



University of South-Eastern Norway
Faculty of technology, natural sciences and
maritime sciences

Master's Thesis (60 ECTS)
Department of natural sciences and
environmental health
Spring 2018

Dag-Roal Wisløff

Effects of boreal forest wildfire on levels of metal and PAH in lacustrine sediments



Water is the first cause, the *archē*, the fundamental principle
of all things.

Thales of Miletus (6th century BC)

University of South-Eastern Norway

Faculty of technology, natural sciences and maritime sciences

Department of Natural Sciences and Environmental Health

Gullbringvegen 36 (Hallvard Eikas plass)

N-3800 Bø (TELEMARK)

www.usn.no

© 2018 Dag-Roar Wisløff

Abstract

Entire catchments rich in acidic peatland, ponds, streams and lakes burned during a large boreal forest wildfire in Mykland (South-Eastern Norway) in 2008. Wildfire liberates accumulated metals, while incomplete combustion of organic matter generates PAHs. As post-wildfire runoff and erosion rates increase, migration of metals and PAHs from terrestrial to aquatic systems is intensified. If undisturbed, sediments are reliable environmental archives that document deposition history and provide information on particle-bound substances such as metals and PAHs.

By measuring concentration levels in surface / sub-surface sediments two years after the fire, this study seeks to explore lacustrine sediments in eight lakes as recipient depots of metals and PAHs mobilized, produced and redistributed during combustion and ensuing processes of boreal forest wildfire. In present study, elevated levels of metals and PAHs in surface sediments are not traceable compared to sub-surface sediments. The results demonstrate a decline in PAH levels, as well as for several metals. Metal concentrations depict a more complex pattern than the marked PAH decline. The results do however reflect regional trends of reduced atmospheric deposition of metals and PAHs during the decade preceding the fire. Nonetheless, surface sediments are polluted with several PAH_{HMW} (i.e. PYR, BaA, CHR, BbF, BkF, BghiP, IcdP, DBa3A), Hg_{LOI} and Pb in six or more lakes. Half of the lakes are polluted with Zn, Cd, Hg, ACNLE and FLU. In addition to reduced input of LRTAP in the area, several mechanisms and processes, like mixing of lake bed sediments thru bioturbation; post-depositional degradation and removal thru biotics' ingestion; re-mobilization thru resuspension of sediments and diffusion across the sediment-water interface, among others, may co-account to the post-fire decline of metals and PAHs. To conclude, surface sediments share no signal of any metal / PAH contamination in response to wildfire, strong enough to counter the general decline documented for these substances in the region.

As climate moves towards more “wildfire weather” with intensified drought, heavier thunderstorms and more wind, fire is expected to shift from a natural part of an evolved ecosystem, to more frequent and severe wildfires, most often ignited by reckless act of man. Intensified post-fire rainfall events increase the mobility of released contaminants that has accumulated in forest soil and flora, posing a considerable hazard to catchment ecosystems and waterbodies. In an ecotoxicological perspective, lacustrine sediments contaminated with metals and PAHs present a threat to water quality, aquatic

ecosystems and biodiversity due to the high toxicity, environmental persistence and bioavailability of these substances. Environmental contaminants released from aquatic sediments can be absorbed by flora and fauna if on a bioaccessible state, and through bioaccumulation and / or biomagnification, ultimately end up in humans. Forest catchments with low levels of contaminants in soil and waterbodies are literally vital to life. However, the supply of sufficient water quality and quantity is seriously challenged at global level by the impacts of natural and anthropogenic activities, including wildfire.

Keywords:

Boreal forest wildfire, lake sediments, heavy metal, PAH, polyarene, Pyrowater

Front page aquarelle: illustrator Helgafo

Sammendrag

I 2008 brant 26 km² boreal skog sør i Norge (Mykland), den største skogbrannen i moderne, norsk historie. Skogbrann kan mineralisere organisk bundet metall akkumulert i jordsmonn og flora etter mange års deponert, lufttransportert forurensning.

Ufullstendig forbrenning av organisk materiale produserer PAH-er. Etter hvert som erosjon og avrenning øker som følge av brann, intensiveres transporten av frigjorte metaller og PAH fra terrestriske til akvatiske systemer, hvor stoffene potensielt sedimenterer. Uforstyrrede sediment er pålitelige miljøarkiv som dokumenterer deponeringshistorien til partikkelbundne stoffer som metaller og PAH.

Ved å måle konsentrasjonsnivåer i overflatesediment og underliggende sedimentsjikt i åtte ferskvannsinnsjøer to år etter Mykland-brannen, forsøker dette studiet å utforske hvorvidt sediment mottar og deponerer metaller og PAH mobilisert, produsert og omfordelt som følge av brann og etterfølgende prosesser. Studiet kan ikke spore økt nivå av metaller / PAH i noen av de undersøkte overflatesedimentene, sammenliknet med de respektive underliggende sedimentsjikt. Resultatene viser nedgang i konsentrasjonsnivå av PAH og flere metaller. Metallkonsentrasjonene tegner et mer komplekst bilde sammenliknet med til den klare reduksjonen for PAH. Resultatene speiler likevel den regionale nedgangen i atmosfærisk avsatt metall og PAH gjennom tiåret forut for brannen. På tross av den generelle konsentrasjonsreduksjonen, er overflatesedimentene i seks innsjøer så forurenset av PAH_{HMV} (dvs. PYR, BaA, CHR, BbF, BkF, BghiP, IcdP, DBa3A), Hg_{GT} og Pb at miljøtilstanden kan karakteriseres som dårlig. Halvparten av innsjøene er tilsvarende forurenset med Zn, Cd, Hg, ACNLE and FLU. I tillegg til regionens reduserte tilførsel av LRTAP, kan en rekke mekanismer og prosesser (for eksempel bioturbasjon; re-mobilisering; diffusjon), være bidragsgivende til den påviste reduksjonen. For å konkludere viser overflatesedimentene ingen tegn til økt avsetning av metaller eller PAH etter brannen, sterkt nok til å motvirke den generelle nedgangen dokumentert for regionen.

I takt med at klimaet endres mot mer «skogbrannvær» med økt tørke, kraftigere tordenvær og sterkere vind, er skogbrann i ferd med å forlate sin posisjon som naturlig ledd i suksesjonen av økosystemer, til å bli mer hyppige og alvorlige, oftest antent som følge av menneskelig uaktsomhet. Mer intens og hyppig nedbøraktivitet etter brann øker mobiliteten til frigjort forurensning akkumulert i jordsmonn og vegetasjon. Dette utgjør en betydelig risiko for miljøet i hele nedbørsfeltet, inkludert vannforekomstene. I et

økotoksikologisk perspektiv representerer akvatiske sedimenter forurenset med metaller og PAH en trussel mot vannkvalitet, akvatiske økosystemer og biologisk mangfold, på grunn av stoffenes høye toksisitet, persistens og mulige biotilgjengelighet. Gjennom bioakkumulering og / eller biomagnifikasjon utgjør biotilgjengelige metaller og PAH en trussel mot akvatisk liv, og kan potensielt ende opp i mennesket. Lave nivå av miljøgifter i boreal skog og vannsystemer er bokstavelig talt livsviktig. På tross av dette utfordres tilførselen av tilstrekkelig mengde vann av tilfredsstillende kvalitet globalt, som følge av menneskelige handlinger, inkludert skogbrann.

Table of contents

Abstract	3
Sammendrag	6
Table of contents	8
Preface	10
1 Introduction	11
2 Aim of study	16
3 Background	17
3.1 Metals and PAHs in post-wildfire soil and ash	19
3.2 PWF effects on soil properties, runoff and erosion.....	20
3.3 Fire regime and associated variables	21
3.4 Metals	21
3.5 Polycyclic aromatic hydrocarbons – polyarenes.....	22
4 Material and methods	24
4.1 Area description	24
4.1.1 Study site and catchment area	24
4.1.2 Lakes.....	25
4.2 Sediment sampling and material.....	28
4.2.1 Material	29
4.3 Sample preparations and chemical analyses.....	32
4.3.1 Radiometric dating of sediments using ²¹⁰ Pb and ¹³⁷ Cs	32
4.3.2 Calculating sediment loss on ignition (LOI).....	34
4.3.3 Metals in sediments; sample pre-treatment and analyses.....	35
4.3.4 PAHs in sediments; sample pre-treatment and analyses.....	37
4.4 Statistical analyses	37
4.4.1 Principal component analyses (PCA)	38
4.4.2 Correlations	39
4.4.3 Cluster analyses (CA).....	40
4.4.4 Parent PAH isomer ratios (IR).....	40
4.4.5 Transformation of data	41
4.4.6 Qualified majority - Identifying metal fluctuations with depth.....	43
5 Results	45
5.1 Dating of sediments	45
5.1.1 Hundsvatn (cf. Appendix 1)	47

5.1.2 Rasvassvatn (cf. Appendix 1).....	48
5.1.3 Jordtjenn _{con} (cf. Appendix 1).....	49
5.2 Lake sediments' organic matter content (LOI).....	49
5.3 Metals in sediments ($\mu\text{g g}^{-1}$).....	51
5.3.1 Metal outlier analysis.....	52
5.3.2 Metals and sediment organic matter (LOI).....	54
5.3.3 Dominant metal concentrations.....	55
5.3.4 Depth profile on metal concentration fluctuation thru time.....	56
5.3.5 PCA on measured metal concentrations.....	58
5.3.6 Metal correlations.....	59
5.3.7 Clustering of depths, lakes and metals.....	61
5.4 PAHs in sediments ($\mu\text{g kg}^{-1}$).....	63
5.4.1 PAHs and sediment organic matter (LOI).....	65
5.4.2 PAH outlier analysis.....	65
5.4.3 Dominant PAH concentrations.....	67
5.4.4 Depth profile on PAH concentration fluctuation thru time.....	68
5.4.5 PCA on LOI-normalized PAH concentrations.....	70
5.4.6 Scatter plot of PAH correlations.....	71
5.4.7 Clustering of depths, lakes and PAH _{LR}	72
5.4.8 PAH relative abundances – Log ratio (LR) biplot.....	74
5.5 Metal and PAH distribution in relation to lake parameters.....	75
6 Discussions.....	78
6.1 Aim of study and results.....	78
6.2 Sampling campaign, material and time lapse since fire.....	79
6.2.1 Dating and mixing of sediments.....	82
6.2.2 Analytical techniques.....	83
6.3 Metals, PAHs and sediment organic matter (LOI).....	84
6.4 PAH and metal mobility - terrestrial soil burn off and organic matter decline.....	87
6.5 PWF degradation of PAHs.....	88
6.6 PWF metal removal.....	89
6.7 Metal distribution in relation to lake basin environmental factors, RT & metal clustering ..	90
6.8 Partitioning of correlated metals – source apportionment.....	92
6.9 Wind and smoke plume dispersal.....	94
7 Conclusions.....	97
References.....	99
Tables and figures.....	116
List of tables and figures.....	129
Appendix.....	137

Preface

The present work is a master's thesis in Environmental Science at University of South-Eastern Norway (USN), Faculty of technology, natural sciences and maritime sciences. There is an appended section (both *Tables and figures*, and *Appendix*) to the document, consisting of tables and figures referred to in the text, and a report on sediment dating (Appendix 1). Espen Lydersen, professor in limnology at Department of Natural Sciences and Environmental Health (USN), is the main supervisor to this work. Senior research scientist Eirik Fjeld at Norwegian Institute for Water Research (NIVA) is the co-supervisor. Espen, the door to your office is always open when there is a need to talk thru a topic, which I truly appreciate. Eirik, your comprehensive insight, spiced with humour bone-dry as any Bond martini, has been genuinely inspirational. To both; I highly value your guidance, support and not least patience during the process of completing this work. Also, I would like to thank NIVA on a general basis for the analyses performed, and Gamma Dating Centre Copenhagen for the sediment timelines of deposition.

Since the present work is a master's thesis and not a research paper, and because the results from the material investigated are negative, a broader review of analysis, methods and techniques are described. This is done to highlight some of the work that has been put down to get to the results and the knowledge behind.

To you, my darling sweet heart, for all your love and support;

For du gylte kvar ein augneblink med hugen fri.

Odd Nordstoga, Dagane (2006)

The sampling campaign in Mykland was the memorable initiation of this work. Now it is time to terminate it.



Dag-Roal Wisløff

Master's candidate

University of South-Eastern Norway

Bø (Telemark, Norway), Mai 2018

1 Introduction

Wildfire is one of the major disturbances in nature (Costa, Calvão & Aranha 2014), burning large areas of forested land each year (Chuvieco, Giglio & Justice 2008). Initially, wildfires occur without any influence from humans, being an integral element in the dynamics of the fire-prone boreal coniferous forest biome, shaping forest structure and composition since late Devonian (Shakesby & Doerr 2006; Perera & Buse 2014). Yet, as *Homo sapiens* learned to ignite fire, the majority of wildfires have become of anthropogenic origin, causing socioeconomic and environmental concern (Tishkov 2004; FAO 2007) in the “Anthropocene” (Stoermer & Crutzen 2000).

Lit by a spark from the tire chains of a forwarder, 26 km² of forested land surrounding the small village Mykland in southern Norway, burned in 2008 (Nygaard & Brean 2014). Immediate environmental consequences were reported (Lydersen *et al.* 2014). Samples of runoff water from the burnt area the weeks following fire, revealed elevated concentrations of metals (Ni, Cu, Zn, Cd, Hg, Pb). One year after the fire, raised concentrations of polycyclic aromatic hydrocarbons (PAH) in lake sediments were reported, while metal concentrations in runoff water approached pre-fire levels (Høgberget 2010). Raised levels of metals in “pyrowater” (i.e. surface waters within a burnt catchment impacted by wildfire) are also reported from the 1999 wildfire in Tyresta (Naturvårdsverket 2006) and 2014 wildfire in Västmanland (Köhler, Wallmann & McKie 2017), both in Sweden.

PAH is a group of organic molecules resistant to degradation under natural conditions, while metal is a group of inorganic chemical elements that are neither created, nor degradable in an orthodox manner. Both metals and PAHs are associated with adverse effects on ecosystems and wildlife, attracting considerable scientific and political attention (UNECE 1998b; UNECE 1998a; Douben 2003; AMAP 2005). Being persistent, relatively volatile and with the property to adsorb on solid particles, metals and PAHs have potential for global dispersal (Christensen *et al.* 2008) through biotic and abiotic compartments (Wilson & Symon 2004). Thus, these chemical compounds are listed as environmental pollutants by the 1979 United Nations Economic Commission for Europe’s (UNECE) Convention on Long-Range Transboundary Air Pollution (CLRTAP) (UNECE 1979; UNECE 1998b; UNECE 1998a).

Metals and PAHs deposited on and accumulated within soil and biota (Greenberg 2003; Kabata-Pendias 2011), are mobilized during combustion processes of wildfire (García-

Falcón, Soto-González & Simal-Gándara 2006; Vergnoux *et al.* 2011; Odigie & Flegal 2014). As incomplete combustion of organic matter (OM) also *generates* PAHs, wildfire is considered a natural source of PAH origin (Kim, Oh & Chang 2003; Choi 2014).

Soils and lacustrine sediments are repository compartments for metals and PAHs (Okafor & Opuene 2007; Yao & Gao 2007; Kabata-Pendias 2011; Luo *et al.* 2013). After wildfire sources of contaminants, soil erosion rates and runoff generation increase, amplifying transport of particles and colloids from terrestrial to aquatic environments, including associated metals and PAHs (Smith *et al.* 2011). In waters, metals and PAHs have propensity to adsorb on depositing particles and potentially persist in sediments for a long time (Christensen *et al.* 2008). Consequently, wildfires have potential to contaminate surrounding waterbodies and accompanying sediments (Silva *et al.* 2016).

In an ecotoxicological perspective, contaminated sediments pose a hazard to aquatic ecosystems, both directly (e.g. ingestion) and indirectly, as bioturbation, diffusion and sediment resuspension re-mobilize contaminants accumulated in sediments and enrich their levels in the above water column (Chen & White 2004; Sprovieri *et al.* 2007; Yao & Gao 2007; Bouloubassi *et al.* 2012; Zeng *et al.* 2013; Breedveld *et al.* 2015). As part of implementing the European Union's *Water Framework Directive* (EU-WFD 2000/60/EC), the Norwegian guide for *classification of environmental status in waters*, states that such re-mobilization is to be considered as emissions (Committee of Directorates 2013).

Studies show that contaminants leaking from sediments become bioavailable and absorbed by plants, animals and humans, with a tendency to bioaccumulate in the organism and biomagnify (most organisms metabolize PAHs sufficiently and thus, biomagnification is prevented (Abdel-Shafy & Mansour 2016)) through the food web (Ignatavièius, Sakalauskienė & Oškinis 2006; Okafor & Opuene 2007; Yao & Gao 2007; Wang *et al.* 2012). Hence, concentrations of metals and PAHs in sediments are important issues in environmental science (Yao & Gao 2007; Zeng *et al.* 2013). Accumulation of metals and PAHs in living organisms has gained considerable attention. A topic of concern in this context is the combined effects of coinciding contamination, as environmental compartments contaminated with metals frequently are reported to contain high amounts of PAHs (Shen, Lu & Hong 2006).

Due to the relative higher rates of deposition, in comparison to re-mobilization and decomposition, sediments represent a sink where numerous contaminants may accumulate (Sprovieri *et al.* 2007). If undisturbed, vertical, stratified sections of dated sediment cores offer environmental records of deposited metals and PAHs, permitting concentration levels to be assessed in terms of temporal and spatial impact on aquatic systems (Müller, Grimmer & Böhnke 1977; Mai *et al.* 2002; Muri, Wakeham & Faganeli 2003; Okafor & Opuene 2007). A wide range of environmental programs like the Arctic Monitoring and Assessment Programme (AMAP 2005) have for long recognized these “depots” as reliable environmental archives, providing information on and documenting pollution history of a number of particle-bound substances such as metals and PAHs (Müller, Grimmer & Böhnke 1977; Appleby 2001; Last & Smol 2001; Rose, *et al.*, 2004; Lepanea, *et al.*, 2007; Rognerud *et al.* 2008; Committee of Directorates 2013). By analysing sediment cores, it is possible to date inputs and determine the extent, source, distribution and hazard potential of contaminants in a historical perspective. A prerequisite to permit such studies is that the substances evaluated have a certain particle affinity or being their own particles. In addition, the inputs may not be easily dissolvable or decomposable by microbial activity and/or other diagenetic changes within the sediment. Both metals and PAHs to a large extent fulfil these criteria (Müller, 1977). Furthermore, mixing of sediments should be restricted. According to Guo *et al.* (2010), post-depositional mixing processes are limited in lacustrine systems.

On a general basis, pollutants accumulated in sediments are studied thoroughly, both in Nordic countries as well as internationally. There is a predominance of studies performed in industrialized areas compared to studies of pristine environments (Müller, Grimmer & Böhnke 1977; Last, Smol & Birks 2001; Donahue, Allen & Schindler 2006; Yao & Gao 2007; Christensen *et al.* 2008; Wang *et al.* 2010; Eide *et al.* 2011). Papers revising post-wildfire (PWF) export of metals and PAHs into rural lakes and sediments are scarce, despite extensive research on wildfire (Kasischke & Stocks 2000; Thomas & McAlpine 2010), metals (Markert & Friese 2000) and PAHs (Harvey 1997; Douben 2003).

Most PWF research on PAHs pay attention to effects on soils (García-Falcón, Soto-González & Simal-Gándara 2006; Kim, Choi & Chang 2011; Vergnoux *et al.* 2011; Choi 2014), waters (Olivella *et al.* 2006; Vila-Escalé, Vegas-Vilarrúbia & Prat 2007; Smith *et al.* 2011) and air (Estrellan & Iino 2010). Only a limited number of studies

have emphasized aspects of PWF PAH levels in sediments (Gabos *et al.* 2001; Olivella *et al.* 2006; Vila-Escalé, Vegas-Vilarrúbia & Prat 2007). Kim, Oh and Chang (2003) address the need of more research on this topic.

According to reviews by Smith *et al.* (2011), Stankov Jovanovic *et al.* (2011) and (Abraham, Dowling & Florentine 2017), there is also a lack of research on PWF export of metals. Most studies on the topic focus merely on mercury (Hg) (Cinnirella & Pirrone 2006; Kelly *et al.* 2006; Biswas *et al.* 2007; Finley, Swartzendruber & Jaffe 2009; Navrátil *et al.* 2009; Burke *et al.* 2010; Moreno, Fjeld & Lydersen 2016) or levels in ash/residues (Pereira & Úbeda 2010; Odigie & Flegal 2014; Pereira *et al.* 2014; Campos *et al.* 2015), stormwater runoff (Stein *et al.* 2012) or soils and flora (Stankov Jovanovic *et al.* 2011; Sosorova, Merkusheva & Ubugunov 2013). Only singular studies encompass PWF metal levels in freshwater sediments (Odigie *et al.* 2016), still primarily on Hg (Caldwell, Canavan & Bloom 2000; Rothenberg *et al.* 2010). Both the latter papers utter the necessity of more research related to this topic. Concerning contributions by natural (e.g. forest fire) sources to atmospheric metal contamination, Nriagu (1989, and references therein) remains the primary reference cited, as stated by Richardson (2001).

A warmer climate is expected to alter global wildfire regimes (i.e. intensity, frequency, duration, fuel composition, severity etc.) and the geographic distributions of wildfires. In which way and to what extent still is uncertain (Krawchuk *et al.* 2009). However, an overall increase in wildfire frequency is expected in the circumpolar boreal forest region (Flannigan *et al.* 2009).

The knowledge about wildfire in the southern boreal and boreonemoral vegetation zones of Fennoscandia is scarce (Storaunet *et al.* 2008). To meet this knowledge gap, the project Pyrowater was initiated. As part of the project this thesis describes temporal and spatial patterns of 9 metals (V, Cr, Co, Ni, Cu, Zn, Cd, Hg, Pb) and 18 PAH species (NAP, ACNLE, ACNE, FLE, PA, ANT, DBTHI, FLU, PYR, BaA, CHR, BbjF, BkF, BaP, BeP, BghiP, IcdP, DBa3A) in lacustrine sediments of five wildfire affected lakes and three nearby control lakes (nomenclature in table 10 and 11, Tables and figures). Sediments are sampled two years after the fire and include age determination measurements of the sampled sediments.

The metals and PAHs investigated are selected on the basis of the two 1998 Aarhus protocols on *heavy metals* (UNECE 1998a) and *persistent organic pollutants (POPs)*

(UNECE 1998b), the United States Environmental Protection Agency (U.S. EPA) list of priority pollutants (U.S. EPA 2012), the EU-WFD 2000/60/EC amended list of priority substances (directive 2013/39/EU) (European Commission 2013), and substances commonly considered environmental pollutants in ecotoxicology and environmental science (Rognerud *et al.* 2008).

Note that some PAHs are grouped together as a single compound; Benzo[b]fluoranthene and Benzo[j]fluoranthene as Benzo[bj]fluoranthene (BbjF); Dibenz[a,c]anthracene, Dibenz[a,h]anthracene and Dibenz[a,j]anthracene as Dibenz[ac+ah+aj]anthracene (DBa3A), and that the sum of all sampled PAHs are denoted $\Sigma\text{PAH}_{\text{EPA16+2}}$. The figures EPA16+2 refers to the 16 PAHs on the United States Environmental Protection Agency's list of priority pollutants, plus the two additional PAHs DBTHI and BeP in this study.

Regarding metal analyses, this paper is concerned with total concentrations of the different metals, including elemental species, their ions and compounds. Being aware of the objections to such usage when environmental impact of contaminated sediments are discussed (e.g. mobility, bioavailability and potential toxicity, cf. Yao and Gao (2007)), total metal concentrations serve as a useful indicator when assessing sediment contamination (Baran & Tarnawski 2015), and are widely used in numerous environmental programs (Roig *et al.* 2016). Analysis of total metal concentrations are in accordance with the objective of this study, which seeks to explore lacustrine sediments as recipient depots of metals and PAHs following a boreal forest wildfire.

2 Aim of study

Mykland sites in an area of Norway that receives substantial amounts of metals and PAHs from continental Europe as Long-Range Transboundary Air Pollution (LRTAP). The deposited contaminants accumulate in soils and vegetation, from where they can be liberated during wildfire (Naturvårdsverket 2006; Høgberget 2010).

Aquatic ecosystems are particularly sensitive to pollution because of the structure in their food web, and because waterbodies are at the receiving end of effluents (Yao & Gao 2007). Lake bed sediments are formed by substances altered through atmospheric deposition, flow of debris from discharge areas (allochthonous) and endogenic matter (autochthonous) (Gilbert 2003). As wildfire amplify soil erosion and runoff, especially during PWF rainfall events, increased amounts of PWF particles, colloids and dissolved compounds, including mobilized metals and PAHs, are expected to be transported from terrestrial surfaces to streams and lakes, including fallout from fire-generated smoke plumes and wind dispersal of wildfire residuals (Certini 2005; García-Falcón, Soto-González & Simal-Gándara 2006; Ryan, Dwire & Dixon 2011; Smith *et al.* 2011; Choi 2014; Odigie & Flegal 2014). In waters, metals and PAHs have propensity to adsorb on depositing particles and potentially persist in sediments for a long time (Christensen *et al.* 2008). Assumably, wildfire affected waterbodies show elevated concentrations of metals and PAHs in their corresponding bed sediments (Caldwell, Canavan & Bloom 2000; Gabos *et al.* 2001; Olivella *et al.* 2006; Vila-Escalé, Vegas-Vilarrúbia & Prat 2007; Rothenberg *et al.* 2010); a potential secondary source of pollution hazardous to life (Sprovieri *et al.* 2007; Yao & Gao 2007; Zeng *et al.* 2013).

When examining the fate of metals and PAHs in nature, it is important to identify emission sources, transport pathways and various recipient depots (Kim, Choi & Chang 2011). To evaluate lacustrine sediments as recipient depots of metals and PAHs mobilized and redistributed during combustion processes of boreal forest wildfire and ensuing processes, the objective of this thesis is to study whether PWF concentration levels of metals and PAHs in lacustrine surface sediments of six fire affected lakes are elevated compared to sub-surface concentration levels (representing pre-fire conditions). Also, three control lakes outside the perimeter of the burnt area are sampled for comparison purposes, as well as pre-industrial depth sections as reference material. All lakes are sampled two years after the fire.

3 Background

In the early summer of 2008 Mykland was struck by a vast forest wildfire that lasted for six days (9th – 14th of June), with persisting smouldering fires for another six days (15th – 20th of June).

Weather conditions preceding the fire were dry, with only 2.1 mm precipitation the last 38 days prior to ignition. A forest wildfire hazard index (The Norwegian Fire Weather Index, FWI) compiled by the Norwegian Meteorological Institute (NMI) from Nelaug meteorological station, showed very high fire danger (WBKZ [Waldbrandkennziffer] >70) already May 10th, and an increase to almost 240 ignition day (Nygaard & Brean 2014).

The wildfire is recognized as the largest in Norway since 1844 (Nygaard & Brean 2014), with more than 90 % (120 000 m³) of the forest within a 26 km² area, almost totally burnt (Storaunet *et al.* 2008; Lydersen *et al.* 2014). Whole catchments rich in acidic peatland, ponds, streams and lakes burned, providing a unique opportunity to study ecotoxicological and limnological effects of wildfire on a boreal conifer forest landscape typical to large parts of Norway (Høgberget 2010).

Limited national data on aquatic effects of domestic boreal forest wildfire (Storaunet *et al.* 2008), and the expected increase in wildfire frequency in Fennoscandia, as a consequence of climate change, (Flannigan *et al.* 2009), makes an imperative for such research.

By this means, two sections of the area ravaged by fire were considered of national value by the Norwegian government. As a consequence *Myklandsvatna* (7.111 km²) and *Jurdalsknuten* (3.477 km²) were declared national nature reserves the 26th of June 2009 (Lovdata.no 2009a; Lovdata.no 2009b) to secure research and long-term monitoring / succession (figure 1).

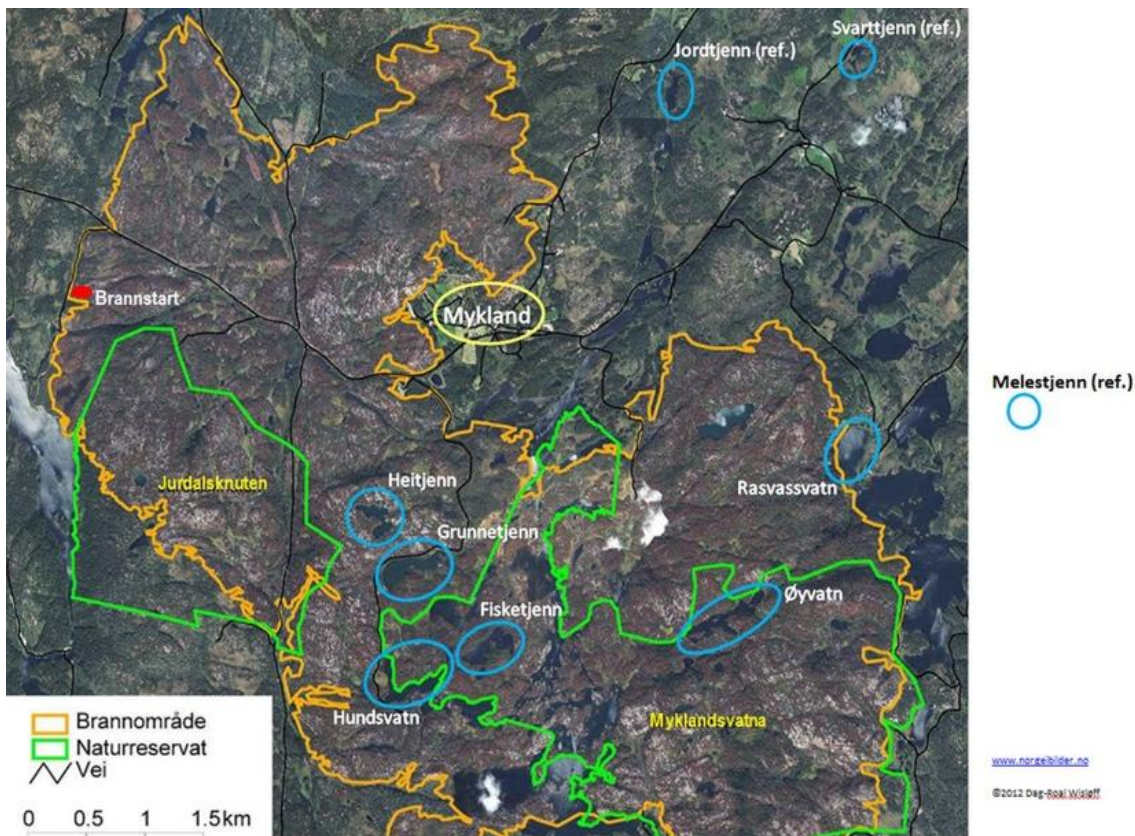


Figure 1 The perimeter of the burnt area is outlined ochre yellow, while the two nature reserves Jurdalsknuten and Myklandsvatna are outlined bright green. Sampled lakes are circled blue. Lakes with the suffix ref. are control lakes outside the perimeter of the fire. Solid red dot marks start of fire (Brandrud, Bratli & Sverdrup-Thygeson 2010).

Following the resolutions, several research projects were initiated (i.a. by *The Norwegian Biodiversity Information Centre*), among them the Research Council of Norway's (RCN) project *Pyrowater – Wildfire effects on biogeochemistry of soil and surface water*, established in October 2009 and led by Telemark University College (TUC, now University of South-Eastern Norway, USN). The project derives from EU's Water Framework Directive 2000/60/EC, which Norway has acceded (NOKUT 2010; UiO 2010; RCN 2013).

As the title imply, *Pyrowater* is an interdisciplinary study of chemical and biological effects in aquatic ecosystems impacted by wildfire, including the fate of metals and PAHs. This paper is part of the project.

During post-fire extinction operations in Mykland, Norwegian Institute for Air Research (NILU) measured elevated concentrations of the PAH retene (RET) in samples of air at Birkenes observatory (17th – 18th of June), approximately 26 km linear distance south of the wildfire area. RET is generated thru thermal degradation of resin compounds in

softwood. In ambient air, RET is regarded a marker compound of conifer combustion. The raised RET-values at Birkenes probably owed to the forest fire in Mykland that passed off during this period (Ramdahl 1983; Aas 2009).

Increased concentrations of Ni, Cu, Zn, Cd, Hg and Pb in samples of runoff water from the burnt area were reported the weeks following fire, as well as elevated concentrations of PAHs in lake sediments one year after the fire (Høgberget 2010).

Wildfires impact both on a local/regional scale and globally (Singh *et al.* 2010; Heilman *et al.* 2013; Robichaud *et al.* 2013). The effect of fire on ecosystems is heterogeneous and complex, involving biotic and abiotic factors with consequences at several spatial and temporal scales (Neary, Ryan & DeBano 2005). Massive landscape changes within and downstream of the burnt area (Robichaud *et al.* 2013) disrupt the initial equilibrium between separate components of the forest (Sosorova, Merkusheva & Ubugunov 2013), having profound influence on soils and waters (Costa, Calvão & Aranha 2014). Factors responsible for hydrological responses to fire are site and burn specific, intricately linked to terrestrial, fire-induced alterations, involving ash, soil and landscape changes (Neary, Ryan & DeBano 2005). The degree of PWF sedimentological changes in watersheds depend largely on landscape susceptibility to erosion, the timing and magnitude of rain events (c.f. torrent rain) that follow fire, and the burn (Ryan, Dwire & Dixon 2011).

The literature on wildfire, sediment contamination, metals and PAHs are extensive, diverse and complex. To highlight research relevant to this thesis, and the probability of the *a priori* hypothesis (elevated concentration levels of metals and PAHs in PWF lake sediments should be expected compared to pre-fire conditions), a comprehensive background section on the most relevant variables related to PWF effects on soils / ash in respect to metal and PAH contamination, is given. A brief review of some PAH properties and differences between metals and PAHs is given.

3.1 Metals and PAHs in post-wildfire soil and ash

When vegetation cover and detritus burn, soil characteristics are modified. Soil OM declines markedly and alkaline cations bound to organics are released through fire induced mineralization (Certini 2005). The combustion residues left in the wildfire area are charred material and ash products, rich in the base cations Na⁺, Mg²⁺, K⁺, Ca²⁺ (Lydersen *et al.* 2014) and other transition metal ions (i.e. Mn²⁺, Fe²⁺, Zn²⁺) (Pereira *et*

al. 2014). The mineralization of soil OM may also release other metals bound to organics (Høgberget 2010). A study by Odigie and Flegal (2014) reported increased concentrations of transition metals Co, Ni, Cu, Zn and Pb (post-transition metal) in ash after a fire in a chaparral and mixed conifer Californian forest. Moreover, Sosorova, Merkusheva and Ubugunov (2013) and Stankov Jovanovic *et al.* (2011) reported increased concentrations of transition metals Cr and Cd in PWF soils.

Also, studies demonstrate increased PAH concentrations in PWF soils (Vergnoux *et al.* 2011; Choi 2014) and in ash derived from forest biomass combustion (Kim, Choi & Chang 2011).

3.2 PWF effects on soil properties, runoff and erosion

During fire, soils are associated with steep temperature gradients below the surface, triggering organic compounds that volatilize to move downwards and condense on the cooler soil particles, causing water repellence. As a result, a continuous negatively charged water-repellent sub-surface soil layer forms, reducing soil permeability. This “tin-roof” effect is enhanced by an increase in soil bulk density, as soil porosity decreases, due to aggregate collapse and clogging of voids by ash and dispersed clay minerals (Ice, Neary & Adams 2004; Certini 2005; Verma & Jayakumar 2012; Xue, Li & Chen 2014). A review by Certini (2005) provides further discussion on wildfire effects on soil properties in forests.

Despite little information on fire induced hydrological and geomorphological impacts in the boreal forests, the role of wildfire as a forceful hydrogeomorphological agent is widely recognized (Shakesby & Doerr 2006). The water repellent soil, together with losses of protective vegetative cover, leave the forest exposed to agents of denudation (e.g. sun, wind, precipitation/rain splash etc.) and increase PWF runoff and erosion rates (Neary, Ryan & DeBano 2005), including wind dispersal of ash (Kim, Choi & Chang 2011). Increased runoff and erosion after wildfire intensify transport of both metals and PAHs from terrestrial to aquatic systems, especially during rainstorm events (Luo *et al.* 2013; Odigie & Flegal 2014), which is considered the primary variable for the PWF response processes (Moody *et al.* 2013).

3.3 Fire regime and associated variables

In addition to the hydrogeomorphological regime, wildfires' effects on the environment depend on the fire regime (e.g. density, frequency, size, distribution and time of fire) (Chuvieco, Giglio & Justice 2008; Moody *et al.* 2013). The fire regime is closely connected to atmospheric conditions (i.e. weather and climate), anthropogenic activity (e.g. forestry, land use, prescribed burning, fire suppression), natural disturbances (e.g. insect pests, storm tree-breakage) and fire severity / ecological impact (i.e. intensity / energy release and duration of fire), which is controlled by several environmental (e.g. amount, nature and moisture of live and dead fuel, temperature, soil, bedrock, wind speed, topography) factors that influence the combustion and PWF processes (Certini 2005; Chuvieco, Giglio & Justice 2008; Keeley 2009; Krebs *et al.* 2010; Bento-Gonçalves *et al.* 2012).

3.4 Metals

Metals are among the inorganic, rudimentary constituents of Earth's crust. Dependent on the composition of the lithosphere, metal concentrations vary across geographic regions. Because metals are neither created, nor degradable in an orthodox manner, they differ fundamentally from organic substances like PAHs (Bowen 1979; Markert & Friese 2000).

Natural processes as weathering, erosion and volcanic activity, release metals into ecosystems (Callender 2003). Once mobilized, metals move through various environmental compartments depending on several biotic and abiotic processes, i.e. the biogeochemical cycling (Garrett 2000). Especially atmospheric and fluvial (e.g. riverine waters) transport of metals are crucial pathways between ecosystems, but also migrating species, anthropogenic wastes, transport etc. are of concern (Callender 2003; Brimble *et al.* 2009).

Dependent on residence time, atmospheric dynamics and their species, many metals have substantial long-range air transport potential before they precipitate into terrestrial and aquatic systems as either wet or dry deposition (Kabata-Pendias & Mukherjee 2007; Feng & Yang 2008). Because metals tend to associate with particles (Sigg, Sturm & Kistler 1987) they have potential to accumulate in soils and aquatic sediments (>99 %), but do also dissolve in the water column (Salomons 1998) or are taken up by biota (Stankov Jovanovic *et al.* 2011).

Numerous physical, chemical and biological processes can convert metals from one species to another. The most important factors regulating species composition and the balance between retention and mobility of metals and other contaminants, is pH, Eh and the presence of complexing agents (ligands) such as organic matter and anions (e.g. fluoride, chloride, and sulphate) (Salomons 1998).

As forest fire fuels dominantly consist of plant material, adsorbed and absorbed metals in soils and flora are latent to be released and redistributed after wildfires (Shcherbov, Strakhovenko & Sukhorukov 2008; Kabata-Pendias 2011).

Natural background (geogenic) concentrations of metals are generally present at concentration levels normally not harmful to any organisms. Some metals, like Mn, Fe, Co, Cu and Zn, are even essential micronutrients, while metals as Cd, Hg and Pb, play no known biological essential role (Stankov Jovanovic *et al.* 2011).

In this study the term *metal* refers to the nine elements V, Cr, Co, Ni, Cu, Zn, Cd, Hg and Pb, grouped as transition (V, Cr, Co, Ni, Cu, Zn, Cd, Hg) and post-transition (Pb) metals in the periodic table of elements. Several papers refer to these metals as *heavy metals* (e.g. Breivik *et al.* 2004; Yao & Gao 2007). Others criticise such terminology as being meaningless (Duffus 2002; Hodson 2004), thus a clarification is needed.

According to Adriano (2001, page 4) these elements (i.e. V, Cr, Co, Ni, Cu, Zn, Cd, Hg and Pb) “occur in natural and perturbed environments in small amounts and that, when present in sufficient bioavailable concentrations, are toxic to living organisms.”

Throughout this thesis Adriano’s definition is adopted, and *metal* will serve as a generic term encompassing the nine listed metals.

3.5 Polycyclic aromatic hydrocarbons – polyarenes

Polycyclic aromatic hydrocarbons (PAH) constitute a large group of structurally diverse organic molecules of two or more fused benzene rings (Neff 1979; Harvey 1997; Douben 2003). Due to their low hydrogen:carbon ratios, PAHs represent a very stable class of hydrocarbons (Ravindra, Sokhi & Van Grieken 2008).

PAHs have both natural (e.g. forest fires and volcanic eruptions) and anthropogenic (i.e. coal/wood burning and, petrol/diesel oil combustion) origin (Tobiszewski & Namieśnik 2012), derived by various processes of pyrolysis-pyrosynthesis (Hwang, Wade & Sericano 2003), as a result of either combustion (*pyrogenic* origin), petroleum formation

(*petrogenic* origin), diagenesis (*diagenetic* origin, e.g. perylene and retene) or biosynthesis (*biogenic* origin) (Soclo, Garrigues & Ewald 2000; Burgess, Ahrens & Hickey 2003; Ruus *et al.* 2009; Barakat *et al.* 2012). Anthropogenic loadings usually outweighs the natural ones, being responsible for the general PAH increase during the 20th century (Grimalt *et al.* 2004).

Simultaneously with PAH accumulation in ecosystems, degradation takes place. In sediments, PAHs' omnipresence suggests that accumulation dominate degradation processes (Soclo, Garrigues & Ewald 2000).

PAHs usually occur as complex mixtures in the environment (Ravindra, Sokhi & Van Grieken 2008). It is not feasible to analyse and quantify all various PAH compounds which are generated. A common approach is to analyse a number of individual PAHs and the total sum of these. Abundant PAHs of ecotoxicological concern are primarily PAH compounds with 2 – 6 benzene rings (U.S. EPA 2012). Pyrogenic PAHs rarely have a single origin, whereas numerous petrogenic PAHs have, suggesting a link between source and distribution. In aquatic ecosystems pyrogenic PAHs are the dominant of the two (Burgess, Ahrens & Hickey 2003).

The matter from which PAHs originate and their formation process determine the structure of PAHs, thus also their properties and fate (distribution and transformation/degradation) (Douben 2003). In general, the more benzene rings the less degradable. During low temperature processes, such as burning of wooden material, low molecular weight (LMW) PAHs are typically produced, while high temperature processes (e.g. combustion of fossil fuels in petrol engines), generates high molecular weight (HMW) PAHs (Tobiszewski & Namieśnik 2012). According to a study by Vergnoux *et al.* (2011) on impact of forest fires on PAH levels in soils, wildfires generate mainly PAH_{LMW} (NAP, ACNE, FLE, PA, ANT, FLU, PYR), which are the preferentially volatilized, leached and degraded ones, at least when considering PAH impact in proximity to the fire (Denis *et al.* 2012).

In Tables and figures basic properties and abbreviations on 24 PAHs relevant to this study are listed (table 11), while table 12 compare LMW (2-3 benzene rings) and HMW (4-6 benzene rings) PAHs. Abbreviations may differ between reports. The purpose is to show property differences between compounds.

National emissions of metals and PAHs, and temporal trends in emission inventories, are found in Appendix 2.

4 Material and methods

4.1 Area description

Mykland is a small village in the rural inlands of Froland municipality (Aust-Agder County) in southern Norway, approximately 34 km linear distance north-west of the coastal town Arendal. The 2008 Mykland forest wildfire started west of the village and east of Mjålandsvatn, spreading north-east and south-east (figure 24, Tables and figures).

The burnt forest lies within a part of Norway which historically has received considerably amounts of long-range transported airborne pollutants from central Europe, including metals, PAHs and strong acids (Aamot, Steinnes & Schmid 1996). Since the 1980's, annual monitoring studies of long-range transboundary air pollutants (LRTAP, metals and PAHs included) through atmospheric (air and precipitation) supply have been performed at Birkenes observatory sampling station, approximately 27 km linear distance south of Mykland (Aas 2009; Aas 2010; Aas 2011). Once a year reports on pollution effects in waters (Schartau 2011), forests (Andreassen 2011) and their summaries (Schartau *et al.* 2011) have been published in parallel.

As result of human activities, great parts of Mykland's forests have burned through history. Extensive logging has clear cut the forest several times since the 18th century (Mykland 1967; Mykland 1970; Mykland 1998; Mykland *et al.* 2009).

A historical review of Mykland are told in Mykland (1967); Mykland (1970); Mykland (1998) and Mykland *et al.* (2009).

4.1.1 Study site and catchment area

Mykland's conifer forest landscape is dominated by Scots pine (*Pinus sylvestris*, constitutes 97 % of the tree species in the burnt locality) and various heather species, with sporadic habitats of rare thermophilic deciduous trees. The area belongs to a clearly oceanic vegetation section in the transition between a southern boreal (north) and boreonemoral (other parts) vegetation zone (Moen, Lillethun & Odland 1999; Brandrud, Bratli & Sverdrup-Thygeson 2010). The terrain is representative for the region, characterized by hilly inland forests and acidic peatland, ponds, streams and lakes (21 % of the burnt area), with a shallow and patchy soil cover on exposed

bedrocks with little uncompacted material and other superficial and glacial deposits. 74 % of the scorched surface is subjected to forestry, 5 % is impediment (Storaunet *et al.* 2008; Brandrud, Bratli & Sverdrup-Thygeson 2010).

The barren forest ground on hard Precambrian bedrock (granites and gneisses) (Brandrud, Bratli & Sverdrup-Thygeson 2010; NGU.no 2012), makes the forests little resistant to acidification, well known conditions in Norwegian nature. This type of forest is considered most prone to wildfire (Skogbrukets Kursinstitutt 2009; Vest-Agder 2017). The burnt land's vertical extent stretches about 250 meters; from Stormyrhølen in south-east at approximately 150 m.a.s.l., to Store Færås/Lauvåsheia in the north at close to 400 m.a.s.l. (Geological Survey of Norway 2018).

Further descriptions of the area (Solvang 2005) and PWF effects, are reported in Storaunet *et al.* (2008) and Nygaard and Brean (2014). PWF effects on fungi, lichens and insects are described in Brandrud, Bratli and Sverdrup-Thygeson (2010).

4.1.2 Lakes

Within the Pyrowater project, water chemistry and biology has been assessed monthly during the first four PWF years (2009-2012) in nine Mykland lakes (Lydersen *et al.* 2014; Moreno, Fjeld & Lydersen 2016). As this paper is an integral part of the project, the lakes considered herein are identical to the ones monitored, not selected from statistical methods but on a discretionary basis, primarily according to the following:

- negligible pre-fire and post-fire influence by human activities and land use (e.g. silviculture/forestry and agriculture),
- location upstream of management actions (i.e. liming),
- accessibility by road for use of boat,
- position within the burnt ground (only relevant to the six, direct fire affected lakes, designated as “burnt”) and
- position outside, but in proximity to the wildfire affected area (only relevant to the three control lakes considered unaffected by fire, mapping pre-fire conditions, designated as “unburnt” and denoted *con.*).

All nine lakes belong to the same drainage basin, Tovdalvassdraget, draining to the main river Tovdalsåna. Six lakes (of which all are burnt); Fisketjenn (228+ m.a.s.l.), Hundsvatn (228- m.a.s.l.), Grunnetjenn (233 m.a.s.l.), Heitjenn (278 m.a.s.l.) and Øyvatt (255 m.a.s.l.), are sited within a sub drainage basin of Tovdalvassdraget,

Uldalsåna (area west of Tovdalvassdraget's drainage divide, draining to Tveitåna tributary river unit), while Rasvassvatn (173 m.a.s.l.), Jordtjenn_{con} (228+ m.a.s.l.), Svarttjenn_{con} (191 m.a.s.l.) and Melestjenn_{con} (222 m.a.s.l.), are located in the adjacent and protected sub drainage basin, *Austrebekken*, east of the drainage divide, draining to Austrebekken tributary river unit (Norwegian Environment Agency 2018; Norwegian Water Resources and Energy Directorate 2018). Fisketjenn and Øyvatn are part of Myklandsvatna nature reserve (figure 25, Tables and figures). Note that one of the burnt lakes, Heitjenn 278, is excluded from the analysis in this study (ch. 4.2.1)

Fisketjenn, Hundsvatn, Grunnetjenn, Heitjenn, Rasvassvatn and Øyvatn are direct fire affected lakes found within the burnt ground, while Jordtjenn_{con} Svarttjenn_{con} and Melestjenn_{con} are situated outside the burnt area (north and east of fire). The latter three lakes are considered unaffected sites for comparison, and thereby serve as control lakes, mapping pre-fire concentrations of metals and PAHs in lake bottom sediments. Worth noting is Rasvassvatn's location along the outside of the perimeter of fire, limiting its spread. Nonetheless, the dominant part of Rasvassvatn's catchment ($\approx 90\%$) lies within the fire area (Lydersen *et al.* 2014) (figure 1).

In spite of Tovdalvassdraget being the cradle of acid rain research in Norway, no pre-wildfire water chemistry data exists for the nine lakes, but lakes are regarded as dilute and acidic (Lydersen *et al.* 2014). According to morphometric data (table 1) and the Norwegian guide on classifications of waters (Committee of Directorates WFD 2015), the studied lakes classify as small ($<0.5\text{ km}^2$), shallow (3 – 15 m) forest (200 – 800 m.a.s.l.) lakes. Rasvassvatn (surface area of 0.89 km^2 , maximum depth 15 meters) differ from this categorization to some degree, and classify as a middle-sized lake ($0.5 < \text{lake} < 5\text{ km}^2$). Høgberget (2010) categorize the direct wildfire affected lakes as oligotrophic (nutrient poor) with varying dystrophy (amount of humus content). Grunnetjenn, Heitjenn (depth 2.5 m, which classify as very shallow) and Øyvatn are wind exposed, shallow (depth 3.0 m) mono-/polymictic (too shallow to be more than briefly thermally stratified during ice-free seasons) waters (Lydersen *et al.* 2016; Moreno, Fjeld & Lydersen 2016).

Many lakes and streams have been artificially limed during the last decades as a countermeasure towards increased acidification in the region. The nine monitored lakes are located upstream the limed lakes (Lydersen *et al.* 2014).

Table 1 Lake morphometric data, catchment characteristics and precipitation data retrieved through the Pyrowater project (by Lydersen) and Lydersen et al. (2014). Lakes impacted by fire (burnt) are also to a varying degree impacted by PWF logging. The three control lakes (unburnt) are located adjacent to the burnt area, outside the perimeter of the fire.

	Fisketjenn _{burnt}	Hundsvatn _{burnt}	Grunnetjenn _{burnt}	Rasvassvatn _{burnt}	Øyvatn _{burnt}	Jordtjenn _{unburnt}	Svarttjenn _{unburnt}	Melestjenn _{unburnt}
Norwegian watercourse number	020.BB5Z	020.BB5Z	020.BB5Z	020.C2Z	020.BB5Z	020.C2Z	020.C2Z	020.C2Z
Norwegian lake number	10061	10033	10024	9948	10045	9816	9804	147913
Latitude	N58 36.549	N58 36.413	N58 36.906	N58 37.446	N58 36.675	N58 38.956	N58 39.118	N58 37.598
Longitude	E8 17.194	E8 16.770	E8 16.515	E8 20.165	E8 19.037	E8 18.721	E8 20.220	E8 22.063
Altitude, min. (masl.)	229	228	231	173	255	228	191	222
Altitude, max. (masl.)	245	320	293	360	316	464	464	243
Catchment area, CA (km ²)	0,23	2,63	0,86	1,23	1,09	2,87	6,86	0,13
Lake area, LA (km ²)	0,06	0,15	0,07	0,89	0,07	0,02	0,02	0,01
Lake area, LA:CA (%)	24,5	5,7	7,8	72,4	6,6	0,8	0,3	7,0
Maximum depth (m)	6	13	3	15	3	10	7	6
Lake volum (1000 m ³)	109	648	72	4573	77	75	46	19
Draining ratio, CA:LA	4,09	17,59	12,74	1,38	15,18	121,61	334,63	14,29
Residence time (yr)	0,40	0,21	0,07	3,18	0,06	0,02	0,01	0,12
Residence time (days)	146,14	75,94	25,94	1160,92	21,68	8,29	2,11	44,60
pH	4,77	4,92	5,29	4,89	5,79	5,29	5,43	5,30
TOC (mg C/l)	4,91	5,10	4,10	3,54	4,88	5,52	6,98	9,16
Annual precipitation (mm)	1182	1184	1178	1169	1183	1183	1152	1184
Summer precipitation (mm)	483	484	482	482	483	481	482	487
Winter precipitation (mm)	700	700	695	687	700	666	670	697
Annual discharge (mm)	746	753	731	745	802	806	760	781
Average annual discharge (l s ⁻¹ km ⁻²)	23,6	23,9	23,2	23,6	25,4	25,5	24,1	24,8
Normal low discharge (l s ⁻¹ km ⁻²)	0,0	0,5	0,5	0,6	0,4	0,3	0,3	0,0
Evapotranspiration (mm)	436	431	447	424	381	340	392	403
Evapotranspiration (%)	36,9	36,4	37,9	36,2	32,2	29,7	34,0	34,0
Average annual temperature (°C)	5,0	4,9	4,9	4,9	5,0	4,7	4,8	5,2
Summer temperature (°C)	12,0	11,9	11,9	11,8	12,0	11,6	11,8	12,2
Winter temperature (°C)	0,0	-0,1	-0,1	-0,1	0,1	-0,3	-0,3	0,2
Agricultural area (%)	0,0	0,0	0,0	0,0	0,0	1,3	2,0	5,2
Bog (%)	29,8	22,0	10,7	7,8	11,8	7,8	13,3	8,6
Lake (%)	26,8	12,4	11,9	12,5	8,1	3,0	1,8	15,7
Forest (%)	37,5	61,0	70,4	78,2	79,3	85,4	81,7	62,4
Naked mountain (%)	0,0	0,0	0,0	0,0	0,0	0,0	0,0	0,0
Urban area (%)	0,0	0,0	0,0	0,0	0,0	0,0	0,0	0,0
Burnt (%)	≈ 100 %	≈ 100 %	≈ 100 %	≈ 90 %	≈ 100 %	0 %	0 %	0 %
Logged after the fire	No	No	Partially	Extensively	No	No	No	No

In advance of sediment sampling, available information associated with the actual lakes, did not reveal influence by silviculture or land-use to any extent, but the three control lakes are slightly affected by agriculture, and Melestjenn_{con} has periodically been impacted by road salting (NaCl) during icy winter conditions. Retrospectively it became apparent that in September 2009, powdered limestone was unexpectedly dumped into a stream entering Svarttjenn_{con}, with significant effects on pH, Ca²⁺ and alkalinity (Lydersen *et al.* 2014). Moreover, extensive PWF logging were conducted in the catchment of Rasvassvatn (Høgberget 2010), and to some degree in the catchments of Grunnetjenn and Heitjenn as well (Lydersen *et al.* 2014).

Additional information on PWF effects on lake chemistry is reported in Høgberget (2010) and Lydersen *et al.* (2014), on fish in Høgberget and Kleiven (2013) and a general description of Tovdalvassdraget, including flora, fauna, liming history etc., can be found in Weideborg (2010).

4.2 Sediment sampling and material

Water column concentrations of contaminants are often temporal and spatial diverged, which is a challenge for representative sampling. Sediments, on the other hand, are more stable environmental compartments that integrate and preserve contaminants over time (Karbassi, Nabi-Bindhendi & Bayati 2005). Even low concentration levels in the water column can accumulate to considerable concentrations in sediments (Okafor & Opuene 2007), focusing in the deeper parts of the lake; the accumulation zone (Likens & Davis 1975).

Using a boat, one sediment core from the accumulation zone of each of the nine lakes (ch. 4.1.2) were retrieved (7th – 8th of June 2010) with a modified "Kajak-Brinkhurst gravity corer" (Mudroch & Azcue 1995) having exchangeable tubes. The applied tube had an inner diameter of 8.3 cm with walls sharpened on a lathe to approximately 2 mm of thickness in the lower region, which contributes to smooth sediment penetration in soft sediments, leaving surface sediments undisturbed by sampling.

To prevent loss of surface sediment ("blow-off") and compaction ("shortening") of the sediment core, the sediment fetcher was attached to a rope, gently lowered by hand to the lake bottom, and then tightly controlled submerged into the sediment (Blomqvist 1991). On the rise, when the fetcher approached the water surface, the tube was corked at the bottom and top so that the entire tube remained filled with sediment and overlying water. The method prevents mixing of surface sediment. The overlying water was then removed with a siphon (Rognerud *et al.* 2008).

Sediment cores were visually judged during fieldwork. Only cores with apparently undisturbed sediment-water interfaces and a uniform mixture of fine particles, have been used for this study. To minimize disturbance of the flocculent surface sediments, the cores were immediately after retrieval extruded and sectioned in field (Rognerud *et al.* 2000).

The procedure described provides representativeness when sampling short (<30 cm) lake sediment cores (Stephenseon, et al., 1996).

Each of the nine sediment cores were horizontally sectioned in four 1.0 cm thick vertical intervals (depth 0-1 cm [categorized as 0.5 cm]; 1-2 cm [categorized as 1.5 cm]; 2-3 cm [categorized as 2.5 cm]; 3-4 cm [categorized as 3.5 cm]) from the top, plus a 1.0 cm thick pre-industrial reference layer at approximately 33.0 ± 11.5 cm (categorized as

33.0 cm) depth for seven of the cores, i.e. Hundsvatn (44-45 cm); Heitjenn (42-43 cm); Rasvassvatn (35-36 cm); Øyvatn (33-34 cm); Jordtjenn_{con} (21-22 cm); Svarttjenn_{con} (36-37 cm) and Melestjenn_{con} (36-37 cm). The upper outtakes were split in two for both metal and PAH analyses, respectively. All samples were placed separately in small, plastic cups for metal analyses (nine cores times four depth intervals, plus seven pre-industrial reference layers) and glowed glass containers for PAH analyses (nine cores times four depth intervals), labelled and stored cool and dark (Rognerud *et al.* 2008). Coordinates of the sampled lakes are found in table 1. Weather data during sampling are appended in table 13 (Tables and figures).

4.2.1 Material

As Heitjenn is omitted from the analysis (cf. below), the data matrix relies on eight separate sediment cores (one from each of the investigated lakes) sectioned at four depth intervals (ch. 4.2) and split in two for both metal and PAH analyses.

In addition, samples from the deeper (depth 33.0 cm) section of the sediment cores were obtained from six of the lakes (i.e. Hundsvatn, Rasvassvatn, Øyvatn, Jordtjenn_{con}, Svarttjenn_{con} and Melestjenn_{con}). These six outtakes were used for assessing pre-industrial reference values of metals.

Thus, the applied number of samples for statistical analyses sum to 38 (eight lakes times four depths + six reference depths) for metals and 32 (eight lakes times four depths) for PAHs, a total of 70 sediment core outtakes.

Exclusion of Heitjenn

The headwater lake Heitjenn is a small and very shallow (depth <3.0 m) lake located on top of a hill, draining to Grunnetjenn. With flat surrounding topography, only a minor catchment (limited runoff provides little terrestrial inflow of PWF material), few surrounding trees and little aquatic vegetation, Heitjenn proves to be wind exposed. Such conditions indicate total mixing of both water masses and the upper part of lake bottom sediments (Herb & Stefan 2005), questioning the suitability of Heitjenn's sediments as PWF impact records.

Heitjenn is at risk of giving an unrepresentative picture of changes in metal and PAH loadings between sediment depths, hence omitted from further statistical analyses.

With Heitjenn being excluded, the total numbers of lakes investigated are eight (five burnt lakes plus three control lakes).

Being shallow mono-/polymictic lakes, Grunnetjenn and Øyvavn share some of Heitjenn's characteristics, which should be considered in the further analysis. Compared to Heitjenn, the two lakes seem less wind exposed due to topography and remaining PWF forest stands (burnt and unburnt). Also, lake morphometrics (e.g. catchment area and lake volume) differ in comparison to Heitjenn. In conclusion, it seems rational to include both Grunnetjenn and Øyvavn in the data matrix.

Explorative pre-analyses of metal and $\Sigma\text{PAH}_{\text{EPA16+2}}$ levels in lake bottom sediments reveal only minor concentration changes throughout the sediment column in Heitjenn (figure 26, Tables and figures), unlike the other lake sediments. This underpins the exclusion of Heitjenn and inclusion of Grunnetjenn and Øyvavn.

Manganese (Mn) and Iron (Fe)

In southern Norway sediment concentrations of manganese (Mn) and iron (Fe) originate from local geochemical sources. Mn and Fe are redox sensitive elements known for their metal complexing potential. A redox-driven migration of Mn and Fe across the sediment-water interface may occur if sediment surfaces become anoxic (reductive conditions dissolve Mn and Fe), for instance during stagnation in thermally stratified lakes.

Several metals (Co, Ni, Cu, Zn, Cd, Pb etc.) do not undergo redox reactions themselves, but are associated to hydrous oxides of Mn and Fe dissolved in anaerobic environments. Adsorbed to Mn-/Fe-(hydr)oxides, metals are transported through the sediment column as Mn and Fe migrate upward and diffuse into the hypolimnion. In the aqueous phase, Mn and Fe oxidize and precipitate, and the adsorbed metals coprecipitate.

Studies *in situ* have shown that this does not occur to any substantial extent in forest lakes in areas of southern Norway (e.g. Mykland) that have been subjected to acidification, due to rapid complex formation in the sediment when oxides are reduced.

If Fe diffuses out of the sediment under anoxic conditions at the sediment surface, metals like Co, Ni, Cu, Zn, Cd, Pb etc. are already effectively bound to other complexes and are virtually non-mobile in the sediment. Even at acidified or anaerobic conditions there are complexing agents enough to keep metals immobile (Rognerud, Fjeld & Løvik 1999; Rognerud *et al.* 2008).

Since the vertical migration of Mn/Fe-(hydr)oxides could cause a false signal of increasing PWF deposits of these two elements and probably also some disturbance to the data, and because Mn/Fe hardly carry any of the metals in scope of this study, Mn and Fe are not discussed further (measured concentration levels in sediments in table 4 (ch. 5.3). An exception exists when metal correlations are analysed. Because Fe mainly is of local geochemical origin (Rognerud, Fjeld & Løvik 1999) it is of interest to test whether any of the metals correlate (table 19 and 20, Tables and figures) to Fe in terms of source apportionment.

Exclusion of PER

The origin of PER in sediments is a matter of continuous discussion, and its formation mechanisms remain uncertain (Grimalt *et al.* 2004; Bertrand *et al.* 2013). Generally, it is believed that PER is formed *in situ* from precursor materials (Fan *et al.* 2011; van Drooge *et al.* 2011; Booij, Arifin & Purbonegoro 2012). Due to the possible *in situ* formation of PER and the continuing modelling debate, PER is omitted from the data matrix.

An exclusion of PER is supported by statistical explorative pre-analyses which find no correlations ($-0.09 < r < 0.28$) between PER and the other PAHs (figure 20, ch. 5.4.6). Lack of correlations correspond to an assumption that PER originate from a source not related to the other PAHs investigated (Budzinski *et al.* 1997). Further, high and increasing concentrations of PER with sediment depth in several of the lakes, suggest biogenic input (Budzinski *et al.* 1997). Biogenic PAHs are beyond the focus of this paper. With PER being excluded from further analyses, the total numbers of PAHs (Σ PAH) are 18, denoted Σ PAH_{EPA16+2}.

Depth section 2.5 cm omitted from illustrations

Within the pre-fire industrial sediment section (depth range: 3.5 – 1.5 cm) there is a rather pronounced metal concentration decline at 2.5 cm (intermediate depth) in some lakes (i.e. Rasvassvatn, Jordtjenn_{con}, Svarttjenn_{con}). Since intermediate fluxes are not in the scope of this paper, the 2.5 cm depth segment is omitted from sediment profile illustrations to ease interpretation and picture a more consistent metal concentration progress through time.

In all other analysis (PCA, clustering etc.) depth section 2.5 cm is included. (e.g. figure 9 in ch. 5.3.4, and figure 18 in ch. 5.4.4).

4.3 Sample preparations and chemical analyses

Radiometric dating of sediments has been performed at the Gamma Dating Centre, Institute of Geography, University of Copenhagen (Appendix 1). All other non-statistical analytical procedures were performed at The Norwegian Institute for Water Research (NIVA) accredited laboratory in Oslo. Protocol descriptions are presented on the basis of two NIVA-reports on metal and PAH contamination of freshwater lake sediment in Norway (Rognerud *et al.* 2007; Rognerud *et al.* 2008).

4.3.1 Radiometric dating of sediments using ^{210}Pb and ^{137}Cs

A sediment section will typically represent sediments that have been deposited over a period of time. Accurate sediment timelines are of crucial importance when interpreting lacustrine sediments as records of pollution history. One of the most essential methods in establishing such chronologies is by radiometric techniques measuring the decay of radioactive isotopes. In environmental science measuring the decay of lead radioisotope ^{210}Pb has been widely used for this purpose (Appleby 2001).

The decay, or (radio)activity of ^{210}Pb , is determined by counting the gamma (γ) photons ^{210}Pb radiates, denoted Bq kg^{-1} (Smol 2009). Such activity measurements enable age specification at the limits of each sediment sample slice. In order to generate a sediment chronology, ^{210}Pb activity is determined at several depths intervals (Mabit *et al.* 2014).

^{210}Pb is a natural product of the ^{238}U (uranium) decay series (figure 2). The radioactive half-life ($t_{1/2}$) of ^{238}U to ^{226}Ra (radium) is 4.51×10^9 yr., while the $t_{1/2}$ of ^{226}Ra to ^{222}Rn (radon) is 1602 years. ^{222}Rn is a noble gas and the parent isotope of ^{210}Pb (i.e. ^{210}Pb is derived from ^{226}Ra via ^{222}Rn).

^{226}Ra occurs naturally in rocks and soils. Theoretically, ^{226}Ra should be in equilibrium with ^{210}Pb in geological material but owing to the diffusion of gaseous ^{222}Rn to air, disequilibrium of ^{226}Ra to ^{210}Pb occurs since concentrations of ^{222}Rn , which generates ^{210}Pb , is reduced.

In lake bed sediments, the total ^{210}Pb ($^{210}\text{Pb}_{\text{tot}}$) activity consists of two components; one atmospheric fallout component of ^{210}Pb in excess of the ^{226}Ra concentrations at site, termed *excess ^{210}Pb* ($^{210}\text{Pb}_{\text{ex}}$), and one ^{210}Pb component derived from *in situ* decay of ^{226}Ra , termed *supported ^{210}Pb* ($^{210}\text{Pb}_{\text{sup}}$). $^{210}\text{Pb}_{\text{sup}}$ is in equilibrium with ^{226}Ra

concentrations at site. The basis of radiometric tracer applications is provided by the rate of decline in $^{210}\text{Pb}_{\text{ex}}$ activity (or γ -radiation) with depth (Mabit *et al.* 2014).

A fraction of the $^{210}\text{Pb}_{\text{ex}}$ isotopes deposited on lake surfaces and its catchments is transported to the lake bed and integrated in the sediment record. As sediments successively become buried by more recent deposits, the $^{210}\text{Pb}_{\text{ex}}$ activity acts as a natural clock, recording the time since deposition on the bed of the lake (Appleby 2008).

Since environmental conditions (e.g. mixing of surficial sediments by biological or physical processes, or conditions that alter the pattern of sediment focusing and cause variations in the ^{210}Pb supply) could influencing on the reliability of ^{210}Pb radiometric dating, techniques that validate the results, using independent chronological evidence, are of importance. A widely applied independent dating technique uses sediment records of the artificial radioisotope ^{137}Cs (cesium) (Appleby 2008).

Atmospheric fallout of ^{137}Cs is a valuable soil redistribution tracer, introduced into the atmosphere as result of nuclear weapon testing (from the beginning in 1954 to its peak in 1963, shortly after the test-ban treaty) and the Chernobyl nuclear power plant accident in 1986. Where there is a good qualitative record of atmospheric fallout, sediments corresponding to these events can be identified, and thus dated. Basic principles of radiometric technique and independent dating using ^{137}Cs “validators”, are described in Appleby (2001).

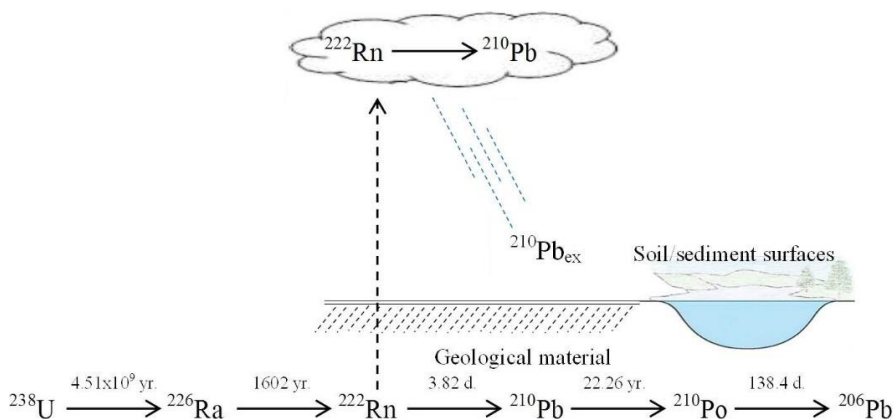


Figure 2 ^{238}U decay series concerned with production of ^{210}Pb . Illustration shows the principal radionuclides (without sub-chains) and their radioactive half-lives. $^{210}\text{Pb}_{\text{ex}}$ activity = $^{210}\text{Pb}_{\text{tot}}$ activity – ^{226}Ra activity (which equals the $^{210}\text{Pb}_{\text{sup}}$) (Appleby 2001; Mabit *et al.* 2014). Po is the chemical element polonium (atomic number 84).

In April 2011, three sediment cores (Hundsvatn, Rasvassvatn and Jordtjenn_{con}) were dated by analysing the activity of ²¹⁰Pb, ²²⁶Ra and ¹³⁷Cs via gamma spectrometry¹ at the Gamma Dating Centre, Institute of Geography, University of Copenhagen. The measurements were carried out on a Canberra low-background germanium (Ge) detector². ²¹⁰Pb was measured via its γ -peak at 46.5 keV, ²²⁶Ra via its “granddaughter” ²¹⁴Pb which peaks at 295 and 352 keV, and ¹³⁷Cs via its peak at 661 keV.

CRS-modelling³ has been applied on the profiles using a modified method (Appleby 2001) where the activity below 14 cm (Rasvassvatn; below 15 cm) is calculated (individually for each of the three sediment cores dated) on the basis of the regression (separate regressions for each report) shown as figure 2 in each of the three reports appended (Appendix 1) on dating of sediments (Gamma Dating Centre Copenhagen 2011).

4.3.2 Calculating sediment loss on ignition (LOI)

Sediments’ ability to accumulate contaminants is governed by sediment physicochemical properties. This applies to the content of sediment organic matter (OM) and grain size in the inorganic fraction. The possibility that metals and organic contaminants (e.g. PAHs) will accumulate is considerably greater in sediments with high OM content and small inorganic particulates (e.g. silt and clay), than in sediments with low OM content and a coarse fractions of inorganic material (e.g. sand and gravel) (Løvik 2010).

Calculations of (weight) loss on ignition (LOI) estimates the percentage proportion of OM in a sediment sample, given in dry weight (DW; percentages [%] of dry matter [DM]). In sediment samples with LOI >5 %, it is likely that organic carbon (OC) analogues approximately 50 % of the organic matter ($OC_{sed} \approx \frac{LOI}{2}$). If LOI >10 %, small variations in LOI will not affect the metal and PAH analysis to any noticeable degree.

Norwegian Pollution Control Authority’s national program for pollution monitoring (Norwegian National lake survey [NLS] 2004 – 2006) of sediment contaminants (i.e. metals, PAH and PCB), report high LOI values in surface (0.0 – 0.5 cm) and sub-surface (0.5 – 1.0 cm) sediments in Norway (median values \approx 33.0 %). This resembles an OC content of 16.5 %. Sediments of forest freshwater lakes in southern Norway have in general high OC content (figure 3, Rognerud *et al.* 2008).

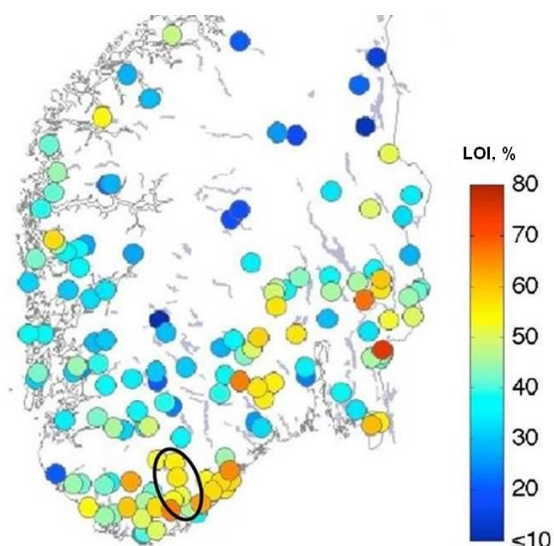


Figure 3 Figure of organic carbon content (as LOI) in lakes in Southern Norway (Rognerud *et al.* 2008). The area surrounding Mykland is circled black.

To calculate LOI, an outtake of every sediment sample was dried at 60 °C, homogenized (individually) and separately sieved to obtain the <70 µm fraction analysed for LOI. A new outtake of each dried, sieved and homogenized material was done, singly weighed (dry weight; DW) and burnt (“ignited”) at 520 °C. The remaining matter, residue on ignition (ROI), was also singly weighed for all outtakes (Rognerud *et al.* 2008).

LOI is the organic matter that burns off during ignition. Its weight was obtained finding the difference (Δ weight) between DW and ROI ($LOI = DW - ROI$).

When ROI was known, LOI in percentages was calculated by individually subtracting each samples’ ROI divided by 10, from hundred ($LOI = 100 - \frac{ROI}{10}$).

4.3.3 Metals in sediments; sample pre-treatment and analyses

Sediment concentrations of nine (i.e. V, Cr, Co, Ni, Cu, Zn, Cd, Hg, Pb) metals are analysed. All concentrations of metals in lake sediments are given as dry weight (DW), denoted $\mu\text{g g}^{-1}$.

Pre-treatment

From each sediment sample used for LOI calculations, an 0.5 g outtake of ROI was homogenized and digested in a Teflon tube with nitric acid (HNO_3), and then autoclaved at 120 °C and 2 atm. for 30 minutes, according to Norwegian Standards (NS) 4770:1994 (Standards-Norway 1994).

This is the most frequently used protocol to digest sediment samples for conventional metal analyses as it limits the contribution of mineral particles from the local bedrock, thus provide a better description of the anthropogenic metal contribution in sediments (Rognerud *et al.* 2007; Rognerud *et al.* 2008).

HR-ICP-MS analyses

Analyses of metals in sediments were performed using a High Resolution Inductively Coupled Plasma Mass Spectrometry (HR-ICP-MS). In HR-ICP-MS a high resolution (HR) mass spectrometer (MS) with an inductively coupled plasma (ICP) source (Thermo Finnigan Element 2) is used to discriminate ions that interfere in traditional ICP-MS. The HR-ICP-MS is considered the most sensitive among ICP-MS-techniques, with detection limits corresponding to metal concentrations in sediments in the range of ng/g. A further and more detailed description of NIVAs analytical methods on metals are found in Rognerud *et al.* (2008).

Quality control

To control the quality of all measurements, a variety of certified reference materials are used. This includes a NIVA-developed internal sediment sample from Bjørvika, Oslo harbour (Norway), as well as *Marine Sediment Reference Materials for Trace Metals and other Constituents*, HISS-1 and MESS-3, from the National Research Council Canada, Institute for National Measurement Standards' (NRC-INMS 1997; NRC-INMS 2000).

Regular tests of sediment reference samples are taken at NIVA. NIVA also participate 2 – 4 times per year in the internationally recognized intercalibration program for metals in sediments, *Quasimeme*, almost always achieving results within the accepted uncertainty for measurements of the priority metals (Rognerud, et al., 2007).

Random comparisons with ICP-AES (Inductively Coupled Plasma - Atomic Emission Spectrometry) are also conducted periodically. These data provide a good indication of whether the method of measurement using HR-ICP-MS is reliable. Such a comparison, performed on analyses of sediments from Oslo harbour, has shown that the deviations are generally below 10% for those metals where the concentration is high enough to provide good comparisons.

4.3.4 PAHs in sediments; sample pre-treatment and analyses

Sediment concentrations of 18 (i.e. NAP, ACNLE, ACNE, FLE, PA, ANT, DBTHI, FLU, PYR, BaA, CHR, BbjF, BkF, BaP, BeP, BghiP, IcdP, DBa3A) PAH species are analysed. All concentrations of PAHs in lake sediments are given as dry weight (DW), denoted $\mu\text{g kg}^{-1}$ DM.

Pre-treatment

Outtakes (8-12 g) of wet material from each of the initial sediment samples were individually mixed with HydroMatrixTM, supplied with deuterated internal standards, and then extracted by Accelerated Solvent Extraction (ASE) technique. The extraction was done at 100 °C and 2000 psi using a mixture of dichloromethane (CH_2Cl_2) and cyclohexane (C_6H_{12}). With the use of gel permeation chromatography (GPC), the extract was concentrated and cleaned (Rognerud *et al.* 2007).

GC/MSD analyses and quality control

Analyses were done with a Gas Chromatograph/Mass Selective Detector (GC/MSD). In the GC/MSD each single compound's molecule ion is registered within a certain time interval and quantified using both internal and external standards. Along with each extraction series, a certified reference material (NIST SRM 1944) was analysed as part of quality control (Rognerud *et al.* 2007).

4.4 Statistical analyses

To uncover and illustrate potential patterns, influences and similarities / dissimilarities among multivariate data, the statistical methods principal components analysis (PCA), correlation analysis (CA) and cluster analysis, are considered effective tools. These approaches have been used successfully in many studies of metal and PAH contamination of sediments (Guo *et al.* 2013; Wu *et al.* 2014). Multivariate statistical techniques reduce the dimensionality of a data set, while the relationships that are present in the original data are attempted preserved.

The statistical analyses are driven by the computer programs JMP[®] 13.2.1 (SAS Institute Inc 2016), which also has been used to generate sediment depth profiles of LOI and measured metal and PAH concentrations. Such profiles serve as a useful tool to illustrate variations in concentration levels through time, and to detect possible resemblances between sediment organic matter content, metals and PAHs.

The basic principles of PCA and CA are described herein as presented in the latest national lake survey (i.e. NLS 3, 2004 – 2006) on freshwater sediment pollution of metals and PAHs in Norway (Rognerud *et al.* 2008).

Outlier analysis

Observations of high influence on summary statistics might be considered outliers if the effect of removing them from the dataset is disproportionately large.

A Jackknife Distance (JD) outlier analysis (significance level $\alpha = 0.05$) reveals data points that may have a diverging character and / or hold extra influence on the analysis' results. The JD outlier analysis measures distances with respect to the correlation (i.e. Pearson's product moment correlation coefficients) structure and do not include the observation itself.

A data point may be considered an outlier because it positions outside the density ellipse on correlations, and by that violating the correlation structure, rather than because it is an outlier in any of the coordinate directions (SAS Institute 2016).

Samples positioning above the Upper Control Limit (UCL; blue dotted line) in the JD outlier plot are regarded outliers and should be subject to further consideration as they can be of high influence.

4.4.1 Principal component analyses (PCA)

The purpose of a PCA is to reduce the dimensionality of a data set by representing the main trend in the data as complete as possible by using as few components as possible. These components are linear combinations of the original variables. The first principal component (PC 1) is the linear combination of the original, standardized variables with maximum variance (i.e. maximum eigenvalue in linear algebra). The next principal component (PC 2) has the second highest eigenvalue and is orthogonal (i.e. uncorrelated) to the first (PC 1) etc. The contributions of the original variables to the different principal components are given by their eigenvectors. These coefficients are used in a linear combination of the original variables to produce the principal components.

The results of a PCA can be displayed graphically in a *biplot* (a biplot combines a score plot and a loading plot in one figure [e.g. figure 23, ch. 5.5]). All eigenvectors are plotted as arrows in a coordinate diagram, with the principal components (PC 1, PC 2,

PC 3,... [...], PC N etc.) as axes. Scores of the individual observations are plotted as points in the same diagram. Each arrow's length describes the vectors relative importance (loading), and the angle between them shows how correlated they are. Closely correlated variables point in the same direction, while negatively correlated variables point in opposite directions. Non-correlated variables are perpendicular (Rognerud *et al.* 2007; Rognerud *et al.* 2008).

4.4.2 Correlations

Probable relationships, or correlations, between individual entities (e.g. metal or PAH) in a data matrix can be calculated pairwise, and variables liable to covary can be identified. The degree of correlations is assigned coefficients between -1 and 1 (i.e. correlation coefficient; r), where 0 is no correlation (i.e. no linear relationship, often termed *the null hypothesis*), and -1 or 1 indicates a 100 % negative or positive correlation, respectively (i.e. there is a perfect linear relationship). The stronger the correlation, the farther r diverge from zero (i.e. r measure the strength of a correlation by approaching -1 or 1). In other words, r determines the degree to which a variable will change as consequence of alterations in the other, associated variable.

Correlations are considered statistically significant if r is sufficiently large or sufficiently small (i.e. negative correlation) with a probability, ρ , equal to, or less than, 0.05 ($\rho \leq 0.05$). This means there is a 5 % risk, or less, that a result occurs by chance (Wheater & Cook 2000; Esbensen *et al.* 2001). The significance of r can either be calculated ($r \geq \frac{2}{\sqrt{n}}$, where n is the total number of samples, prerequisite: $n \geq 5$ (Walsh 1998)), or evaluated by consulting tables listing threshold values of r at different levels of significance (i.e. α , usually set to 0.05 as the ρ) and sample sizes (n), alternatively accessing online databases (e.g. (Soper 2018)). A significant correlation does not mean that causal relationships exist between variables (Wheater & Cook 2000; Esbensen *et al.* 2001).

Threshold values of r for significant correlations ($\alpha = 0.05$, thus $\rho \leq 0.05$) at different sample sizes (n) are found in table 14 (Tables and figures). r values are calculated according to Walsh (1998), hence, considered conservative.

4.4.3 Cluster analyses (CA)

The purpose of a cluster analyses is to organize multivariate observations (entities with multiple measured characteristics) into groups in a way that “members” within the various groups have the most properties in common, while groups diverge from one another. This rests upon the phenomenon that data is not likely to be distributed evenly in a multi-dimensional space, but rather gather in groups with similar locality, called “clusters”. No *á priori* hypotheses regarding the data are put forward using such method. Consequently, there is no need for hypothesis testing.

Cluster analyses detect structures in the data without explaining why they exist. Thus, cluster analyses provide a useful starting point for further exploratory examinations of the data.

The results of a cluster analyses are displayed graphically in a *dendrogram*. This is a hierarchically structured tree-diagram showing all individual observations organized in a way that when combined with other observations, they form clusters.

The cluster analyses technique used is called *hierarchical clustering*, a robust method insensitive to very deviant observations (statistical “outliers”) (Rognerud *et al.* 2007; Rognerud *et al.* 2008).

4.4.4 Parent PAH isomer ratios (IR)

Relative abundance of PAHs is a frequently used diagnostic tool designating PAH origin sources (Dickhut *et al.* 2000; Sprovieri *et al.* 2007; Galarneau 2008; Leung, Cheung & Wong 2013). Every origin of PAH mixtures demonstrates specific characteristics (“fingerprint signatures”) dependent on the process producing the PAHs. This feature makes it possible to distinguish certain PAHs from each other, offering them as possible environmental tracers of PAH emission sources (Liu *et al.* 2009).

Explorative analysis of the sampled lake sediments from Mykland are not able to identify such “fingerprints” because of high degree of co-variation between individual PAH compounds (figure 29, Tables and figures). Thus, source identification with the use of molecular composition is hardly possible (Rognerud, Fjeld & Løvik 1997). Consequently, no source identification using isomer ratios are presented herein.

4.4.5 Transformation of data

There are some aspects to the data that should be commented, as these at least have potential to influence on the results of the analysis.

LOI values are sediment specific and represent the content of organic matter in sediments at a given depth the moment the sample is retrieved, just like the values of metal and PAH concentrations. This is not valid for pH and total organic carbon (TOC), which are dynamic water quality parameters. pH and TOC are measured at an unspecified time differing from that of the sediment sampling campaign and is given as static numbers. Measured pH and TOC values vary only across lakes, not vertically with sediment depths. Residence time (time from a substance enters till it flows out of a lake) is like pH and TOC a static measure related to features of the water masses, varying only across lakes, not with sediment depths (table 1, ch. 4.1.2).

Furthermore, LOI is a percentage measure that sum to 100 (cf. *ArcSin square root transformation of proportional data* below).

To depict concentration fluctuations of magnitude (e.g. figure 9 in ch. 5.3.4 and figure 18 in ch. 5.4.4), there is a need to reduce spread of data. Thus, concentration values are logged (natural logarithm, ln) (Emerson & Soto 1982).

ArcSin square root transformation of proportional data

Environmental data provided by field investigations are often given as proportions, or percentages of a totality (e.g. amount of organic matter in lake bed sediments). If a considerable quantity of observations in a data series hold values outside the range of 30 – 70 %, it is common practice to normalize the data. One of the recommended methods is the ArcSin Square Root (ASSR) transformation; $\sin^{-1}(\sqrt{\frac{p}{100}})$. Note that the percentage data, p , is converted to decimal numbers ($\frac{p}{100}$) in the ASSR transformation.

The primarily effect of an ASSR transformation is to pull the distribution of data points out at the ends of the inverted *sigmoid curve*. Such expansion of the scale empowers small alterations in p (e.g. going from 0.94 to 0.96) to influence more strongly on the ASSR scale.

However, intermediate values of the original percentage data (p) share a close to linear relationship to ASSR. Thus, the ASSR transformation is not effective when the majority of observations are found *within* the range of 0.30 – 0.70. Consequently, if the majority

of data points fall in the 0.30 – 0.70 range, ASSR transformation is not required (Lacey 2012; Clewer & Scarisbrick 2013).

Log-ratio (LR); relative abundance of an entity expressed in relation to a total

In compositional data sets, where all entity values in a sample series sum to a unit value (e.g. 100 % or 1), loadings of single entities to the total, cannot vary independently. As the proportion of one entity increase, the proportion of the remaining entities correspondingly decline. This phenomenon is called constant-sum constraint (CSC), a mathematical property embedded within any compositional data set expressed as fractions of a given sum. As CSC induce correlations and potentially conceal true relationships among variables, CSC violate basic assumptions upon which standard statistical analyses are designed.

It should be noted that the CSC does not disappear if one or more of the original variables are removed from the initial data set. Although the sample series of such modified data not sum to a unit value by principle, it still sums to the unit value withdrawn the omitted variable(s).

The effects of CSC on correlation matrices can be diminished if raw percentage data are expressed as logarithms (ln) of ratios (“proportions”), where the numerator is the individual sample entities’ (X_1, X_2, X_3, \dots etc.) percentage (%) contribution to the total data series, and the denominator is the geometric mean (GM) of these percentages. In accordance with this, a log-ratio transformed (LR) sample value (S) can be expressed as

$$S_{LR} = \ln\left(\frac{\%X_1}{GM}\right),$$

where the GM can be calculated as

$$GM = \sqrt[n]{\%X_1 * \%X_2 * \dots * \%X_n},$$

and n is the number of entities in a data series.

After application of the log-ratio transformation on all entities, adding up the S_{LR} (log-ratio transformed sample value) sum to zero (i.e. $S_{LR_1} + S_{LR_2} + S_{LR_3} + \dots + S_{LR_n} = 0$). A proper interpretations of structures in compositional data sets is enabled (Kucera & Malmgren 1998).

In the cluster analyses herein, relative relationships between PAH compounds (i.e. PAH_{LR}) are used. In consequence, it has no bearing on the analyses whether

$\Sigma\text{PAH}_{\text{EPA16+2}}$ is high or low, as it is (dis)similarities between individual compounds that are important to elucidate (Kucera & Malmgren 1998; Rognerud *et al.* 2007).

Concentration levels below detection limit

The multivariate statistical methods applied (PCA, CA and cluster analyses) cannot tolerate missing data for any variables. In environmental studies, an often used method to meet this restraint simply replace values below detection limit (i.e. data with obtained values lower than the precision level under which the data were generated) with half that limit to reduce bias (Kucera & Malmgren 1998; Rognerud *et al.* 2007; Rognerud *et al.* 2008; Inengite, Oforika & Osuji 2012). With Heitjenn being excluded from further analyses (ch. 4.2.1), this is applicable only for ACNLE in Svarttjenn_{con}'s surface sediment, where $2 \mu\text{g kg}^{-1}$ is replaced by $1 \mu\text{g kg}^{-1}$.

LOI-normalization of metal and PAH concentrations in sediments

In aquatic environments, metals tend to associate with rapid settling organic particles (Rognerud *et al.* 2008; Rognerud *et al.* 2013). This is attributed to the large particulate surface and surface charge in this fraction (Horowitz 1985).

As for metals, PAHs have high affinity for organic matter (Opuene, Agbozu & Ekeh 2007; Rognerud *et al.* 2008). This is due to the hydrophobic/lipophilic nature of PAHs (Barakat *et al.* 2012).

To enable comparison of metal and PAH concentrations in various lake sediments, and to reveal sediment enrichment patterns, measured concentration values are normalized to sediment OM (i.e. LOI) content, when correlated to LOI (Kuijpers, et al., 1993; Rognerud *et al.* 2007). This normalization is done by calculating the sample's organic fraction (ch. 4.3.2) and adjust the measured concentrations according to this (LOI-normalized concentration = measured concentration divided by $\frac{\text{LOI}}{100}$ (Dean 1974; Heiri, et al., 2001; Santisteban *et al.* 2004)). The procedure is the same for metals and PAHs.

Concentrations of LOI-correlated metals and PAHs are given as LOI-normalized proportions of dry matter (DM), denoted $\mu\text{g g}^{-1}$ (metal) and $\mu\text{g kg}^{-1}$ (PAH), respectively.

4.4.6 Qualified majority - Identifying metal fluctuations with depth

Attempting to identify prevailing trends of measured metal concentration fluctuations in Mykland sediments has been a difficult task. As an attempt to solve this challenge, metal fluctuations are considered only in absolute digits; as an increase, a decline or as

unaltered, from one depth to a shallower. Minor numerical changes may represent a substantial change in percentages. For instance, a Cd concentration decline from $1.90 \mu\text{g g}^{-1}$ at depth 1.5 cm to $1.10 \mu\text{g g}^{-1}$ at depth 0.5 cm in Melestjenn_{con}, seems like a modest numerical reduction ($\div 0.80 \mu\text{g g}^{-1}$, cf. table 4 in ch. 5.3), while representing a notable reduction ($\div 42.11 \%$) in percentages (table 16, Tables and figures).

Whether metals within a lake demonstrate a concentration decline or increase is identified by using a non-statistic approach; *qualified majority*. Qualified majority (QM) is a method often used in decision making, like voting over a proposal of great significance. The threshold required to obtain QM is set in advance of voting, typically to $\frac{2}{3}$ or $\frac{3}{4}$ of all votes (e.g. §115 in the Constitution of the Kingdom of Norway). In this study the threshold value is set to $\geq \frac{3}{4}$, which is to be considered a rather strict criterion. This means that at least $\frac{3}{4}$ of the nine measured metals, regardless of which, in a single lake's sediment must either all decline or all increase from one depth to a shallower to consider that particular lake to hold a tendency of declining / increasing metal concentrations.

There is a possibility that single metals demonstrate a mutual decline / increase from one depth to a shallower across several lakes, without belonging to any lake that fulfil the $\geq \frac{3}{4}$ criteria (for metals) to be regarded a lake with declining / increasing metal concentrations. To capture such tendencies, these metal fluctuations are presented individually as metals to decline / increase across lakes. A more detailed description of the use of QM is found in Appendix 4.

5 Results

The results of this study present major spatial and temporal trends in the data set. The matrix analysed comprise quantitative data on nine metals and 18 PAHs, obtained from eight boreal forest freshwater lake sediment cores collected in southern Norway early June 2010. Five of the lakes are located within a forest area totally burnt by wildfire in June 2008. Three of the lakes serve as non-burnt, pre-fire control lakes outside the burnt forest area.

One sediment core is obtained from each of the eight investigated lakes, with four sample outtakes from every core at 1.0 cm depth intervals, labelled 0.5, 1.5, 2.5 and 3.5 cm. Each outtake is split in two for metal and PAH analysis, respectively. In addition to these 64 samples (eight lakes, times four outtakes, times two), outtakes are retrieved from the deeper section of the sediment core in six of the lakes (i.e. Hundsvatn, Rasvassvatn, Øyvatn, Jordtjenn_{con}, Svarttjenn_{con}, Melestjenn_{con}) and analysed for metals as pre-industrial references.

5.1 Dating of sediments

The year of sedimentation has been analysed on three lake bed sediment cores (i.e. Hundsvatn, Rasvassvatn and Jordtjenn_{con}) by Gamma Dating Centre, Copenhagen (Appendix 1). All three sediment cores show high surface content of $^{210}\text{Pb}_{\text{ex}}$. The chronologies of the cores are considered fairly accurate due to the tendencies of an exponential decline of $^{210}\text{Pb}_{\text{ex}}$ with depth.

The calculated flux of $^{210}\text{Pb}_{\text{ex}}$ in Rasvassvatn ($83 \text{ Bq m}^{-2} \text{ y}^{-1}$) and Jordtjenn_{con} ($72 \text{ Bq m}^{-2} \text{ y}^{-1}$) are about the same as the estimated local atmospheric supplies. Hundsvatn has a calculated flux of $^{210}\text{Pb}_{\text{ex}}$ ($42 \text{ Bq m}^{-2} \text{ y}^{-1}$), about half the estimated local atmospheric supplies (based on Appleby 2001).

The content of ^{137}Cs peaks around depth 2.0 cm. Below this depth ^{137}Cs content is generally low. Calculated chronologies of ^{137}Cs peak activity are consistent with the expected Chernobyl origin (1986) of the sampled material. The activity of ^{137}Cs at depths dated to well before these isotopes were released into nature (around the mid 1950's), suggests that the isotope is not completely immobile in these sediments (Gamma Dating Centre Copenhagen 2011. Report appended; Appendix 1).

Table 2 Sediment age (yr), year of deposition and accumulation rates ($\text{kg m}^{-2} \text{yr}^{-1}$) for lakes Hundsvatn, Rasvassvatn and Jordtjenn_{con}. All data assembled from the appended report (Appendix 1) on dating of core Hundsvatn, Rasvassvatn and Jordtjenn_{con} (Gamma Dating Centre Copenhagen 2011).

Depth (cm)	Hundsvatn					Rasvassvatn					Jordtjenn _{con}				
	Age (yr)	Error age (±yr)	Date (yr)	Acc. rate ($\text{kg m}^{-2} \text{yr}^{-1}$)	Error acc. rate ($\text{kg m}^{-2} \text{yr}^{-1}$)	Age (yr)	Error age (±yr)	Date (yr)	Acc. rate ($\text{kg m}^{-2} \text{yr}^{-1}$)	Error acc. rate ($\text{kg m}^{-2} \text{yr}^{-1}$)	Age (yr)	Error age (±yr)	Date (yr)	Acc. rate ($\text{kg m}^{-2} \text{yr}^{-1}$)	Error acc. rate ($\text{kg m}^{-2} \text{yr}^{-1}$)
0	0		2010			0		2010			0		2010		
0,5	4	1	2006	0,04	0,00	1	1	2009	0,1	0,01	4	1	2006	0,04	0,00
1,5	13	2	1997	0,04	0,00	6	1	2004	0,07	0,01	15	2	1995	0,04	0,00
2,5	27	2	1983	0,03	0,00	12	1	1998	0,06	0,01	28	2	1982	0,04	0,00
3,5	44	2	1966	0,03	0,00	18	1	1992	0,08	0,01	43	2	1967	0,05	0,01
4,5	55	3	1955	0,04	0,01	22	1	1988	0,1	0,01	55	3	1955	0,06	0,01
5,5	68	3	1942	0,03	0,00	26	1	1984	0,14	0,02	70	4	1940	0,05	0,01
6,5	79	4	1931	0,03	0,01	29	1	1981	0,16	0,03	81	4	1929	0,06	0,01
7,5	89	5	1921	0,04	0,01	32	1	1978	0,17	0,02	90	5	1920	0,07	0,01
8,5	98	6	1912	0,05	0,04	36	2	1974	0,13	0,01	103	7	1907	0,05	0,02
9,5	99	6	1911	0,38	4,06	40	2	1970	0,11	0,02	115	7	1895	0,05	0,05
10,5	106	6	1904	0,06	0,02	45	2	1965	0,12	0,02	125	8	1885	0,07	0,02
11,5	119	7	1891	0,04	0,01	51	2	1959	0,1	0,01	144	12	1866	0,04	0,02
12,5	131	10	1879	0,04	0,02	57	2	1953	0,11	0,02	159	17	1851	0,05	0,12
13,5	173	15	1837	0,01	0,01	63	2	1947	0,09	0,01	176	18	1834	0,04	0,02
14,5						71	1	1939	0,08	0,00					
33,0 ±11,5	506		1504 ^a			162		1848 ^a			269		1741 ^a		

^aCalculated

Table 2 organize accumulation rates ($\text{kg m}^{-2} \text{yr}^{-1}$), year of deposition and sediment age (yr) at depths 0.5; 1.5; 2.5; 3.5 [...], 14.5 cm and reference depths (33.0 ±11.5 cm) for lakes Hundsvatn, Rasvassvatn and Jordtjenn_{con}. All data originate from Gamma Dating Centre Copenhagen's report on dating of sediments (Appendix 1).

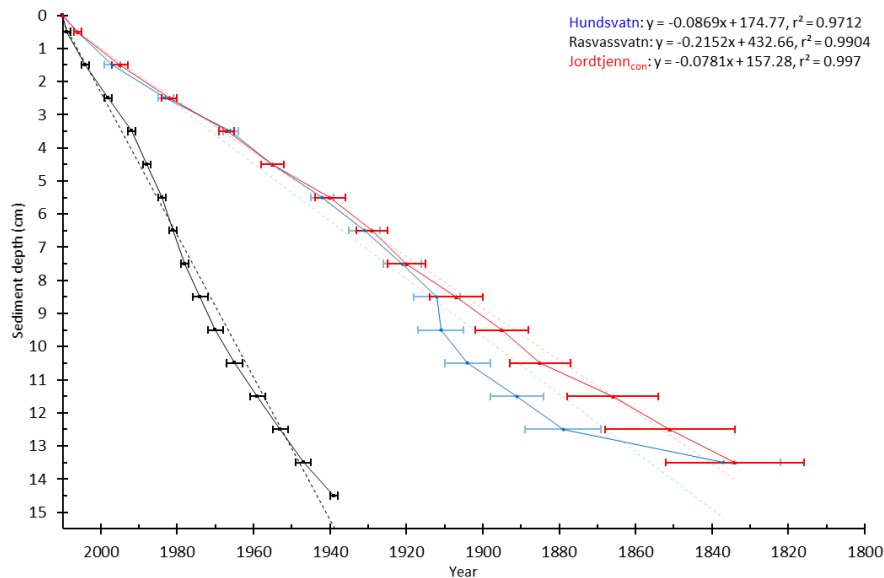


Figure 4 Graphic illustration of how sediment age (year of sedimentation) increases with increasing sediment depth (cm) in Hundsvatn, Rasvassvatn and Jordtjenn_{con}. The figure is generated on data from the appended report (Appendix 1) on dating of sediments, presented in table 2.

Based on data in table 2, figure 4 illustrates sediment age (year of sedimentation) with increasing depth (cm), while sedimentation rates (cm yr^{-1}) are graphically described in figure 5. There are four outliers (depths 9.5, 10.5, 11.5 and 12.5 cm) in Hundsvatn (figure 5). If these are excluded, $y = 0.081x$ ($r^2 = 0.99$), which is similar to Jordtjenn_{con}.

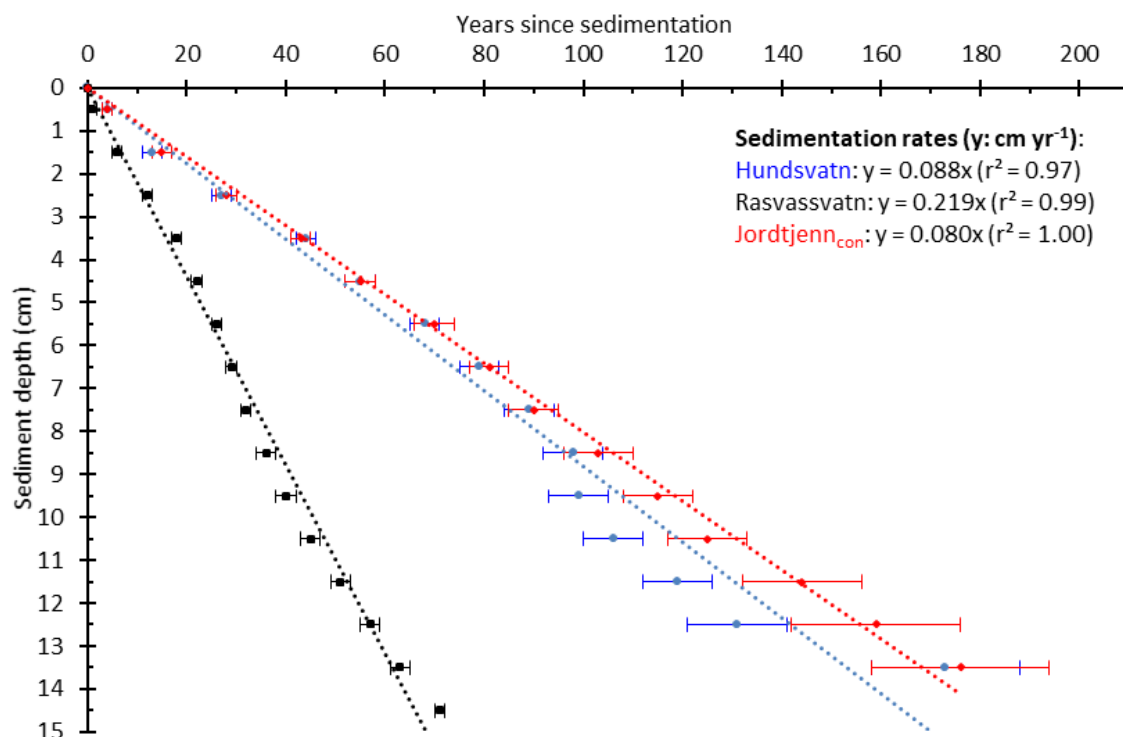


Figure 5 Sedimentation rates (cm yr^{-1}) for the lakes Hundsvatn, Rasvassvatn and Jordtjenn_{con}, generated on data from the appended report (Appendix 1) on dating of sediments, presented in table 2. Hundsvatn has four outliers (depths 9.5; 10.5; 11.5 and 12.5). $y = 0.081x$ ($r^2 = 0.99$) when the four outliers are excluded. This is similar to Jordtjenn_{con}.

5.1.1 Hundsvatn (cf. Appendix 1)

The analysis of sediment core Hundsvatn dates the sample outtake at depth 0.5 cm to year 2006 ± 1 yr. At depth 1.5 cm the sediment outtake is dated year 1997 ± 2 yr. There is no increased accumulation rate between the two depths (accumulation rate $0.04 \text{ kg m}^{-2} \text{ yr}^{-1}$ and error rate $0.00 \text{ kg m}^{-2} \text{ yr}^{-1}$ for both). According to these results, Hundsvatn's surface sediment contains pre-fire (< year 2008) matter at depth 0.5 cm (year 2006 ± 1 yr) (table 2).

Assuming a near linear (constant) age rate between the two uppermost sediment sample outtakes (depth 0.5 cm and 1.5 cm), the year of the interface between surface and subsurface (i.e. depth 1.0 cm) sediments can be calculated from the data in table 2: Due

to the slightly exponential decline of age vs. depth (figure 4), values are rounded to the highest year. This is considered a fairly conservative estimate. An exponential decay slope will give an age value closer to that of depth 0.5 cm, than to the one at depth 1.5 cm.

The formulas used to calculate the interface-date_{1.0 cm} (Bjørnes & Hovde 1973):

- Intermediate (surface/subsurface) date (*Intermediate date*_{1.0 cm}):

$$\text{Intermediate date}_{1.0 \text{ cm}} = \text{date}_{0.0 \text{ cm}} - \frac{\text{age}_{0.5 \text{ cm}} + \text{age}_{1.5 \text{ cm}}}{n}$$

n is the total number of samples (here; $n = 2$) included in the calculations.

- Standard deviation for complex results (S_R) at *Intermediate date*_{1.0 cm} ($S_{R_{1.0 \text{ cm}}}$):

$$S_{R_{1.0 \text{ cm}}} = \sqrt{\frac{SD_{0.5 \text{ cm}}^2 + SD_{1.5 \text{ cm}}^2}{n}}$$

$SD_{0.5 \text{ cm}}$ and $SD_{1.5 \text{ cm}}$ is the standard deviations (here; error age) at increasing depths (here; 0.5 cm and 1.5 cm, respectively).

$$\text{Intermediate date}_{1.0 \text{ cm (Hundsvatn)}}: 2010_{0.0 \text{ cm}} - \frac{4_{0.5 \text{ cm}} + 13_{1.5 \text{ cm}}}{2} \approx \underline{\underline{2002}}$$

$$S_{R_{1.0 \text{ cm (Hundsvatn)}}} = \sqrt{\frac{1_{0.5}^2 + 2_{1.5}^2}{2}} \approx \underline{\underline{2}}$$

$$\text{Interface date}_{1.0 \text{ cm (Hundsvatn)}} \equiv \underline{\underline{2002 \pm 2 \text{ yr.}}}$$

5.1.2 Rasvassvatn (cf. Appendix 1)

The analysis of sediment core Rasvassvatn dates the sample outtake at depth 0.5 cm to year 2009 ± 1 yr. At depth 1.5 cm the sediment outtake is dated year 2004 ± 1 yr. The accumulation rate increases from subsurface (0.07 kg m⁻² yr⁻¹) to surface (0.10 kg m⁻² yr⁻¹), both with an error rate of 0,01 kg m⁻² yr⁻¹. According to these results, Rasvassvatn's surface sediment sample contains predominantly post-fire (\geq year 2008) matter at depth 0.5 cm (year 2009 ± 1 yr) (table 2).

Assuming a near constant age rate, although not as confident as for Hundsvatn, between the two uppermost sediment samples, there may be a fair amount of pre-fire (< year 2008) matter in Rasvassvatn's surface sediment too. The year of the interface between

surface and subsurface (i.e. depth 1.0 cm) in Rasvassvatn can be calculated as described for Hundsvatn (ch. 5.1.1) from the data in table 2:

$$\text{Intermediate date}_{1.0 \text{ cm (Rasvassvatn)}}: 2010_{0.0 \text{ cm}} - \frac{1_{0.5 \text{ cm}} + 6_{1.5 \text{ cm}}}{2} \approx \underline{2007}$$

$$S_{R_{1.0 \text{ cm (Rasvassvatn)}}} = \sqrt{\frac{1_{0.5}^2 + 1_{1.5}^2}{2}} = \underline{1}$$

$$\text{Interface date}_{1.0 \text{ cm (Rasvassvatn)}} \equiv \underline{2007 \pm 1 \text{ yr.}}$$

5.1.3 Jordtjenn_{con} (cf. Appendix 1)

The analysis of sediment core Jordtjenn_{con} dates the sample outtake at depth 0.5 cm to year 2006 ±1 yr. At depth 1.5 cm the sediment outtake is dated year 1995 ±2 yr. There is no increased accumulation rate between the two depths (accumulation rate 0.04 kg m⁻² yr⁻¹ and error rate 0.00 kg m⁻² yr⁻¹ for both). According to these results, Jordtjenn_{con}'s surface sediment contains pre-fire (< year 2008) matter at depth 0.5 cm (year 2006 ±1 yr.) (table 2). The results are very similar to those of Hundsvatn.

With the assumptions as for Hundsvatn (a near linear age rate between the two uppermost sediment sample outtakes at depth 0.5 cm and 1.5 cm), the year of the interface between surface and subsurface (i.e. depth 1.0 cm) in Jordtjenn_{con} is calculated as described for Hundsvatn (ch. 5.1.1) from the data in table 2:

$$\text{Intermediate date}_{1.0 \text{ cm (Jordtjenn}_{con})}: 2010_{0.0 \text{ cm}} - \frac{4_{0.5 \text{ cm}} + 15_{1.5 \text{ cm}}}{2} \approx \underline{2001}$$

$$S_{R_{1.0 \text{ cm (Jordtjenn}_{con})}} = \sqrt{\frac{1_{0.5}^2 + 2_{1.5}^2}{2}} \approx \underline{2}$$

$$\text{Interface date}_{1.0 \text{ cm (Jordtjenn}_{con})} \equiv \underline{2001 \pm 2 \text{ yr.}}$$

With these calculations in mind, it is important to recognize that surface sediments may contain substantial amounts of pre-fire matter.

5.2 Lake sediments' organic matter content (LOI)

Table 3 display sediment organic matter content expressed by LOI (%) for all eight lake bed sediments investigated. Calculated LOI_{median} on all lakes at all depths is 56.2 % (std. 12.75). Across lakes LOI_{median} values are high at all depths (LOI_{median} range; 48.8_{depth 1.5 cm} – 59.7_{depth 0.5 cm} %), typical for the region (Rognerud *et al.* 2008), while LOI_{median}

values calculated *within* lakes, range from 43.0_{Svarttjenn} to 68.3_{Hundsvatn} %. Downcore single-lake fluctuations range from 86.8_{Fisketjenn 0.5 cm} to 32.5_{Svarttjenn 2.5 cm} %.

The OC_{min} value is 16.3 % ($\frac{32.50}{2}$), while OC_{max} is 43.4 % ($\frac{86.80}{2}$) and OC_{median} is 28.1 % ($\frac{56.15}{2}$) (ch. 4.3.2).

Table 3 Simple statistics on sediment OM content in Mykland lake bed sediments; OC_{min} value = 16.3 % ($\frac{32.50}{2}$), OC_{max} = 43.4 % ($\frac{86.80}{2}$) and OC_{median} = 28.1 % ($\frac{56.15}{2}$).

Depth (cm)	Fisketjenn LOI (%)	Hundsvatn LOI (%)	Grunnetjenn LOI (%)	Rasvassvatn LOI (%)	Øyvavn LOI (%)	Jordtjenn _c LOI (%)	Svarttjenn _c LOI (%)	Melestjenn _c LOI (%)	LOI at single depth interval across all lakes				
									Max.	Min.	Mean	Median	Std.
0,5	86,80	73,70	45,40	64,30	41,80	55,10	50,10	65,10	86,80	41,80	60,29	59,70	15,19
1,5	62,20	41,40	42,20	59,80	38,10	55,40	36,60	59,70	62,20	36,60	49,43	48,80	10,83
2,5	58,90	86,50	44,50	63,10	41,10	56,90	32,50	61,10	86,50	32,50	55,58	57,90	16,57
3,5	65,50	68,40	44,30	58,80	43,30	60,00	43,00	61,70	68,40	43,00	55,63	59,40	10,46
33,0		62,30		62,60	39,30	50,10	49,30	54,70	62,60	39,30	53,05	52,40	8,85
Max.	86,80	86,50	45,40	64,30	43,30	60,00	50,10	65,10	LOI for all lakes at all depths				
Mean	68,35	66,46	44,10	61,72	40,72	55,50	42,30	60,46	86,80	Max. (Fisketjenn 0,5 cm)			
Median	63,85	68,40	44,40	62,60	41,10	55,40	43,00	61,10	54,88	Mean			
Min.	58,90	41,40	42,20	58,80	38,10	50,10	32,50	54,70	32,50	Min. (Svarttjenn _{con} 2,5 cm)			
Std.	12,59	16,61	1,35	2,32	2,05	3,59	7,73	3,78	12,75	Std.			

The majority of LOI values are within a 40 % interval range, mostly between 30 – 70 %. Only two LOI measures (i.e. 86.8_{Fisketjenn 0.5 cm} and 86.5_{Hundsvatn 2.5 cm}) out of 38 samples, differ from this. On basis of the span (LOI values within the near linear 30 – 70 % range, ch. 4.4.5 *Arcsin square root transformation of proportional data*) shown in table 3, the reason to perform ASSR transformation on LOI values is not met for these data. Consequently, LOI % data are used.

Vertical depth profiles of LOI fluctuations throughout the sediment column (figure 6) reconstruct historical changes in sediment OC content. It is evident that sediment OC levels follow a relatively uniform pattern through time (depth) and across lakes (space), with Fisketjenn’s LOI peak at 0.5 cm and Hundsvatn as the most distinct exceptions. Also, Svarttjenn_{con} show spread in the data (std. 7.73). Only Jordtjenn_{con} display a decline in LOI from sub-surface (55.4 %) to surface (55.1 %) sediments.

Comparing LOI concentrations at depth 3.5 against 1.5 cm, LOI declines (increase in Rasvassvatn), while LOI increases (decline in Jordtjenn_{con}) when comparing depth 1.5 against 0.5 cm.

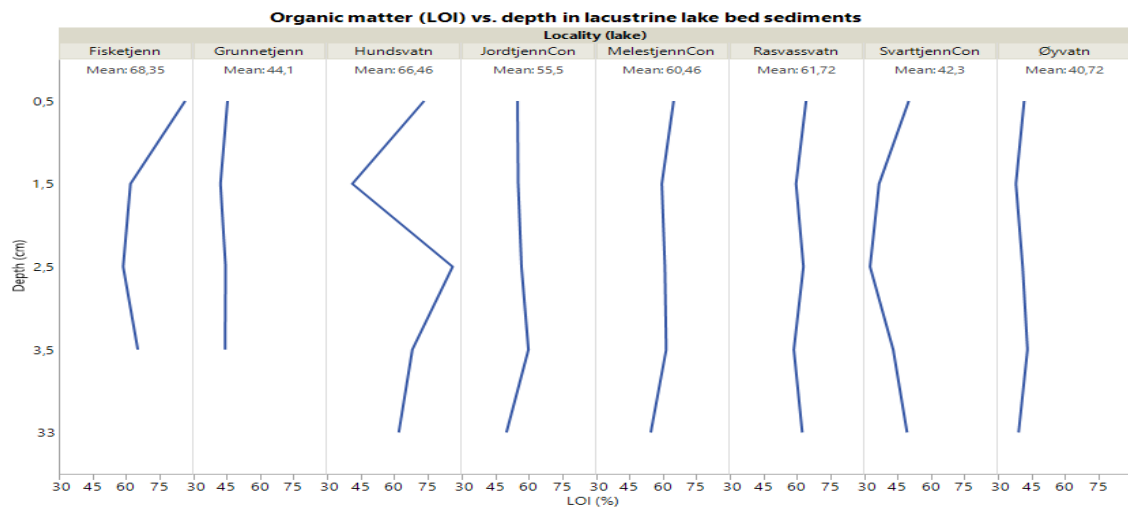


Figure 6 Vertical depth profiles of LOI fluctuations throughout the sediment column. LOI levels follow a relatively uniform pattern with depth and across lakes, with Fisketjenn's LOI peak at 0.5 cm and Hundsvatn being the most distinct exceptions.

5.3 Metals in sediments ($\mu\text{g g}^{-1}$)

Measured metal concentrations are displayed in a colour coded table (table 4), classifying sediment environmental conditions (ECC; Environmental Conditions Class, scale range from I – V) on basis of the governing material, as described in the Norwegian classification guide M-608 on *Quality standards for water, sediment and biota* (Norwegian Environment Agency 2016) (table 15, Tables and figures).

In terms of metal pollution, environmental conditions in surface sediments classify as *Bad* (ECC IV orange; acute toxic effects at short-term exposure) for Hg_{LOI} in five lakes and *Moderate* (ECC III yellow; chronic effects when long-term exposure) in Øyvatn (conditions classify *Good* in Svarttjenn_{con} and Melestjenn_{con}). For Pb environmental conditions are classified as *Moderate* (ECC III) in all lakes except Svarttjenn_{con}, which are classified as *Good* (ECC II green; not toxic effects). Environmental conditions in surface sediments contaminated with Zn, Cd and Hg classify as *Moderate* (ECC III) in Fisketjenn (minus Zn), Hundsvatn, Rasvassvatn, Jordtjenn_{con} (minus Hg) and Melestjenn_{con} (Zn only) (table 4).

Table 4 Metal concentrations in sediments. Colours code for ECC for metals in lacustrine sediments according to the Norwegian classification guide M-608 (Norwegian Environment Agency 2016). Blue code for Class I (background), green for Class II (good), yellow Class III (moderate), orange Class IV (bad) and Red class V (very bad) (table 15, Tables and figures). LOI-normalized metal concentrations for Cd_{LOI}, Cu_{LOI}, Pb_{LOI} and Hg_{LOI} are included (cf. ch. 5.3.2 Metals and sediment organic matter). There are no environmental class for V (Vanadium) and Co (not colour-coded). Also, measured concentrations of Mn and Fe are included in the table, but not evaluated against environmental condition class.

Locality (lake)	Depth (cm)	ROI (g/kg)	LOI (%)	OC (50% of LOI)	Acc. Rate (kg m ⁻² y ⁻¹)	Year of deposition	Cd (µg/g DW)	Cd _{LOI}	Co (µg/g DW)	Cr (µg/g DW)	Cu (µg/g DW)	Fe (µg/g DW)	Mn (µg/g DW)	Ni (µg/g DW)	Pb (µg/g DW)	Pb _{LOI}	V (µg/g DW)	Zn (µg/g DW)	Hg (µg/g DW)	Hg _{LOI}	
Fisketjenn	0,5	132	86,8	43,40			2,30	2,65	1,50	12,5	35,5	40,9	11200	24,9	15,4	196	226	26,9	132	0,712	0,820
Fisketjenn	1,5	378	62,2	31,10			2,70	4,34	1,60	12,0	35,4	56,9	10700	24,8	15,7	219	352	26,4	209	0,608	0,977
Fisketjenn	2,5	411	58,9	29,45			2,40	4,07	1,70	11,3	28,4	48,2	10500	25,3	15,3	208	353	24,8	242	0,514	0,873
Fisketjenn	3,5	345	65,5	32,75			1,60	2,44	1,40	9,40	21,1	32,2	9430	22,8	13,0	156	238	20,1	173	0,386	0,589
Hundsvatn	0,5	263	73,7	36,85	0,40	2006 ±1	2,50	3,39	1,60	14,6	33,1	44,9	7330	37,0	15,7	139	189	29,6	171	0,573	0,777
Hundsvatn	1,5	586	41,4	20,70	0,40	1997 ±2	4,10	9,90	1,70	15,5	38,9	94,0	5770	35,5	19,8	213	514	29,5	361	0,710	1,171
Hundsvatn	2,5	135	86,5	43,25	0,30	1983 ±2	4,70	5,43	1,60	13,0	36,9	42,7	5700	33,4	16,8	266	308	25,2	450	0,719	0,831
Hundsvatn	3,5	316	68,4	34,20	0,30	1966 ±2	3,80	5,56	1,60	11,6	30,6	44,7	6120	33,0	14,2	247	361	21,8	337	0,625	0,914
Hundsvatn	44,5	377	62,3	31,15		1504 _{calc}	0,100	0,161	1,10	9,80	16,00	25,7	8990	57,2	12,0	3,00	4,82	14,6	23,0	0,098	0,157
Grunnetjenn	0,5	546	45,4	22,70			1,10	2,42	1,60	17,5	30,3	66,7	16000	31,4	20,3	164	361	31,1	133	0,362	0,797
Grunnetjenn	1,5	578	42,2	21,10			1,90	4,50	2,20	16,2	29,8	70,6	17000	29,0	20,5	210	498	27,4	243	0,396	0,938
Grunnetjenn	2,5	555	44,5	22,25			1,60	3,60	3,50	13,6	24,9	56,0	21800	28,3	21,0	195	438	21,6	273	0,286	0,643
Grunnetjenn	3,5	557	44,3	22,15			1,20	2,71	4,30	11,6	18,3	41,3	26400	27,8	20,3	155	350	18,6	174	0,188	0,424
Rasvassvatn	0,5	357	64,3	32,15	0,10	2009 ±1	2,60	4,04	8,30	26,8	52,7	82,0	35200	47,8	28,7	232	361	44,2	292	0,738	1,15
Rasvassvatn	1,5	402	59,8	29,90	0,07	2004 ±1	2,70	4,52	9,10	24,4	52,0	87,0	35900	51,1	26,3	248	415	38,2	292	0,719	1,20
Rasvassvatn	2,5	369	63,1	31,55	0,06	1998 ±1	1,60	2,54	2,90	9,1	23,7	37,6	20500	93,8	7,70	107	170	25,9	145	0,618	0,979
Rasvassvatn	3,5	412	58,8	29,40	0,08	1992 ±1	2,00	3,40	7,90	22,0	42,5	72,3	30300	48,9	23,3	215	366	32,6	211	0,548	0,932
Rasvassvatn	35,5	374	62,6	31,30		1848 _{calc}	0,200	0,319	2,20	24,0	49,1	78,4	16800	53,9	17,7	6,70	10,7	27,4	56,3	0,127	0,203
Øyvatn	0,5	582	41,8	20,90			0,77	1,84	1,80	11,1	17,8	42,6	30200	62,2	14,9	136	325	28,5	121	0,257	0,615
Øyvatn	1,5	619	38,1	19,05			1,50	3,94	1,80	11,8	20,6	54,1	23300	53,4	15,8	188	493	26,8	226	0,313	0,822
Øyvatn	2,5	589	41,1	20,55			2,10	5,11	2,00	11,3	21,4	52,1	22800	52,0	15,4	192	467	23,3	279	0,315	0,766
Øyvatn	3,5	567	43,3	21,65			2,10	4,85	2,30	9,60	18,3	42,3	23100	47,6	14,1	175	404	18,3	299	0,288	0,665
Øyvatn	33,5	607	39,3	19,65			0,200	0,509	2,90	7,10	10,7	27,2	34800	45,2	12,0	5,90	15,0	13,4	52,9	0,085	0,216
Jordtjenn _{con}	0,5	449	55,1	27,55	0,40	2006 ±1	2,80	5,08	3,00	12,4	33,4	60,6	21200	78,9	12,0	141	256	30,3	294	0,463	0,840
Jordtjenn _{con}	1,5	446	55,4	27,70	0,40	1995 ±2	2,60	4,69	3,60	11,1	37,4	67,5	24800	103	10,0	142	256	28,3	291	0,298	0,538
Jordtjenn _{con}	2,5	431	56,9	28,45	0,40	1982 ±2	1,90	3,34	4,10	10,0	27,6	48,5	26100	113	9,50	128	225	27,8	246	0,406	0,714
Jordtjenn _{con}	3,5	400	60,0	30,00	0,50	1967 ±2	2,40	4,00	6,70	30,4	56,3	93,8	36500	47,2	27,3	221	368	57,8	273	0,248	0,413
Jordtjenn _{con}	21,5	499	50,1	25,05		1741 _{calc}	0,500	1,00	1,70	7,70	21,7	43,3	20200	85,5	5,60	10,0	20,0	23,5	54,9	0,075	0,150
Svarttjenn _{con}	0,5	499	50,1	25,05			1,00	2,00	1,50	7,00	22,5	44,9	16600	35,7	7,30	63,5	127	29,9	102	0,239	0,477
Svarttjenn _{con}	1,5	634	36,6	18,30			0,81	2,21	2,60	8,90	17,8	48,6	17300	65,8	7,30	50,4	138	32,3	87,8	0,141	0,385
Svarttjenn _{con}	2,5	675	32,5	16,25			0,60	1,85	2,60	9,80	16,7	51,4	17500	76,5	7,20	47,9	147	32,8	75,5	0,149	0,458
Svarttjenn _{con}	3,5	570	43,0	21,50			1,20	2,79	2,00	8,70	21,1	49,1	14800	52,6	9,00	73,9	172	26,7	117	0,223	0,519
Svarttjenn _{con}	36,5	507	49,3	24,65			0,200	0,406	1,00	4,00	14,5	29,4	7560	41,2	6,20	7,40	15,0	14,3	36,0	0,080	0,162
Melestjenn _{con}	0,5	349	65,1	32,55			1,10	1,69	1,30	5,70	20,6	31,6	12200	26,4	8,70	74,7	115	19,2	141	0,223	0,343
Melestjenn _{con}	1,5	403	59,7	29,85			1,50	2,51	1,90	7,30	23,8	39,9	14200	34,2	11,0	103	173	22,6	209	0,303	0,508
Melestjenn _{con}	2,5	389	61,1	30,55			2,00	3,27	2,60	8,40	25,4	41,6	16000	40,2	12,0	124	203	24,9	216	0,335	0,548
Melestjenn _{con}	3,5	383	61,7	30,85			2,70	4,38	2,60	9,00	26,2	42,5	14800	44,4	13,0	142	230	24,3	266	0,378	0,613
Melestjenn _{con}	36,5	453	54,7	27,35			0,100	0,183	0,700	4,70	10,7	19,6	7570	26,6	7,00	6,90	12,6	10,5	25,0	0,115	0,210

5.3.1 Metal outlier analysis

A Jackknife Distances outlier analysis is run on the data matrix (*all metals in all lakes at all depths*) to reveal probable outliers. Two sediment samples are identified as outliers (significance level $\alpha = 0.05$) as they position above the blue, dotted line which indicates the Upper Control Limit (UCL = 5.15) (figure 7).

Among the burnt lakes, Rasvassvatn at reference depth 33.0 cm positions as an outlier. Jordtjenn_{con} 3.5 positions as an outlier among the control lakes. Rasvassvatn diverge from the other lakes at depth 33.0 cm in having a peak in Cr and Cu concentrations (table 4). Concentration levels for Cr and Cu in Rasvassvatn 33.0 (pre-industrial depth) are greater than for Rasvassvatn 3.5 (industrial depth). No other lakes, except Co in

Øyvåtn, display greater metal concentrations in pre-industrial sediments compared to industrial depth 3.5 cm. Jordtjenn_{con} diverge from the other lakes at depth 3.5 cm as V, Cr, Co, Ni, Cu, Zn, Cd and Pb concentrations peak at 3.5 cm (table 4). A similar peak is also seen in other (e.g. Rasvassvatn 3.5), but not with the same magnitude and number of metals.

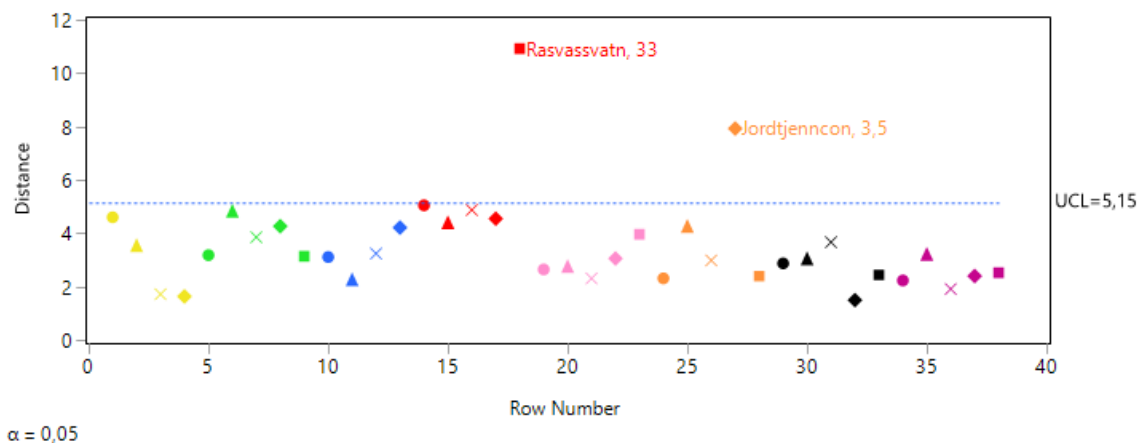


Figure 7 A Jackknife Distances outlier analysis at significance level $\alpha = 0.05$ identify two outliers positioned above the blue, dotted line which indicates the Upper Control Limit (UCL = 5.15); one sample from the burnt lake Rasvassvatn at reference depth 33.0 cm, and one from the control lake Jordtjenn_{con} at industrial depth 3.5 cm.

Consulting a scatter plot (figure 11, ch. 5.3.6) Jordtjenn_{con} 3.5 positions outside the density ellipses almost exclusively for V, Cr and Cu (comparably high concentrations), often close to and in the direction of the fit line. Hg correlations to V, Cr and Cu sites Jordtjenn_{con} 3.5 almost orthogonal to the fit line with an influential distance (relatively high concentrations of V, Cr and Cu, and low concentrations of Hg when compared against each other). Rasvassvatn 33.0 resides outside the density ellipses for Cr and Cu (comparably high concentrations) in combination with relatively low concentrations of the correlating metal, and almost orthogonal to the fit line with a variable, yet mostly weighty, distance. Note how Rasvassvatn (depth 3.5, 1.5 and 0.5 cm) positions outside the density ellipse for Co.

If LOI is included in the Jackknife Distances outlier analysis on *all metals* in *all lakes* at *all depths*, three sediment samples are identified as outliers (figure 8) at significance level $\alpha = 0.05$. Outliers position above the blue, dotted line that indicates the Upper Control Limit (UCL = 5.49).

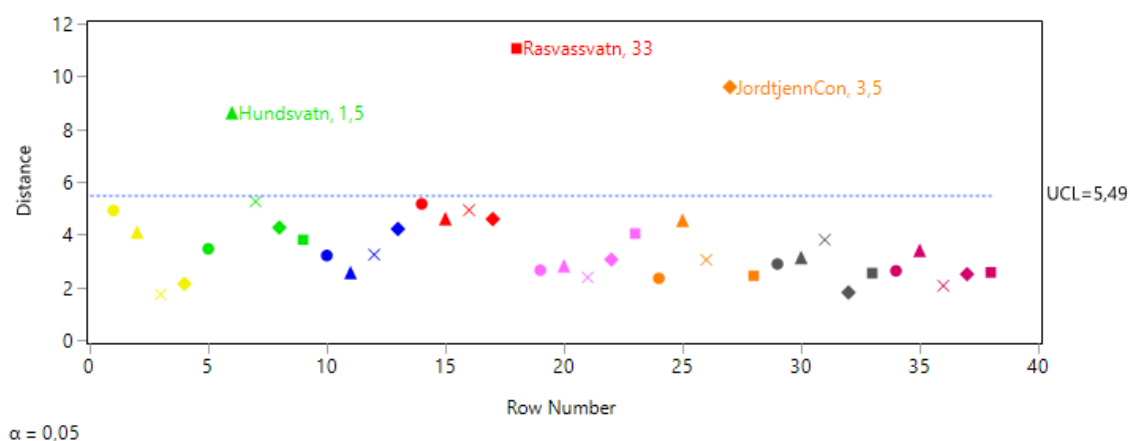


Figure 8 Hundsvatn at depth 1.5 cm, Rasvassvatn at reference depth 33.0 cm and Jordtjenn_{con} at industrial depth 3.5 cm position as outliers if LOI is included in the Jackknife Distances outlier analysis on all metals in all lakes at all depths.

Hundsvatn diverge from the other lakes at depth 1.5 cm in having a big drop in LOI compared to LOI values at the other depths of Hundsvatn (table 4).

Metal outliers are not excluded from further analysis. Nonetheless, it is important to identify outliers as they may be strongly influential and require extra attention.

5.3.2 Metals and sediment organic matter (LOI)

Table 5 lists metal-to-LOI correlations when *all metals* in *all lakes* at *all depths* are included in the data matrix (no outliers excluded). Sample size is 38 ($n = 38$) and significance level set to $\alpha = 0.05$. Metal-to-LOI correlation coefficient $r > 0.3244$ holds a probability $\rho \leq 0.05$, which means there is less than 5 % probability that correlations with $r > 0.3244$ (shaded green) appear by chance. If reference depths 33.0 cm are excluded from the correlation analysis, the Pb-to-LOI correlation holds $r = 0.3579$ ($\rho = 0.0443$).

From table 5 it is evident that only Cu, Cd and Hg correlate to sediment organic matter (LOI). A further examination of these correlations reveals that the degree of metal association to sediment organic matter is negligible when considering metal-to-LOI correlations at specified depths (outliers Hundsvatn 1.5, Rasvassvatn 33.0 and Jordtjenn_{con} 3.5 are excluded at specified depths). Explorative analysis of metal-to-LOI correlations at single depths with outliers included, do not influence strength (r) or probability (ρ) of the correlations to an extent which alters the results. Only at depth section 2.5 cm individual metals (i.e. Cu, Cd and Hg) correlate significantly to LOI. Additionally, Hg is significantly correlated to LOI at depth 3.5 cm and closely

correlated to LOI in the PWF sediment section, however just below the 0.707 r -threshold for significant correlation (cell shaded light green). The latter is seen for Cd at 1.5 cm as well (cell shaded light green).

Table 5 Metal-to-LOI correlation coefficients on all metals in all lakes at all depths (no outliers excluded). Cells shaded green indicate significant correlations ($r > 0.3244$, $\alpha = 0.05$). Light green cells mark correlation coefficient just below threshold values of significance. Outliers Hundsvatn 1.5, Rasvassvatn 33.0 and Jordtjenn_{con} 3.5 are excluded for metal-to-LOI correlations at specified depths.

Depth	LOI	Cd	Co	Cr	Cu	Ni	Pb	V	Zn	Hg
All depths ($n=38$, $r > 0.3244$, $\alpha = 0.05$)		0,4470	0,0380	0,1799	0,4472	0,1414	0,2843	0,0675	0,2457	0,5531
Industrial depths ($n=32$, $r > 0.3536$, $\alpha = 0.05$)		0,5423	0,0427	0,1184	0,4471	0,1040	0,3579	0,0138	0,2842	0,6428
0.5 cm ($n=8$, $r > 0.7071$, $\alpha = 0.05$)		0,6076	0,0509	0,0866	0,4363	0,0852	0,3365	-0,0980	0,1061	0,7003
1.5 cm ($n=7$, $r > 0.7559$, $\alpha = 0.05$) ¹		0,7426	0,3372	0,2036	0,6753	0,2348	0,3501	-0,0369	0,5112	0,6518
2.5 cm ($n=8$, $r > 0.7071$, $\alpha = 0.05$)		0,8592	-0,3064	0,1291	0,9120	0,1524	0,5654	-0,2624	0,6737	0,9094
3.5 cm ($n=7$, $r > 0.7559$, $\alpha = 0.05$) ²		0,6732	-0,0868	0,1824	0,5233	0,0377	0,5749	0,1639	0,4108	0,8280
33.0 cm ($n=5$, $r > 0.8944$, $\alpha = 0.05$) ³		-0,3233	-0,7907	0,3383	0,2666	-0,0044	-0,4207	-0,0555	-0,7999	0,5021
Pre-industrial ($n=6$, $r > 0.8165$, $\alpha = 0.05$)		-0,3033	-0,4417	0,5887	0,5709	0,4184	-0,3513	0,3657	-0,3434	0,6763

¹Outlier Hundsvatn 1.5 cm excluded

²Outlier Jordtjenn_{con} 3.5 cm excluded

³Outlier Rasvassvatn 33.0 cm excluded

Since Hg correlates with LOI at three depths (depths 3.5, 2.5 and 0.5 cm), and because the properties of Hg differ from the other metals in its high affinity to organic material (Lydersen, Löfgren & Arnesen 2002), LOI-normalized concentrations of Hg are presented parallel to measured Hg concentrations (table 4, ch. 5.3). For comparison purposes also Cu_{LOI}, Cd_{LOI} and Pb_{LOI} are presented in the table. It seems that depth 2.5 cm has an influence on Cu and Cd correlations to LOI when metal-to-LOI correlations for *all metals in all lakes at all depths* (no exclusion of outliers) are considered simultaneously. In present paper depth 2.5 cm is of little interest and hence LOI-normalized values of Cu and Cd are not included in tables and figures etc. Further analysis use measured metal concentration levels for all metals, and not LOI-normalized metal concentrations.

5.3.3 Dominant metal concentrations

Dominant metal concentrations in Mykland sediments are of interest. Examining sub-surface (depth 1.5 cm) and surface (depth 0.5 cm) sediments across lakes, reveals an increasing metal concentration order (prevailing trend on median values of measured metal concentration levels) of Hg < Co < Cd < Cr < Ni < V < Cu < Zn / Pb at both depths (i.e. before and after the wildfire, respectively). The prevailing trend (on median

values of measured metal concentration levels) in pre-industrial reference sediments (depth 33.0 cm) follow an increasing order of Hg < Cd < Co < Pb < Cr < Ni < V < Cu < Zn. Note how Pb positions with Zn in the upper (depths 1.5 and 0.5 cm) sediments, compared to the relatively lower concentration levels of Pb in reference (depth 33.0 cm) sediments (highlighted yellow) (table 6). Within boxes outlined in black, increasing order may be disrupted (shaded grey). Including / excluding outliers have no influence on the metal order or the declining / increasing trend of metal concentration levels.

Table 6 Increasing metal concentration order (prevailing trend of median values) from left to right. Within boxes outlined in black, increasing order may be disrupted (shaded grey) when considering single lakes. Note how Pb positions with Zn in the upper (depth 1.5 and 0.5 cm) sediments, compared to the relatively lower concentration levels of Pb in reference (depth 33.0 cm) sediments (highlighted yellow).

	Hg <	Hg (LOI) <	Co <	Cd <	Cr <	Ni <	V <	Cu <	Pb <	Zn
Median (0.5)	0.41	0.79	1.60	1.70	12.45	15.15	29.75	31.70	140.0	137.0
Median (1.5)	0.35	0.88	2.05	2.25	11.90	15.75	27.85	32.60	199.0	234.5
Median (33.0)	0.09	0.18	1.40	0.20	7.40	9.50	14.45	15.25	6.80	44.45

Despite the differentiated positioning of Pb between pre-industrial and present sediments, it is evident that the metal concentration order remains relatively unaltered through time (in between depths) and space (across lakes). Full table on measured metal concentration order and % decline / increase across depths in table 16 and 31 (Tables and figures).

5.3.4 Depth profile on metal concentration fluctuation thru time

Depth profiles on sediment LOI and Ln-logged (to reduce spread) metal concentrations illustrate the historic variations in sediment organic matter content and metal load for all eight lakes studied (figure 9). LOI-normalized concentrations of Hg are included.

Due to the complexity of the results, the number of depths illustrated are reduced to enhance visual interpretation / patterns. Full sediment profile including depth 2.5 cm is found in Tables and figure (figure 28). To uncover predominant trends of metal fluctuations from one depth to a shallower, a concentration decline / increase is identified by using qualified majority (ch. 4.4.6 and Appendix 4).

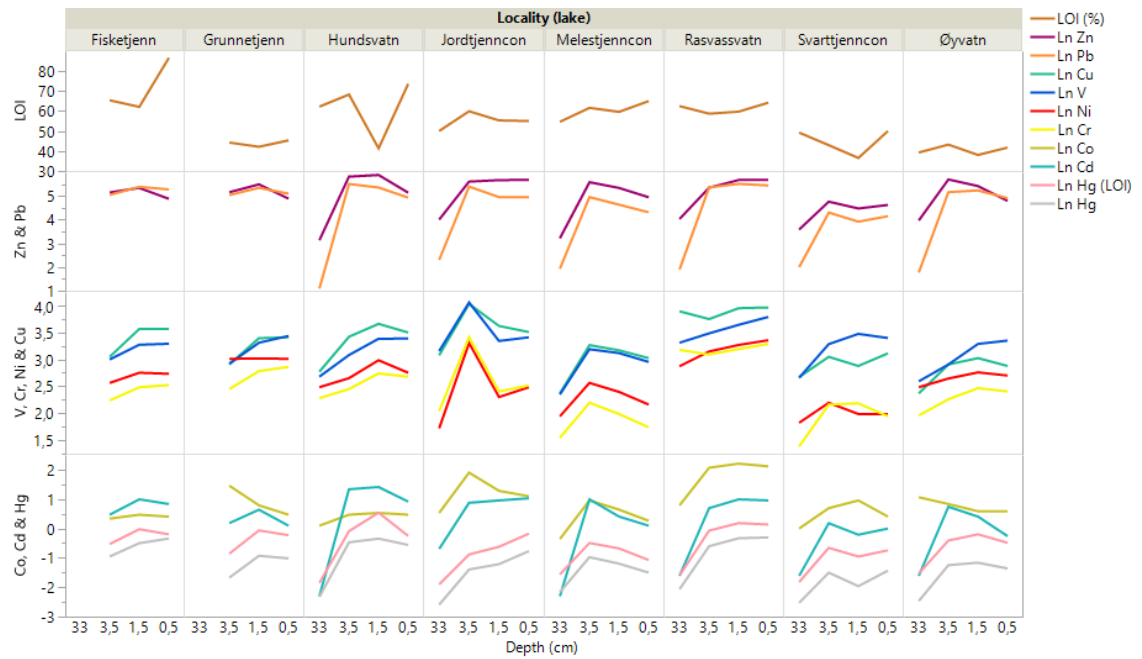


Figure 9 Depth profiles on sediment LOI and Ln-logged (to reduce spread) metal concentrations illustrate the historic variations in sediment organic matter content and metal load for all eight lakes studied. LOI-normalized concentrations of Hg are included. Due to the complexity of the results, the number of depths illustrated are reduced (depth 2.5 cm omitted) to enhance visual interpretation / patterns.

Pre-industrial (depth 33.0 cm) deposits against industrial deposits

Despite the lack of any obvious relationship between metals and LOI when plotted against each other with depth, metals share some resemblances in downcore concentration fluctuations. The most explicit tendency is increasing metal (including Hg_{LOI}) concentrations from pre-industrial to industrial time (at any depth) in all eight lakes. Exceptions worth noticing are the Cr and Cu decline in Rasvassvatn (Cr is unaltered comparing depth 33.0 against 1.5 cm in Rasvassvatn) and Co decline in Øyvavn (all from depth 33.0 cm to the overlaying sediment section; depth 3.5 cm). Throughout the sediment, Co keeps declining from one depth section toward the shallower (Co is unaltered from depth 1.5 to 0.5 cm in Øyvavn).

Industrial deposits in advance of the fire (depth 3.5 against 1.5 cm)

A noticeable trend is seen when comparing depth 3.5 cm against depth 1.5 cm; concentrations increase for several metals in the *burnt lake* sediments (isolated exceptions are the Zn and Cd decline in Øyvavn, a Pb decline in Hundsvatn and a Co decline in Grunnetjenn and Øyvavn), while a *decline* is seen in the *control lakes*

Jordtjenn_{con}, Svarttjenn_{con} and Melestjenn_{con}. Note that in Jordtjenn_{con} Zn, Cd and Hg / Hg_{LOI} increase, while in Svarttjenn_{con} V, Cr and Co increase.

Pre-fire (depth 1.5 cm) deposits against PWF (depth 0.5 cm) deposits

To unveil any trend in metal fluctuations from pre-fire to PWF sediments, lakes are seen collectively. Five (i.e. Fisketjenn, Hundsvatn, Grunnetjenn, Øyvavn, Melestjenn_{con}) of the eight lake sediments sampled, hold declining concentration levels from sub-surface to surface sediments for six (i.e. Co, Ni, Zn, Cd, Hg_{LOI}, Pb) or more out of the nine measured metals (which metals to decline beyond the six listed, differ between lakes). Co, Ni, Zn, Cd, Hg_{LOI} and Pb also decline in other lakes than five listed above (which lakes beyond the five listed, differ between metals to decline). In Rasvassvatn, Jordtjenn_{con} and Svarttjenn_{con}, five to six metals *increase* from sub-surface to surface sediments (metals to increase differ between lakes). Cr, Cu and Hg decline / increase in half of the lake sediments (considered *no tendency*), of which a decline is seen in Hundsvatn, Øyvavn and Melestjenn_{con}. Co is the only metal to decline in all eight lake sediments from depth 1.5 to 0.5 cm, while V increases in six lakes within that sediment section. In terms of meeting the requirements of a qualified majority (ch. 4.4.6) the results outlined above are specified in Appendix 4.

5.3.5 PCA on measured metal concentrations

A PCA run on *all metals* (measured concentrations) in *all lakes at all depths* (outliers Rasvassvatn 33.0 and Jordtjenn_{con} 3.5 included) illustrates that two dimensions (PC 1; 63.6 % plus PC 2; 19.7 %) in the component space account for 83.3 % (cumulative percentage) of the total variance in the data set (figure 10). The third dimension (PC 3) and on, has an eigenvalue below one (0.4905), thus it accounts for less variance than the original variable (which would have a variance of one). It is therefore of little influence (UCLA 2018). Hence, the results propose two explanatory factors for metal concentrations in the sampled lake sediments.

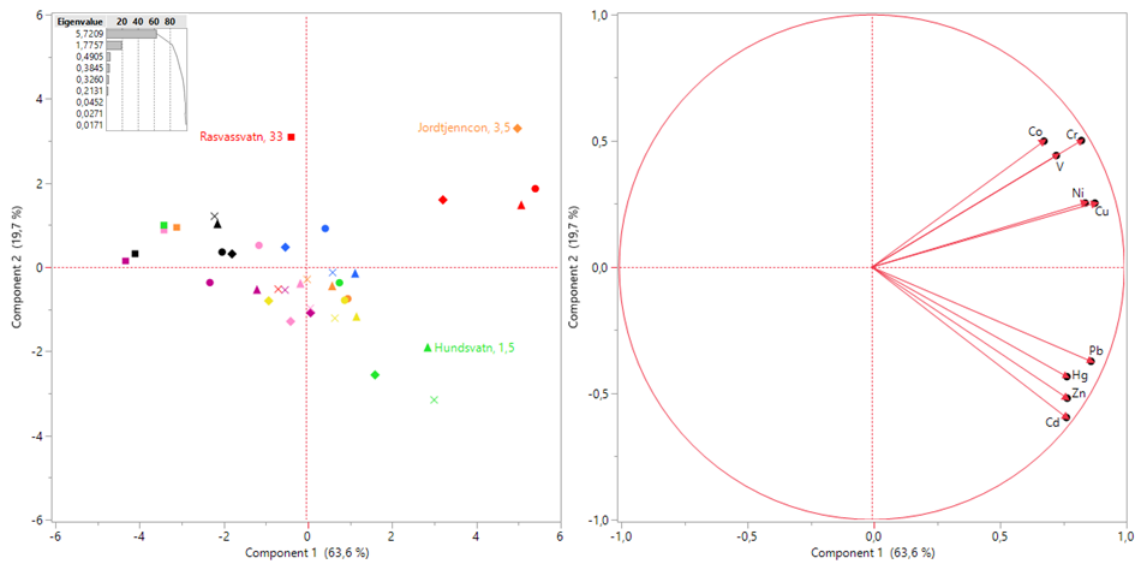


Figure 10 PCA on all metals (measured concentrations) in all lakes at all depths (the outliers Rasvassvatn 33.0 and Jordtjenn_{con} 3.5 included). Score plot to the left and loading plot to the right. Squares represent reference depth 33.0 cm, diamonds match depth 3.5 cm, triangles correspond to sub-surface / pre-fire sediments and solid dots symbolise surface / PWF sediments (depth 0.5 cm). Xs represent the intermediate section (2.5 cm) of the industrial pre-fire sediment. The scree plot (upper left corner) propose two explanatory factors (eigenvalue 0.4905). 83.3 % of all the variance in the dataset can be explained by two principal components (PC 1 63.6 % plus PC 2 19.7 %).

All nine metals load positively and fairly equal along PC 1 (table 17, Tables and figures). Such an arrangement implies correlations between metals. Based on the positioning in the loading plot (figure 10, right), metals seem to arrange in two sets; V, Cr, Co, Ni, Cu, and Zn, Cd, Hg, Pb. The score plot (figure 10, left) shows that Rasvassvatn and Jordtjenn_{con} 3.5 exert influence on V, Cr, Co, Ni and Cu loadings, and that Hundsvatn impacts the Zn, Cd, Hg and Pb loadings in a negative direction along PC 2 (table 17, Tables and figures). The remaining lakes position close to the centre of the plot and are of little influence. Nonetheless, reference depths cluster uttermost to the left along PC 1 (figure 10, left), in the opposite direction of metal positioning in the loading plot. Such clustering indicates that metal concentrations are at its minimum in the pre-industrial sediments.

5.3.6 Metal correlations

The results of the PCA require further exploration of relationships between metals, without influence from pre-industrial matter (sediment depth 33.0 cm). A scatter plot

(figure 11) on all metals across all lakes at all *industrial* depths (pre-industrial reference depth excluded, outliers included), reveals whether metals correlate, the significance and strength (proximity of strong correlations: $r > 0.7$) of possible correlations, and if there is any linearity between correlations. A correlation table and a probability table are found in Tables and figures (table 19 and 20, respectively).

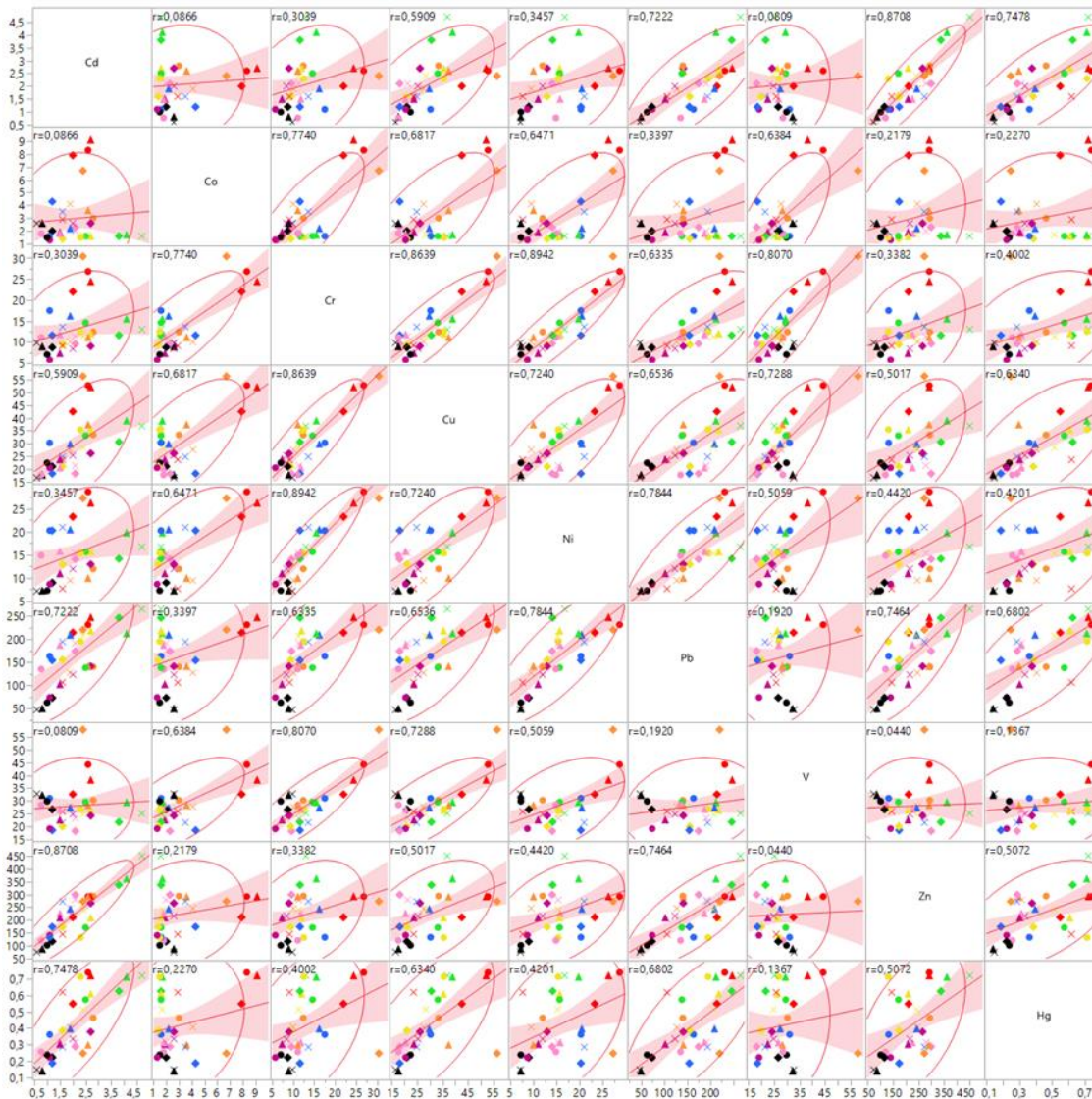


Figure 11 Scatter plot including all metals at all industrial depths in all lakes (pre-industrial reference depth excluded, outliers included). $n = 32$, $r > 0.3536$, $\alpha = 0.05$. Solid circles represent sediment depth 0.5 cm, triangles 1.5 cm, crosses 2.5 cm and diamonds 3.5 cm. Yellow represent Fisketjenn, green Hundsvatn, blue Grunnetjenn, red Rasvassvatn, pink Øyvatt, orange Jordtjenn_{con}, black Svarttjenn_{con} and deep purple Melestjenn_{con}. Orange diamonds represent Jordtjenn_{con} 3.5.

The threshold value for significant correlations is calculated according to Walsh (1998); When all lakes at all industrial depths are included, the number of samples (n) sum to

32, which gives a correlation coefficient $r > 0.3536$ at significance level $\alpha = 0.05$ (table 14, Tables and figures).

The scatter plot (figure 11) demonstrates strong correlations within the two clustered groups seen in the PCA loading plot (figure 10, right); *V, Cr, Co, Ni, Cu*, and *Zn, Cd, Hg, Pb*. Ni, Cu and Pb correlate to most metals in both groups, while V and Co only correlates to Cr, Ni and Cu. Rasvassvatn and Jordtjenn_{con} 3.5 strongly influence on several metal correlations, especially Co correlations to Cr, Ni and Cu. A correlation-tree of strong correlations (proximity of strong correlations: threshold $< r > 0.7$) is displayed in figure 12 (left).



Figure 12 Correlation-tree of strong (threshold $< r > 0.7$) correlations (left), and weak (threshold $< r < 0.5$) correlations (right).

Some correlations (e.g. Hg to Cr / Ni, and Ni to Zn) are weak (proximity of weak correlations: threshold $< r < 0.5$) and hold low linearity, even if correlations are significant ($r > 0.3536$). A correlation-tree of weak correlations is displayed in figure 12 (right). Co differs from the general picture, as no linear relationship to the other metals seems to exist. Yet, correlations are significant with medium strength (proximity of medium strong correlations: $0.5 < r < 0.7$). Lack of linearity hint that Co concentrations may be influenced by other factors than the rest of the metals, while good correlations suggest one common source of origin (Müller, Grimmer & Böhnke 1977; Wang et al. 2010).

The scatter plot (figure 11) confirms what is illustrated in the PCA score plot (figure 10, left); Hundsvatn, Rasvassvatn and Jordtjenn_{con} 3.5 pull on several metals (i.e. *Zn, Cd, Hg, Pb*, and *V, Cr, Co, Ni, Cu*, respectively).

5.3.7 Clustering of depths, lakes and metals

A hierarchical two-way clustering dendrogram (method = ward) run on *all metals* at *all depths* for *all lakes* (outliers included), demonstrates that lakes rather than depths tend to cluster (figure 13, excluding the two outliers Rasvassvatn 33.0 and Jordtjenn_{con} 3.5 makes clustering of lakes even more apparent).

In the dendrogram each lake holds a specific colour, depths are identified by their figures, while clusters are grouped together. Metals are found beneath the “pixed” dendrogram mosaic, divided into two groups (*V, Cr, Co, Ni, Cu*, and *Zn, Cd, Hg, Pb*). Values (i.e. concentration level) of each variable (i.e. metals) relative to the others are presented on a continuous three colour scale; red colours represent high metal concentrations, while blue colours represent low metal concentrations.

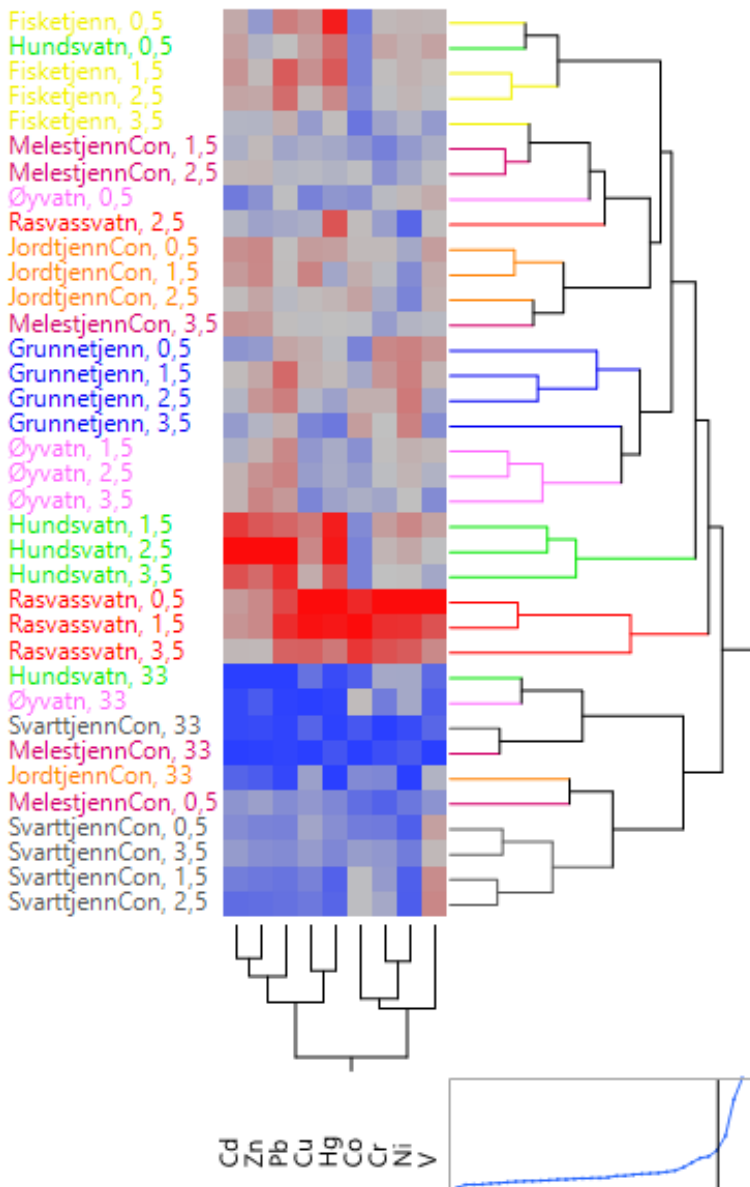


Figure 13 A hierarchical two-way clustering dendrogram (method = ward) on all metals (outliers included), demonstrates that lakes rather than depths tend to cluster. Each lake is given a specific colour, depths are identified by their figures, while clusters are grouped together. The scree-plot at the bottom right corner indicates the recommended number of clusters (at knee point).

Red colour fading to grey represents declining metal concentration levels, while blue colour fading to grey represents increasing metal concentration levels.

The scree plots below the dendrograms (figure 13, bottom right) propose the best suitable number of clusters in the material. The line crossing the “knee point” in the scree plot indicates four clusters (i.e. figure 14), which are (starting at top):

1. Fisketjenn 0.5 to Grunnetjenn 3.5
2. Hundsvatn 1.5, Hundsvatn 2.5 and Hundsvatn 3.5
3. Hundsvatn 33.0 – Melestjenn_{con} 0.5*
4. Rasvassvatn 0.5, Rasvassvatn 1.5, Rasvassvatn 3.5 and Jordtjenn_{con} 3.5

*The third cluster-group consists of two sub-clusters (plus the outlier Rasvassvatn 33.0 positioning as its own sub-cluster). Reference depths Hundsvatn 33.0, Øyvatn 33.0, Svarttjenn_{con} 33.0 and Melestjenn_{con} 33.0 compose the first sub-cluster, while control lake Svarttjenn_{con} holds the major part of sub-cluster two. Jordtjenn_{con} 33.0 positions as a member of the second sub-cluster.

Sediment segments of equal depth do not cluster in the dendrogram. According to this, sediment sections of equal depth have comparatively little in common (interlake dissimilarities) regarding metal concentrations. On the contrary, lakes cluster, proposing intralake similarities. These similarities are downcore in each sediment column (temporal), not across lake sediment samples of equal depth (spatial).

Surface sediments of Fisketjenn and Hundsvatn cluster, as well as surface sediments of Grunnetjenn and Øyvatn. This divergent clustering is evaluated by conferring the scree plot, promoting the number of clusters to be four. Dividing the material into four clusters will include the deeper sections of Fisketjenn, Grunnetjenn and Øyvatn. Although Hg concentrations in Fisketjenn 0.5 are among the highest, inclusion of several depths in this cluster points towards other variables than depth responsible for that cluster.

At the bottom of the dendrogram, metals divide in two clusters; V, Cr, Co, Ni, and Cu, Zn, Cd, Hg, Pb.

5.4 PAHs in sediments ($\mu\text{g kg}^{-1}$)

Measured PAH concentrations are displayed in a colour coded table (table 7), classifying sediment ECC on basis of the governing material, as described in the

Norwegian classification guide M-608 (Norwegian Environment Agency 2016) (table 21, Tables and figures).

In terms of PAH pollution, environmental conditions in surface sediments classify as *Bad* (ECC IV) to *Very bad* (ECC V) for PAH_{HMW} CHR, BbjF, BkF, BghiP, IcdP and DBa3A in ≥6 lakes. For PAHs NAP_{LMW}, ANT_{LMW}, PYR_{HMW} and BaA_{HMW}, environmental conditions are classified as *Moderate* (ECC III) to *Bad* (ECC IV) in ≥7 lakes.

Table 7 PAH concentrations in lacustrine sediments. Colours code for ECC for PAHs in lacustrine sediments according to the Norwegian classification guide M-608 (Norwegian Environment Agency 2016). Blue code for Class I (background), green for Class II (good), yellow Class III (moderate), orange Class IV (bad) and Red class V (very bad). There are no environmental class for DBTHI, BeP, PER (biogenic) or ΣPAHs (not colour-coded).

Locality (lake)	Depth (cm)	LOI (%)	Year of deposition	Acc. Rate (g m ⁻² y ⁻¹)	MFP °C (ug/kg DW)	ACNLE °C (ug/kg DW)	ACNLE °F (ug/kg DW)	ACNE °C (ug/kg DW)	ACNE °F (ug/kg DW)	FILE °C (ug/kg DW)	FILE °F (ug/kg DW)	PA °C (ug/kg DW)	PA °F (ug/kg DW)	ANT °C (ug/kg DW)	DBTHI (ug/kg DW)	FLU °C (ug/kg DW)	PYR °C (ug/kg DW)	BAAC °C (ug/kg DW)	CHR °C (ug/kg DW)	BBBF °C (ug/kg DW)	BNFC °C (ug/kg DW)	BEF °C (ug/kg DW)	BAP °C (ug/kg DW)	PER °C (ug/kg DW)	BGHP °C (ug/kg DW)	ICDP °C (ug/kg DW)	DBA3A °C (ug/kg DW)	ZPAH _{HMW} °C (ug/kg DW)	ZPAH _{HMW} °F (ug/kg DW)	ECPA48 (C)
Fiskeljønn	0.5	86.8			161	49.5	26.5	112	829	829	112	2189	1382	889	2535	5415	1728	2765	1118	910	2985	3111	599	26106	23264	15665				
Fiskeljønn	1.5	62.2			225	65.9	43.4	154	1206	177	3055	2090	1286	3376	7556	2412	3859	1608	1527	4341	3377	4341	836	36746	32772	21640				
Fiskeljønn	2.5	58.9			204	56.0	45.8	115	1121	161	2716	1868	1171	3056	6791	2207	3396	1460	2037	3735	3905	747	32856	29360	19542					
Fiskeljønn	3.5	65.5			137	39.7	36.6	73.3	809	107	67.2	1985	1282	748	2137	4427	1359	2290	931	2595	2443	2595	473	21942	19585	12809				
Hundsvatn	0.5	73.7	2006 ±1	0.40	217	50.2	19.0	85.5	896	111	93.6	2171	1628	1058	2442	6513	2035	2985	1628	611	2442	2578	434	27388	24309	16906				
Hundsvatn	1.5	41.4	1997 ±2	0.40	604	184	70.0	338	2899	459	338	7488	6039	4589	9179	26570	7971	11836	7005	1570	9662	10386	1836	107452	95278	68140				
Hundsvatn	2.5	86.5	1983 ±2	0.30	335	127	37.0	220	1965	324	208	4855	4162	3353	5318	16185	5202	7977	5087	936	6705	7168	1272	70499	62314	43919				
Hundsvatn	3.5	68.4	1966 ±2	0.30	336	108	35.1	205	2047	336	190	4825	4240	3070	5117	14327	4825	7018	4678	965	6433	6871	1155	65816	58608	40380				
Grunnetjønn	0.5	45.4			141	41.9	9.69	30.8	529	44.1	37.4	859	419	242	1123	2643	639	1167	308	121	1278	1432	220	11164	9959	6749				
Grunnetjønn	1.5	42.2			185	40.3	15.6	52.1	806	85.3	61.6	1374	711	427	1919	4265	1090	1951	592	474	2275	2607	403	18900	16847	11488				
Grunnetjønn	2.5	44.5			157	31.5	15.1	47.2	697	87.6	53.9	1236	674	427	1551	3596	989	1753	584	1191	2157	2247	360	16682	14856	9910				
Grunnetjønn	3.5	44.3			99.3	18.5	12.2	33.9	406	58.7	31.6	745	406	226	767	2032	519	948	316	1964	1219	1287	199	9324	8344	5445				
Rasvassvatn	0.5	64.3	2009 ±1	0.10	249	65.3	28.0	104	1260	140	90.2	2488	2177	1384	3421	10731	3110	5288	2333	529	3888	4044	684	41485	36107	25956				
Rasvassvatn	1.5	59.8	2004 ±1	0.07	351	110	36.8	184	2508	284	167	4849	4248	3010	5853	18395	5518	8696	4682	1070	7191	7525	1271	74980	66117	46805				
Rasvassvatn	2.5	63.1	1998 ±1	0.06	317	109	33.3	174	2377	301	158	5071	4120	2694	5230	13312	5230	8686	3962	1585	8399	8716	1537	68399	61585	40988				
Rasvassvatn	3.5	58.8	1992 ±1	0.08	272	85.0	25.5	136	1871	238	124	4082	3231	2041	4082	10374	3741	5102	3061	1701	6973	7313	1207	53959	48733	32092				
Øvåtn	0.5	41.8			206	45.5	12.4	38.3	478	45.5	35.9	718	407	230	933	2392	478	1148	383	122	1292	1411	208	10462	9278	6242				
Øvåtn	1.5	38.1			220	68.2	15.5	49.9	682	81.4	57.7	1234	735	420	1680	4724	919	2178	682	341	2441	2625	394	19207	16971	11664				
Øvåtn	2.5	41.1			221	90.0	17.3	53.5	706	90.0	60.8	1285	803	511	2068	5596	1119	2676	827	706	3163	3406	487	23161	20424	14236				
Øvåtn	3.5	43.3			166	62.4	12.2	41.6	624	80.8	53.1	993	716	439	1755	4850	1062	2286	693	1316	2771	3002	416	20024	17684	12383				
Jordtjønn _{kon}	0.5	55.1	2006 ±1	0.40	200	45.4	18.1	56.3	563	94.4	58.1	1289	1125	653	1525	5808	1597	2722	1107	962	2359	2541	381	22142	19361	13811				
Jordtjønn _{kon}	1.5	55.4	1995 ±2	0.40	181	48.7	18.1	65.0	614	114	59.6	1444	1318	776	1751	6679	6859	3249	1336	1516	2708	3069	487	30774	27466	21137				
Jordtjønn _{kon}	2.5	56.9	1982 ±2	0.40	176	47.5	17.6	65.0	598	104	56.2	1318	1213	756	1757	6151	1670	2988	1248	1933	2636	2812	439	24051	21007	15009				
Jordtjønn _{kon}	3.5	60.0	1967 ±2	0.50	127	28.3	15.8	45.0	433	73.3	36.7	817	733	467	850	3667	983	1833	800	2333	1667	1833	267	14676	12806	8993				
Svartjønn _{kon}	0.5	50.1			73.9	2.00	9.78	20.0	174	18.8	13.2	259	194	85.8	240	519	144	259	128	1078	279	259	45.9	2724	2452	1495				
Svartjønn _{kon}	1.5	36.6			112	19.4	15.8	22.4	254	26.2	20.2	410	273	126	328	738	199	383	199	929	383	383	68.3	3959	3557	2153				
Svartjønn _{kon}	2.5	32.5			114	23.7	19.1	26.2	338	36.9	29.5	646	431	197	554	1200	338	615	338	769	646	646	117	6317	5672	3505				
Svartjønn _{kon}	3.5	43.0			130	30.2	21.2	39.5	465	58.1	46.5	1140	791	395	1116	2279	698	1163	651	1209	1256	1302	233	11814	10605	6805				
Melesjønn _{kon}	0.5	65.1			89.1	16.9	12.1	27.6	323	32.3	18.4	538	369	154	430	1121	369	588	261	1997	691	691	117	5828	5241	3232				
Melesjønn _{kon}	1.5	59.7			101	18.4	15.7	40.2	486	58.6	33.5	955	653	335	888	2178	737	1089	503	1675	1256	1256	218	10820	9697	6214				
Melesjønn _{kon}	2.5	61.1			162	39.3	36.0	80.2	949	110	70.4	1964	1358	655	1637	4092	1408	1964	998	1358	2291	2455	428	20694	18660	11831				
Melesjønn _{kon}	3.5	61.7			211	63.2	32.4	94.0	1151	131	89.7	2431	1621	924	2431	5024	1572	2431	1475	1556	2755	2917	502	25856	23335	15057				

Class limits for Dibenz(a,h)Anthracene (DBa(hA)) used

Class limits for Benzo(b)Fluoranthene (BbF) used

Environmental conditions class in lacustrine sediments on PAH_{LMW} (according to M-608)

Environmental conditions in lakes Fisketjenn, Hundsvatn and Rasvassvatn are classified as *Moderate* (ECC III) to *Bad* (ECC IV) for ACNLE_{LMW} and FLU (plus Jordtjenn_{con}, ECC IV for FLU) (table 7).

5.4.1 PAHs and sediment organic matter (LOI)

A correlation matrix run on measured PAH concentrations against LOI, demonstrates good ($r > 0.5$) PAH-to-LOI correlations ($\rho < 0.002$) and strong ($r > 0.7$) PAH-to-PAH correlations (table 8). Consequently, measured PAH concentrations are LOI-normalized (table 22, Tables and figures).

Table 8 Correlation matrix on singular PAHs and LOI. PAH-to-PAH correlations are strong ($r > 0.7$). PAH-to-LOI correlations (shaded green) are good ($r > 0.5$) with significant correlation probabilities ($\rho < 0.02$).

	NAP *C	ACNLE *	ACNE *	FLE *	PA *	ANT *	DBTHI	FLU *	PYR *	BAA *C	CHR *C	BBJF *C	BKF *C	BEP	BAP *C	BGHIP *	ICDP *C	DBA3A *C	LOI (%)
NAP *C	1	0,9762	0,8117	0,9649	0,9535	0,9656	0,9783	0,9674	0,9701	0,9682	0,9807	0,9795	0,8936	0,9773	0,9670	0,9486	0,9524	0,9499	0,5757
ACNLE *	0,9762	1	0,7835	0,9560	0,9465	0,9671	0,9705	0,9590	0,9617	0,9688	0,9706	0,9672	0,8825	0,9696	0,9653	0,9568	0,9614	0,9572	0,5419
ACNE *	0,8117	0,7835	1	0,8864	0,8186	0,8295	0,8507	0,8636	0,8200	0,7950	0,8500	0,7866	0,7109	0,7953	0,7663	0,7936	0,7903	0,8242	0,6626
FLE *	0,9649	0,9560	0,8864	1	0,9508	0,9803	0,9883	0,9829	0,9720	0,9722	0,9802	0,9557	0,8736	0,9611	0,9576	0,9473	0,9483	0,9614	0,6450
PA *	0,9535	0,9465	0,8186	0,9508	1	0,9735	0,9507	0,9874	0,9862	0,9675	0,9787	0,9565	0,8770	0,9623	0,9601	0,9819	0,9811	0,9811	0,5855
ANT *	0,9656	0,9671	0,8295	0,9803	0,9735	1	0,9839	0,9892	0,9927	0,9911	0,9796	0,9672	0,9025	0,9733	0,9829	0,9748	0,9775	0,9788	0,5925
DBTHI	0,9783	0,9705	0,8507	0,9883	0,9507	0,9839	1	0,9805	0,9766	0,9839	0,9817	0,9684	0,8801	0,9685	0,9755	0,9433	0,9471	0,9534	0,5793
FLU *	0,9674	0,9590	0,8636	0,9829	0,9874	0,9892	0,9805	1	0,9912	0,9795	0,9895	0,9604	0,8857	0,9661	0,9673	0,9789	0,9790	0,9858	0,6165
PYR *	0,9701	0,9617	0,8200	0,9720	0,9862	0,9927	0,9766	0,9912	1	0,9929	0,9845	0,9780	0,9090	0,9826	0,9886	0,9779	0,9794	0,9792	0,5900
BAA *C	0,9682	0,9688	0,7950	0,9722	0,9675	0,9911	0,9839	0,9795	0,9929	1	0,9781	0,9815	0,9025	0,9845	0,9972	0,9616	0,9652	0,9646	0,5646
CHR *C	0,9807	0,9706	0,8500	0,9802	0,9787	0,9796	0,9817	0,9895	0,9845	0,9781	1	0,9814	0,8932	0,9833	0,9687	0,9738	0,9749	0,9792	0,5809
BBJF *C	0,9795	0,9672	0,7866	0,9557	0,9565	0,9672	0,9684	0,9604	0,9780	0,9815	0,9814	1	0,9196	0,9983	0,9837	0,9536	0,9577	0,9528	0,5435
BKF *C	0,8936	0,8825	0,7109	0,8736	0,8770	0,9025	0,8801	0,8857	0,9090	0,9025	0,8932	0,9196	1	0,9222	0,9070	0,8948	0,9017	0,8955	0,5332
BEP	0,9773	0,9696	0,7953	0,9611	0,9623	0,9733	0,9685	0,9661	0,9826	0,9845	0,9833	0,9983	0,9222	1	0,9850	0,9620	0,9654	0,9617	0,5708
BAP *C	0,9670	0,9653	0,7663	0,9576	0,9601	0,9829	0,9755	0,9673	0,9886	0,9972	0,9687	0,9837	0,9070	0,9850	1	0,9517	0,9563	0,9513	0,5454
BGHIP *	0,9486	0,9568	0,7936	0,9473	0,9819	0,9748	0,9433	0,9789	0,9779	0,9616	0,9738	0,9536	0,8948	0,9620	0,9517	1	0,9995	0,9973	0,5732
ICDP *C	0,9524	0,9614	0,7903	0,9483	0,9811	0,9775	0,9471	0,9790	0,9794	0,9652	0,9749	0,9577	0,9017	0,9654	0,9563	0,9995	1	0,9966	0,5689
DBA3A *C	0,9499	0,9572	0,8242	0,9614	0,9811	0,9788	0,9534	0,9858	0,9792	0,9646	0,9792	0,9528	0,8955	0,9617	0,9513	0,9973	0,9966	1	0,5913
LOI (corr.)	0,5757	0,5419	0,6626	0,6450	0,5855	0,5925	0,5793	0,6165	0,5900	0,5646	0,5809	0,5435	0,5332	0,5708	0,5454	0,5732	0,5689	0,5913	1
LOI (proba.)	0,0006	0,0014	<,0001	<,0001	0,0004	0,0004	0,0005	0,0002	0,0004	0,0008	0,0005	0,0013	0,0017	0,0006	0,0012	0,0006	0,0007	0,0004	<,0001

5.4.2 PAH outlier analysis

To reveal possible outliers in the data matrix, a Jackknife Distances outlier analysis is run on all measured PAH concentration levels in *all lakes at all depths*. As much as 10 out of 32 (>30 %) sediment samples are identified as outliers (positioned above the blue, dotted line that indicates the Upper Control Limit [UCL = 10.32]) with respect to the correlation structure (figure 14). As for the metal outlier analysis, Hundsvatn (all depths), Rasvassvatn (all depths) and Jordtjenn_{con} (depth 1.5 cm) stand out. In addition, Fisketjenn 0.5 positions as an outlier. Several of the outliers have just crossed the UCL-line and hold a limited vertical distance to the data points below the UCL-line. This implies that the chance that these particular outliers being part of any differing sediment process affecting their concentration levels, is low (i.e. Fisketjenn 0.5, Hundsvatn 0.5 and Rasvassvatn [all depths]). Hundsvatn 1.5, 2.5 and 3.5 have an increased distance to

the UCL-line and the other data points, while Jordtjenn_{con} 1.5 is positioned as an extreme.

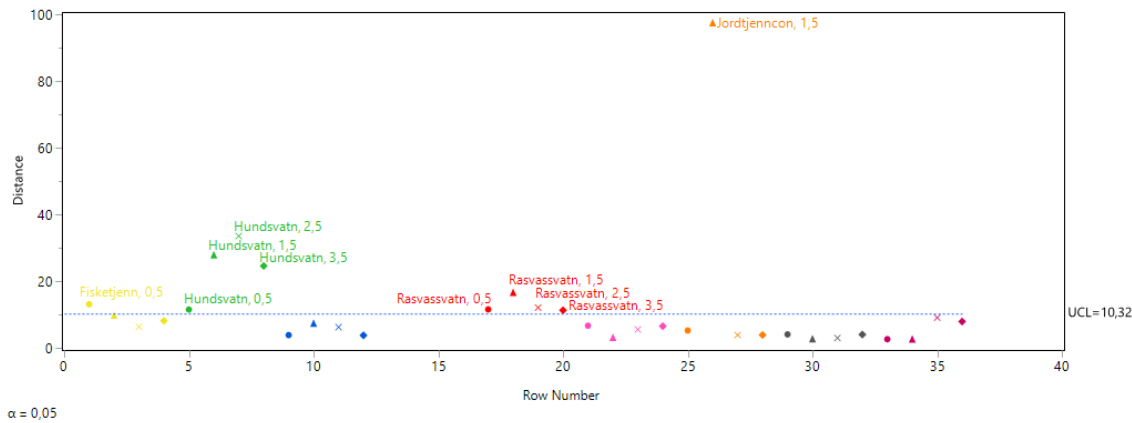


Figure 14 A Jackknife Distances outlier analysis at significance level $\alpha = 0.05$ identify Fisketjenn 0.5, Hundsvatn (all depths), Rasvassvatn (all depths) and Jordtjenn_{con} 1.5 as outliers (positioning above the blue, dotted line that indicates the Upper Control Limit [UCL = 10.32]).

A fit $Y (\Sigma PAH_{EPA16+2})$ by $X (LOI \%)$ residual plot (figure 15) reveals that Hundsvatn and Rasvassvatn have much higher concentrations of PAHs than expected, when compared to the content of sediment organic matter (LOI).

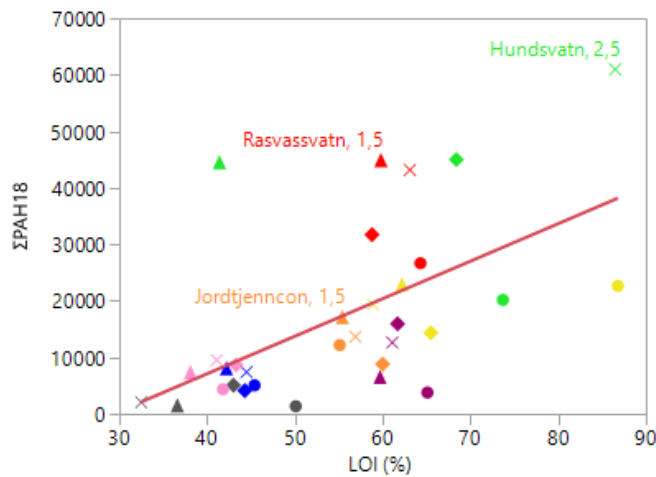


Figure 15 A Fit $Y (\Sigma PAH_{EPA16+2})$ by $X (LOI \%)$ residual plot reveals that Hundsvatn and Rasvassvatn have much higher concentrations of PAHs than expected, when plotted against the content of sediment organic matter (LOI).

Consulting table 7 on measured PAH concentrations, a BKF peak in Jordtjenn_{con} 1.5 is found, and both Hundsvatn and Rasvassvatn have high ΣPAH concentrations at all depths, except a marked drop in Hundsvatn 0.5. Furthermore, Hundsvatn has a high

content of LOI, with large fluctuations between depths 2.5 (86.5 %) and 1.5 (41.4 %) cm.

The scatter plot in figure 19 (ch. 5.4.6) run on all measured PAHs (i.e. individual PAHs) confirms the results from the residual plot (figure 15). Hundsvatn and Rasvassvatn position along the fit line towards the upper right within each scatterplot on PAH correlations, mostly within the density ellipse. Hundsvatn 2.5 has the most extreme positioning as it situates almost exclusively in the upper right corner for all individual PAH-to-PAH correlations. Such positioning shows that both corresponding PAHs hold high concentration levels, compared to PAH concentrations in other lakes or at other depths. In the scatter plot, Jordtjenn_{con} 1.5 positions outside the density ellipses only for BkF. BkF positions almost orthogonal to the fit line with a weighty distance and with relatively high concentration levels compared to the corresponding PAHs. Still, BkF holds significant and strong correlations, including pronounced linearity, to all other PAHs.

From this it is decided to include all outliers in further analysis is taken. Still, outliers can be strongly influential and should be kept under observation.

5.4.3 Dominant PAH concentrations

Which of the sampled PAHs to dominate sediment concentrations, are of interest. Concentration levels (LOI-normalized) and fluctuation patterns with sediment depth reveals that $\Sigma\text{PAH}_{\text{LMW}}$ have the lowermost levels at all sampled depths in all lakes when compared to $\Sigma\text{PAH}_{\text{HMW}}$, which hold the highest concentration levels. ΣPAH concentration fluctuations follow a homogenous pattern downcore in the sediment and across lakes (figure 16). PAH_{LMW} follow an increasing concentration order (prevailing trend on median concentrations) of $\text{ACNE} < \text{ACNLE} < \text{FLE} / \text{DBTHI} < \text{ANT} < \text{NAP} < \text{PA}$ through the whole sediment column, while the increasing order of PAH_{HMW} is $\text{DBA3A} < \text{BaA} < \text{BaP} < \text{PYR} < \text{FLU} / \text{BkF} < \text{CHR} < \text{BEP} / \text{BghiP} < \text{IcdP} < \text{BbjF}$. Considering both PAH_{LMW} and PAH_{HMW} together, the prevailing trend on median concentration levels follow an increasing order of $\text{ACNE} < \text{ACNLE} < \text{FLE} / \text{DBTHI} < \text{ANT} < \text{NAP} < \text{DBA3A} < \text{BaA} < \text{PA} < \text{BaP} < \text{PYR} < \text{BkF} / \text{FLU} < \text{CHR} < \text{BEP} / \text{BghiP} < \text{IcdP} < \text{BbjF}$ (figure 17, ch. 5.4.4). Note how PA (PAH_{LMW}) positions between BaA and BaP (both PAH_{HMW}).

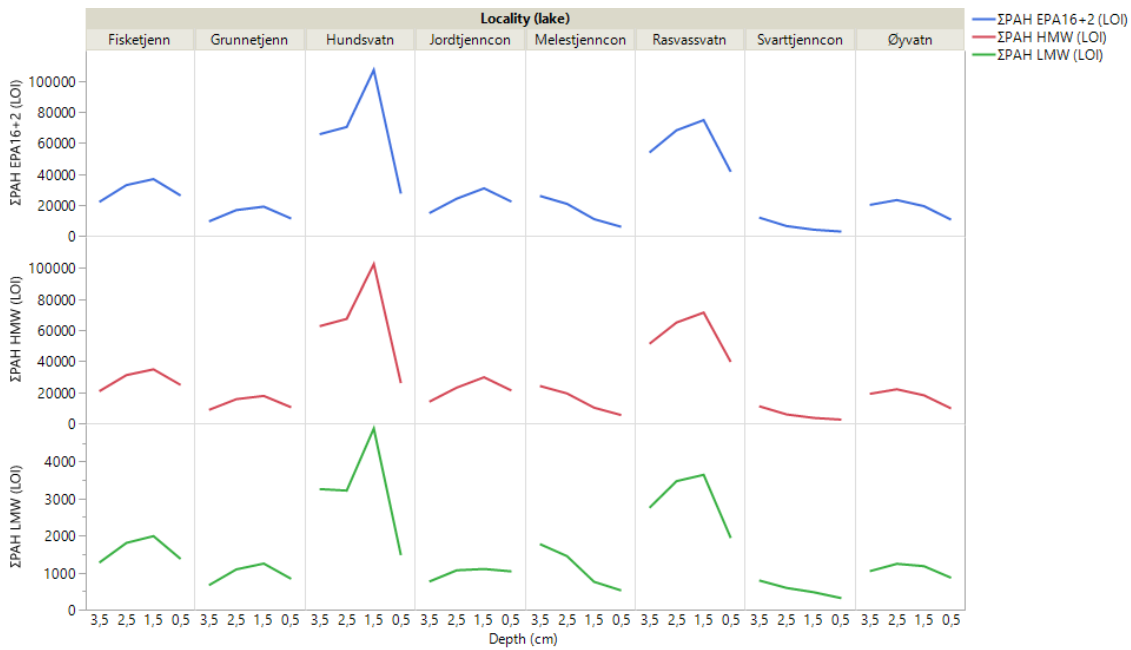


Figure 16 Concentration fluctuations with sediment depth across lakes reveals the prevailing concentration order of three PAH totals in Mykland lake bed sediments; ΣPAH_{LMW} in the lowermost section and ΣPAH_{HMW} in the intermediate section. The upper panel is $\Sigma PAH_{EPA16+2}$.

5.4.4 Depth profile on PAH concentration fluctuation thru time

Vertical fluctuations of single PAH concentrations (LOI-normalized) across lakes are compared to reveal any (dis)similarities relevant to wildfire impact (figure 17). To ease visual interpretation, the number of depths illustrated are reduced (depth 2.5 cm omitted, all depths in figure 30, Tables and figures). An aspect worth noting is the lower concentration levels of PAH_{LMW} (i.e. NAP, ACNLE, ACNE, FLE, ANT and DBTHI) relative to the PAH_{HMW} (FLU, PYR, BaA, CHR, BbjF, BkF, BaP, BeP, BghiP, IcdP, DBa3A) and the positioning of PA_{LMW} , as seen in chapter 5.4.3.

There is a general trend of increasing PAH concentrations from the deepest (depth 3.5 cm) sediment section to sub-surface (depth 1.5 cm) for all PAHs / $\Sigma PAH_{EPA16+2}$ (figure 16 and 17) in Fisketjenn, Hundsvatn, Grunnetjenn, Rasvassvatn and Jordtjenn_{con}. The control lakes Svarttjenn_{con} and Melestjenn_{con} differ from this, with declining PAH / $\Sigma PAH_{EPA16+2}$ concentrations in this sector. In Øyvatt, there is a minute $\Sigma PAH_{EPA16+2}$ decline, mostly due to a concentration drop in PAH_{HMW} (e.g. IcdP, BGHIP, BkF). Several PAH_{LMW} (e.g. NAP, ACNE, FLE) increase.

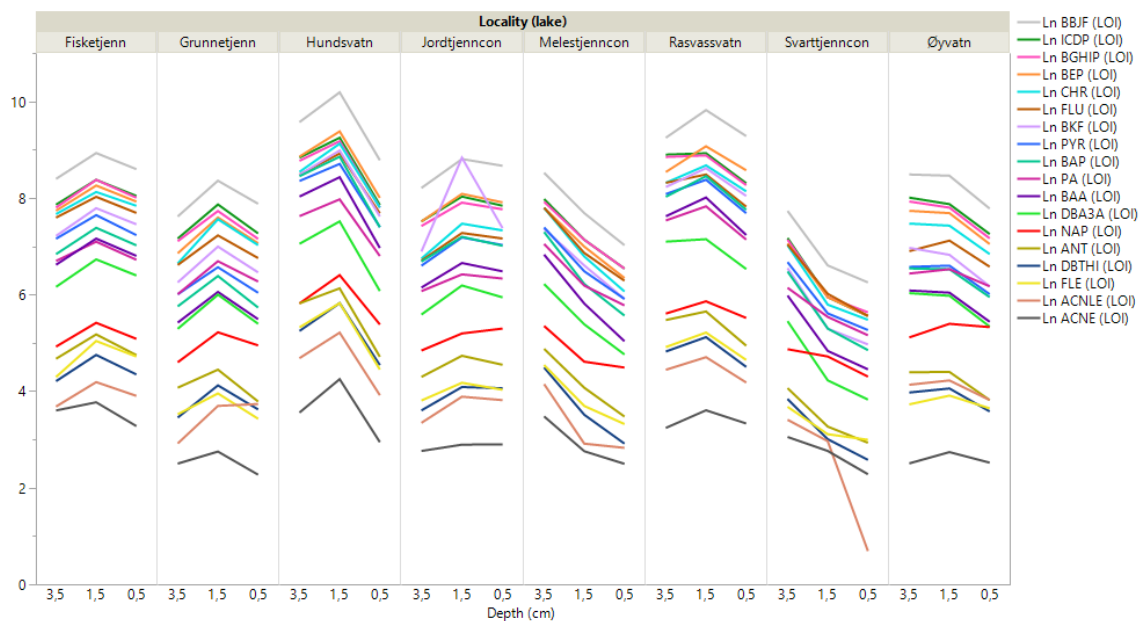


Figure 17 All individual PAH_{LOI} concentrations, and consequently $\Sigma PAH_{EPA16+2}$, increase from sediment section 3.5 to 1.5 in Fisketjenn, Hundsvatn, Grunnetjenn, Rasvassvatn and Jordtjenn_{con}. In Svarttjenn_{con} and Melestjenn_{con} there is a general concentration decline for all single PAH_{LOI} . In Øyvavn all PAH_{LMW} (including FLU) increase from depth 3.5 to 1.5 cm, while all PAH_{HMW} decline (PYR_{HMW} increase). Consequently, $\Sigma PAH_{EPA16+2}$ displays a minute decline in Øyvavn. From depth 1.5 to 0.5 cm all individual PAH_{LOI} concentrations, and consequently $\Sigma PAH_{EPA16+2}$, decline in all lakes; Fisketjenn, Hundsvatn, Grunnetjenn (ACNLE_{LMW} increases), Rasvassvatn, Øyvavn, Jordtjenn_{con} (NAP_{LMW} increases), Svarttjenn_{con} and Melestjenn_{con}. The number of depths illustrated are reduced (depth 2.5 cm omitted) to enhance visual interpretation / patterns.

From sub-surface to surface sediments, all PAHs follow the same declining trend (figure 17, percentage reductions in table 24, Tables and figures). No peak is projected for any PAH compound on a general basis, nor for the PAH totals (figure 16, ch. 5.4.3). Some single PAHs (i.e. ACNLE_{LMW} in Grunnetjenn, and NAP_{LMW} in Jordtjenn_{con}) increase slightly from sub-surface to surface and hence, differ somewhat from the prevailing trend of a sub-surface to surface PAH decline.

The individual PAHs follow the pattern of $\Sigma PAH_{EPA16+2}$. Within lakes, the lines representing single PAHs keep roughly the same distance through the sediment profile (consequently lines do not cross, BEP in Rasvassvatn, and NAP in Svarttjenn_{con} being two of the few exceptions), expressing that concentration levels of single PAHs fluctuate at comparable rates within lakes, and that their temporal relative abundances

persist. Across lakes, the order of the lines is unaltered (as is the distance between them), reflecting that the spatial (across lakes) relative PAH composition stays about unaffected, independent of initial PAH concentration levels.

5.4.5 PCA on LOI-normalized PAH concentrations

A PCA on Ln PAH_{LOI} at all depths for all lakes (outliers included), illustrates that 93.3 % of the total variance in the data can be explained by one principal component (PC 1). PC 2 explains only 3.1 % (figure 18). From the scree plot (figure 18, upper left) it is evident that the second dimension (PC 2) of the PCA has an eigenvalue below one (0.5529). It is therefore of little influence, as it accounts for less variance than the original variable (which would have a variance of one) (UCLA 2018). Hence, the results propose one explanatory factor for PAH concentrations in the sampled lake sediments.

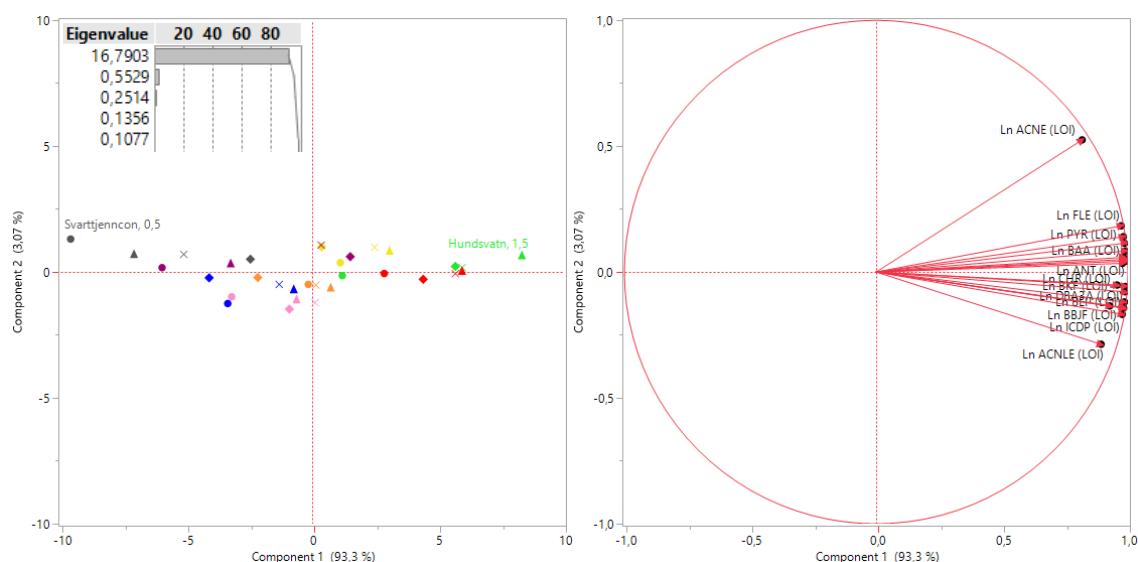


Figure 18 93.3 % of all the variance in the dataset can be explained by one principal component (PC 1) when running a PCA on Ln PAH_{LOI} at all depths for all lakes (outliers included). Solid dots represent PWF sediments, triangles represent pre-fire sediments, while diamond squares represent the deepest sediment layer (depth 3.5 cm).

In the loading plot (figure 18, right) individual PAH compounds load positively and quite equal along PC 1 (table 23, Tables and figures). Such arrangement implies correlations between PAHs (table 8, ch. 5.4.1). Based on positioning, ACNE seems to differ somewhat from the other PAHs. From the score plot (figure 18, left) it is apparent that Hundsvatn and Rasvassvatn exerts great influence on all PAH loadings.

Interestingly, sub-surface (depth 1.5 cm) sediments have higher scores than their

corresponding surface sediment sections along PC 1. Such pattern implies diminishing PAH concentrations from pre-fire (sub-surface) to post-fire (surface) sediments.

Excluding outliers Hundsvatn 1.5, 2.5, 3.5, Rasvassvatn 1.5 and Jordtjenn_{con} 1.5 (the ones with the greatest distance to the UCL-line) does not alter the results to any noteworthy degree; the second explanatory variable still has an eigenvalue below one (0.7940), suggesting one explanatory variable. The two dimensions PC 1 (91.4 %) plus PC 2 (4.4 %) account for 95.8 % of the total variance in the data. The positioning of the PAHs, including ACNE, is not interrupted (not shown).

5.4.6 Scatter plot of PAH correlations

A scatter plot (figure 19) on Ln PAH_{LOI} (all lakes at all depths, outliers included) confirms strong linear correlations among all PAHs (correlation coefficient threshold value for significant ($\alpha = 0.05$) correlations calculated according to Walsh (1998); $n = 32$, $r > 0.3536$). Since the excluded PAH PER has no bearing on the analyses, Ln PER_{LOI} is included in the scatter plot to illustrate the lack of correlation ($r \leq 0.2649$) with other PAHs (ch. 4.2.1). A weak ($r = 0.3753$) correlation with low probability ($p = 0.0343$) and no linearity between PER and ACNE, is seen.

The scatter plot demonstrates the same tendency as the results from the PCA; strong ($r > 0.7$) positive correlations with a pronounced linearity between all PAHs. Only a singular exception correlate below the 0.7 threshold value for strong correlations; ACNLE to ACNE ($r = 0.6445$). Note positioning of Hundsvatn 1.5 (outlier) for NAP, ACNE and DBTHI correlations, Jordtjenn_{con} 1.5 (outlier) for BKF correlations (increased concentrations relative to corresponding PAHs) and positioning of Svarttjenn_{con} 0.5 for ACNLE.

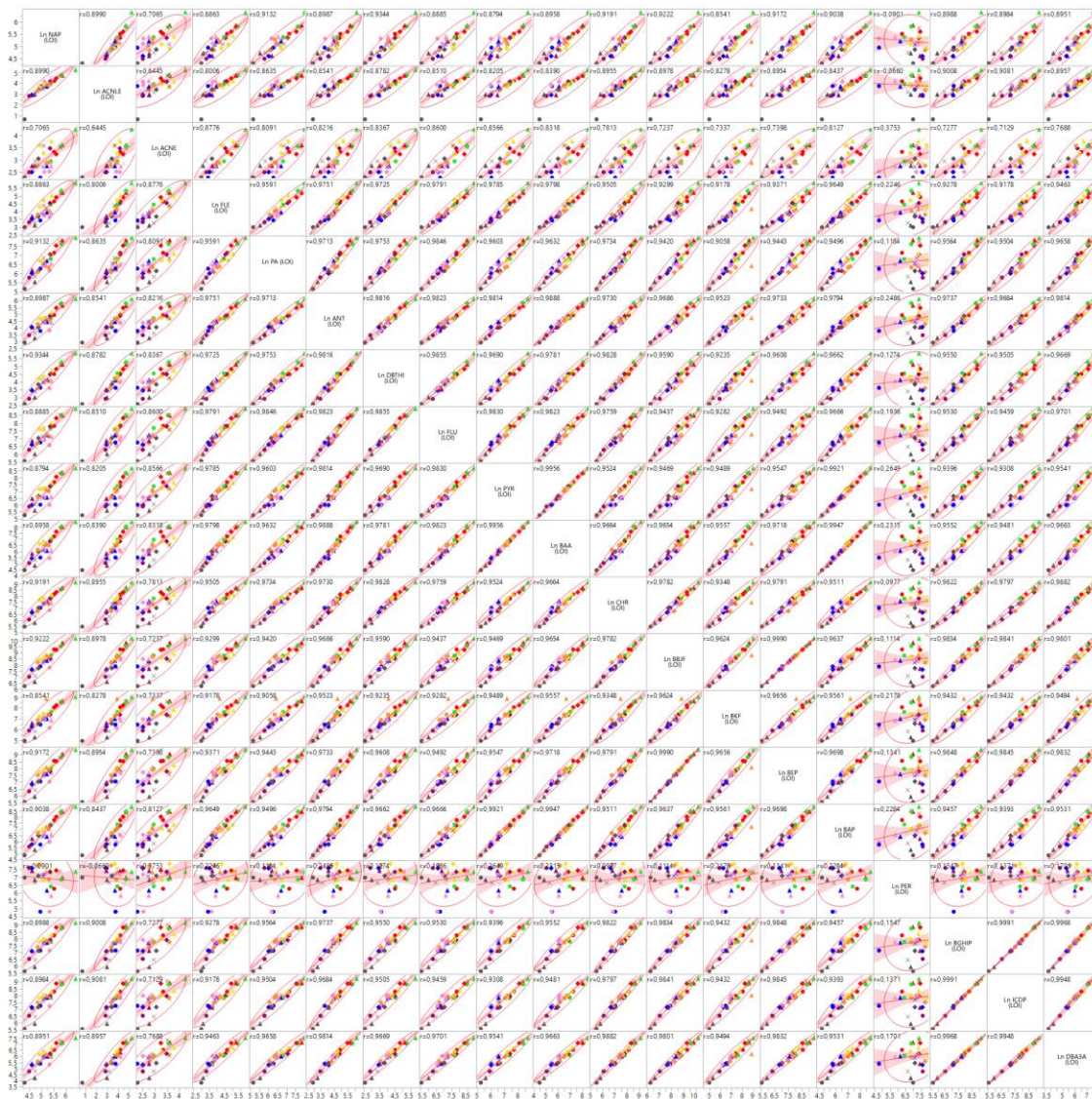


Figure 19 Scatter plot on Ln PAH_{LOI} correlation. The matrix displays strong ($r > 0.7$), positive and linear correlations between all PAHs, except PER ($r \leq 0.2649$). Only a singular exception correlate below the 0.7 threshold value of strong correlations; ACNLE to ACNE ($r = 0.6445$).

5.4.7 Clustering of depths, lakes and PAH_{LR}

A hierarchical two-way clustering dendrogram (method = ward) is run on LR converted PAH concentrations (LR PAH). In the figure each lake holds a specific colour, depths are identified by their figures, while clusters are grouped together. LR PAH are found beneath the “pixeled” dendrogram mosaic, divided into LR PAH_{LMW} (ACNE < FLE < DBTHI < ANT < NAP < PA) and FLU_{HMW} to the left, and LR PAH_{HMW} DBA3A < BaA < BaP < PYR < BkF < CHR < BEP < BghIP < IcdP < BbjF) and ACNLE_{LMW} to

the right. In the transition between the two groups ACNLE (PAH_{LMW}) and FLU (PAH_{HMW}) positions.

Weighting (i.e. contribution to the $\Sigma\text{PAH}_{\text{EPA16+2}}$) of each variable (i.e. LR PAH) relative to the others are represented on a continuous three colour scale; red colours represent high LR PAH contributions to the PAH total, while blue colours represent low LR PAH contributions. Red colour fading to grey represents declining relative contributions, while blue colour fading to grey represents increasing relative contributions (figure 20). The scree plot below the dendrogram (bottom right) propose the best suitable number of clusters in the material. The line crossing the “knee point” in the scree plot indicates four clusters (starting at the top):

1. Fisketjenn 0.5 – Melestjenn_{con} 0.5
2. Svarttjenncon 0.5 – Svarttjenn_{con} 2.5
3. Grunnetjenn 0.5 – Grunnetjenn 3.5
4. Hundsvatn 0.5 – Jordtjenn_{con} 1.5

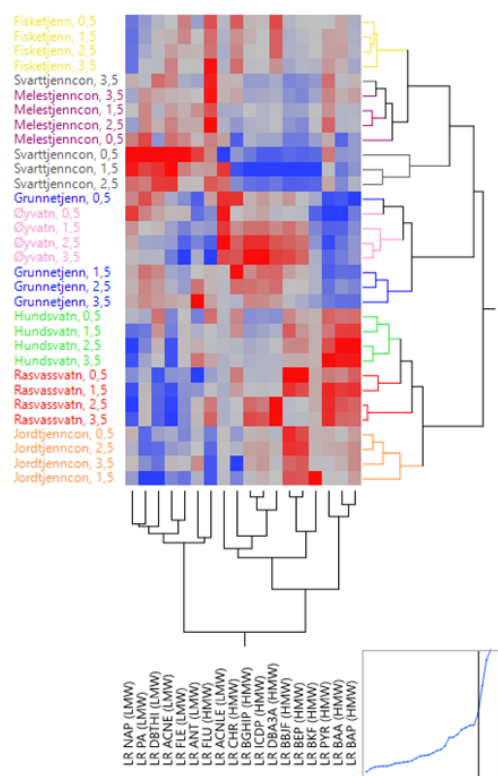


Figure 20 A hierarchical two-way clustering dendrogram (method = ward) run on LR converted PAH concentrations, demonstrates that lakes rather than depths tend to cluster. Each lake is given a specific colour, depths are identified by their figures, while clusters are grouped together (to the right). The scree-plot at the bottom right corner indicates the recommended number (i.e. four) of clusters (at “knee point”).

The dendrogram demonstrates that lakes rather than depths tend to cluster. When sediment segments of equal depth do not cluster, these sections have comparatively

little in common (interlake dissimilarities) regarding PAH concentrations. Instead lakes cluster, proposing intralake similarities. These similarities are downcore in each sediment column (temporal), not across lake sediment samples of equal depth (spatial).

5.4.8 PAH relative abundances – Log ratio (LR) biplot

A PCA (outliers included) on LR PAHs (ch. 4.4.5) displays the same clustering tendency between lakes rather than depths, as the dendrogram. Examining one lake (markers of identical colour in the biplot) at the time, it is evident that there is little difference in how surface (solid circles) sediments relative to corresponding deeper sections position in the biplot. Thus, similarities are greater within each lake (all depth sections within each lake cluster), than between sediment sections of equal depth (sections of equal depths do not cluster across lakes) (figure 21).

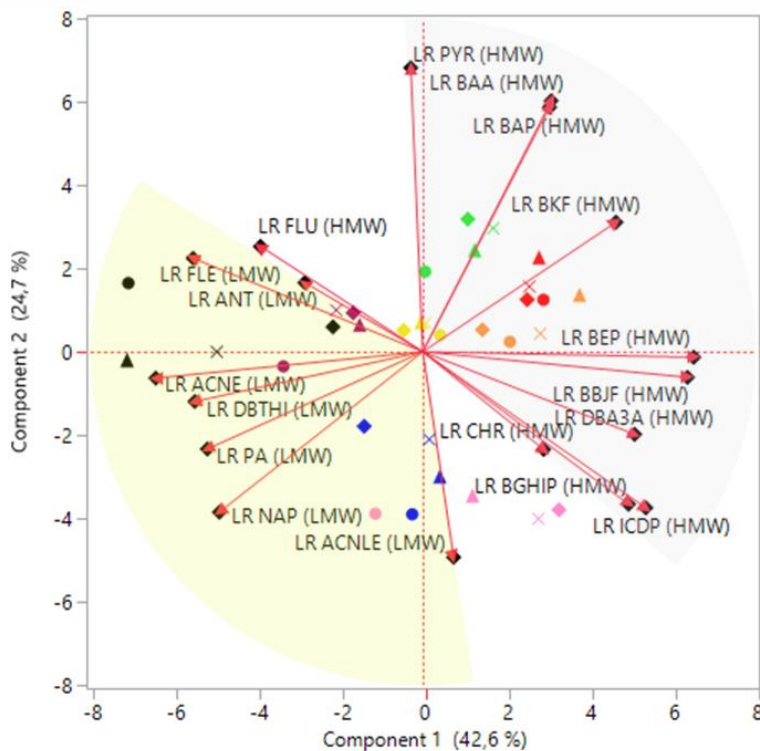


Figure 21 A PCA biplot on LR PAH conclude that 77.9 % of all variance in the dataset can be expressed by three principal components. BeP_{HMW} , $BbjF_{HMW}$, $IcdP_{HMW}$, $DBa3A_{HMW}$, $BghiP_{HMW}$ and BkF_{HMW} load along PC 1 (42.6 %), while along PC 2 (24.7 %) PYR_{HMW} , BaA_{HMW} and BaP_{HMW} load. Lakes rather than depths tend to cluster. There is little difference in how the two uppermost sediment sections position in the biplot.

77.9 % of the variance in the dataset can be expressed by three principal components. PAH_{HMW} (shaded grey) tend to load in the opposite direction of PAH_{LMW} (shaded khaki). BEP_{HMW}, BBJF_{HMW}, ICDP_{HMW}, DBA3A_{HMW}, BGHIP_{HMW} and BKF_{HMW} load along PC 1 (42.6 %), while along PC 2 (24.7 %) PYR_{HMW}, BAA_{HMW} and BAP_{HMW} load (table 9).

Table 9 Formatted loading matrix from the PCA on LR PAH (outliers included). Cells shaded green indicate weighty loads on a principal component (PC). Red digits load in the opposite direction (negatively) of black digits (positively) along the PCs. BeP_{HMW}, BbjF_{HMW}, ICDP_{HMW}, DBA3A_{HMW}, BGHIP_{HMW} and BKF_{HMW} load along PC 1 (42.6 %), while along PC 2 (24.7 %) PYR_{HMW}, BaA_{HMW} and BaP_{HMW} load.

Eigenvalue	PC 1 (42.6%)	PC 2 (24.7%)	PC 3 (10.6%)	PC 4 (7.7%)
	7.6590	4.4478	1.9072	1.3876
LR BEP (HMW)	0,9158	-0,0183	-0,2527	0,0088
LR BBJF (HMW)	0,8948	-0,0865	-0,2440	-0,0438
LR ICDP (HMW)	0,7539	-0,5272	0,2837	0,2342
LR DBA3A (HMW)	0,7161	-0,2788	0,5809	0,1388
LR BGHIP (HMW)	0,6955	-0,5148	0,3617	0,2934
LR BKF (HMW)	0,6534	0,4377	-0,1914	0,1672
LR PYR (HMW)	-0,0405	0,9589	0,0799	-0,0520
LR BAA (HMW)	0,4338	0,8476	0,1366	-0,1611
LR BAP (HMW)	0,4284	0,8258	-0,1624	-0,1134
LR FLE (LMW)	-0,7766	0,3158	0,1157	0,1568
LR FLU (HMW)	-0,5490	0,3561	0,6367	-0,2934
LR CHR (HMW)	0,4085	-0,3297	0,5249	-0,5495
LR ANT (LMW)	-0,3989	0,2333	0,2844	0,7196
LR ACNE (LMW)	-0,9029	-0,0889	-0,0943	0,1356
LR DBTHI (LMW)	-0,7710	-0,1679	0,0724	-0,3032
LR ACNLE (LMW)	0,1040	-0,6936	-0,3329	-0,3258
LR PA (LMW)	-0,7285	-0,3284	0,3026	-0,0226
LR NAP (LMW)	-0,6878	-0,5414	-0,3939	0,0922

5.5 Metal and PAH distribution in relation to lake parameters

To uncover possible influences and correlations among the data, ΣPAH_{EPA16+2}, LOI and lake parameters (i.e. residence time [RT], total organic carbon [TOC], pH) have been introduced to the PCA (figure 22) on metal concentrations (outliers included, pre-industrial depth 33.0 cm excluded).

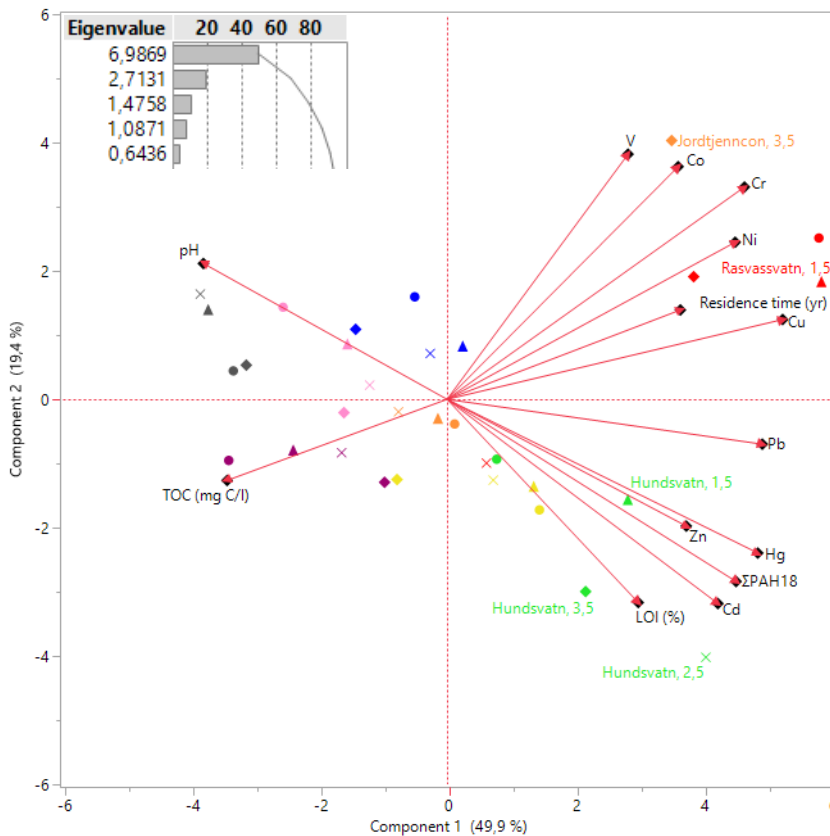


Figure 22 PCA on metals, $\Sigma\text{PAH}_{\text{EPA16+2}}$, LOI, TOC, pH and RT (depths 3.5 – 0.5, outliers included). Three dimensions (PC 1; 49.9 %, PC 2; 19.4 % and PC 3; 10.5 %) in the component space account for 79.8 % (cumulative percentage) of the total variance in the data set. The fourth dimension (PC 4) and on, has an eigenvalue <1.0871, and accounts for little of the variance.

Three dimensions (PC 1; 49.9 %, PC 2; 19.4 % and PC 3; 10.5 %) account for 79.8 % of the variance in the data. The fourth dimension (PC 4) and on has an eigenvalue <1.0871, and thus accounts for little of the variance. All parameters load positively along PC 1, except pH and TOC which load in the opposite direction. Along PC 2 metals are split in two clusters (V, Cr, Co, Ni, and Zn, Cd, Hg, respectively) loading in opposite directions (table 18, Tables and figures). From the PCA Hundsvatn score on Zn, Cd, Hg, Pb, $\Sigma\text{PAH}_{\text{EPA16+2}}$ and LOI loadings, while Rasvassvatn and Jordtjenn_{con} 3.5 score on V, Cr, Co, Ni, Cu and RT loadings. pH is negatively correlated to LOI and TOC is negatively correlated to RT. This means that metal concentrations are strongly influenced by Hundsvatn, Rasvassvatn and Jordtjenn_{con} 3.5, with the RT of Rasvassvatn and LOI content in Hundsvatn's sediments being important parameters.

A correlation matrix (table 19, Tables and figures) run on the data confirms the clustering of metals seen in the PCA. Cu, Zn, Cd, Hg and Pb correlate ($n = 32, r$

>0.3536 , $\alpha = 0.05$) to $\Sigma\text{PAH}_{\text{EPA16+2}}$ ($0.5015 \leq r \leq 0.8708$) and each other, while only Cu, Cd and Hg correlate to LOI. Negative pH correlations to Cu, Cd and Hg are good ($-0.4992 \leq r \leq -0.7590$). Hg and Pb correlate negatively to TOC. The metals in the V, Cr, Co and Ni cluster correlate to each other and RT (not V), but not to LOI, $\Sigma\text{PAH}_{\text{EPA16+2}}$ or pH. Ni and Cr correlate (negatively) to TOC. Note that Cu correlates to V, Cr, Co, Ni, Zn, Cd, Hg, Pb, $\Sigma\text{PAH}_{\text{EPA16+2}}$, RT, LOI and pH (negatively). To test whether any metals correlate to Fe in terms of source apportionment (ch. 4.2.1), Fe is included in the correlation matrix; the metal cluster V, Cr, Co, Ni and RT correlates to Fe ($0.4450 \leq r \leq 0.8021$). Mn correlations are not shown in the table 19 (not correlated to any metals but Fe [$r = 0.3903$] and Ni [$r = -0.3362$]). A table with correlation probabilities are found in Tables and figures (table 20).

6 Discussions

6.1 Aim of study and results

Sediment contaminants in Mykland have, including wildfire, several natural and anthropogenic origins. Natural sources are attributed to weathering of bedrock, while anthropogenic sources comprise regional point (e.g. high temperature industry) and diffuse (e.g. shipping and offshore activities in the maritime sector) sources, in addition to LRTAP (Aamot, Steinnes & Schmid 1996; Rognerud *et al.* 2008). Lacustrine waterbodies are probable recipients of metals and PAHs mobilized and redistributed during combustion and ensuing processes of wildfire (Abraham, Dowling & Florentine 2017). In waters, metals and PAHs have propensity to adsorb on settling particles and become incorporated into lake bed sediments. Deposits potentially persist for a long time. Assumingly, wildfire affected waterbodies show elevated concentrations of metals and PAHs in bed sediments, representing a latent source of pollution hazardous to life, as metals and PAHs are at risk of being re-mobilized from the sediment (Sprovieri *et al.* 2007; Yao & Gao 2007; Christensen *et al.* 2008; Zeng *et al.* 2013).

To evaluate lacustrine sediments as repository depots of metals and PAHs from a boreal forest wildfire in the Fennoscandian Peninsula, temporal and spatial concentrations of nine metals and 18 PAHs in lake bed sediments are described. The analyses rely on sample outtakes at four depth intervals from eight separate freshwater sediment cores, retrieved in 2010, two years after the fire. Five cores originate from separate freshwater lakes within the perimeter of the burnt area, while three cores derive from nearby, unburnt control lakes, representing pre-fire conditions. In addition, six pre-industrial depths are sampled (only metal concentrations analysed).

The results reveal that all⁴ surface sediments are polluted with several PAH_{HMW} (i.e. PYR, BaA, CHR, BbjF, BkF, BghiP, IcdP, DBa3A), NAP_{LMW}, ANT_{LMW} and Pb (ECC III – V). Half of the lakes (i.e. Fisketjenn 0.5, Hundsvatn 0.5, Rasvassvatn 0.5 and Jordtjenn_{con} 0.5) are polluted with ACNLE_{LMW} (not Jordtjenn_{con} 0.5) FLU_{HMW}, BaP_{HMW}, Zn (not Fisketjenn 0.5, but Melestjenn_{con} 0.5), Cd and Hg (not Jordtjenn_{con} 0.5) (ECC III – IV). For ACNE_{LMW}, FLE_{LMW}, PA_{LMW}, DBTHI_{LMW}, BeP_{HMW}, V, Cr, Co, Ni and Cu ECC is either good (ECC ≤II) or there is no environmental quality standard (EQS) for the substance.

Depth profiles on measured metal concentrations and LOI-normalized PAH concentrations show a declining trend when pre-fire sediments are held against PWF sediments. Fisketjenn, Hundsvatn, Grunnetjenn, Øyvatn and Melestjenn_{con} display declining concentration levels from sub-surface to surface sediments for Co, Ni, Zn, Cd, Hg_{LOI} and Pb (ch. 5.3.4). All PAHs follow the same declining trend from sub-surface to surface sediments (ch. 5.4.4). No distinct peak in PWF concentration levels of metals or PAHs is detected. Two separate cluster analyses on metals (ch. 5.3.7) and PAHs (ch. 5.4.7), respectively, group lakes rather than depths. These clusters question temporal (downcore) contrasting trends. It appears that a given depth have more in common with divergent depths within the lake (temporal similarities), rather than sediment sections of corresponding depth across lakes (spatial differences). Sediment sections of equal depth cluster only for pre-industrial (depth 33.0 cm) sediments (PCA and cluster analysis on metals, ch. 5.3.5 and 5.3.7, respectively). Surface sediments that potentially share a signal of fire impact, do not. Thus, surface sediments hold no properties that are mutual across lakes, to form a cluster which separate PWF sediments from the other depths. In terms of metal and PAH concentration levels and composition, a distinguishable metal / PAH impacted PWF sediment section is not expressed by the cluster analyses.

In other words, surface sediments share no signal of any metal and / or PAH contamination in response to wildfire, strong enough to counter the general decline documented for these substances in the region (Rognerud *et al.* 2008). In contrast to the anticipated concentration increase in burnt lakes (Hegna 1986; Naturvårdsverket 2006; Høgberget 2010; Vergnoux *et al.* 2011; Odigie & Flegal 2014; Köhler, Wallmann & McKie 2017), there is a decline. This is in accordance with regional trends described in national surveys on pollutants in air, precipitation, vegetation and lake sediments (e.g. Rognerud *et al.* 2008). The initial increase in metals and PAHs seen in water samples during the first PWF rainstorm event, is untraceable two years after the fire (Høgberget 2010).

To evaluate the results, wildfire and PWF processes are of relevance, as are environmental factors, analytical techniques and the sampling campaign.

6.2 Sampling campaign, material and time lapse since fire

Without adequate care, sampling procedure can become the weakest link in a study. Non-representative or incorrectly collected or stored samples, may lead to erroneous

conclusions. To design an efficient sampling strategy, location selection criteria and sampling technique are of critical importance.

In shallow zones of a lake there is a continuous shift between sedimentation and resuspension, while in the deepest part, the accumulation zone, sedimentation will be dominant. It is crucial that sediments are derived from the accumulation zone material to ensure representative time trends to be mapped (e.g. deposits settle chronologically and are undisturbed). In Nordic forest lakes with surface area less than 1 km², the accumulation zone occurs from approximately two meters depth, with sediments typically consisting of a homogeneous mixture of fine grained particles, depositing at rates about $1.2 \pm 0.5 \text{ mm yr}^{-1}$. As lakes in Mykland are small forest lakes (Melestjenn_{con} 0.01 km² [min.] and Rasvassvatn 0.89 km² [max.]), the accumulation zone is expected at a few meters depth, if not wind exposed (Rognerud, Fjeld & Løvik 1999; Rognerud & Fjeld 2001; Rognerud *et al.* 2008). With a depth of three meters, Grunnetjenn and Øyvavn are the shallowest of the sampled lakes. It is reasonable to assume that sediment samples obtained from the deepest part of these lakes will be suitable for detecting any historical change in deposition of contaminants.

Identifying locations where lake bed sediments likely hold representativeness is most sufficiently determined on basis of *a priori* information about the region (e.g. geology and processes influencing on sediment distribution) and knowledge about bottom dynamics (e.g. accumulation rates) (International Atomic Energy Agency 2003). Such information can be obtained through online database resources (e.g. *ngu.no*; bedrock geology – *kartverket.no*; aerial photography [*norgebilder.no*] and topography [*hoydedata.no*] – *nve.no*; hydrological data, lake morphometrics, drainage patterns and basins – *nibio.no*; land use etc.). In this study, much of this information have been collected *ad hoc*. On the contrary, regional (Rognerud, Fjeld & Løvik 1997; Rognerud *et al.* 1997) and national lake surveys (Rognerud & Fjeld 1990; Rognerud, Fjeld & Løvik 1999; Rognerud *et al.* 2008) have provided valuable information in advance of the sampling campaign, on processes to influence on sediment distribution. Likewise, two research reports (Storaunet *et al.* 2008; Høgberget 2010) on the environmental impact of the 2008 Mykland wildfire, published during the first two years following fire, have been taken into account as supplementary information. On basis of the outlined preparations, it is considered that the retrieved sediment cores (both burnt and unburnt) hold representativeness and should not bias the study.

In retrospect, influence of topography (e.g. steep hill northwest of Rasvassvatn) and vegetation cover (e.g. Heitjenn excluded from the analysis because of both its location on top of a hill and lack of surrounding vegetation) may have been somewhat underrated; the results from Rasvassvatn positions as an outlier, with elevated concentration levels of several constituents compared to other lakes. On the other hand, the number of headwater lakes that position within the perimeter of the fire, is limited. Lakes are generally shallow (e.g. Grunnetjenn and Øyvatn), with the risk of sediment mixing. Some lakes are influenced by land use (the three control lakes are slightly affected by different kinds of land use, including road salt [NaCl]) or have been limed. To secure some robustness in the data, the number of sampled lakes should not be decimated, and if all parameters with possible influence on the analysis should be considered, it would be a difficult task to find suitable lakes for sediment sampling. Besides, the results of the analysis show rather strong correlations among the data, suggesting common influences and that sampled sediments capture the general picture. The extensive PWF logging conducted in the catchment of Rasvassvatn (Høgberget 2010), and to some degree in the catchments of Grunnetjenn, was not known in advance of the sampling campaign. Neither was the dumping of powdered limestone into a stream entering Svarttjenn_{con} (ch. 4.1.2).

To enable comparison of samples retrieved from sites with diverse environmental conditions, it is of paramount importance with standardized sampling techniques, guidelines for sample storage, and that sample preparations fulfil analytical requirements (International Atomic Energy Agency 2003). To meet these necessities, sampling protocols are followed as described in chapter 4, Material and methods (and references therein). Still, bottom sediments are soft and fluffy. Not using an echo sounder (or its similar) to locate the sediment-water interface when lowering the sediment fetcher, may result in loss of surface sediment (“blow-off”) and / or compaction (“shortening”) of the sediment core, if submerging the sediment fetcher into the sediment to rapid or abruptly.

Sampling fluffy soft bottom sediments with a depositing rate about $1.2 \pm 0.5 \text{ mm yr}^{-1}$ (Rognerud & Fjeld 2001) makes variations within a two years (years since the burn) time interval difficult to capture. Margins are minute on a millimetre scale, making sediment core sectioning (without segment mixing) demanding. Further, removal of sediment cores’ overlying water by siphon, makes flocculent surface sediments prone to

disturbance, risking loss of sediment matter from the sediment-water interface. Only sediment cores (visually inspected and judged during fieldwork) with an apparently undisturbed sediment-water interface, a homogenous colour (no smell of H₂S) and uniform mixture of fine particles, have been used for this study. The homogenous results suggest that loss of top sediment matter or shortening unlikely occurred, since deviant concentration levels supposedly would appear across lakes. Nonetheless, capturing only PWF material in a 10 mm thick surface sample retrieved only two years after fire, is not likely. Even if splitting the uppermost sediments in <5 mm thin sections, pre-fire matter is to be expected.

6.2.1 Dating and mixing of sediments

Age chronologies on sediment cores Hundsvatn, Rasvassvatn and Jordtjenn_{con} are derived from radiometric dating of sediments at depth 0.5, 1.5, 2.5, [...], 14.5 cm. Sediment concentrations of metals and PAHs represent 1.0 cm thick sediment sections (0.0 – 1.0, 1.0 – 2.0, 2.0 – 3.0, 3.0 – 4.0 and a reference section at depth 33.0 ± 11.5 cm). Conservative calculations of sediment age at the interface (i.e. at depth 1.0 cm) between surface (i.e. depth section 0.0 – 1.0 cm) and sub-surface (i.e. depth section 1.0 – 2.0 cm) sediments in Hundsvatn (ch. 5.1.1) and Jordtjenn_{con} (ch. 5.1.3), estimate deposition year to 2002 ± 2 yrs. / 2001 ± 2 yrs., respectively, while in Rasvassvatn to year 2007 ± 1 yr (ch. 5.1.2). Assuming the accumulation rates of Hundsvatn and Jordtjenn_{con} represent the sampled lakes better than Rasvassvatn does, which has diverging catchment characteristics (steep and basin-shaped catchment, larger lake volume, greater residence time and subjected to extensive PWF logging), it becomes obvious that the sampled surface sediments (depth 0.0 – 1.0 cm, termed 0.5 cm and regarded post-fire sediments) can be expected to contain considerable amounts of *pre*-fire material from year 2001/2002 ± 2 yrs. to mid-2008, and less PWF (from mid-2008 to mid-2010) material. A stable accumulation rate points toward a proportion of approximately 20 % (two out of ten years) PWF matter. Pre-fire matter dominates (80 %) the sample outtake.

Along with the general concentration decline of metals and PAHs in surface sediments, vast contributions of pre-fire matter can govern sediment concentrations of these chemicals, such that a possible fire signal is camouflaged.

Also, post-depositional processes, typically confined to the upper sediment stratum or across the sediment-water interface, may redistribute the initial chronology of sediments

(including metal and / or PAH carrying particles) or deplete contaminant concentrations, questioning the sampled sediment profiles reliability in terms of reconstructing deposition histories. As metals and PAHs become allocated to deeper sediments through sediment mixing, input pulses in the upper sediments tends to be homogenized, and variations in the original accumulation history can be reduced or eliminated. Sediment mixing is caused by a variety of geochemical processes and physical events (e.g. strong wind, water currents, wave action or flooding). None the less, the most frequent process resulting in sediment surface disturbances is the activity of benthic organisms, referred to as bioturbation (physical reworking of sediments by feeding and/or burrowing activities of all kinds of organisms⁵).

Whether surface sediments have undergone mixing processes can be diagnosed with a radioisotope tracer, like lead ²¹⁰Pb. Rather than the expected exponential decay pattern associated with no mixing and constant sedimentation, mixed surface sediments display a distinct flattening in radioactivity in the upper profile (Outridge & Wang 2015). In Mykland, surface sediments do not show any sign of such, leading to an assumption of restricted surface sediment mixing. Similarities between sediment profiles of metal and PAH concentration fluctuations with sediment depth (across lakes), supports this assumption. Moreover, in the accumulation zone of small Norwegian forest lakes, influences of bioturbation on sediment mixing is minor, mainly because the stock of benthic species is relatively modest and consists of small individuals, such as *Chironomid larvae*, *Oligochaeta*, and *Pisidium* (Rognerud, Fjeld & Løvik 1999). This should not lead to the conclusion of no PWF sediment mixing at all in Mykland.

6.2.2 Analytical techniques

PAH analyses were done with a Gas Chromatograph/Mass Selective Detector (GC/MSD). Denis *et al.* (2012) discuss the use of GC/MSD when analysing PAHs produced during natural fires. High performance liquid chromatography with fluorescence detector (HPLC/FLD) demonstrate to be superior to GC/MSD for detecting low concentrations of sedimentary PAHs derived from forest fires. A concern is the limit of detection because PAHs are typically studied as pollutants in concentrations much higher than those produced by wildfires. PAHs are easily detected using GC/MSD when concentrations are high. However, HPLC/FLD detects and selects for PAHs at greater sensitivities. The HPLC/FLD's sensitivity and selectivity is particularly important for detecting and quantifying PAHs where only small volumes of

sediment are available. Concentration levels below detection limit have only been valid for one substance (ACNLE) in one sample (Svarttjenn_{con} 0.5) in this study (ch. 4.4.5). The sensitivity and selectivity (some PAHs are grouped together as a single compound, cf. Introduction) of GC/MSD have been sufficient for this study.

6.3 Metals, PAHs and sediment organic matter (LOI)

Lake sediments ability to reflect changes in metal and PAH deposits depends on the nature of the sediment, especially the content of organic matter (expressed by LOI). General LOI tendencies across lakes should be emphasized, while downcore single-lake fluctuations are of less importance (Rognerud, Fjeld & Løvik 1999). When sediment LOI >10 %, LOI will not affect the metal and PAH analysis to any influential degree, as long as the inter-lake differences are not too extensive (ch. 4.3.2 and Rognerud *et al.* 2008). Organic matter content in the sampled Mykland lake bed sediments (ch. 5.2) is high (all LOI values exceeds 30 %), and interlake differences of LOI_{median} span within a narrow 10 % interval range (54.3 % ± approximately 10 %). These features meet the above referred criteria for sediments to reflect deposition history of metals and PAHs.

In accordance with previous studies (Rognerud, Fjeld & Løvik 1999), the variations in organic matter content from pre-industrial to surface sediments in Mykland, are limited. When comparing LOI_{median} reference (52.40 % at 33.0 cm) to LOI_{median} surface (59.70 % at 0.5 cm) sediments across lakes, values are quite equal (about 14 % increase), proposing decomposition of sediment organic matter in Mykland lakes to be a slow process, where the general sediment structure is stable on century long time scales, and thus, well suited as archives of deposition history.

Metals and LOI

In sediments deposited within industrial time, Cu, Cd, Hg and Pb correlate to LOI ($0.4 < r < 0.6$) (table 5, ch. 5.3.2), each other and $\Sigma\text{PAH}_{\text{EPA16+2}}$ (table 19, Tables and figures). Correlations suggest one common source of origin (Budzinski *et al.* 1997; Soclo, Garrigues & Ewald 2000). When associated to organic matter, that source is thought to be atmospheric deposition (Rognerud, Fjeld & Løvik 1999). Since Hundsvatn score on Cu, Cd, Hg, Pb and LOI loadings (figure 22, ch. 5.5), an assumption can be made; levels of these metals in Hundsvatn are dominated by atmospheric deposition.

Hg and Pb form strong complexes to soil organic matter and mobility is less sensitive to pH reductions. Reduced pH even enhances binding of Hg to humus. Therefore, concentrations of Hg and Pb in lake sediments are often dominated by atmospheric deposition directly onto lake surfaces, and hence, LOI association is expected in sediments. Nonetheless, rapid soil mineralization, like wildfire induced mineralization of soil organic matter, can liberate Hg and Pb and increase transport to receiving waterbodies. There is little evidence for that to have happened in Mykland, even for the mobile element Cd (mobilize from soils through acidification, but to a lesser extent associate to settling particles in acidic lake environments) (Rognerud & Fjeld 1990; Rognerud, Fjeld & Løvik 1999).

The lack of correlations between V, Cr, Co, Ni, Zn and LOI needs further examination. Parvaresh *et al.* (2010) suggest scarcity of variation in these parameters as explanatory factor. Even though median values of LOI span within a narrow spatial (LOI fluctuations across lakes) and temporal (vertical differences of LOI) range, as described above, measured concentrations of LOI still vary at considerably rates (LOI % across lakes at depth 2.5 cm range from 32.5 – 86.5, LOI % across depths within one lake [Fisketjenn] range from 58.9 – 86.8), and measured metal concentrations vary comparably.

Rognerud, Fjeld and Løvik (1999) propose geochemical dominance on metal concentration levels when not associated to LOI. This seems like a more plausible explanation. Since Rasvassvatn score on V, Cr, Co, Ni and RT loadings (figure 22, ch. 5.5), an assumption can be made; levels of these metals in Rasvassvatn are dominated by geochemical sources.

The two metal clusters (i.e. V, Cr, Co, Ni and Zn, which are *not* correlated to LOI, and Cu, Cd, Hg and Pb, which *are* correlated to LOI, cf. ch. 5.3.5 and 5.3.7) are influenced to a diverging degree by atmospheric deposition and geochemical weathering, as described in Rognerud, Fjeld and Løvik (1999). To this there should be noted that the area surrounding Hundsvatn is rather flat, consist of several bogs, while extensive parts of Rasvassvatn's catchment are quite steep and have been subjected to extensive PWF logging by the use of a forwarder (ch. 4.1.2 and Høgberget 2010).

The lack of V, Cr, Co, Ni and Zn correlations to LOI might signal that not every lake or sediment is equally suited to reflect different loads of pollutants, due to natural conditions and anthropogenic activities.

PAHs and LOI

PAHs are correlated ($r > 0.7$) (table 8, ch. 5.4.1). Such good correlations suggest one common source of origin (Budzinski *et al.* 1997; Soclo, Garrigues & Ewald 2000). PAHs also correlate to LOI ($r > 0.5$, $\rho < 0.002$). When associated to organic matter, that source is thought to be atmospheric deposition of LRTAP and domestic sources (Rognerud, Fjeld & Løvik 1999). Since no peak in PAH concentration in surface sediments is detected, PAHs in Mykland's surface sediments are most likely dominated by PAHs originating from LRTAP and domestic sources.

In the biplot on LR PAH (figure 21 and table 9, ch. 5.4.8), HMW PAHs BeP, BbF, ICDP, DBA3A, BGHIP and BkF load along PC 1 (42.6 %), while HMW PAHs PYR, BaA and BaP load along PC 2 (24.7 %). Within both groups, PAHs correlate, suggesting one common source of origin (Budzinski *et al.* 1997; Soclo, Garrigues & Ewald 2000). The HMW PAHs BeP and BaP are the two most well-known carcinogens, both mainly derived from petrogenic sources (Oliveira *et al.* 2011). According to a study by (Vergnoux *et al.* 2011) on impact of forest fires on PAH levels in soils, wildfires generate mainly PAH_{LMW}, at least when considering PAH impact in proximity to the fire (Denis *et al.* 2012). PAH_{LMW} are volatile and prone to degradation compared to PAH_{HMW}. In the biplot, LR PAH_{HMW} (positively) and LR PAH_{LMW} (negatively) load in opposite directions. Two years after the 2008 Mykland wildfire, there is little evidence of a fire impact on sediment PAH concentrations and composition.

Also seen in the biplot, the two PAH clusters (i.e. BeP and BaP, respectively) are not correlated. The BeP-cluster loading along PC 1, consists of PAHs with higher molecular weight than PAHs in the BaP-cluster (cf. table 11, Tables and figures). Considering the LOI-association of all PAHs, and that they share a common source of origin (i.e. atmospheric deposition of "petrogenic PAHs" from domestic sources and LRTAP), BeP, BbF, ICDP, DBa3A, BGHIP and BkF in Mykland sediments possibly originate from sources with somewhat differing proximity to Mykland, than the comparable lighter PYR, BaA and BaP (greater potential of aerial transport (Rognerud *et al.* 2007)). In the biplot Hundsvatn score on these concentrations.

6.4 PAH and metal mobility - terrestrial soil burn off and organic matter decline

Within a catchment, forest floor soils may act as a source of pollution long after deposition of contaminants, because forest soil is a strong adsorbent (complexing ligands) for metals (Rognerud, Fjeld & Løvik 1999). Wildfire induced mineralization of soil organic matter liberate these metals accumulated in vegetation and soil (Naturvårdsverket 2006; Høgberget 2010; Pereira & Úbeda 2010; Bladon *et al.* 2014). Furthermore, wildfire combustion of OM can decompose soil humus (Bleken, Mysterud & Mysterud 1997; Neary, Ryan & DeBano 2005) and produce PAHs. Soil OM declines, while PWF levels of metals and PAHs (in soils) are raised due to deposition of ash (Kim, Oh & Chang 2003; Lydersen *et al.* 2014). Increased PWF runoff and erosion intensify the transport of both metals and PAHs from terrestrial to aquatic systems, especially during rainstorm events (Naturvårdsverket 2006; Høgberget 2010; Luo *et al.* 2013; Odigie & Flegal 2014), which is considered a primary variable for the PWF response processes (Moody *et al.* 2013). Due to their abilities to form complexes, organic matter and humic substances have key functions in transport and supply of metals and PAHs to aquatic environments. No pre-fire data exist on TOC values in surface waters around Mykland, but Lydersen *et al.* (2014) and Høgberget (2010) argue for a possible PWF TOC decline within the first PWF year, owing to combustion of OM during fire. Fan *et al.* (2011) report that declining inputs of organic matter in lakes might be somewhat linked to a decline in Σ PAH.

Wildfire, and its prelude, drought, mineralize organically bound sulfur (S) to sulfate (SO_4^{2-}) and oxidize inorganic sulfide (S^{2-}) to sulfate. Subsequently, sulfate follow the drainage water as sulfuric acid (H_2SO_4) during PWF heavy rain discharge. This process has an acidifying effect, as it produces hydrons (H^+), thus increasing the mobility of metals (Naturvårdsverket 2006; Høgberget 2010). Høgberget (2010) finds this scenario likely in Mykland and record increased PWF acidification in burnt lakes. Lydersen *et al.* (2014) also document increased acidification during the first PWF hydrological episodes in the burnt Mykland lakes. Strong acid anions, as Cl^- but primarily SO_4^{2-} , are mobilized from terrestrial to aquatic systems at a faster rate than base cations (ΣBC), leading to a decline in lake acid neutralizing capacity (ANC: $[\Sigma\text{BC}] - [\text{SAA}]$), with subsequent increase in hydrons (pH decline). This is in accordance with previous

studies on base-poor boreal forest streams (Bayley *et al.* 1992), similar to conditions in large parts of Norwegian nature.

In other terms, pulses of increased PWF runoff during torrential rain, containing acidic drainage water, metals as dissolved ions, PAHs, particles and low levels of organic matter, enters the thermally stratified lakes (Lydersen *et al.* 2014). The lowered pH and reduced amounts of TOC in lake waters, restrict metal and PAH sedimentation (Rognerud, Fjeld & Løvik 1999; Skjelkvåle *et al.* 2008). Consequently, ionic metals and PAHs bound to ash (Lydersen *et al.* 2014) or other particles with low settling velocities (Smith *et al.* 2011), may wash through the lake system, rather than deposit, especially during rainstorm events like the one on August 13th 2008 (Bladon *et al.* 2014).

Along with the general decline in atmospheric supply of pollutants in the Mykland region, the amount of acid rain has declined considerably during the latest decades. Thus, Mykland is much less susceptible to acidification episodes and subsequent consequences. Although, the small forest lakes of Mykland are the most vulnerable (Schartau 2011; Lydersen *et al.* 2014; Nizzetto, Aas & Warner 2017).

6.5 PWF degradation of PAHs

Contrary to metal elements, PAHs are subjected to several degradation mechanisms, such as chemical oxidation, photolysis, volatilization and biodegradation. Biological degradation is regarded as the most influential mechanism, and a wide variety of algal, fungal and bacterial species have the potential to degrade / transform PAHs (Ghosal *et al.* 2016).

It is difficult to diagnose to which extent PWF PAHs are degraded in the sampled lakes or in the terrestrial environment, but it should be considered that PWF PAH concentration levels may be affected by one or several of the parameters mentioned above. For instance, solar radiation is likely to increase, both onto soils and lake surfaces, when forest vegetation is burnt off.

The sampled lakes are shallow and oligotrophic, with a varying degree of dystrophy (Høgberget 2010). Relatively low nutrient content within a lake, leads to low productivity and generally clear waters due to the limited algae growth. High water transparency allows light to penetrate further into the water masses and makes photolysis possible. On the other hand, several factors counter photolytically

degradation, for instance if PAH molecules are shielded from sunlight. Lydersen *et al.* (2014) report declining PWF water transparency (despite reduction in TOC), which attenuates sunlight penetrating the water column. Also, PAHs deposited in PWF ash (Smith *et al.* 2011) become shielded from sunlight if the PAH molecules are sorbed to ash particles which allow them to deposit inside the ash particle structure. The trend of a PAH decline in surface sediments speak against extensive protection from PAH degradation (Abdel-Shafy & Mansour 2016). Instead, it is an interesting notion that sulfate (SO_4^{2-}) can enhance biodegradation of sediment PAHs (Yan *et al.* 2012).

6.6 PWF metal removal

Areas most exposed to LRTAP are generally also areas most vulnerable to supply of acid rain, like southern Norway (Rognerud, Fjeld & Løvik 1999), an area little resistant to acidification (Lydersen *et al.* 2014). Water pH and TOC content are important parameters for the transport of metals from terrestrial surfaces to lakes (as metals are liberated more easily in acidic water) and subsequent sedimentation. Thus, most metals (e.g. Ni, Cu, Zn, Cd, Pb) appear as free cations in waters with low pH. Mobile elements such as Ni, Zn and Cd (mobilized from soils through acidification), associate to a lesser extent to settling particles in acidic lake environments (Rognerud & Fjeld 1990; Rognerud, Fjeld & Løvik 1999), while Hg and Pb form strong complexes to soil organic matter. Mobility is less sensitive to reductions in pH, compared to Ni, Zn and Cd. Reduced pH even enhances binding of Hg to humus. Rapid soil mineralization, like wildfire induced mineralization of soil organic matter, can liberate Hg and Pb and increase transport to receiving waterbodies (Rognerud & Fjeld 1990).

The most striking result from the PWF sampling campaign in Mykland, is the lack of a fire signal on metal and PAH concentrations in surface sediments compared to sub-surface sediments. Still, sediments are polluted (ch. 6.1). The decline is in accordance with regional trends describing reduced supply of pollutants in air, precipitation, vegetation and lake sediments (Nizzetto, Aas & Warner 2017). In unburnt areas, like where the control lakes are located, an analogous decline would be expected in lake sediments. In this study the results display a decline similar to the regional trend, most pronounced for PAHs in Svarttjenn_{con} and Melestjenn_{con} (ch. 5.4.4). Metals decline only in Melestjenn_{con} (ch. 5.3.4). Somewhat surprisingly, this decline is also seen in the five burnt lakes (ch. 5.4.4).

PWF drainage water from the burnt catchments holds low pH and contribute to reduced lake pH, compared to unburnt sites. This may reduce sedimentation of metals entering lakes, and may also re-mobilize metals from sediments, thus reducing sediment concentrations (ch. 6.4). For instance, the LOI-associated metals Cd and Hg decline from sub-surface to PWF sediments in all burnt lakes. It is tempting to ask if not the PWF Cd and Hg increase in Jordtjenn_{con} and Svarttjenn_{con} (ch. 5.3.4) is an inversed fire signal; atmospheric deposition of fire-generated metals increase sediment concentrations of Cd and Hg in lakes which are located in proximity to the fire, and that hold less acidic water (higher pH compared to burnt, PWF acidified lakes). This is left to speculations.

In the region surrounding Mykland, deposited metals like Co, Ni, Cu, Zn, Cd, Pb etc. are generally associated to sediment OM or bound in the sediment mineral fraction, and unlikely affected by redox-driven migration of Mn-/Fe-(hydr)oxides after deposition (ch. 4.2.1). It is reasonable to assume, that for metals only indirectly affected by redox reactions (e.g. Co, Ni, Cu, Zn, Cd, Pb), altered concentration levels in sediments could relate to historical changes in loads. However, concentrations of mobile metals such as Zn and Cd, may decline in sediments by acidification, as a lower proportion of the total concentration binds to depositing particles in an acidic environment (Rognerud, Fjeld & Løvik 1999; Rognerud *et al.* 2008).

In general, declining pH, RT and lake depth reduce the chance of sedimentation for most metals analysed in this study (Rognerud & Fjeld 1990).

6.7 Metal distribution in relation to lake basin environmental factors, RT & metal clustering

A lake's capacity as sediment trap (proportion of material that deposits permanently) increases with increasing lake volume and water RT. Still, annual sediment growth will often be greater in lakes with short RT because the total inflow of allochthonous material from the discharge area is greater (Rognerud, Fjeld & Løvik 1999). Among the sampled Mykland lakes RT (τ) vary considerably. The RT of Rasvassvatn is 1160.9 days (τ_{\max}), which is 3.2 years. Compared to this, Svarttjenn_{con}, which has a RT of 2.1 days (τ_{\min}), appear closer to a lotic than lentic waterbody. The median RT value is 35.3 days, τ_{average} is 185.7 days. Hundsvatn has a RT of 75.9 days. Variation in lake volume between Hundsvatn and Rasvassvatn is major. Hundsvatn (lake volume 648 000 m³) has

six times the lake volume of Fisketjenn (109 000 m³), and Rasvassvatn (4 573 000 m³) has seven times that of Hundsvatn. How short RT increases sediment growth is not reflected in the lakes' respective accumulation rates. Hundsvatn and Jordtjenn_{con} have stable accumulation rates (0.04 kg⁻² yr⁻¹), while Rasvassvatn on the other hand, has a varying and higher accumulation rate, reaching from 0.06 / 0.07 kg⁻² yr⁻¹ in the years before fire, to 0.10 kg⁻² yr⁻¹ after fire (table 2, ch. 5.1). This is the opposite of what would be expected (short RT followed by high accumulation rates).

Relative concentration levels of V, Cr, Co, Ni and Cu are greater in Rasvassvatn (which has long RT accompanied by greater accumulation rate) at depth 3.5, 1.5 and 0.5 cm, compared to the other lakes. In figure 10 (ch. 5.3.5), Rasvassvatn score on the loadings of these metals. When not LOI associated (table 5, ch. 5.3.2), these metals are expected to have geochemical origin (Rognerud, Fjeld & Løvik 1999). Relative concentration levels of the LOI correlated metals Cd, Hg, Pb and ΣPAH_{EPA16+2} (table 19 and 20, Tables and figures) are greater in Hundsvatn at depth 3.5 and 1.5 in comparison to the other lakes. In figure 10 (ch. 5.3.5), Hundsvatn score on loadings of these metals.

Correlations between Cd, Hg, Pb and PAHs in sediments are reported by Müller, Grimmer and Böhnke (1977) and suggested by Wang *et al.* (2004) to have shared sources. When LOI associated, Cd, Hg, Pb and PAHs are believed to origin from atmospheric deposition, mainly as LRTAP (Rognerud, Fjeld & Løvik 1999).

Comparing Hundsvatn and Rasvassvatn when considering the splitting of metals into two clusters, the two lakes have some similar characteristics. They are the deepest (depth 13.0 meters and 15.4 meters, respectively) and largest (lake area 0.15 km² and 0.89 km², respectively), and together with Fisketjenn (pH 4.8), they also have the lowest pH (4.9) of the sampled lakes. In Grunnetjenn, Jordtjenn_{con}, Svarttjenn_{con}, Melestjenn_{con} and Øyvavn (pH 5.8), pH is 5.3/5.4 (table 1, ch. 4.1.2). Both Hundsvatn and Rasvassvatn are dimictic (temperature stratified during summer) (Lydersen *et al.* 2016) and experienced a drop in pH (pH 4.4 in Hundsvatn and 4.8 in Rasvassvatn) during a PWF rain storm event (rainfall: 119 mm) in August 13th 2008 (Lydersen *et al.* 2014).

On the contrary, Hundsvatn is a smaller (lake area 0.15 km²) lake compared to Rasvassvatn (lake area 0.89 km²). The two lakes are situated on each side of a drainage divide. Hundsvatn is the downstream lake of both Fisketjenn and Grunnetjenn, located within a rather flat and larger (2.63 km²) catchment area, consisting of bogs (Høgberget & Kleiven 2013) which are less burnt. Rasvassvatn is positioned close to a quite steep

hillside within a smaller (1.23 km²) catchment subjected to extensive PWF logging with the use of a forwarder (ch. 4.1.2 and Høgberget 2010), while there has been no such activity in the area surrounding Hundsvatn. Reduction of vegetative cover by forest harvesting generally increases average surface runoff volume. Consequently, discharge for a given area of land will peak (Suryatmojo *et al.* 2013).

With the diverging accumulation rates and surface sediment age (ch. 5.1) in mind, sediments in Rasvassvatn contain mostly material from the PWF years 2008 – 2010, while sediments in Hundsvatn contain considerably amounts of pre-fire matter (years 2002 ±2 yr – 2010). It is to be expected that the splitting of metals into two clusters (i.e. *Zn, Cd, Hg, Pb, and V, Cr, Co, Ni, Cu*) is affected by a combination of the topography surrounding Hundsvatn (including probable effects of bogs that are not burnt, and Hundsvatn being a downstream lake of four lakes of which three are burnt) and Rasvassvatn (increased inflow of inorganic particles [cf. Høgberget 2010], increased accumulation rate and less pre-fire matter), and the long RT and the PWF logging in Rasvassvatn's catchment (Lydersen *et al.* 2016). Lake RT is a poorly explored factor in previous studies of wildfire effects on lakes (Lydersen *et al.* 2014).

Interestingly, the outlier Jordtjenn_{con}, which RT is only 8.3 days, also influence considerably on the divide clustering of metals (high concentration levels at depth 3.5 cm compared to the other lakes).

6.8 Partitioning of correlated metals – source apportionment

Within the sediment all metals correlate (Co does not correlate to Cd or Hg), nonetheless, partitioning into two clusters; *Zn, Cd, Hg, Pb, and V, Cr, Co, Ni, Cu* (figure 13, ch. 5.3.7). Within each cluster, correlations are stronger than across clusters (figure 19, Tables and figures). In the PCA (figure 10, chapter 5.3.5) reference depths (33.0 cm) cluster to the left. The splitting of metals into two separate clusters is strongly influenced by the industrial section of lakes Hundsvatn (influence on Zn, Cd, Hg and Pb), Rasvassvatn and Jordtjenn_{con} 3.5 (both lakes influence on V, Cr, Co, Ni and Cu). Jordtjenn_{con} 3.5 is an outlier in the data analysis, as well as Rasvassvatn 33.0. Fisketjenn, Grunnetjenn, Øyvavn, Jordtjenn_{con} (i.e. depth 0.5, 1.5 and 2.5 cm) and Melestjenn_{con} are positioned close to the centre of the PCA and hardly influence on the split (Rognerud, Fjeld & Løvik 1999). Metal concentrations in sediments deposited within industrial time are determined by local geochemistry and contributions from both

natural and anthropogenic atmospheric deposits. Rognerud, Fjeld and Løvik (1999) describe the dominant source of origin for the two groups of metals; *V, Zn, Cd, Hg, Pb* mainly originating from LRTAP, and *Cr, Co, Ni, Cu* from local sources, including geochemical origin. *V* may also have geochemical origin (Rognerud, Fjeld & Løvik 1999).

Along the coast of southern Norway, deposited metals and PAHs in lacustrine sediments mainly originate from continental Europe (as result of long-range atmospheric transport), regional industry (including off-shore activities) and, to a far lesser extent, local geochemical weathering (Rognerud *et al.* 2008). In environmental studies of sediment contaminants, strong correlations of different chemicals / groups of chemicals indicate that sediment substances are associated and may originate from the same source, while weak correlations point towards mixed sources (Müller, Grimmer & Böhnke 1977; Soclo, Garrigues & Ewald 2000; Wang *et al.* 2010). When LOI-associated, metals and PAHs are believed to originate (on both continental and regional scale) from atmospheric deposition (Rognerud, Fjeld & Løvik 1997; Rognerud *et al.* 1997). Based on the dominant sources of origin, deposited metals and PAHs in Mykland are believed to originate primarily from continental Europe as LRTAP, in addition to regional industry. LRTAP of *Zn, Cd, Hg* and *Pb* seems to be more explicit in Hundsvatn compared to the other lakes. The slightly differing pattern of *V, Cr, Co, Ni* and *Cu* indicates regional influences to be somewhat more pronounced, at least in Rasvassvatn, and / or that influences by geochemical weathering is possible (Berg & Steinnes 1997; Rognerud *et al.* 1997; Rognerud, Fjeld & Løvik 1999).

Support for such source apportionment is the (lack of) metal correlations to Fe. Sediment concentrations of *Cu, Zn, Cd, Hg* and *Pb* are not correlated to Fe, while *V, Cr, Co* and *Ni* are (table 19 and 20, Tables and figures). As Fe is mainly of local geochemical origin, this is interesting. The pattern is in accordance with assumptions that *Zn, Cd, Hg* and *Pb* (LOI-correlated / not Fe-correlated) concentrations are more influenced by LRTAP than *V, Cr, Co* and *Ni* (Fe-correlated / not LOI-correlated), which could be relatively more affected by local sources. When not LOI associated (table 5, ch. 5.3.2), *V, Cr, Co* and *Ni* concentrations can be expected to be influenced by geochemical sources (Rognerud, Fjeld & Løvik 1999). This is in accordance with the results from the PCA, as it suggests two explanatory variables (ch. 5.3.5).

6.9 Wind and smoke plume dispersal

The wildfire in Mykland was a postlude climax of a long crescendo with extreme drought. During the burn, strong winds governed (Nygaard & Brean 2014). Heat-induced convective lofting carried giant smoke plumes from the intense fire high up in the air, where they blew to sea.



Figure 23 Smoke from the 2008 Mykland wildfire was lofted high in the air and blown to sea. Photo: Erik Holand (Nygaard & Brean 2014).

Lofting of wildfire generated smoke plumes is generally followed by horizontal airborne transport to locations distant from the fire (Heilman *et al.* 2014), where fallout (i.a. Cr, Ni, Cu, Zn, Cd, Pb and PAHs) from the plumes deposits and possibly mobilize into adjacent aquatic environments (Yuan *et al.* 2008; Kim, Choi & Chang 2011; Abraham, Dowling & Florentine 2017). This mechanism reduces the amounts of metals and PAHs reaching lake bed sediments within the perimeter of the burnt area to such an extent that a sediment amplitude may not be recorded for these substances (Denis *et al.* 2012). This scenario is likely to have been part of the 2008 wildfire in Mykland. Not only were there strong winds and dry conditions (sufficient oxygen supply enhance combustion, more matter burn off and formation of hydrocarbons is restricted), but observations of unusually high concentrations of RET (ch. 3), registered at Birkenes observatory at the end of the smouldering fire, document such transport (Schartau 2009). In Denmark, beyond the vicinity of the fire, people could smell and see smoke

coming in from the sea while fire brigades moved out (Gjerstad 2008). As wind turned more westerly, smoke reached Sweden. On satellite images from the 12th and 13th of June 2008, shot by U.S. National Oceanic and Atmospheric Administration (NOAA) / The Norwegian Meteorological Institute (MET), a smoke plume rising from Mykland and crossing the North Sea is easily detected (Rommetveit 2008).

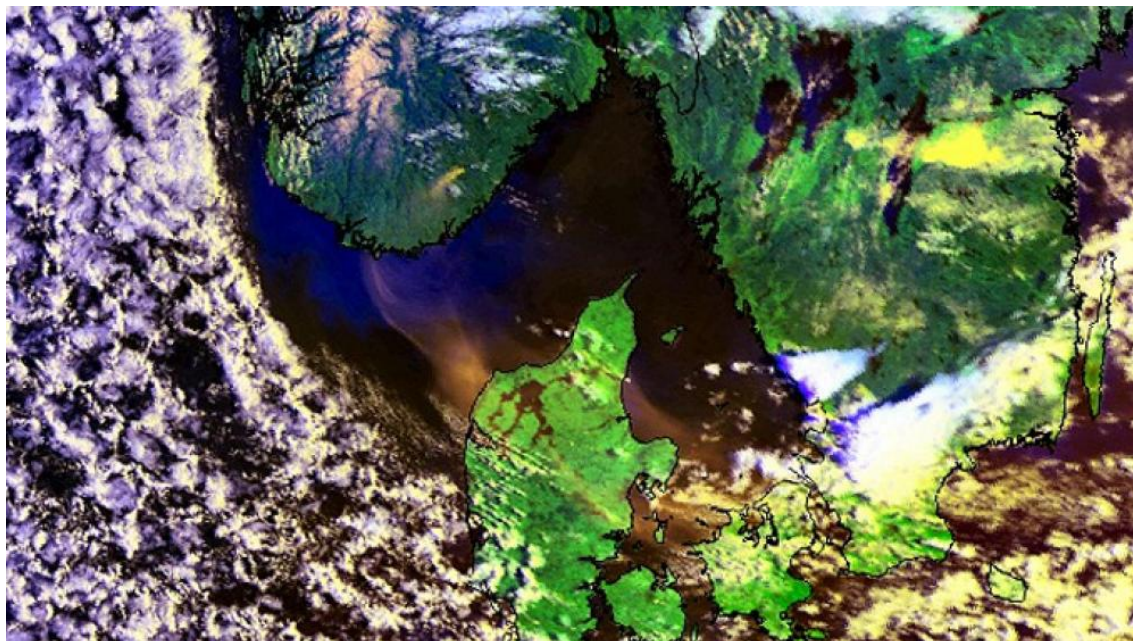


Figure 24 Satellite image of the wildfire smoke plume drifting from Mykland across the North Sea to Denmark on the 12th of June 2008 (Gjerstad 2008). Photo: NOAA/MET.no

Wildfire reduce ground cover and leave the ash covered soils exposed to wind and UV radiation (Whicker, Pinder & Breshears 2006). Increased solar radiation cause more effective vaporization and photodegradation of PAHs (especially PAH_{LMW}).

Immediately after the burn, soil surface blackening (from charring) causes a decline in albedo and an increase in surface temperatures (Veraverbeke *et al.* 2010). Airmasses are subsequently lofted due to the increased temperature, and wind is liable to increase on a local scale.

In Mykland, prolonged PWF drought (Lydersen *et al.* 2014) left the burnt area dry, hydrophobic, warm and wind exposed. Wind dissipation of PWF ash (Kim, Choi & Chang 2011) containing metals and PAHs (Lydersen *et al.* 2014) in the weeks following the fire, should be regarded a factor with possible influence on metal and PAH concentrations in surface sediments. A processes not considered herein, is reduction in soil hydrophobicity by fire, specifically in plots burned more than once (Abraham, Dowling & Florentine 2017), like in Mykland (ch. 4.1). In such scenario, percolation of

metals and PAHs upon wetting from PWF sprinkle precipitation is thinkable, consequently reducing the amount of metals and PAHs reaching the burnt lakes (Driscoll, Otton & Iverfeldt 1994).

In the view of forests already burnt by fire within industrial time, contaminants accumulated in forest biota and soils are expected to be reduced, at least for a “reasonable” period. Hence, the potential to affect downstream waterbodies can be limited (Bladon *et al.* 2014).

Another process that can bear upon the levels of metals and PAHs in PWF sediments, is the PWF uptake of metals and PAHs by biota, reducing sediment concentrations (Stankov Jovanovic *et al.* 2011; Sosorova, Merkusheva & Ubugunov 2013).

Several additional mechanisms and processes described in the literature (e.g. Neary, Ryan & DeBano 2005; Keeley 2009), can be expected to influence on the results to a varying degree. For instance, may enhanced PWF runoff increase the amount of uncontaminated, inorganic particles entering a lake. If these particles deposit, surface sediment concentrations of metals and PAHs can be “diluted”, so that a PWF signal is “camouflaged” (Neary, Ryan & DeBano 2005). During the Mykland sampling campaign, the retrieved sediment cores were visually inspected for coarse particles and larger grains. Only cores with an apparently uniform mixture of fine particles, have been used for this study (ch. 4.2), and it is not likely that “dilution” has taken place.

7 Conclusions

Forest wildfire used to be a natural prelude to secondary succession. At present, eight out of ten forest fires are caused by reckless activities of man (Lehtonen *et al.* 2014; Balch *et al.* 2017), mobilizing pollutants accumulated for decades in soil and flora (Greenberg 2003; Kabata-Pendias 2011). By measuring concentration levels in surface and sub-surface sediments two years after the 2008 Mykland wildfire, this paper sought to explore lacustrine sediments in eight lakes as recipient depots of metals and PAHs mobilized, produced and redistributed during combustion and ensuing processes of boreal forest wildfire.

The study shows that the elevated levels of metals and PAHs in runoff water during the primary PWF rainstorm event in Mykland, as reported by Høgberget (2010), are not traceable in surface sediments. In contrast to an anticipated concentration increase (Hegna 1986; Naturvårdsverket 2006; Vergnoux *et al.* 2011; Odigie & Flegal 2014), results demonstrate a decline in PAHs (ch. 5.4.4) and most metals (ch. 5.3.4). Several mechanisms and processes (ch. 6) may co-account to such results.

The decline is in agreement with regional trends of atmospheric deposits (Rognerud, Fjeld & Løvik 1999; Rognerud *et al.* 2008). Nonetheless, PWF sediments in $\geq 6/8$ of the lakes are polluted with PAH_{HMW}, Hg_{LOI} and Pb (ECC III-V). Half of the PWF sediments are polluted with Zn, Cd, Hg, ACNLE and FLU (ECC III – IV, cf. chs. 5.3 and 5.4) (Norwegian Environment Agency 2016), probably from atmospheric deposition, as most of these substances associate to LOI (Rognerud, Fjeld & Løvik 1999). It is not likely they originate from the fire (no concentration peak in surface sediments, ch. 6.1).

In an ecotoxicological perspective, lacustrine sediments contaminated with metals and PAHs pose a hazard to water quality, aquatic ecosystems and biodiversity due to the high toxicity, environmental persistence and bioavailability of these substances (Silva *et al.* 2016). Contaminants released from aquatic sediments can be absorbed by flora and fauna in the waterbody and benthic zone. Thru bioaccumulation and / or biomagnification, multiple impacts to organisms can be expected, including adverse effects on sediment-dwelling populations and changes in the structure and composition of resident communities. Ultimately, PWF contaminants may end up in humans. (Ignatavičius, Sakalauskienė & Oškinis 2006; Okafor & Opuene 2007; Yao & Gao 2007; Wang *et al.* 2012; Abraham, Dowling & Florentine 2017).

Watershed management constitutes the basis of water regulations and policies governing surface and groundwater resources (e.g. EU-WFD 2000/60/EC). In this context wildfire is importantly relevant as it is the most severe disturbance regime in boreal forests. A changing climate seems to move towards more “wildfire weather”, facing raised wildfire frequency, intensity and duration (Flannigan *et al.* 2009). Forest catchments with low levels of contaminants in soil and waterbodies are vital to provide functional habitats for wildlife. Also, urban areas rely heavily on water from such areas. More than 31 % of the global land of forested watersheds, filter and store high quality water. Thus, healthy catchment environments are a premise for the supply of potable and irrigation water, in addition to industrial and recreational use. However, supplying communities with sufficient water quality and quantity is seriously challenged by the impacts of natural and anthropogenic activities, including wildfire (Abraham, Dowling & Florentine 2017).

References

- Aamot, E., Steinnes, E. & Schmid, R. (1996) Polycyclic aromatic hydrocarbons in Norwegian forest soils: Impact of long range atmospheric transport. *Environmental Pollution*, **92**, 275-280.
- Aas, W. (2009) *Overvåking av langtransportert forurenset luft og nedbør : atmosfærisk tilførsel, 2008*. Norwegian Institute for Air Research (NILU), Oslo.
- Aas, W. (2010) *Overvåking av langtransportert forurenset luft og nedbør : atmosfærisk tilførsel, 2009. Monitoring of long-range transported air pollutants annual report for 2009*. Norwegian Institute for Air Research (NILU), Oslo.
- Aas, W. (2011) *Overvåking av langtransportert forurenset luft og nedbør : atmosfærisk tilførsel, 2010. Monitoring of long-range transported air pollutants annual report for 2010*. Norwegian Institute for Air Research (NILU), Oslo.
- Abdel-Shafy, H.I. & Mansour, M.S.M. (2016) A review on polycyclic aromatic hydrocarbons: Source, environmental impact, effect on human health and remediation. *Egyptian Journal of Petroleum*, **25**, 107-123.
- Abraham, J., Dowling, K. & Florentine, S. (2017) Risk of post-fire metal mobilization into surface water resources: A review. *Science of The Total Environment*, **599**, 1740-1755.
- Adriano, D.C. (2001) *Trace Elements in Terrestrial Environments: Biogeochemistry, Bioavailability, and Risks of Metals*. Springer.
- AMAP (2005) AMAP Assessment 2002: Heavy Metals in the Arctic. *Arctic Monitoring and Assessment Programme*. Arctic Monitoring and Assessment Programme, Norway.
- Andreassen, K. (2011) *Overvåkingsprogram for skogskader : årsrapport for 2010. Norwegian monitoring programme for forest damage annual report for 2010*. Norsk institutt for skog og landskap, Ås.
- Appleby, P.G. (2001) Chronostratigraphic Techniques in Recent Sediments. *Tracking Environmental Change Using Lake Sediments* (eds W. Last & J. Smol), pp. 171-203. Springer Netherlands.
- Appleby, P.G. (2008) Three decades of dating recent sediments by fallout radionuclides: a review. *The Holocene*, **18**, 83-93.
- Appleby, P.G., Oldfield, F., Thompson, R., Huttunen, P. & Tolonen, K. (1979) ²¹⁰Pb dating of annually laminated lake sediments from Finland. *Nature*, **280**, 53-55.
- Balch, J., Bradley, B., Abatzoglou, J., Chelsea Nagy, R., Fusco, E.J. & Mahood, A. (2017) Human-started wildfires expand the fire niche across the United States. *PNAS - Proceedings of the National Academy of Sciences of the United States of America*, **114**, 2946-2951.
- Barakat, A.O., Mostafa, A., El-Sayed, N.B., Wade, T.L. & Sweet, S.T. (2012) Polycyclic Aromatic Hydrocarbons (PAHs) in Surface Sediments of Lake Manzala, Egypt. *Soil and Sediment Contamination: An International Journal*, **22**, 315-331.

- Baran, A. & Tarnawski, M. (2015) Assessment of heavy metals mobility and toxicity in contaminated sediments by sequential extraction and a battery of bioassays. *Ecotoxicology*, **24**, 1279-1293.
- Bayley, S.E., Schindler, D.W., Parker, B.R., Stainton, M.P. & Beaty, K.G. (1992) Effects of forest fire and drought on acidity of a base-poor boreal forest stream: similarities between climatic warming and acidic precipitation. *Biogeochemistry*, **17**, 191-204.
- Bento-Gonçalves, A., Vieira, A., Úbeda, X. & Martin, D. (2012) Fire and soils: Key concepts and recent advances. *Geoderma*, **191**, 3-13.
- Berg, T. & Steinnes, E. (1997) Recent trends in atmospheric deposition of trace elements in Norway as evident from the 1995 moss survey. *Science of The Total Environment*, **208**, 197-206.
- Bertrand, O., Montargès-Pelletier, E., Mansuy-Huault, L., Losson, B., Faure, P., Michels, R., Pernot, A. & Arnaud, F. (2013) A possible terrigenous origin for perylene based on a sedimentary record of a pond (Lorraine, France). *Organic Geochemistry*, **58**, 69-77.
- Biswas, A., Blum, J.D., Klaue, B. & Keeler, G.J. (2007) Release of mercury from Rocky Mountain forest fires. *Global biogeochemical cycles*, **21**, 1-13.
- Bjørnes, H. & Hovde, P. (1973) *Fysiske målinger*, 2. utg. edn. Universitetsforl., Oslo.
- Bladon, K.D., Emelko, M.B., Silins, U. & Stone, M. (2014) Wildfire and the Future of Water Supply. *Environmental Science & Technology*, **48**, 8936-8943.
- Bleken, E., Mysterud, I. & Mysterud, I. (1997) Forest fire and environmental management – a technical report on forest fire as an ecological factor. Directorate for fire & explosion prevention and department of biology, University of Oslo.
- Blomqvist, S. (1991) Quantitative sampling of soft-bottom sediments: problems and solutions. *Marine ecology progress series*, **72**, 295-304.
- Booij, K., Arifin, Z. & Purbonegoro, T. (2012) Perylene dominates the organic contaminant profile in the Berau delta, East Kalimantan, Indonesia. *Marine Pollution Bulletin*, **64**, 1049-1054.
- Bouloubassi, I., Roussiez, V., Azzoug, M. & Lorre, A. (2012) Sources, dispersal pathways and mass budget of sedimentary polycyclic aromatic hydrocarbons (PAH) in the NW Mediterranean margin, Gulf of Lions. *Marine Chemistry*, **142-144**, 18-28.
- Bowen, H.J.M. (1979) *Environmental chemistry of the elements*. Academic Press, London.
- Brandrud, T.E., Bratli, H. & Sverdrup-Thygeson, A. (2010) Dokumentasjon av sopp, lav og insekter etter Frolandbrannen. Norwegian Forest and Landscape Institute (NFLI), Ås.
- Breedveld, G., Ruus, A., Bakke, T., Kibsgaard, A. & Arp, H.P. (2015) Guidelines for risk assessment of contaminated sediments. (ed. N.E. Agency), pp. 106. Norwegian Environment Agency, Oslo.
- Breivik, K., Ilyin, I., Mano, S., Travnikov, O. & Aas, W. (2004) EMEP - Heavy metals: transboundary pollution of the environment. **2**.

- Brimble, S.K., Foster, K.L., Mallory, M.L., Macdonald, R.W., Smol, J.P. & Blais, J.M. (2009) High arctic ponds receiving biotransported nutrients from a nearby seabird colony are also subject to potentially toxic loadings of arsenic, cadmium, and zinc. *Environmental Toxicology and Chemistry*, **28**, 2426-2433.
- Budzinski, H., Jones, I., Bellocq, J., Piérard, C. & Garrigues, P. (1997) Evaluation of sediment contamination by polycyclic aromatic hydrocarbons in the Gironde estuary. *Marine Chemistry*, **58**, 85-97.
- Burgess, R.M., Ahrens, M.J. & Hickey, C.W. (2003) Geochemistry of PAHs in Aquatic Environments: Source, Persistence and Distribution. *PAHs: An Ecotoxicological Perspective*, pp. 35-45. John Wiley & Sons, Ltd.
- Burke, M., Hogue, T., Ferreira, M., Mendez, C., Navarro, B., Lopez, S. & Jay, J. (2010) The Effect of Wildfire on Soil Mercury Concentrations in Southern California Watersheds. *Water, Air, & Soil Pollution*, **212**, 369-385.
- Caldwell, C.A., Canavan, C.M. & Bloom, N.S. (2000) Potential effects of forest fire and storm flow on total mercury and methylmercury in sediments of an arid-lands reservoir. *Science of The Total Environment*, **260**, 125-133.
- Callender, E. (2003) 9.03 - Heavy Metals in the Environment—Historical Trends. *Treatise on Geochemistry* (eds H.D. Holland & K.K. Turekian), pp. 67-105. Pergamon, Oxford.
- Campos, I., Vale, C., Abrantes, N., Keizer, J.J. & Pereira, P. (2015) Effects of wildfire on mercury mobilisation in eucalypt and pine forests. *CATENA*, **131**, 149-159.
- Certini, G. (2005) Effects of fire on properties of forest soils: a review. *Oecologia*, **143**, 1-10.
- Chen, G. & White, P.A. (2004) The mutagenic hazards of aquatic sediments: a review. *Mutation Research/Reviews in Mutation Research*, **567**, 151-225.
- Choi, S.-D. (2014) Time trends in the levels and patterns of polycyclic aromatic hydrocarbons (PAHs) in pine bark, litter, and soil after a forest fire. *Science of The Total Environment*, **470–471**, 1441-1449.
- Christensen, G.N., Evenset, A., Rognerud, S., Skjelkvåle, B.L., Palerud, R., Fjeld, E. & Røyset, O. (2008) National lake survey 2004-2006, part III: AMAP : status of metals and environmental pollutants in lakes and fish from the Norwegian part of the AMAP region. *National lake survey* (ed. G.N. Christensen). Norwegian Pollution Control Authority (SFT), Oslo.
- Chuvieco, E., Giglio, L. & Justice, C. (2008) Global characterization of fire activity: toward defining fire regimes from Earth observation data. *Global Change Biology*, **14**, 1488-1502.
- Cinnirella, S. & Pirrone, N. (2006) Spatial and temporal distributions of mercury emissions from forest fires in Mediterranean region and Russian federation. *Atmospheric Environment*, **40**, 7346-7361.
- Clewer, A.G. & Scarisbrick, D.H. (2013) *Practical Statistics and Experimental Design for Plant and Crop Science*. Wiley.
- Committee of Directorates (2013) Klassifisering av miljøtilstand i vann: Økologisk og kjemisk klassifiseringssystem for kystvann, grunnvann, innsjøer og elver. *Norsk klassifiseringssystem for vann i henhold til vannforskriften* (ed. The Norwegian

- Environment Agency), pp. 230. The Committee of Directorates (CD) for implementation of the EU Water Framework Directive (EU-WFD), Trondheim.
- Committee of Directorates WFD (2015) Klassifisering av miljøtilstand i vann. (ed. Ministry of Climate and Environment). Norwegian Environment Agency,, www.vannportalen.no.
- Costa, M.R., Calvão, A.R. & Aranha, J. (2014) Linking wildfire effects on soil and water chemistry of the Marão River watershed, Portugal, and biomass changes detected from Landsat imagery. *Applied Geochemistry*, **44**, 93-102.
- Darwin, C. (1881) *The formation of vegetable mould through the action of worms, with observations on their habits*. John Murray, London.
- Dean, W.E. (1974) Determination of carbonate and organic matter in calcareous sediments and sedimentary rocks by loss on ignition; comparison with other methods. *Journal of Sedimentary Research*, **44**, 242-248.
- Debertin, K. & Helmer, R.G. (1988) *Gamma- and X-ray spectrometry with semiconductor detectors*. North-Holland.
- Denis, E.H., Toney, J.L., Tarozo, R., Scott Anderson, R., Roach, L.D. & Huang, Y. (2012) Polycyclic aromatic hydrocarbons (PAHs) in lake sediments record historic fire events: Validation using HPLC-fluorescence detection. *Organic Geochemistry*, **45**, 7-17.
- Dickhut, R.M., Canuel, E.A., Gustafson, K.E., Liu, K., Arzayus, K.M., Walker, S.E., Edgecombe, G., Gaylor, M.O. & MacDonald, E.H. (2000) Automotive Sources of Carcinogenic Polycyclic Aromatic Hydrocarbons Associated with Particulate Matter in the Chesapeake Bay Region. *Environmental Science & Technology*, **34**, 4635-4640.
- Donahue, W., Allen, E. & Schindler, D. (2006) Impacts of Coal-Fired Power Plants on Trace Metals and Polycyclic Aromatic Hydrocarbons (PAHs) in Lake Sediments in Central Alberta, Canada. *Journal of Paleolimnology*, **35**, 111-128.
- Douben, P.E.T. (2003) *PAHs: an ecotoxicological perspective*. Wiley, Chichester.
- Driscoll, C.T., Otton, J.K. & Iverfeldt, Å. (1994) Trace Metals Speciation and Cycling. *Biogeochemistry of small catchments; a tool for environmental research* (eds B. Moldan & J. Cerny), pp. 301-322. Scientific Committee on Problems of the Environment, International Council of Scientific Unions, United Nations Environment Programme.
- Duffus, J.H. (2002) "Heavy metals" - a meaningless term? *Pure and Applied Chemistry*, **74**, 793-807.
- Eide, I., Berg, T., Thorvaldsen, B., Christensen, G., Savinov, V. & Larsen, J. (2011) Polycyclic Aromatic Hydrocarbons in Dated Freshwater and Marine Sediments Along the Norwegian Coast. *Water, Air, & Soil Pollution*, **218**, 387-398.
- Emerson, J. & Soto, M. (1982) Transforming data. *Understanding robust and exploratory data analysis* (eds D. Hogalin, F. Mosteller & J.W. Tukey). Wiley, New York.
- Esbensen, K.H., Guyot, D., Westad, F. & Houmøller, L.P. (2001) *Multivariate data analysis - in practice: an introduction to multivariate data analysis and experimental design*. Camo, Oslo.

- Estrellan, C.R. & Iino, F. (2010) Toxic emissions from open burning. *Chemosphere*, **80**, 193-207.
- European Commission (2013) Directive 2013/39/EU of the European parliament and the council of 12 August 2013 amending Directives 2000/60/EC and 2008/105/EC as regards priority substances in the field of water policy. *Directive 2013/39/EC* (ed. E.U. (EU)), pp. 17. The European parliament and the council of the European union.
- Fan, C.-W., Shiue, J., Wu, C.-Y. & Wu, C.-Y. (2011) Perylene dominance in sediments from a subtropical high mountain lake. *Organic Geochemistry*, **42**, 116-119.
- FAO (2007) Fire management - global assesment 2006. *FAO forestry paper*. Food and Agriculture Organization (FAO) of the United Nations (UN), Rome.
- Feng, B. & Yang, H. (2008) Metal Pollution in Lake System and its Reconstruction by Using Lake Sediments. *Bioinformatics and Biomedical Engineering, 2008. ICBBE 2008. The 2nd International Conference on*, pp. 3689-3692.
- Finley, B.D., Swartzendruber, P.C. & Jaffe, D.A. (2009) Particulate mercury emissions in regional wildfire plumes observed at the Mount Bachelor Observatory. *Atmospheric Environment*, **43**, 6074-6083.
- Flannigan, M., Stocks, B., Turetsky, M. & Wotton, M. (2009) Impacts of climate change on fire activity and fire management in the circumboreal forest. *Global Change Biology*, **15**, 549-560.
- Gabos, S., Ikononou, M.G., Schopflocher, D., Fowler, B.R., White, J., Prepas, E., Prince, D. & Chen, W. (2001) Characteristics of PAHs, PCDD/Fs and PCB in sediment following forest fires in northern Alberta. *Chemosphere*, **2001**, 709-719.
- Galarneau, E. (2008) Source specificity and atmospheric processing of airborne PAHs: Implications for source apportionment. *Atmospheric Environment*, **42**, 8139-8149.
- Gamma Dating Centre Copenhagen (2011) Dating of core Hundsvatn, Rasvassvatn and Jordtjenn. (ed. T.J. Andersen). University of Copenhagen.
- García-Falcón, M.S., Soto-González, B. & Simal-Gándara, J. (2006) Evolution of the Concentrations of Polycyclic Aromatic Hydrocarbons in Burnt Woodland Soils. *Environmental Science & Technology*, **40**, 759-763.
- Garrett, R.G. (2000) Natural Sources of Metals to the Environment. *Human and Ecological Risk Assessment: An International Journal*, **6**, 945-963.
- Geological Survey of Norway (2018) National areal information - Norway, Svalbard and ocean areas. *Applications*. Geological Survey of Norway - Norges geologiske undersøkelse (NGU), geo.ngu.no.
- Ghosal, D., Ghosh, S., Dutta, T.K. & Ahn, Y. (2016) Current State of Knowledge in Microbial Degradation of Polycyclic Aromatic Hydrocarbons (PAHs): A Review. *Frontiers in Microbiology*, **7**, 1369.
- Gilbert, R. (2003) Lacustrine sedimentation. *Sedimentology* (ed. C.W. Finkl), pp. 661-667. Springer Netherlands.
- Gjerstad, S. (2008) Røyklegger Danmark. TV 2, www.tv2.no.

- Greenberg, B.M. (2003) PAH Interactions with Plants: Uptake, Toxicity and Phytoremediation. *PAHs: An Ecotoxicological Perspective*, pp. 263-273. John Wiley & Sons, Ltd.
- Grimalt, J.O., van Drooge, B.L., Ribes, A., Fernández, P. & Appleby, P. (2004) Polycyclic aromatic hydrocarbon composition in soils and sediments of high altitude lakes. *Environmental Pollution*, **131**, 13-24.
- Guo, J., Wu, F., Luo, X., Liang, Z., Liao, H., Zhang, R., Li, W., Zhao, X., Chen, S. & Mai, B. (2010) Anthropogenic input of polycyclic aromatic hydrocarbons into five lakes in Western China. *Environmental Pollution*, **158**, 2175-2180.
- Guo, W., Zhang, H., Xu, Q., Tang, Z., Feng, Y. & Xu, X. (2013) Distribution, Sources, and Risk of Polycyclic Aromatic Hydrocarbons in the Core Sediments from Baiyangdian Lake, China. *Polycyclic Aromatic Compounds*, **33**, 108-126.
- Harvey, R.G. (1997) *Polycyclic aromatic hydrocarbons*. Wiley-VCH, New York.
- Hegna, K. (1986) Sammenlikning av vann- og sedimentkjemi mellom et 6-9 år gammelt skogbrannområde og et ikke-brent skogsområde i Telemark. K. Hegna, Oslo.
- Heilman, W.E., Liu, Y., Urbanski, S., Kovalev, V. & Mickler, R. (2013) Wildland fire emissions, carbon, and climate: Plume rise, atmospheric transport, and chemistry processes. *Forest Ecology and Management*.
- Heilman, W.E., Liu, Y., Urbanski, S., Kovalev, V. & Mickler, R. (2014) Wildland fire emissions, carbon, and climate: Plume rise, atmospheric transport, and chemistry processes. *Forest Ecology and Management*, **317**, 70-79.
- Heiri, O., Lotter, A.F. & Lemcke, G. (2001) Loss on ignition as a method for estimating organic and carbonate content in sediments: reproducibility and comparability of results. *Journal of Paleolimnology*, **2001**, 101-110.
- Herb, W.R. & Stefan, H.G. (2005) Dynamics of vertical mixing in a shallow lake with submersed macrophytes. *Water resources research*, **41**.
- Hodson, M.E. (2004) Heavy metals—geochemical bogey men? *Environmental Pollution*, **129**, 341-343.
- Horowitz, A.J. (1985) A primer on trace metal-sediment chemistry. *United States Geological Survey, Water Supply Paper*, **2277**.
- Hwang, H.-M., Wade, T.L. & Sericano, J.L. (2003) Concentrations and source characterization of polycyclic aromatic hydrocarbons in pine needles from Korea, Mexico, and United States. *Atmospheric Environment*, **37**, 2259-2267.
- Høgberget, R. (2010) Forest fire in Mykland, SE Norway in 2008. Results from two years of chemical investigations in water. The Norwegian Institute for Water Research (Norsk Institutt for Vannforskning; NIVA), Grimstad.
- Høgberget, R. & Kleiven, E. (2013) Prøvefiske i tre innsjøer innenfor brannlokaliteter i Mykland, Aust-Agder : grunnlagsdata før antatte effekter etter skogbrannen i 2008. The Norwegian Institute for Water Research (NIVA), Oslo.
- Ice, G.G., Neary, D.G. & Adams, P.W. (2004) Effects of Wildfire on Soils and Watershed Processes. *Journal of Forestry*, **102**, 16-20.
- Ignatavičius, G., Sakalauskienė, G. & Oškinis, V. (2006) Influence of land fires on increase of heavy metal concentrations in river waters of Lithuania. pp. 46-51. Taylor & Francis Group.

- Inengite, A.K., Oforika, N.C. & Osuji, L.C. (2012) Sources of polycyclic aromatic hydrocarbons in an environment urbanised by crude oil exploration. *Environment and natural resources research*, **2**, 62-70.
- International Atomic Energy Agency (2003) *Collection and Preparation of Bottom Sediment Samples for Analysis of Radionuclides and Trace Elements*. INTERNATIONAL ATOMIC ENERGY AGENCY, Vienna.
- Kabata-Pendias, A. (2011) *Trace Elements in Soils and Plants*, Fourth Edition edn. Taylor & Francis, United States of America (New York).
- Kabata-Pendias, A. & Mukherjee, A.B. (2007) *Trace elements from soil to human*. Springer, Berlin.
- Karbassi, A.R., Nabi-Bindhendi, G.R. & Bayati, I. (2005) Environmental geochemistry of heavy metals in a sediment core off Bushehr, Persian Gulf. *Journal of Environmental Health Science and Engineering*, **2**, 255-260.
- Kasischke, E.S. & Stocks, B.J. (2000) *Fire, climate change, and carbon cycling in the boreal forest*. Springer, New York.
- Keeley, J.E. (2009) Fire intensity, fire severity and burn severity: a brief review and suggested usage. *International Journal of Wildland Fire*, **18**, 116-126.
- Kelly, E.N., Schindler, D.W., St. Louis, V.L., Donald, D.B. & Vladicka, K.E. (2006) Forest fire increases mercury accumulation by fishes via food web restructuring and increased mercury inputs. *Proceedings of the National Academy of Sciences*, **103**, 19380-19385.
- Kim, E.-J., Choi, S.-D. & Chang, Y.-S. (2011) Levels and patterns of polycyclic aromatic hydrocarbons (PAHs) in soils after forest fires in South Korea. *Environmental Science and Pollution Research*, **18**, 1508-1517.
- Kim, E.-J., Oh, J.-E. & Chang, Y.-S. (2003) Effects of forest fire on the level and distribution of PCDD/Fs and PAHs in soil. *Science of The Total Environment*, **311**, 177-189.
- Krawchuk, M.A., Moritz, M.A., Parisien, M.-A., Van Dorn, J., Hayhoe, K. & Chave, J. (2009) Global Pyrogeography: the Current and Future Distribution of Wildfire (Global Pyrogeography). *PLoS ONE*, **4**, e5102.
- Krebs, P., Pezzatti, G.B., Mazzoleni, S., Talbot, L.M. & Conedera, M. (2010) Fire regime: history and definition of a key concept in disturbance ecology. *Theory in Biosciences*, **129**, 53-69.
- Kucera, M. & Malmgren, B.A. (1998) Logratio transformation of compositional data: a resolution of the constant sum constraint. *Marine Micropaleontology*, **34**, 117-120.
- Kuijpers, A., Dennegård, B., Albinsson, Y. & Jensen, A. (1993) Sediment transport pathways in the Skagerrak and Kattegat as indicated by sediment Chernobyl radioactivity and heavy metal concentrations. *Marine Geology*, **111**, 231-244.
- Köhler, S.J., Wallmann, K. & McKie, B. (2017) Skogsbranden i Västmanland 2014 - Utvärdering av effekter på vattenkvalitet och vattenlevande organismer i och runt brandområdet. Swedish University of Agricultural Sciences.
- Lacey, L.A. (2012) *Manual of Techniques in Invertebrate Pathology*. Elsevier Science.

- Last, W.M. & Smol, J.P. (2001) *Tracking environmental change using lake sediments, Vol. 2, Physical and geochemical methods*. Kluwer Academic, Dordrecht.
- Last, W.M., Smol, J.P. & Birks, H.J.B. (2001) *Tracking environmental change using lake sediments*. Kluwer Academic Springer, Dordrecht.
- Lee, B.-K. & Vu, V.T. (2010) Sources, Distribution and Toxicity of Polyaromatic Hydrocarbons (PAHs) in Particulate Matter. *Air Pollution* (ed. V. Villanyi). Sciyo.
- Lehtonen, I., Ruosteenoja, K., Venäläinen, A. & Gregow, H. (2014) The projected 21st century forest-fire risk in Finland under different greenhouse gas scenarios. **19**, 127-139.
- Lepanea, V., Varvasb, M., Viitaka, A., Alliksaarc, T. & Heinsalu, A. (2007) Sedimentary record of heavy metals in Lake Rõuge Liinjärv, southern Estonia. *Estonian journal of earth sciences*, **56**, 221-232.
- Leung, A.O.W., Cheung, K.C. & Wong, M.H. (2013) Spatial distribution of polycyclic aromatic hydrocarbons in soil, sediment, and combusted residue at an e-waste processing site in southeast China. *Environmental Science and Pollution Research*, 1-16.
- Likens, G.E. & Davis, M.B. (1975) Post-Glacial History of Mirror Lake and Its Watershed In New Hampshire, U. S. A.: An Initial Report. *Verhandlungen Internationale Vereinigung Limnologie*, **19**, 982-993.
- Liu, Y., Chen, L., Huang, Q.-H., Li, W.-Y., Tang, Y.-J. & Zhao, J.-F. (2009) Source apportionment of polycyclic aromatic hydrocarbons (PAHs) in surface sediments of the Huangpu River, Shanghai, China. *Science of The Total Environment*, **407**, 2931-2938.
- Lovdata.no (2009a) FOR 2009-06-26 nr 885: Forskrift om verneplan for skog. Vedlegg 2. Fredning av Myklandsvatna naturreservat, Froland kommune, Aust-Agder. (ed. T.R.N.M.o.t.E. Miljøverndepartementet). Justis- og politidepartementet.
- Lovdata.no (2009b) FOR 2009-06-26 nr 886: Forskrift om verneplan for skog. Vedlegg 3. Fredning av Jurdalsknuten naturreservat, Froland kommune, Aust-Agder. (ed. T.R.N.M.o.t.E. Miljøverndepartementet). Justis- og politidepartementet.
- Luo, X., Zheng, Y., Wu, B., Lin, Z., Han, F., Zhang, W. & Wang, X. (2013) Impact of carbonaceous materials in soil on the transport of soil-bound PAHs during rainfall-runoff events. *Environmental Pollution*, **182**, 233-241.
- Lydersen, E., Høgberget, R., Holtan, M., Darrud, M. & Moreno Vicente, C. (2016) *Effects of wildfire on water chemistry and perch (Perca fluviatilis) populations in some acidic lakes in southern Norway*.
- Lydersen, E., Høgberget, R., Moreno, C.E., Garmo, Ø.A. & Hagen, P.C. (2014) Effects of wildfire on the water chemistry of dilute, acidic lakes in southern Norway. *Biogeochemistry*, **119**, 109-124.
- Lydersen, E., Löfgren, S. & Arnesen, R.T. (2002) Metals in Scandinavian Surface Waters: Effects of Acidification, Liming, and Potential Reacidification. *Critical Reviews in Environmental Science and Technology*, **32**, 73-295.
- Løvik, J.E. (2010) Overvåking av miljøgifter i Hunnselv-vassdraget i Vestre Toten kommune i 2009. Norsk institutt for vannforskning, Oslo.

- Mabit, L., Benmansour, M., Abril, J.M., Walling, D.E., Meusburger, K., Iurian, A.R., Bernard, C., Tarján, S., Owens, P.N., Blake, W.H. & Alewell, C. (2014) Fallout ^{210}Pb as a soil and sediment tracer in catchment sediment budget investigations: A review. *Earth-Science Reviews*, **138**, 335-351.
- Mai, B.-X., Fu, J.-M., Sheng, G.-Y., Kang, Y.-H., Lin, Z., Zhang, G., Min, Y.-S. & Zeng, E.Y. (2002) Chlorinated and polycyclic aromatic hydrocarbons in riverine and estuarine sediments from Pearl River Delta, China. *Environmental Pollution*, **117**, 457-474.
- Markert, B. & Friese, K. (2000) *Trace elements: their distribution and effects in the environment*. Elsevier, Amsterdam.
- Moen, A., Lillethun, A. & Odland, A. (1999) *Vegetation*. Norwegian Mapping Authority, Hønefoss.
- Moody, J.A., Shakesby, R.A., Robichaud, P.R., Cannon, S.H. & Martin, D.A. (2013) Current research issues related to post-wildfire runoff and erosion processes. *Earth-Science Reviews*, **122**, 10-37.
- Moreno, C.E., Fjeld, E. & Lydersen, E. (2016) The effects of wildfire on mercury and stable isotopes ($\delta^{15}\text{N}$, $\delta^{13}\text{C}$) in water and biota of small boreal, acidic lakes in southern Norway. *Environmental Monitoring and Assessment*, **188**, 178.
- Mudroch, A. & Azcue, J.M. (1995) *Manual of aquatic sediment sampling*. Lewis Publishers, London.
- Muri, G., Wakeham, S.G. & Faganeli, J. (2003) Polycyclic aromatic hydrocarbons and black carbon in sediments of a remote alpine Lake (Lake Planina, northwest Slovenia). *Environmental Toxicology and Chemistry*, **22**, 1009-1016.
- Mykland, K. (1967) Mykland : ei bygd i Råbygdelaget : 1 : Gard, ætt, grend. Mykland bygdeboknemnd, Mykland.
- Mykland, K. (1970) Mykland : ei bygd i Råbygdelaget : 2 : Gard, ætt, grend. Mykland bygdeboknemnd, Mykland.
- Mykland, K. (1998) Mykland : ei bygd i Råbygdelaget : 3 : Kultursoga til 1832. *Myklands historie*. Mykland bygdeboknemnd, Mykland.
- Mykland, K., Frigstad, V., Lauvrak, S. & Risdal, M. (2009) *Mykland : ei bygd i Råbygdelaget : 4 : kultursoga 1832-2009*. Mykland bygdeboknemnd, Mykland.
- Müller, G., Grimmer, G. & Böhnke, H. (1977) Sedimentary record of heavy metals and polycyclic aromatic hydrocarbons in Lake Constance. *Naturwissenschaften, Springer-Verlag*, **64**, 427-431.
- Nasher, E., Heng, L.Y., Zakaria, Z. & Surif, S. (2013) Concentrations and Sources of Polycyclic Aromatic Hydrocarbons in the Seawater around Langkawi Island, Malaysia. *Journal of Chemistry*, **2013**, 10.
- Naturvårdsverket (2006) Branden i Tyresta 1999 - dokumentation av effekterna. *Dokumentation av de svenska nationalparkerna* (ed. U. Pettersson). Naturvårdsverket.
- Navrátil, T., Hojdová, M., Rohovec, J., Penížek, V. & Vařilová, Z. (2009) Effect of Fire on Pools of Mercury in Forest Soil, Central Europe. *Bulletin of Environmental Contamination and Toxicology*, **83**, 269-274.

- Neary, D.G., Ryan, K.C. & DeBano, L.F., (eds.) (2005) Wildland fire in ecosystems: effects of fire on soils and water. *General technical report RMRS-GTR-42*, pp. 250. U.S. Department of Agriculture, Forest Service, Utah.
- Neff, J.M. (1979) *Polycyclic aromatic hydrocarbons in the aquatic environment : sources, fates and biological effects*. Applied Science Publ., London.
- NGU.no (2012) Nasjonal berggrunnsdatabase. Norges geologiske undersøkelse.
- Nizzetto, P.B., Aas, W. & Warner, N.A. (2017) Monitoring of environmental contaminants in air and precipitation, annual report 2016. Norwegian Institute for Air Research - Norsk Institutt for Luftforskning (NILU), Norway.
- NOKUT (2010) Søknad om akkreditering av doktorgradsstudium i økologi ved Høgskolen i Telemark. *NOKUTs rapporter* (ed. T. Mørland). Nasjonalt organ for kvalitet i utdanningen (NOKUT).
- Norwegian Environment Agency (2016) Quality standards for water, sediment and biota. *Guidelines*, **2016**, 26.
- Norwegian Environment Agency (2018) Vannmiljø. The Norwegian Environment Agency - Miljødirektoratet (MD), vannmiljo.miljodirektoratet.no.
- Norwegian Water Resources and Energy Directorate (2018) NVE Atlas. *Lake database* (ed. The Norwegian Water Resources and Energy Directorate), pp. NVE map catalogue. The Norwegian Water Resources and Energy Directorate - Norges vassdrags- og energidirektorat (NVE), Oslo.
- NRC-INMS (1997) Marine Sediment Reference Materials for Trace Metals and other Constituents. *HISS-1*. National Research Council Canada, Institute for National Measurement Standards.
- NRC-INMS (2000) Marine Sediment Reference Materials for Trace Metals and other Constituents. *MESS-3*. National Research Council Canada, Institute for National Measurement Standards.
- Nriagu, J.O. (1989) Natural Versus Anthropogenic Emissions of Trace Metals to the Atmosphere. *Control and Fate of Atmospheric Trace Metals* (eds J. Pacyna & B. Ottar), pp. 3-13. Springer Netherlands.
- Nygaard, P.H. & Brean, R. (2014) Dokumentasjon og erfaringer etter skogbrannen i Mykland 2008 : sluttrapport. pp. 33. Norwegian Forest and Landscape Institute, Ås.
- Odigie, K.O. & Flegal, A.R. (2014) Trace metal inventories and lead isotopic composition chronicle a forest fire's remobilization of industrial contaminants deposited in the angeles national forest. *PLoS ONE*, **9**, e107835.
- Odigie, K.O., Khanis, E., Hibdon, S.A., Jana, P., Araneda, A., Urrutia, R. & Flegal, A.R. (2016) Remobilization of trace elements by forest fire in Patagonia, Chile. *Regional Environmental Change*, **16**, 1089-1096.
- Okafor, E.C. & Opuene, K. (2007) Preliminary assessment of trace metals and polycyclic aromatic hydrocarbons in the sediments. *International Journal of Environmental Science & Technology*, **4**, 233-240.
- Oliveira, C., Martins, N., Tavares, J., Pio, C., Cerqueira, M., Matos, M., Silva, H., Oliveira, C. & Camões, F. (2011) Size distribution of polycyclic aromatic hydrocarbons in a roadway tunnel in Lisbon, Portugal. *Chemosphere*, **83**, 1588-1596.

- Olivella, M.A., Ribalta, T.G., de Febrer, A.R., Mollet, J.M. & de las Heras, F.X.C. (2006) Distribution of polycyclic aromatic hydrocarbons in riverine waters after Mediterranean forest fires. *Science of The Total Environment*, **355**, 156-166.
- Opuene, K., Agbozu, I.E. & Ekeh, L.E. (2007) Identification of perylene in sediments: Occurrence and diagenetic evolution. *International Journal of Environmental Science & Technology*, **4**, 457-462.
- Outridge, P.M. & Wang, F. (2015) *The Stability of Metal Profiles in Freshwater and Marine Sediments*.
- Pampanin, D.M. & Sydnes, M.O. (2013) *Polycyclic Aromatic Hydrocarbons a Constituent of Petroleum: Presence and Influence in the Aquatic Environment*.
- Parvaresh, H., Abedi, Z., Farshchi, P., Karami, M., Khorasani, N. & Karbassi, A.R. (2010) *Bioavailability and Concentration of Heavy Metals in the Sediments and Leaves of Grey Mangrove, Avicennia marina (Forsk.) Vierh, in Sirik Azini Creek, Iran*.
- Pereira, P. & Úbeda, X. (2010) Spatial distribution of heavy metals released from ashes after a wildfire. *Journal of Environmental Engineering and Landscape Management*, **18**, 13-22.
- Pereira, P., Úbeda, X., Martin, D., Mataix-Solera, J., Cerdà, A. & Burguet, M. (2014) Wildfire effects on extractable elements in ash from a *Pinus pinaster* forest in Portugal. *Hydrological Processes*, **28**, 3681-3690.
- Perera, A.H. & Buse, L.J. (2014) *Ecology of wildfire residuals in boreal forests*. Wiley Blackwell, Hoboken, NJ.
- Ramdahl, T. (1983) Retene - a molecular marker of wood combustion in ambient air. *Nature*, **306**, 580-582.
- Ravindra, K., Sokhi, R. & Van Grieken, R. (2008) Atmospheric polycyclic aromatic hydrocarbons: Source attribution, emission factors and regulation. *Atmospheric Environment*, **42**, 2895-2921.
- RCN (2013) Wildfire effects on biogeochemistry of soil and surface water. *FoU-satsing* (ed. T.R.C.o. Norway). The Research Council of Norway; RCN (Norges forskningsråd), Prosjektkatalog 2002–2015.
- Richardson, G.M. (2001) Critical review on natural global and regional emissions of six trace metals to the atmosphere.
- Robichaud, P.R., Lewis, S.A., Wagenbrenner, J.W., Ashmun, L.E. & Brown, R.E. (2013) Post-fire mulching for runoff and erosion mitigation: Part I: Effectiveness at reducing hillslope erosion rates. *CATENA*, **105**, 75-92.
- Rognerud, S., Dauvalter, V., Fjeld, E., Skjelkvåle, B., Christensen, G. & Kashulin, N. (2013) Spatial Trends of Trace-Element Contamination in Recently Deposited Lake Sediment Around the Ni–Cu Smelter at Nikel, Kola Peninsula, Russian Arctic. *AMBIO*, **42**, 724-736.
- Rognerud, S. & Fjeld, E. (1990) *Landsomfattende undersøkelse av tungmetaller i innsjøsedimenter og kvikksølv i fisk*. Norwegian Pollution Control Authority (Statens forurensningstilsyn; SFT), Oslo.
- Rognerud, S. & Fjeld, E. (2001) Trace Element Contamination of Norwegian Lake Sediments. *AMBIO: A Journal of the Human Environment*, **30**, 11-19.

- Rognerud, S., Fjeld, E. & Løvik, J.E. (1997) *Regional undersøkelse av miljøgifter i innsjøsedimenter, delrapport 1: Organiske mikroforurensninger*. The Norwegian Institute for Water Research (Norsk Institutt for Vannforskning; NIVA), Oslo.
- Rognerud, S., Fjeld, E. & Løvik, J.E. (1999) *Landsomfattende undersøkelse av metaller i innsjøsedimenter*. The Norwegian Institute for Water Research (Norsk Institutt for Vannforskning; NIVA), Oslo.
- Rognerud, S., Fjeld, E., Løvik, J.E. & Skotvold, T. (1997) *Regional undersøkelse av miljøgifter i innsjøsedimenter, delrapport 2: Tungmetaller og andre sporelementer*. The Norwegian Institute for Water Research (Norsk Institutt for Vannforskning; NIVA), Oslo.
- Rognerud, S., Fjeld, E., Skjelkvåle, B.L., Christensen, G. & Røyset, O.K. (2008) Nasjonal innsjøundersøkelse 2004 - 2006, del 2 sedimenter: forurensning av metaller, PAH og PCB. *National lake survey 2004 - 2006*. Norwegian Pollution Control Authority (Statens forurensningstilsyn; SFT), Oslo.
- Rognerud, S., Fjeld, E., Skjelkvåle, B.L. & Røyset, O.K. (2007) Hydro aluminium Sunndal - PAH, metaller og vannkvalitet i innsjøer i regionen rundt aluminiumsverket. The Norwegian Institute for Water Research (Norsk Institutt for Vannforskning; NIVA).
- Rognerud, S., Hongve, D., Fjeld, E. & Ottesen, R.T. (2000) Trace metal concentrations in lake and overbank sediments in southern Norway. *Environmental Geology*, **39**, 723-732.
- Roig, N., Sierra, J., Moreno-Garrido, I., Nieto, E., Gallego, E.P., Schuhmacher, M. & Blasco, J. (2016) Metal bioavailability in freshwater sediment samples and their influence on ecological status of river basins. *Science of The Total Environment*, **540**, 287-296.
- Rommetveit, A. (2008) Røyken har nådd Sverige. The Norwegian Meteorological Institute (MET), www.yr.no.
- Rose, N.L., Rose, C.L., Boyle, J.F. & Appleby, P.G. (2004) Lake-Sediment Evidence for Local and Remote Sources of Atmospherically Deposited Pollutants on Svalbard. *Journal of Paleolimnology*, **31**, 499-513.
- Rothenberg, S., Kirby, M., Bird, B., DeRose, M., Lin, C.-C., Feng, X., Ambrose, R. & Jay, J. (2010) The impact of over 100 years of wildfires on mercury levels and accumulation rates in two lakes in southern California, USA. *Environmental Earth Sciences*, **60**, 993-1005.
- Ruus, A., Næs, K., Grung, M., Green, N., Bakke, T., Oug, E. & Hylland, K. (2009) Contamination of marine sediments by PAHs - a review. Norwegian institute for water research, www.miljodirektoratet.no.
- Ryan, S.E., Dwire, K.A. & Dixon, M.K. (2011) Impacts of wildfire on runoff and sediment loads at Little Granite Creek, western Wyoming. *Geomorphology*, **129**, 113-130.
- Salomons, W. (1998) Biogeochemistry of contaminated sediments and soils: perspectives for future research. *Journal of Geochemical Exploration*, **62**, 37-40.
- Santisteban, J.I., Mediavilla, R., López-Pamo, E., Dabrio, C.J., Zapata, M.B.R., García, M.J.G., Castaño, S. & Martínez-Alfaro, P.E. (2004) Loss on ignition: a

qualitative or quantitative method for organic matter and carbonate mineral content in sediments? *Journal of Paleolimnology*, **2004**, 287-299.

SAS Institute (2016) *JMP 13 Multivariate Methods*. SAS Institute.

SAS Institute Inc (2016) JMP 13.2.1 statistical software., *JMP 13 Multivariate Methods*. SAS Institute Inc.,

Schartau, A.K. (2009) *Overvåking av langtransportert forurenset luft og nedbør : årsrapport - effekter 2008 = Monitoring long-range transboundary air pollution : effects 2008*. Norsk institutt for vannforskning, Oslo.

Schartau, A.K. (2011) *Overvåking av langtransportert forurenset luft og nedbør : årsrapport - effekter 2010*. Norsk institutt for vannforskning, Oslo.

Schartau, A.K., Fjellheim, A., Walseng, B., Skjelkvåle, B.L., Framstad, E., Halvorsen, G.A., Bruteig, I.E., Røsberg, I., Kålås, J.A., Nordbakken, J.-F., Yttri, K.E., Andreassen, K., Skancke, L.B., Evju, M., Clarke, N., Aarrestad, P.A., Saksgård, R., Manø, S., Solberg, S., Jensen, T.C., Økland, T., Høgåsen, T., Hesthagen, T., Bakkestuen, V., Timmermann, V., Aas, W. & Skjelkvåle, B.L.P.m. (2011) *Overvåking av langtransporterte forurensninger 2010*. Sammendragsrapport.

Shakesby, R.A. & Doerr, S.H. (2006) Wildfire as a hydrological and geomorphological agent. *Earth-Science Reviews*, **74**, 269-307.

Shcherbov, B.L., Strakhovenko, V.D. & Sukhorukov, F.V. (2008) The ecogeochemical role of forest fires in the Baikal region. *Geography and Natural Resources*, **29**, 150-155.

Shen, G., Lu, Y. & Hong, J. (2006) Combined effect of heavy metals and polycyclic aromatic hydrocarbons on urease activity in soil. *Ecotoxicology and Environmental Safety*, **63**, 474-480.

Sigg, L., Sturm, M. & Kistler, D. (1987) Vertical transport of heavy metals by settling particles in Lake Zurich. *Limnology and Oceanography*, **32**, 112-130.

Silva, V., Abrantes, N., Costa, R., Keizer, J.J., Gonçalves, F. & Pereira, J.L. (2016) Effects of ash-loaded post-fire runoff on the freshwater clam *Corbicula fluminea*. *Ecological Engineering*, **90**, 180-189.

Singh, H.B., Anderson, B.E., Brune, W.H., Cai, C., Cohen, R.C., Crawford, J.H., Cubison, M.J., Czech, E.P., Emmons, L., Fuelberg, H.E., Huey, G., Jacob, D.J., Jimenez, J.L., Kaduwela, A., Kondo, Y., Mao, J., Olson, J.R., Sachse, G.W., Vay, S.A., Weinheimer, A., Wennberg, P.O. & Wisthaler, A. (2010) Pollution influences on atmospheric composition and chemistry at high northern latitudes: Boreal and California forest fire emissions. *Atmospheric Environment*, **44**, 4553-4564.

Skjelkvåle, B.L., Rognerud, S., Fjeld, E., Christensen, G. & Røyset, O. (2008) Nasjonal innsjøundersøkelse 2004 - 2006, del I: vannkjemi : status for forsurening, næringssalter og metaller. *National lake survey 2004 - 2006, part I: water chemistry status of acidification, nutrients and metals*. Norwegian Pollution Control Authority (Statens forurensningstilsyn; SFT), Oslo.

Skogbrukets Kursinstitutt (2009) Det skjer ikke hos oss... -om skogbrann og skogbrannvern. (ed. J.E. Vollen).

Skupińska, K., Misiewicz, I. & Kasprzycka-Guttman, T. (2004) Polycyclic aromatic hydrocarbons: physicochemical properties, environmental appearance and

- impact on living organisms. *Acta Poloniae Pharmaceutica - Drug research*, **61**, 233-240.
- Smith, H.G., Sheridan, G.J., Lane, P.N.J., Nyman, P. & Haydon, S. (2011) Wildfire effects on water quality in forest catchments: A review with implications for water supply. *Journal of Hydrology*, **396**, 170-192.
- Smol, J.P. (2009) *Pollution of Lakes and Rivers: A Paleoenvironmental Perspective*. Wiley.
- Soclo, H.H., Garrigues, P. & Ewald, M. (2000) Origin of Polycyclic Aromatic Hydrocarbons (PAHs) in Coastal Marine Sediments: Case Studies in Cotonou (Benin) and Aquitaine (France) Areas. *Marine Pollution Bulletin*, **40**, 387-396.
- Solvang, R. (2005) Biologisk mangfold : kartlegging av naturtyper i Froland kommune 2000-2002. *Biologisk mangfold i Froland*. Fylkesmannen i Aust-Agder, Miljøvernvedelingen, Arendal.
- Soper, D.S. (2018) p-value calculator for correlation coefficients. www.danielsoper.com/statcalc.
- Sosorova, S.B., Merkusheva, M.G. & Ubugunov, L.L. (2013) Pyrogenic changes in microelement content in soils and plants from the pine forests of western Transbaikal. *Contemporary Problems of Ecology*, **6**, 499-508.
- Sprovieri, M., Feo, M.L., Prevedello, L., Manta, D.S., Sammartino, S., Tamburrino, S. & Marsella, E. (2007) Heavy metals, polycyclic aromatic hydrocarbons and polychlorinated biphenyls in surface sediments of the Naples harbour (southern Italy). *Chemosphere*, **67**, 998-1009.
- Standards-Norway (1994) Water analysis - Determination of metals by atomic absorption spectrophotometry, atomization in flame - General principles and guidelines. *NS 4770:1994*. Standards Norway, Norwegian Standards.
- Stankov Jovanovic, V.P., Ilic, M.D., Markovic, M.S., Mitic, V.D., Nikolic Mandic, S.D. & Stojanovic, G.S. (2011) Wild fire impact on copper, zinc, lead and cadmium distribution in soil and relation with abundance in selected plants of Lamiaceae family from Vidlic Mountain (Serbia). *Chemosphere*, **84**, 1584-1591.
- Stein, E.D., Brown, J.S., Hogue, T.S., Burke, M.P. & Kinoshita, A. (2012) Stormwater contaminant loading following southern California wildfires. *Environmental Toxicology and Chemistry*, **31**, 2625-2638.
- Stephenson, M., Klaverkamp, J., Motycka, M., Baron, C. & Schwartz, W. (1996) Coring artifacts and contaminant inventories in lake sediment. *Journal of Paleolimnology*, **15**, 99-106.
- Stoermer, E.F. & Crutzen, P.J. (2000) The Anthropocene. pp. 20. The International Geosphere-Biosphere Programme (IGBP), Global Change Newsletter.
- Storaunet, K.O., Brandrud, T.E., Rolstad, J. & Rolstad, E. (2008) Vurdering av verneverdier og skoghistorie i to områder tilbudt for frivillig vern etter skogbrannen i Mykland i juni 2008. Norwegian Forest and Landscape Institute (NFLI), Ås.
- Suryatmojo, H., Masamitsu, F., Kosugi, K.i. & Mizuyama, T. (2013) Effects of Selective Logging Methods on Runoff Characteristics in Paired Small Headwater Catchment. *Procedia Environmental Sciences*, **17**, 221-229.

- Thomas, P.A. & McAlpine, R. (2010) *Fire in the forest*. Cambridge University Press, Cambridge.
- Tishkov, A.A. (2004) Forest fires and dynamics of forest cover. *Natural Disasters, Encyclopedia of Life Support Systems (EOLSS), UNESCO. Eolss Publishers, Oxford, United Kingdom*.
- Tobiszewski, M. & Namieśnik, J. (2012) PAH diagnostic ratios for the identification of pollution emission sources. *Environmental Pollution*, **162**, 110-119.
- Tsymbalyuk, K.K., Den'ga, Y.M., Berlinsky, N.A. & Antonovich, V.P. (2011) Determination of 16 priority polycyclic aromatic hydrocarbons in bottom sediments of the Danube estuarine coast by GC/MS. *Geo-Eco-Marina*, **17**.
- U.S. EPA (2012) Code of Federal Regulations. *40 (Protection of environment); Chapter I (Environmental protection agency (continued)); Subchapter N (Effluent guidelines and standards)* (ed. U.S.G. United States Environmental protection agency (U.S. EPA)), pp. 653-654. National Archives and Records Administration, Office of the Federal Register, Washington, DC.
- UCLA (2018) Introduction to SAS. *Learning module introduction* (ed. U.S.C. Group). University of California (UCLA), <https://stats.idre.ucla.edu>.
- UiO (2010) Pyrowater - Wildfire effects on biogeochemistry of soil and surface water. University of Oslo (UiO), www.uio.no.
- UNECE (1979) Convention on Long-range Transboundary Air Pollution. *TIAS 10541; 1302 UNTS 217; 18 ILM 1442* (ed. U. Nations). United Nations Economic Commission for Europe, Geneva.
- UNECE (1998a) The Aarhus protocol on heavy metals. (ed. U. Nations). United Nations Economic Commission for Europe, UNECE's 1979 Geneva convention on LRTAP.
- UNECE (1998b) The Aarhus protocol on Persistent Organic Pollutants (POPs). (ed. U. Nations). United Nations Economic Commission for Europe, UNECE's 1979 Geneva convention on LRTAP.
- van Drooge, B.L., López, J., Fernández, P., Grimalt, J.O. & Stuchlík, E. (2011) Polycyclic aromatic hydrocarbons in lake sediments from the High Tatras. *Environmental Pollution*, **159**, 1234-1240.
- Van Mouwerik, M., Stevens, L., Seese, M.D. & Basham, W. (1997) Environmental Contaminants Encyclopedia. (ed. R.J. Irwin). U.S. department of the interior, National Park Service, Water Resources Division, Fort Collins, Colorado.
- Veraverbeke, S., Van De Kerchove, R., Verstraeten, W., Lhermitte, S. & Goossens, R. (2010) *Fire-induced changes in vegetation, albedo and land surface temperature assessed with MODIS*.
- Vergnoux, A., Malleret, L., Asia, L., Doumenq, P. & Theraulaz, F. (2011) Impact of forest fires on PAH level and distribution in soils. *Environmental research*, **111**, 193-198.
- Verma, S. & Jayakumar, S. (2012) Impact of forest fire on physical, chemical and biological properties of soil: A review. *Proceedings of the International Academy of Ecology and Environmental Sciences*, **2**, 168-176.
- Vest-Agder, F.i.A.-o. (2017) ROS Agder. Fylkesmannen.

- Vila-Escalé, M., Vegas-Vilarrúbia, T. & Prat, N. (2007) Release of polycyclic aromatic compounds into a Mediterranean creek (Catalonia, NE Spain) after a forest fire. *Water Research*, **41**, 2171-2179.
- Walsh, D.P. (1998) A simple rule of thumb for statistically significant correlation. pp. 6. Middle Tennessee State University, <http://capone.mtsu.edu/dwalsh/CORRSIG.pdf>.
- Wang, D.-Q., Yu, Y.-X., Zhang, X.-Y., Zhang, S.-H., Pang, Y.-P., Zhang, X.-L., Yu, Z.-Q., Wu, M.-H. & Fu, J.-M. (2012) Polycyclic aromatic hydrocarbons and organochlorine pesticides in fish from Taihu Lake: Their levels, sources, and biomagnification. *Ecotoxicology and Environmental Safety*, **82**, 63-70.
- Wang, G., Mielke, H.W., Quach, V.A.N., Gonzales, C. & Zhang, Q. (2004) Determination of Polycyclic Aromatic Hydrocarbons and Trace Metals in New Orleans Soils and Sediments. *Soil and Sediment Contamination: An International Journal*, **13**, 313-327.
- Wang, X., Yang, H., Gong, P., Zhao, X., Wu, G., Turner, S. & Yao, T. (2010) One century sedimentary records of polycyclic aromatic hydrocarbons, mercury and trace elements in the Qinghai Lake, Tibetan Plateau. *Environmental Pollution*, **158**, 3065-3070.
- Weideborg, M. (2010) Tovdalsvassdraget. Aquateam.
- Wheater, C.P. & Cook, P.A. (2000) *Using statistics to understand the environment*. Routledge, London.
- Whicker, J.J., Pinder, J.E. & Breshears, D.D. (2006) Increased wind erosion from forest wildfire: implications for contaminant-related risks. *Journal of environmental quality*, **35**, 468.
- Wikimedia Commons contributors (2015) Atlas of Norway. Wikimedia Commons, the free media repository.
- Wikipedia contributors (2015) List of municipalities of Norway. Wikipedia, The Free Encyclopedia.
- Wilson, S.J. & Symon, C. (2004) *AMAP assessment 2002 : persistent organic pollutants in the Arctic*. Arctic Monitoring and Assessment Programme (AMAP), Oslo.
- Wu, B., Wang, G., Wu, J., Fu, Q. & Liu, C. (2014) Sources of Heavy Metals in Surface Sediments and an Ecological Risk Assessment from Two Adjacent Plateau Reservoirs. *PLoS ONE*, **9**, e102101.
- Xue, L., Li, Q. & Chen, H. (2014) Effects of a Wildfire on Selected Physical, Chemical and Biochemical Soil Properties in a *Pinus massoniana* Forest in South China. *Forests*, **5**, 2947-2966.
- Yan, Z., Song, N., Cai, H., Tay, J.-H. & Jiang, H. (2012) Enhanced degradation of phenanthrene and pyrene in freshwater sediments by combined employment of sediment microbial fuel cell and amorphous ferric hydroxide. *Enhanced degradation of phenanthrene and pyrene in freshwater sediments by combined employment of sediment microbial fuel cell and amorphous ferric hydroxide*, **199**, 217-225.
- Yao, Z. & Gao, P. (2007) Heavy metal research in lacustrine sediment: a review. *Chinese Journal of Oceanology and Limnology*, **25**, 444-454.

Yr.no (2018) Mykland Froland (Aust-Agder),. Norwegian Meteorological Institute, Norwegian Broadcasting Corporation, www.yr.no.

Yuan, H., Tao, S., Li, B., Lang, C., Cao, J. & Coveney, R.M. (2008) Emission and outflow of polycyclic aromatic hydrocarbons from wildfires in China. *Atmospheric Environment*, **42**, 6828-6835.

Zeng, S., Zeng, L., Dong, X. & Chen, J. (2013) Polycyclic aromatic hydrocarbons in river sediments from the western and southern catchments of the Bohai Sea, China: toxicity assessment and source identification. *Environmental Monitoring and Assessment*, **185**, 4291-4303.

Tables and figures

Table 10 Nomenclature, abbreviations and basic properties for 23 PAHs relevant to this study (based on Rognerud et al. 2007; Tobiszewski & Namieśnik 2012).

Compound	Abbreviation	Chemical formula	No. benzene rings (tot. aromatic rings)	Molecular Weight class (Low or High)	Molecular weight [g mol ⁻¹]	Vapor pressure [mmHg] at 25° C	Log K _{ow} at 25° C	Water solubility [mg L ⁻¹] at 25° C	CAS no. (Chemical Abstract Service)	US-EPA PAH16	Carcinogenic PAH
Naphthalene	NAP	C ₁₀ H ₈	2	LMW	128		3,34	31	91-20-3	x	x
Acenaphthylene	ACNLE	C ₁₂ H ₈	2 (3)	LMW	152	0,029	4,07	16	208-96-8	x	
Acenaphthene	ACNE	C ₁₂ H ₁₀	2 (3)	LMW	154	4,47 x 10 ⁻³	3,98	3,8	83-32-9	x	
Fluorene	FLE	C ₁₃ H ₁₀	2 (3)	LMW	166	3,2 x 10 ⁻⁴	4,9	1,9	86-73-7	x	
Phenanthrene	PA	C ₁₄ H ₁₀	3	LMW	178	6,8 x 10 ⁻⁴	4,45	1,1	85-01-8	x	
Anthracene	ANT	C ₁₄ H ₁₀	3	LMW	178	1,7 x 10 ⁻⁵	4,45	0,04	120-12-7	x	Isomers
Dibenzothiophene	DBTHI	C ₁₂ H ₈ S	2 (3)	LMW	184				132-65-0		
Fluoranthene	FLU	C ₁₆ H ₁₀	3 (4)	HMW	202	5,0 x 19 ⁻⁶	4,9	0,2	206-44-0	x	Isomers
Pyrene	PYR	C ₁₆ H ₁₀	4	HMW	202	6,0 x 10 ⁻⁴	5,32	0,13	129-00-0	x	
Benz[a]anthracene	BaA	C ₁₈ H ₁₂	4	HMW	228	2,2 x 10 ⁻⁸	5,6	0,011	56-55-3	x	x
Chrysene	CHR	C ₁₈ H ₁₂	4	HMW	228	1,2 x 10 ⁻⁵	5,61	0,0019	218-01-9	x	x
Benzo[b]fluoranthene ^a	BbF	C ₂₀ H ₁₂	4 (5)	HMW	252	5,0 x 10 ⁻⁷	6,06	0,0015	205-99-2	x	x
Benzo[j]fluoranthene ^a	BjF	C ₂₀ H ₁₂	4 (5)	HMW	252	5,0 x 10 ⁻⁷	6,06	0,0025	205-82-3	x	x
Benzo[k]fluoranthene	BkF	C ₂₀ H ₁₂	4 (5)	HMW	252	9,6 x 10 ⁻¹¹	6,06	0,008	207-08-9	x	x
Benzo[a]pyrene	BaP	C ₂₀ H ₁₂	5	HMW	252	5,6 x 10 ⁻⁹	6,06	0,0015	50-32-8	x	x
Benzo[e]pyrene	BeP	C ₂₀ H ₁₂	5	HMW	252	5,7 x 10 ⁻⁹	6,44	0,007	192-97-2		
Benzo[g,h,i]perylene	BghiP	C ₂₂ H ₁₂	6	HMW	276	1,03 x 10 ⁻¹⁰	6,5	0,00014	191-24-2	x	
Indeno[1,2,3-c,d]pyrene	IcdP/IP	C ₂₂ H ₁₂	5 (6)	HMW	276	1,0 x 10 ⁻¹¹	6,58	0,00019	193-39-5	x	x
Dibenz[a,c]anthracene ^b	DBaCA	C ₂₂ H ₁₄	5	HMW	278	1,0 x 10 ⁻¹⁰	6,84		215-58-7	x	x
Dibenz[a,h]anthracene ^b	DBaHA	C ₂₂ H ₁₄	5	HMW	278	1,0 x 10 ⁻¹⁰	6,84	0,0005	53-70-3	x	x
Dibenz[a,j]anthracene ^b	DBaJA	C ₂₂ H ₁₄	5	HMW					224-41-9	x	x

^a Benzo[b]jfluoranthene BbjF
^b Dibenz[ac+ah+aj]anthracene DBa3A

Table 11 Comparison of LMW and HMW PAHs (based upon Van Mouwerik et al. 1997, and references therein; Skupińska, Misiewicz & Kasprzycka-Guttman 2004; Lee & Vu 2010; Oliveira et al. 2011; Tsymbalyuk et al. 2011; Nasher et al. 2013; Pampanin & Sydnes 2013).

Low molecular weight (LMW) PAHs	High molecular weight (HMW) PAHs
Consist of 2 – 3 benzene rings (e.g. NAP, ACNLE, ACNE, FLE, PA, ANT, DBTHI)	Consist of 4 – 8 benzene rings (e.g. FLU, PYR, BaA, CHR, BbjF, BkF, BEP, BaP, BghiP, IcdP, DB3A)
Predominance of alkylated PAHs over parent compounds	Predominance of parent compounds over alkylated PAHs
Formed under lower temperatures	Formed under higher temperatures
In general petrogenic (i.e. related to crude oil and its products)	In general pyrogenic (i.e. related to incomplete combustion of organic material such as fossil fuels)
Considered natural	Considered technogenic (anthropogen)
In general more volatile and soluble in water	In general less volatile and soluble in water (hydrophobic/lipophilic)
More rapid breakdown	Great persistence (slow breakdown)
Known to cause acute toxicity to aquatic organisms (greater solubility in water and consequently more bioavailable to aquatic life)	Low acute toxicity, but known mutagens/carcinogens and teratogens (Note: PAHs are not active substances and thus not a mutagen/carcinogen by it self. Only through metabolic biosynthesis [cf. CYP-450] <i>in vivo</i> PAHs can be transformed to such.)
Predominantly found in the gas phase	Predominantly found in particulate phase (low volatility and low solubility favor adherence to solid particles/high affinity for organic carbon in particulate matter), in sediments with concentrations commonly much higher than those detected in surface water (in the range of ug/kg rather than ng/kg)
Greater potential of being transported far from the source	In general deposited closer to the source

Table 12 Nomenclature of (post-)transition metals according to the periodic table of elements.

Nomenclature, (post-)transition metals					
Vanadium	V	Manganese	Mn	Zinc	Zn
Chromium	Cr	Iron	Fe	Cadmium	Cd
Cobalt	Co	Copper	Cu	Mercury	Hg
Nickel	Ni			Lead	Pb

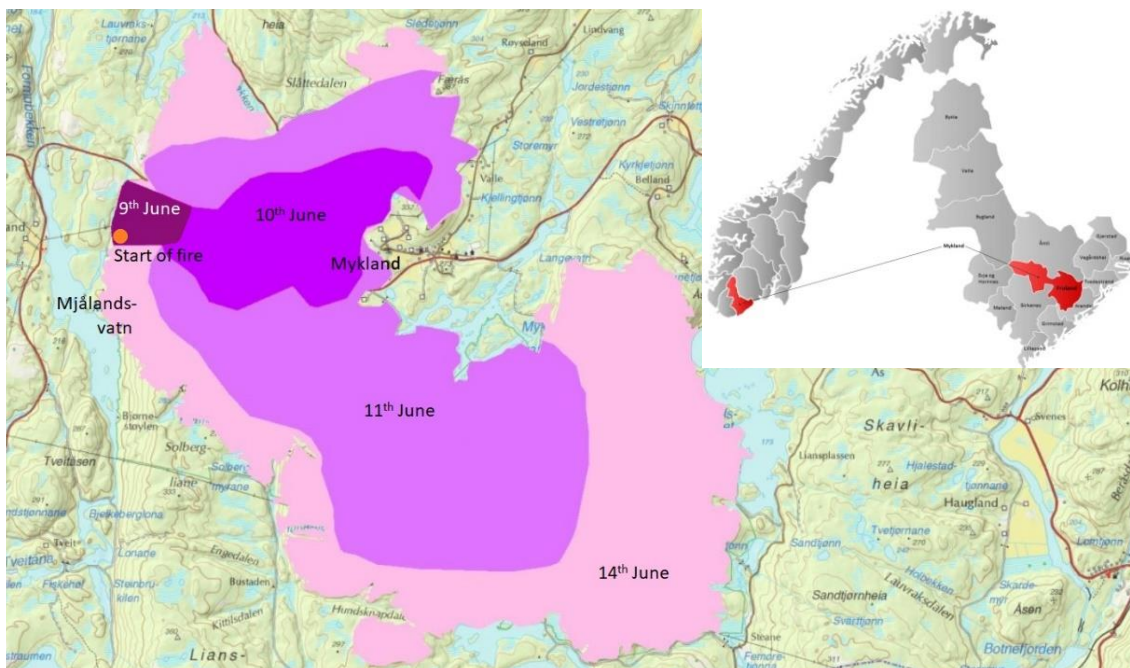


Figure 25 Map of the burnt area, start of fire and its spread (Nygaard & Brean 2014). Upper right corner; Norway with excerpt of Aust-Agder County (furthest right). In the excerpt, Froland municipality is coloured red. Mykland locates in centre of the western part of Froland municipality (own edits of maps from Wikimedia Commons contributors 2015; Wikipedia contributors 2015).

Drainage divide
 Assessed lakes written in **red** (burnt) and **green** (unburnt)

*Part of Myklandsvatna nature reserve

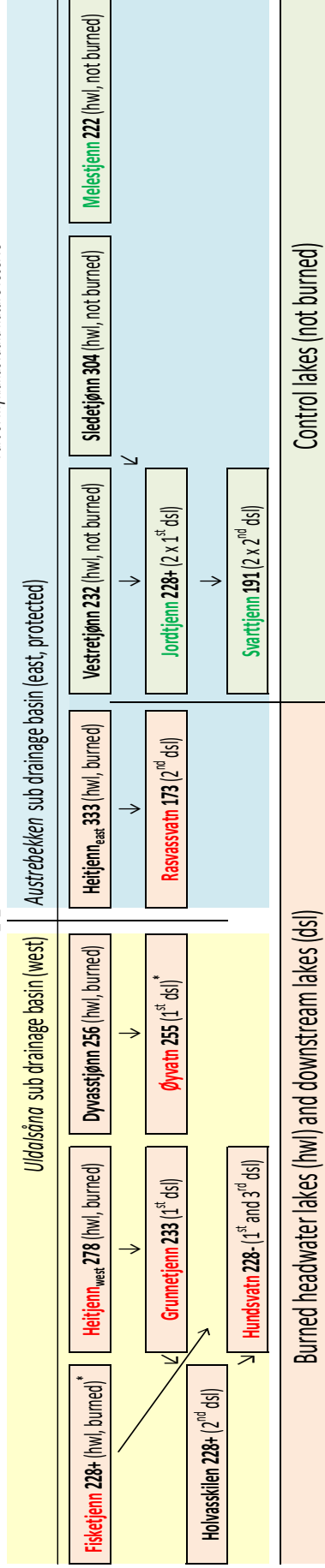








Figure 26 Drainage pattern and meters above sea level (m.a.s.l.) for the eight investigated lakes (all lakes drain to river Toydalsána). Burnt headwater lakes: Hwl Fisketjenn (228+ m.a.s.l.) drains to Hundsvatn (228- m.a.s.l.), Hwl Heitjenn (278 m.a.s.l.) drains via Grumetjenn (233 m.a.s.l.) to Hundsvatn, while Hwl 333 drains to Rasvassvatn (173 m.a.s.l.). Control lakes (not directly affected by fire): Hwl 304 drains via Jordtjenn_{con} (228+ m.a.s.l.) to Svarttjenn_{con} (191 m.a.s.l.). All lakes belong to Toydal drainage basin. Note that the lake just outside the perimeter of the fire, Rasvassvatn, belongs to the same catchment, Austerbekken, as the control lakes.

Table 13 Weather data for the period of the sampling campaign (Yr.no 2018).

Date	Time	Weather	Temp.	Precipitation	Wind	Humidity
7 th of June 2010	08:00		12.9 °C	–	1 m/s from north	77 %
	14:00		17.1 °C	–	1 m/s from east-southeast	58 %
	20:00		18.4 °C	–	1 m/s from south-southeast	45 %
8 th of June 2010	08:00		12.8 °C	–	3 m/s from east-southeast	80 %
	14:00		18.4 °C	–	3 m/s from east-southeast	49 %
	20:00		14.8 °C	–	1 m/s from east	76 %

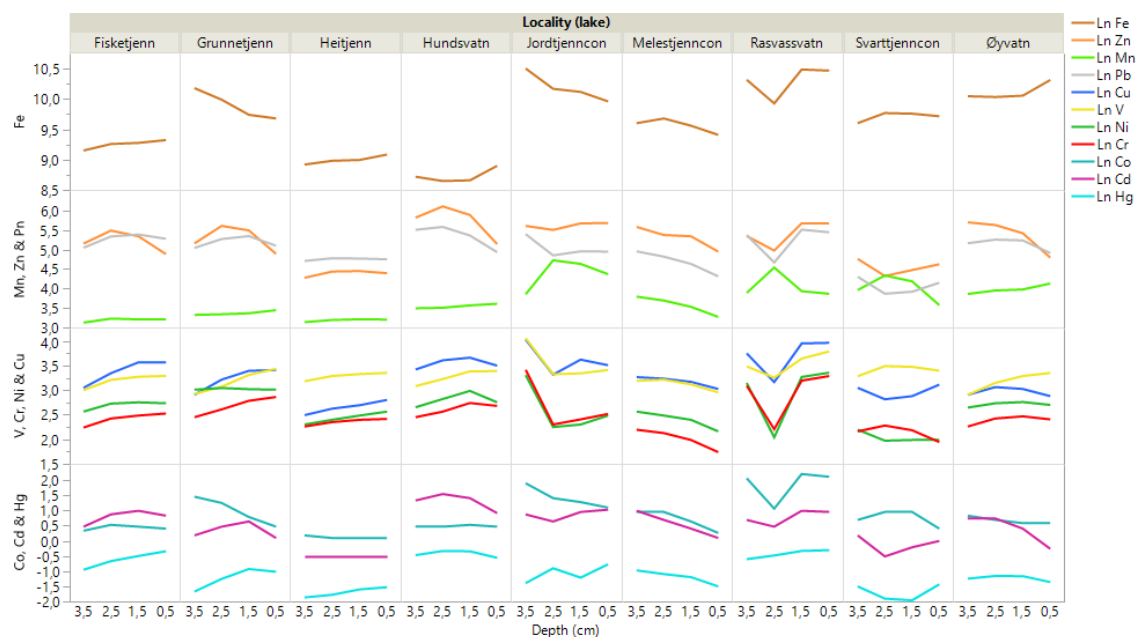


Figure 27 Metal concentration (Ln) fluctuations with depth (industrial sediments), including both Mn, Fe, depth 2.5 cm and the excluded lake Heitjenn. Note how Heitjenn only displays minor alterations in metal concentration levels with sediment depth.

Table 14 Correlation coefficients, r , for different sample sizes, n , according to Walsh (1998); a correlation is significant at level $\alpha = 0.05$ when $n \geq 5$ and $r > \frac{2}{\sqrt{n}}$

n	5	6	7	8	30	32	35	36	38
r	>0.8944	>0.8165	>0.7559	>0.7071	>0.3651	>0.3536	>0.3381	>0.3333	>0.3244

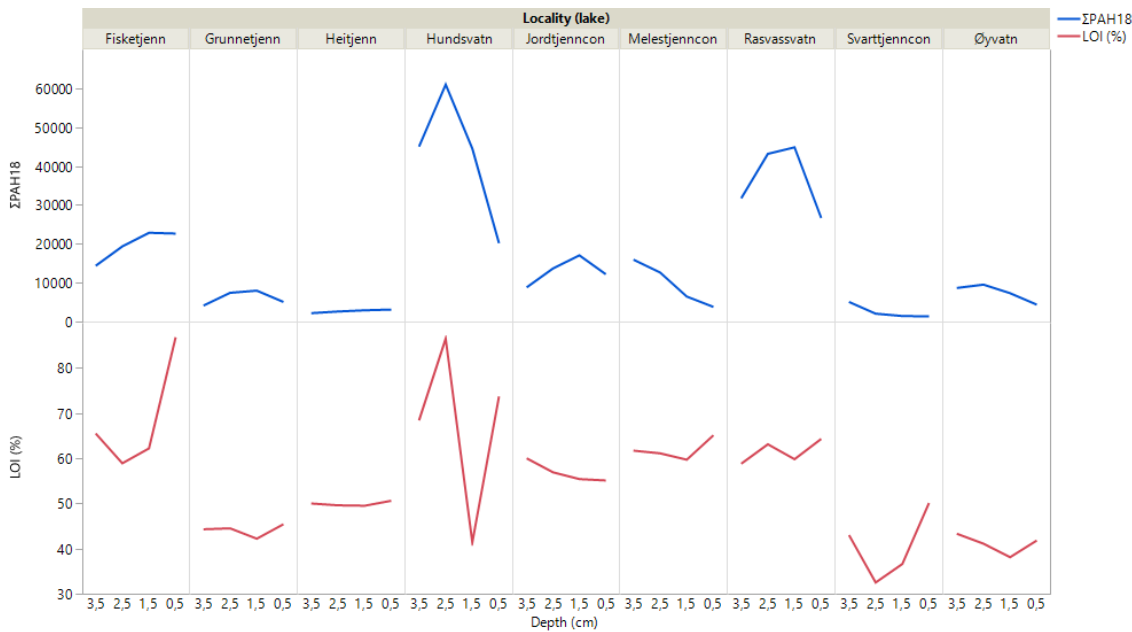


Figure 28 Measured $\Sigma PAH_{EPA16+2}$ and LOI concentration fluctuations with depth. Note how the excluded lake Heitjenn only displays minor alterations in $\Sigma PAH_{EPA16+2}$ concentration levels with sediment depth. Also, worth noting is how depth 2.5 cm, which is omitted from the depth profile illustrations, disrupt interpretation.

Table 15 Environmental quality standards (EQS) and environmental conditions class (ECC) for metals in lacustrine sediments according to M-608; Norwegian classification guide – Quality standards for water, sediment and biota (Norwegian Environment Agency 2016).

Environmental Quality Standards (EQS) for lacustrine sediments			Classes for environmental conditions in lacustrine sediments				
Substance	CAS-no.	EQS _{sed} (mg/kg DM)	I Background (background level)	II Good (no toxic effects)	III Moderate (chronic effects when long-term exposure)	IV Bad (acute toxic effects at short-term exposure)	V Very bad (extensive toxic effects)
Cadmium (Cd)	7440-43-9	2,5 (marine sediments)	0,2	1,5	16	157	>157
Lead (Pb)	7439-92-1	66	25	66	1480	2000	2000-2500
Mercury (Hg)	7439-97-6	0,52 (marine sediments)	0,05	0,52	0,75	1,45	>1,45
Nickel (Ni)	7440-02-0	42 (marine sediments)	30	42	271	533	>533
Copper (Cu) ¹	7440-50-8	84 (marine sediments)	20	210 ²	210 ²	400	>400
Zinc (Zn) ¹	7440-66-6	139	90	139	750	6690	>6690
Chromium (Cr) ¹	7440-47-3	660 (marine sediments)	60	112 ³	112 ³	112 ³	>112

¹River basin specific pollutant (not included in The EU Water Framework Directive 2000/60/EC [WFD]).

²Cu: In lacustrine sediments, upper limit class III is set to the same level as upper limit class II, because the difference between acute and chronic toxicity is minimal (p. 130 in M-241).

³Cr: In lacustrine sediments, upper limit class III and IV is set to the same level as upper limit class II, because the risk of hexavalent chromium (Cr^{VI}) being present (p. 152 in M-241).

Table 16 Increasing (rows from left to right) order of measured metal concentrations at depth 33.0, 1.5 and 0.5 cm. Within outlined cells shaded green, metal order may be disrupted (in some cases also across neighbouring cells outlined and shaded green). Cells shaded yellow pay attention to Pb positioning; in reference sediments actual positioning of Pb is further left relative to the other metals in terms of increasing (left to right) metal concentration order. Vertical columns; declining (red digits) / increasing (expressed as percentages) metal concentrations across depth sections within lakes.

Fisketjenn (µg/g DW): prevailing trend of metals* at depth 0.5 and 1.5	Hg <	Hg (LOI) ¹ <	Cd <	Co <	Cr <	Ni <	V <	Cu <	Pb <	Zn	LOI (%) ²	Acc. Rate (kg m-2 y-1)
Metal concentration@0.5 cm	0,71	0,82	2,30	1,50	12,50	15,40	26,90	35,50	196,00	132,00	86,80	
Δ% (sub-surface to surface)	17,11	-16,08	-14,81	-6,25	4,17	-1,91	1,89	0,28	-10,50	-36,84	39,55	
Metal concentration@1.5 cm	0,61	0,98	2,70	1,60	12,00	15,70	26,40	35,40	219,00	209,00	62,20	
Hundsvatn (µg/g DW): prevailing trend of metals* at depth 0.5 and 1.5	Hg <	Hg (LOI) ¹ <	Cd <	Co <	Cr <	Ni <	V <	Cu <	Pb <	Zn	LOI (%) ²	Acc. Rate (kg m-2 y-1)
Metal concentration@0.5 cm	0,57	0,78	2,50	1,60	14,60	15,70	29,60	33,10	139,00	171,00	73,70	0,40
Δ% (sub-surface to surface)	-19,30	-54,67	-39,02	-5,88	-5,81	-20,71	0,34	-14,91	-34,74	-52,63	78,02	0,00
Metal concentration@1.5 cm	0,71	1,71	4,10	1,70	15,50	19,80	29,50	38,90	213,00	361,00	41,40	0,40
Δ% (reference to sub-surface)	624,49	990,23	4000,00	54,55	58,16	65,00	102,05	143,13	7000,00	1469,57	-33,55	
Metal concentration@44.5 cm	0,10	0,16	0,10	1,10	9,80	12,00	14,60	16,00	3,00	23,00	62,30	
Grunnetjenn (µg/g DW): prevailing trend of metals* at depth 0.5 and 1.5	Hg <	Hg (LOI) ¹ <	Cd <	Co <	Cr <	Ni <	V <	Cu <	Pb <	Zn	LOI (%) ²	Acc. Rate (kg m-2 y-1)
Metal concentration@0.5 cm	0,36	0,80	1,10	1,60	17,50	20,30	31,10	30,30	164,00	133,00	45,40	
Δ% (sub-surface to surface)	-8,59	-15,03	-42,11	-27,27	8,02	-0,98	13,50	1,68	-21,90	-45,27	7,58	
Metal concentration@1.5 cm	0,40	0,94	1,90	2,20	16,20	20,50	27,40	29,80	210,00	243,00	42,20	
Rasvassvatn (µg/g DW): prevailing trend of metals* at depth 0.5 and 1.5	Hg <	Hg (LOI) ¹ <	Cd <	Co <	Cr <	Ni <	V <	Cu <	Pb <	Zn	LOI (%) ²	Acc. Rate (kg m-2 y-1)
Metal concentration@0.5 cm	0,74	1,15	2,60	8,30	26,80	28,70	44,20	52,70	232,00	292,00	64,30	0,10
Δ% (sub-surface to surface)	2,64	-4,54	-3,70	-8,79	9,84	9,13	15,71	1,35	-6,45	0,00	7,53	42,86
Metal concentration@1.5 cm	0,72	1,20	2,70	9,10	24,40	26,30	38,20	52,00	248,00	292,00	59,80	0,07
Δ% (reference to sub-surface)	466,14	492,65	1250,00	313,64	1,67	48,59	39,42	5,91	3601,49	418,65	-4,47	
Metal concentration@35.5 cm	0,13	0,20	0,20	2,20	24,00	17,70	27,40	49,10	6,70	56,30	62,60	
Øyvavn (µg/g DW): prevailing trend of metals* at depth 0.5 and 1.5	Hg <	Hg (LOI) ¹ <	Cd <	Co <	Cr <	Ni <	V <	Cu <	Pb <	Zn	LOI (%) ²	Acc. Rate (kg m-2 y-1)
Metal concentration@0.5 cm	0,26	0,61	0,77	1,80	11,10	14,90	28,50	17,80	136,00	121,00	41,80	
Δ% (sub-surface to surface)	-17,89	-25,16	-48,67	0,00	-5,93	-5,70	6,34	-13,59	-27,66	-46,46	9,71	
Metal concentration@1.5 cm	0,31	0,82	1,50	1,80	11,80	15,80	26,80	20,60	188,00	226,00	38,10	
Δ% (reference to sub-surface)	268,24	279,83	650,00	-37,93	66,20	31,67	100,00	92,52	3086,44	327,22	-3,05	
Metal concentration@33.5 cm	0,09	0,22	0,20	2,90	7,10	12,00	13,40	10,70	5,90	52,90	39,30	
Jordtjenn _{con} (µg/g DW): prevailing trend of metals* at depth 0.5 and 1.5	Hg <	Hg (LOI) ¹ <	Cd <	Co <	Cr <	Ni <	V <	Cu <	Pb <	Zn	LOI (%) ²	Acc. Rate (kg m-2 y-1)
Metal concentration@0.5 cm	0,46	0,84	2,80	3,00	12,40	12,00	30,30	33,40	141,00	294,00	55,10	0,40
Δ% (sub-surface to surface)	55,37	56,22	7,69	-16,67	11,71	20,00	7,07	-10,70	-0,70	1,03	-0,54	0,00
Metal concentration@1.5 cm	0,30	0,54	2,60	3,60	11,10	10,00	28,30	37,40	142,00	291,00	55,40	0,40
Δ% (reference to sub-surface)	297,33	259,32	420,00	111,76	44,16	78,57	20,43	72,35	1320,00	430,05	10,58	
Metal concentration@21.5 cm	0,08	0,15	0,50	1,70	7,70	5,60	23,50	21,70	10,00	54,90	50,10	
Svarttjenn _{con} (µg/g DW): prevailing trend of metals* at depth 0.5 and 1.5	Hg <	Hg (LOI) ¹ <	Cd <	Co <	Cr <	Ni <	V <	Cu <	Pb <	Zn	LOI (%) ²	Acc. Rate (kg m-2 y-1)
Metal concentration@0.5 cm	0,24	0,48	1,00	1,50	7,00	7,30	29,90	22,50	63,50	102,00	50,10	
Δ% (sub-surface to surface)	69,50	23,83	23,46	-42,31	-21,35	0,00	-7,43	26,40	25,99	16,17	36,89	
Metal concentration@1.5 cm	0,14	0,39	0,81	2,60	8,90	7,30	32,30	17,80	50,40	87,80	36,60	
Δ% (reference to sub-surface)	76,25	137,41	305,00	160,00	122,50	17,74	125,87	22,76	581,08	143,89	-25,76	
Metal concentration@36.5 cm	0,08	0,16	0,20	1,00	4,00	6,20	14,30	14,50	7,40	36,00	49,30	
Melestjenn _{con} (µg/g DW): prevailing trend of metals* at depth 0.5 and 1.5	Hg <	Hg (LOI) ¹ <	Cd <	Co <	Cr <	Ni <	V <	Cu <	Pb <	Zn	LOI (%) ²	Acc. Rate (kg m-2 y-1)
Metal concentration@0.5 cm	0,22	0,34	1,10	1,30	5,70	8,70	19,20	20,60	74,70	141,00	65,10	
Δ% (sub-surface to surface)	-26,40	-32,51	-26,67	-31,58	-21,92	-20,91	-15,04	-13,45	-27,48	-32,54	9,05	
Metal concentration@1.5 cm	0,30	0,51	1,50	1,90	7,30	11,00	22,60	23,80	103,00	209,00	59,70	
Δ% (reference to sub-surface)	163,48	141,41	1400,00	171,43	55,32	57,14	115,24	122,43	1392,75	736,00	9,14	
Metal concentration@36.5 cm	0,12	0,21	0,10	0,70	4,70	7,00	10,50	10,70	6,90	25,00	54,70	

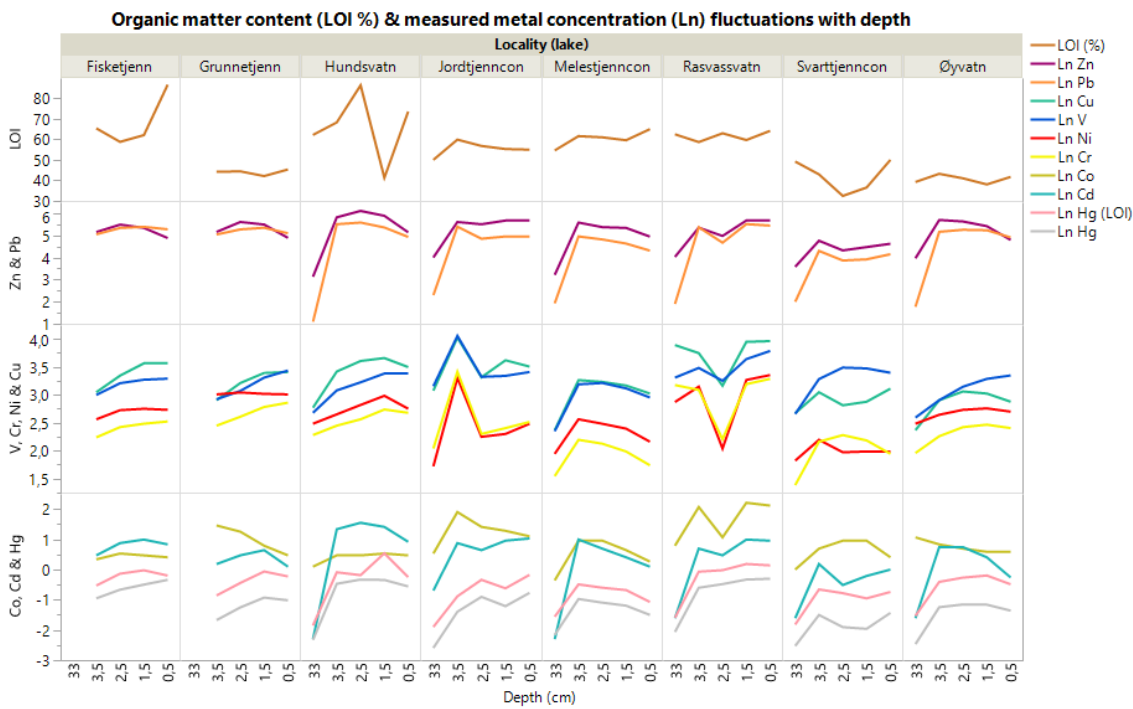


Figure 29 Depth profiles on sediment LOI and Ln-logged metal concentrations illustrate historic variations in sediment organic matter content and metal load for all eight lakes studied. LOI-normalized concentrations of Hg are included. There is no obvious parallel between vertical (depth) variations of metal concentrations and LOI when plotted against each other. Worth noting is how depth 2.5 cm disrupt interpretation.

Table 17 Formatted loading matrix from the PCA on all metals at all depths (outliers included). Cells shaded green indicate weighty loads on a principal component (PC). Red digits load in the opposite direction (negatively) of black digits (positively) along the PC. Metals load positively and quite equal along PC 1. Zn, Cd, Hg and Pb load negatively along PC 2, while V, Cr and Co load positively along PC 2.

	PC 1 (63.6 %)	PC 2 (19.7 %)	PC 3 (5.45 %)
Eigenvalue	5.7209	1.7757	0.4905
Cu	0,8831	0,2538	0,2297
Pb	0,8676	-0,3727	-0,1866
Ni	0,8448	0,2541	-0,4033
Cr	0,8296	0,5014	-0,0393
Zn	0,7735	-0,5187	-0,0724
Hg	0,7722	-0,4336	0,1232
Cd	0,7704	-0,5953	0,1435
V	0,7304	0,4422	0,4102
Co	0,6816	0,4994	-0,1717

Table 18 Formatted loading matrix from the PCA (outliers included) on metals, ΣPAH and lake parameters. Cells shaded green indicate weighty loads on a principal component (PC). Red digits load in the opposite direction (negatively) of black digits (positively) along the PCs. All parameters load positively along PC 1, except pH and TOC which load in the opposite direction. Along PC 2 metals are split in two clusters (V, Cr, Co, Ni, and Zn, Cd, Hg, respectively) loading in opposite directions.

	PC 1 (49.9 %)	PC 2 (19.4 %)	PC 3 (10.5 %)	PC 4 (7.77 %)
Eigenvalue	6.9869	2.7131	1.4758	1.0871
Cu	0,8965	0,2130	-0,0341	0,3335
Pb	0,8421	-0,1195	0,4052	-0,1746
Hg	0,8302	-0,4099	-0,1978	-0,1260
Cr	0,7945	0,5665	0,0905	0,1040
Ni	0,7698	0,4192	0,2759	-0,0975
Cd	0,7235	-0,5447	0,3112	0,2005
Zn	0,6392	-0,3380	0,5867	0,1063
Co	0,6172	0,6207	-0,1609	0,0435
V	0,4835	0,6541	-0,0888	0,4473
ΣPAH18	0,7721	-0,4859	-0,1149	-0,1055
Residence time	0,6232	0,2385	-0,5435	-0,3088
LOI	0,5107	-0,5418	-0,3763	0,3081
pH	-0,6509	0,3624	0,5024	-0,0023
TOC	-0,5876	-0,2163	-0,0983	0,6740

Table 19 Correlation table (n = 32, r > 0.3536, α = 0.05) on metals (including Fe), ΣPAH_{EPA16+2}, pH, TOC, RT and LOI. When considering all metals in all lakes at all industrial depths (outliers included) simultaneously, Cu, Cd and Hg correlate to LOI, which is not seen for the rest of the metals. Metals form in two clusters (shaded in different green colours). Fe correlates to one of them.

	Cd	Co	Cr	Cu	Ni	Pb	V	Zn	Hg	Fe	ΣPAH18	pH	TOC	RT	LOI
Cd	1	0,0866	0,3039	0,5909	0,3457	0,7222	0,0809	0,8708	0,7478	-0,2750	0,8072	-0,4992	-0,2045	0,1135	0,5423
Co	0,0866	1	0,7740	0,6817	0,6471	0,3397	0,6384	0,2179	0,2270	0,8021	0,2240	-0,2001	-0,3699	0,7118	0,0427
Cr	0,3039	0,774	1	0,8639	0,8942	0,6335	0,807	0,3382	0,4002	0,5680	0,3005	-0,2951	-0,5509	0,5068	0,1184
Cu	0,5909	0,6817	0,8639	1	0,7240	0,6536	0,7288	0,5017	0,6340	0,3401	0,5356	-0,5412	-0,3730	0,5015	0,4471
Ni	0,3457	0,6471	0,8942	0,7240	1	0,7844	0,5059	0,4420	0,4201	0,4564	0,2944	-0,2722	-0,5891	0,4157	0,1040
Pb	0,7222	0,3397	0,6335	0,6536	0,7844	1	0,1920	0,7464	0,6802	0,1059	0,6247	-0,4144	-0,6165	0,2965	0,3579
V	0,0809	0,6384	0,8070	0,7288	0,5059	0,1920	1	0,0440	0,1367	0,5508	0,0688	-0,1155	-0,1974	0,3264	0,0138
Zn	0,8708	0,2179	0,3382	0,5017	0,4420	0,7464	0,0440	1	0,5072	0,0042	0,6205	-0,1893	-0,2363	0,0743	0,2842
Hg	0,7478	0,2270	0,4002	0,6340	0,4201	0,6802	0,1367	0,5072	1	-0,1759	0,8679	-0,7590	-0,4662	0,5610	0,6428
Fe	-0,2750	0,8021	0,5680	0,3401	0,4564	0,1059	0,5508	0,0042	-0,1759	1	-0,1886	0,3170	-0,3329	0,4450	-0,2909
ΣPAH18	0,8072	0,2240	0,3005	0,5356	0,2944	0,6247	0,0688	0,6205	0,8679	-0,1886	1	-0,6640	-0,3802	0,5274	0,5756
pH	-0,4992	-0,2001	-0,2951	-0,5412	-0,2722	-0,4144	-0,1155	-0,1893	-0,7590	0,3170	-0,6640	1	0,2858	-0,4735	-0,6876
TOC (mg C/l)	-0,2045	-0,3699	-0,5509	-0,3730	-0,5891	-0,6165	-0,1974	-0,2363	-0,4662	-0,3329	-0,3802	0,2858	1	-0,4658	0,0123
Residence time (yr)	0,1135	0,7118	0,5068	0,5015	0,4157	0,2965	0,3264	0,0743	0,5610	0,4450	0,5274	-0,4735	-0,4658	1	0,2498
LOI (%)	0,5423	0,0427	0,1184	0,4471	0,1040	0,3579	0,0138	0,2842	0,6428	-0,2909	0,5756	-0,6876	0,0123	0,2498	1

Table 20 Correlation probabilities ($n = 32, \rho \leq 0.05$) for metal correlations (including Fe), Σ PAH_{EPA16+2}, pH, TOC, RT and LOI (figure 19).

	Cd	Co	Cr	Cu	Ni	Pb	V	Zn	Hg	Fe	Σ PAH18	pH	TOC	RT	LOI
Cd	<,0001	0,6373	0,0908	0,0004	0,0526	<,0001	0,6597	<,0001	<,0001	0,1277	<,0001	0,0036	0,2617	0,5361	0,0013
Co	0,6373	<,0001	<,0001	<,0001	<,0001	0,0572	<,0001	0,2310	0,2114	<,0001	0,2178	0,2723	0,0372	<,0001	0,8167
Cr	0,0908	<,0001	<,0001	<,0001	<,0001	<,0001	<,0001	0,0583	0,0232	0,0007	0,0947	0,1011	0,0011	0,0031	0,5185
Cu	0,0004	<,0001	<,0001	<,0001	<,0001	<,0001	<,0001	0,0034	<,0001	0,0568	0,0016	0,0014	0,0355	0,0035	0,0103
Ni	0,0526	<,0001	<,0001	<,0001	<,0001	<,0001	0,0031	0,0113	0,0167	0,0087	0,1019	0,1318	0,0004	0,0180	0,5710
Pb	<,0001	0,0572	<,0001	<,0001	<,0001	<,0001	0,2926	<,0001	<,0001	0,5640	0,0001	0,0184	0,0002	0,0994	0,0443
V	0,6597	<,0001	<,0001	<,0001	0,0031	0,2926	<,0001	0,8111	0,4555	0,0011	0,7081	0,5291	0,2787	0,0683	0,9402
Zn	<,0001	0,2310	0,0583	0,0034	0,0113	<,0001	0,8111	<,0001	0,0030	0,9818	0,0002	0,2994	0,1929	0,6861	0,1149
Hg	<,0001	0,2114	0,0232	<,0001	0,0167	<,0001	0,4555	0,0030	<,0001	0,3355	<,0001	<,0001	0,0072	0,0008	<,0001
Fe	0,1277	<,0001	0,0007	0,0568	0,0087	0,5640	0,0011	0,9818	0,3355	<,0001	0,3013	0,0771	0,0627	0,0107	0,1063
Σ PAH18	<,0001	0,2178	0,0947	0,0016	0,1019	0,0001	0,7081	0,0002	<,0001	0,3013	<,0001	<,0001	0,0318	0,0019	0,0006
pH	0,0036	0,2723	0,1011	0,0014	0,1318	0,0184	0,5291	0,2994	<,0001	0,0771	<,0001	<,0001	0,1128	0,0062	<,0001
TOC (mg C/l)	0,2617	0,0372	0,0011	0,0355	0,0004	0,0002	0,2787	0,1929	0,0072	0,0627	0,0318	0,1128	<,0001	0,0072	0,9467
Residence time (yr)	0,5361	<,0001	0,0031	0,0035	0,0180	0,0994	0,0683	0,6861	0,0008	0,0107	0,0019	0,0062	0,0072	<,0001	0,1679
LOI (%)	0,0013	0,8167	0,5185	0,0103	0,5710	0,0443	0,9402	0,1149	<,0001	0,1063	0,0006	<,0001	0,9467	0,1679	<,0001

Table 21 Environmental quality standards (EQS) and environmental conditions class (ECC) for PAHs in lacustrine sediments according to the Norwegian classification guide M-608 Quality standards for water, sediment and biota (Norwegian Environment Agency 2016).

Environmental Quality Standards (EQS) for lacustrine sediments				Classes for environmental conditions in lacustrine sediments				
Substance	Abbreviation	CAS-no.	EQS _{sed} (mg/kg DM)	I Background (background level), NB: µg/kg DM	II Good (no toxic effects), NB: µg/kg DM	III Moderate (chronic effects when long-term exposure), NB: µg/kg DM	IV Bad (acute toxic effects at short-term exposure), NB: µg/kg DM	V Very bad (extensive toxic effects), NB: µg/kg DM
Naphthalene	NAP	91-20-3	0,027 (marine sediments)	2	27	1754	8769	>8769
Acenaphthylene ¹	ACNLE	208-96-8	0,033	1,6	33	85	8500	>8500
Acenaphthene ¹	ACNE	83-32-9	0,10	2,4	96	195	19500	>19500
Fluorene ¹	FLE	86-73-7	0,15	6,8	150	694	34700	>34700
Phenanthrene ¹	PA / PHE	85-01-8	0,78	6,8	780	2500	25000	>25000
Anthracene	ANT	120-12-7	0,0046 (marine sediments)	1,2	4,6	30	295	>295
Fluoranthene ²	FLU / FLT	206-44-0	0,40 (marine sediments)	8	400	400	2000	>2000
Pyrene ¹	PYR	129-00-0	0,084	5,2	84	840	8400	>8400
Benzo[a]Anthracene ¹	BaA	56-55-3	0,06	3,6	60	501	50100	>50100
Chrysene ^{1,3}	CHR	218-01-9	0,28	4,4	280	280	2800	>2800
Benzo[b]Fluoranthene ⁴	BbF	205-99-2	0,14 (marine sediments)	90	140	140	10600	>10600
Benzo[k]Fluoranthene ⁴	BkF	207-08-9	0,14 (marine sediments)	90	135	135	7400	>7400
Benzo[a]Pyrene	BaP	50-32-8	0,18 (marine sediments)	6	183	2300 (freshwater)	13100	>13100
Benzo[g,h,i]Perylene ⁵	BghiP	191-24-2	0,084 (marine sediments)	18	84	84	1400	>1400
Indeno[1,2,3-c,d]Pyrene ⁶	IcdP / IP	193-39-5	0,063 (marine sediments)	20	63	63	2300	>2300
Dibenzo[a,h]Anthracene ¹	DBaA	53-70-3	0,027	12	27	273	2730	>2730

¹River basin specific pollutant (not included in The EU Water Framework Directive 2000/60/EC [WFD]).

²FLU: In lacustrine sediments, upper limit class III is set to the same level as upper limit class II, because the difference between acute and chronic toxicity is minimal (p. 71 in M-241).

³CHR: In lacustrine sediments, upper limit class III is set to the same level as upper limit class II, because there is a general lack of data to calculate acute toxicity, besides differences between acute and chronic toxicity are minimal.

⁴BbF og BkF: In lacustrine sediments, upper limit class III is set to the same level as upper limit class II, because there is a lack of data to calculate acute toxicity. This is accordance with Directive 2013/39/EU (p. 75 in M-241).

⁵Benzo[g,h,i]Perylene: Differences between document TA-3001 (KJUF 2013) and Directive 2013/39/EU has lead to a conclusion where Class II and Class III EQS are set alike (p. 82 in M-241).

⁶Indeno[1,2,3-c,d]Pyrene: In lacustrine sediments, upper limit class III is set to the same level as upper limit class II, because there is a general lack of data to calculate acute toxicity and differences between acute and chronic toxicity are minimal.

Table 22 LOI-normalized PAH concentrations in lacustrine sediments. Colours code for ECC for PAHs in lacustrine sediments according to the Norwegian classification guide M-608 (Norwegian Environment Agency 2016). Blue code for Class I (background), green for Class II (good), yellow Class III (moderate), orange Class IV (bad) and Red class V (very bad). There are no environmental class for DBTHI, BeP, PER (biogenic) or ΣPAHs (not colour-coded).

Locality (lake)	Depth (cm)	LOI (%)	Year of deposition	Acc. Rate (kg m ⁻² y ⁻¹)	NAP-C (µg/kg DW)	ACNLE* (µg/kg DW)	ACNE* (µg/kg DW)	FILE* (µg/kg DW)	PA* (µg/kg DW)	ANT*	DBTHI (µg/kg DW)	FLU* (µg/kg DW)	PYR* (µg/kg DW)	BAA-C (µg/kg DW)	CHR-C (µg/kg DW)	BBJF-C (µg/kg DW)	BKF-C (µg/kg DW)	BEP (µg/kg DW)	BAP-C (µg/kg DW)	PER	BGHP* (µg/kg DW)	ICDP-C (µg/kg DW)	DBASA-C (µg/kg DW)	ΣPAH19 (µg/kg DW)	ΣPAH _{PAH12} (µg/kg DW)	ΣPAH16* (µg/kg DW)	ΣC-PAH8 (C) (µg/kg DW)		
Ffsketjenn	0.5	86.8			161	49.5	26.5	112	829	115	77.2	2169	1382	899	2535	5415	1728	2765	1118	910	2985	3111	599	27016	26106	23284	15565		
	1.5	62.2			225	65.9	43.4	154	1206	177	1206	177	116	3055	2090	1286	3376	7556	2412	3859	1608	1527	4341	836	38273	36746	32772	21640	
	2.5	58.9			204	56.0	46.8	115	1121	161	1121	161	100	2716	1888	1171	3656	6791	2207	3396	1460	2037	3735	3805	747	34893	32856	29380	19542
	3.5	65.5			137	39.7	36.6	73.3	809	107	67.2	1985	67.2	1985	1282	748	2137	4427	1359	2290	931	2595	2443	2595	473	24537	21942	19585	12809
	0.5	73.7			2006 ±1	0.40	217	50.2	19.0	85.5	896	111	93.6	2171	1628	1058	2442	6513	2035	2985	1628	611	2442	2578	434	27999	27388	24309	16906
Hundsvatn	1.5	41.4	1997 ±2	0.40	604	184	70.0	338	2899	459	338	7488	6039	4599	9179	26570	7971	11836	7005	1570	9862	10386	1836	109022	107452	96278	68140		
	2.5	86.5	1983 ±2	0.30	336	127	37.0	220	1965	324	208	4855	4162	3353	5316	16105	5202	7977	5087	986	6705	7168	1272	71436	70499	62314	43919		
	3.5	68.4	1966 ±2	0.30	336	108	35.1	205	2047	336	190	4825	4240	3070	5117	14327	4825	7018	4678	965	6433	6871	1155	66781	65816	58608	40380		
	0.5	45.4			141	41.9	9.69	30.8	529	44.1	37.4	859	419	242	1123	2643	639	1167	308	121	1278	1432	220	11285	11164	9359	6749		
Grunnetjenn	1.5	42.2			185	40.3	15.6	52.1	806	85.3	61.6	1374	711	427	1919	4285	1090	1991	592	474	2275	2607	403	19373	18900	16847	11488		
	2.5	44.5			157	31.5	15.1	47.2	697	87.6	53.9	1236	674	427	1551	3596	989	1753	584	1191	2157	2247	380	17853	16862	14856	9910		
	3.5	44.3			99.3	18.5	12.2	33.9	406	58.7	31.6	745	406	226	767	2032	519	948	316	1964	1219	1287	199	11288	9324	8344	5445		
	0.5	64.3	2009 ±1	0.10	249	65.3	28.0	104	1260	140	90.2	2488	2177	1384	3421	10731	3110	5288	2333	529	3888	4044	684	42014	41485	36107	25956		
Rasvassvatn	1.5	59.8	2004 ±1	0.07	351	110	36.8	184	2508	284	167	4849	4348	3010	5853	18395	5518	8696	4692	1070	7191	7525	1271	76050	74980	68117	46605		
	2.5	63.1	1998 ±1	0.06	317	109	33.3	174	2377	301	158	5071	4120	2894	5230	13312	5230	6656	3962	1585	6399	8716	1537	69894	69399	61585	40988		
	3.5	58.8	1992 ±1	0.08	272	85.0	25.5	136	1871	238	124	4092	3231	2041	10374	3741	5102	3061	1701	6973	7313	1207	55660	53959	48733	32092			
	0.5	41.8			206	45.5	12.4	38.3	478	45.5	35.9	718	407	230	933	2392	478	1148	383	122	1292	1411	208	10584	10462	9278	6242		
Øyvatn	1.5	36.1			220	68.2	15.5	49.9	682	81.4	57.7	1234	735	420	1860	4724	919	2178	682	341	2441	2625	384	19548	19207	16971	11664		
	2.5	41.1			221	90.0	17.3	53.5	706	90.0	60.8	1285	803	511	2068	5596	1119	2876	827	706	3163	3406	487	23866	23161	20424	14236		
	3.5	43.3			166	62.4	12.2	41.6	624	80.8	53.1	993	716	439	1755	4850	1062	2286	693	1316	2771	3002	416	21340	20024	17684	12383		
	0.5	55.1	2006 ±1	0.40	200	45.4	18.1	58.3	583	94.4	58.1	1289	1125	653	1525	5808	1597	2722	1107	982	2359	2541	381	23103	22142	19381	13811		
Svarttjenn _{com}	1.5	59.4	1995 ±2	0.40	181	48.7	18.1	65.0	614	114	59.6	1444	1318	776	1751	6679	6859	3249	1336	1516	2708	3069	487	32291	30774	27466	21137		
	2.5	56.9	1982 ±2	0.40	176	47.5	17.6	65.0	598	104	56.2	1318	1213	756	1757	6151	1670	2988	1248	1933	2636	2812	439	25964	24051	21007	15009		
	3.5	60.0	1967 ±2	0.50	127	28.3	15.8	45.0	433	73.3	36.7	817	733	467	850	3667	983	1833	800	2333	1667	1833	267	17009	14676	12906	8993		
	0.5	50.1			73.9	20.0	9.78	20.0	174	18.8	13.2	259	194	85.8	240	519	144	259	128	1078	279	259	45.9	3802	2724	2452	1495		
Svarttjenn _{com}	1.5	36.6			112	19.4	15.8	22.4	26.4	26.2	20.2	410	273	126	328	738	199	363	199	929	383	383	68.3	4888	3959	3557	2153		
	2.5	32.5			114	23.7	19.1	26.2	338	36.9	29.5	646	431	197	554	1200	338	615	338	769	646	646	117	7086	6317	5672	3505		
	3.5	43.0			130	30.2	21.2	39.5	485	58.1	46.5	1140	791	395	1116	2279	698	1163	651	1209	1256	1302	233	13023	11814	10605	6805		
	0.5	65.1			89.1	16.9	12.1	27.6	323	32.3	18.4	538	369	154	430	1121	369	568	281	1997	691	691	117	7825	5828	5241	3232		
Melestjenn _{com}	1.5	59.7			101	18.4	15.7	40.2	486	58.6	33.5	955	653	335	888	2178	737	1089	503	1675	1256	1256	218	12495	10820	9687	6214		
	2.5	61.1			162	39.3	36.0	80.2	949	110	70.4	1984	1358	655	1637	4092	1408	1964	988	1358	2291	2455	426	22052	20694	18680	11831		
	3.5	61.7			211	63.2	32.4	94.0	1151	131	88.1	2481	1621	924	2431	5024	1572	2431	1475	1556	2755	2917	502	55029	25856	23335	15057		

Class limits for Dibenzo[a,h]Anthracene (DBaH) used

Class limits for Benzo[b]Fluoranthene (BbF) used

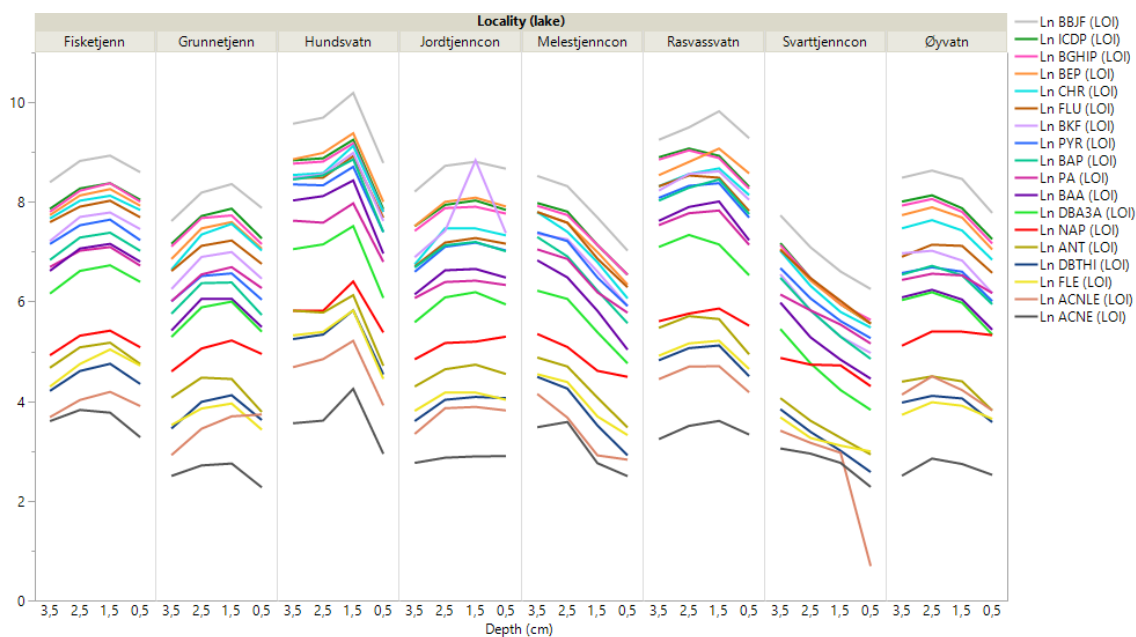


Figure 30 Concentration fluctuations with depth on single Ln PAH_{LOI}.

Table 23 Formatted loading matrix from the PCA on Ln PAH_{LOI} (outliers included).

Cells shaded green indicate weighty loads on a principal component (PC). Red digits load in the opposite direction (negatively) of black digits (positively) along the PCs.

PAHs load positively and quite equal along PC 1. Only ACNE loads along PC 2.

	PC 1 (93,3%)	PC 2 (3,1 %)	PC 3 (1,4%)
Eigenvalue	16.7903	0.5529	0.2514
ANT	0,9919	0,0437	-0,0599
BAA	0,9892	0,0832	-0,0769
DBTHI	0,9887	0,0501	0,0725
CHR	0,9885	-0,0575	0,0186
DBA3A	0,9882	-0,0784	-0,0436
FLU	0,9860	0,1144	0,0096
BEP	0,9857	-0,1188	-0,0694
BBJF	0,9824	-0,1431	-0,0628
BAP	0,9820	0,0581	-0,0737
PYR	0,9812	0,1402	-0,0748
BGHIP	0,9808	-0,1406	-0,0526
PA	0,9781	0,0347	0,0530
ICDP	0,9770	-0,1679	-0,0489
FLE	0,9728	0,1834	-0,0165
BKF	0,9566	-0,0515	-0,2019
NAP	0,9274	-0,1348	0,2373
ACNLE	0,8930	-0,2868	0,2845
ACNE	0,8177	0,5249	0,1681

Table 24 Declining (red digits) / increasing (expressed as percentages) PAH concentrations from sub-surface to surface sediments. Measured ΣPAH_{EPA16+2} concentration levels display a -38 % (median, range -1 to -55 %) decline. When PAHs' association to sediment OM is accounted for, ΣPAH_{EPA16+2} LOI decline with -43 % (median, range -29 to -74 %). With only singular exceptions, all individual PAH concentrations (i.e. both measured PAH concentrations and PAH_{LOI} concentrations) decline. The PAH decline seen in Mykland surface sediments represents the first decade of the 2000s.

Locality (lake)	Depth (cm)	LOI (%)	Year of deposition	Acc. Rate (kg m ⁻² y ⁻¹)	NAP * LOI (µg/kg DW)	ACNLE * LOI (µg/kg DW)	ACNE * LOI (µg/kg DW)	FLE * LOI (µg/kg DW)	PA * LOI (µg/kg DW)	ANT * LOI (µg/kg DW)	DBTHI LOI (µg/kg DW)	FLU * LOI (µg/kg DW)	PYR * LOI (µg/kg DW)	BAA * C LOI (µg/kg DW)	CHR * C LOI (µg/kg DW)	BBJF * C LOI (µg/kg DW)	BKF * C LOI (µg/kg DW)	BEP LOI (µg/kg DW)	BAP * C LOI (µg/kg DW)	BGHP * LOI (µg/kg DW)	ICDP * C LOI (µg/kg DW)	DBA3A * C LOI (µg/kg DW)	EPAH ₁₆₊₂ LOI (µg/kg DW)	EPAH ₁₆₊₂ (% LOI) (µg/kg DW)	Σ-PAH6 (C) LOI (µg/kg DW)
Fiskefjenn	0.50	86.80			161.29	49.54	26.50	111.75	829.49	115.21	77.19	2188.94	1382.49	898.62	2534.56	5414.75	1728.11	2794.98	1117.51	2995.39	3110.60	2910.59	23263.82	28105.99	15564.52
		Δ%			-29.34	-24.85	-38.96	-27.59	-31.21	-34.86	-33.32	-28.34	-33.65	-30.13	-24.93	-28.34	-28.34	-28.34	-30.49	-31.00	-28.34	-28.34	-28.96	-29.01	-28.07
Fiskefjenn	1.50	62.20			226.08	65.92	43.41	154.34	1205.79	176.85	115.76	3054.66	2090.03	1286.17	3376.21	7556.27	2411.58	3858.52	1607.72	4340.84	4340.84	836.01	36745.98	32771.70	21639.87
Hundsvatn	0.50	73.70	2006 ± 1	0.40	217.10	50.20	19.00	85.48	895.52	111.26	93.62	2170.96	1628.22	1058.34	2442.33	6512.89	2035.28	2985.07	1628.22	2442.33	2578.02	434.19	27388.06	24309.36	16906.38
		Δ%			-64.05	-72.65	-72.88	-74.72	-69.10	-75.76	-72.31	-71.01	-73.04	-76.94	-73.39	-75.49	-74.47	-74.78	-76.76	-74.72	-75.18	-76.35	-74.51	-74.49	-75.19
Hundsvatn	1.50	41.40	1997 ± 2	0.40	603.86	183.57	70.05	338.16	2896.55	458.94	338.16	7487.92	6038.65	4589.37	9178.74	26570.05	7971.01	11835.75	7094.83	9661.84	10386.47	1835.75	107451.69	95277.78	68140.10
Grunnetfjenn	0.50	45.40			140.97	41.85	9.69	30.84	528.63	44.05	37.44	869.03	418.50	242.29	1123.35	2843.17	638.77	1167.40	308.37	1277.53	1431.72	220.26	11163.88	9959.03	6748.90
		Δ%			-23.73	3.89	-38.03	-40.85	-34.39	-48.36	-39.22	-37.50	-41.13	-43.20	-41.47	-38.03	-41.40	-41.35	-47.95	-43.94	-45.07	-45.32	-40.93	-40.89	-41.25
Grunnetfjenn	1.50	42.20			184.63	40.28	15.64	52.13	805.69	85.31	61.61	1374.41	710.90	426.54	1919.43	4265.40	1090.05	1990.52	592.42	2274.88	2606.64	402.84	18899.53	16847.39	11488.15
Rasvassvatn	0.50	64.30	2009 ± 1	0.10	248.83	65.32	27.99	104.20	1259.72	139.97	90.20	2488.34	2177.29	1384.14	3421.46	10730.95	3110.42	5287.71	2332.81	3888.02	4043.55	684.29	41485.23	36107.31	25956.45
		Δ%			-29.14	-40.82	-23.91	-43.35	-49.78	-50.76	-46.06	-48.69	-49.92	-54.02	-41.54	-41.66	-43.64	-38.19	-50.18	-45.93	-46.27	-46.16	-44.67	-45.39	-44.31
Rasvassvatn	1.50	59.80	2004 ± 1	0.07	351.17	110.37	36.79	183.95	2508.36	294.28	167.22	4849.50	4347.83	3010.03	5852.84	18394.05	5518.39	8895.65	4882.27	7190.64	7525.08	1270.90	74979.93	66117.06	46605.35
Øyvåtn	0.50	41.80			205.74	45.45	12.44	38.28	478.47	45.45	35.89	717.70	406.70	229.67	933.01	2382.34	478.47	1148.33	382.78	1291.87	1411.48	208.13	10482.20	9277.99	6241.63
		Δ%			-6.68	-33.39	-19.67	-23.24	-29.89	-44.13	-37.85	-41.82	-44.68	-45.31	-44.46	-49.36	-47.92	-47.29	-43.91	-47.08	-46.22	-47.13	-45.53	-45.33	-46.49
Øyvåtn	1.50	38.10			220.47	68.24	15.49	49.87	682.41	81.36	57.74	1233.60	734.91	419.95	1679.79	4724.41	918.64	2178.48	682.41	2440.94	2824.67	393.70	19207.09	16970.87	11564.04
Jordfjenn ₂₀₀₆	0.50	55.10	2006 ± 1	0.40	199.64	45.37	18.15	56.26	562.61	94.37	58.08	1288.57	1125.23	653.36	1524.50	5807.62	1597.10	2722.32	1107.08	2359.35	2540.83	381.13	22141.56	19381.16	13811.25
		Δ%			10.60	-6.90	0.54	-13.42	-8.33	-17.01	-2.50	-10.77	-14.61	-15.82	-12.93	-13.04	-16.72	-16.21	-17.12	-12.86	-17.20	-21.80	-28.05	-29.51	-34.66
Jordfjenn ₁₉₉₅	1.50	55.40	1995 ± 2	0.40	180.51	48.74	18.05	64.98	613.72	113.72	59.57	1444.04	1317.69	776.17	1750.90	6678.70	6859.21	3248.10	1335.74	2707.58	3068.59	487.36	30774.37	27465.70	21137.18
Svartfjenn ₂₀₀₆	0.50	50.10			73.85	2.00	9.78	19.96	173.65	18.76	13.17	259.48	193.61	85.83	239.52	518.96	143.71	259.48	127.74	279.44	259.48	45.91	2724.35	2451.70	1495.01
		Δ%			-34.07	-89.71	-38.28	-10.91	-31.86	-28.47	-34.84	-36.69	-29.14	-31.71	-26.95	-29.65	-27.95	-32.16	-35.95	-26.95	-32.16	-32.79	-31.19	-31.07	-30.56
Svartfjenn ₁₉₉₅	1.50	36.60			112.02	19.40	15.85	22.40	254.10	26.23	20.22	409.84	273.22	125.68	327.87	737.70	199.45	382.51	382.51	382.51	68.31	3959.29	3556.56	2153.01	
Melestfjenn ₂₀₀₆	0.50	65.10			89.09	16.90	12.14	27.65	322.58	32.26	18.43	537.63	368.66	153.61	430.11	1121.35	368.66	568.36	261.14	691.24	691.24	116.74	5827.80	5241.01	3231.95
		Δ%			-11.35	-9.29	-22.93	-31.22	-33.59	-44.98	-44.98	-43.69	-43.57	-54.15	-51.55	-48.50	-49.98	-47.80	-48.03	-44.98	-44.98	-46.39	-46.14	-45.95	-47.99
Melestfjenn ₁₉₉₅	1.50	59.70			100.50	18.43	15.75	40.20	485.76	58.63	33.50	964.77	653.27	335.01	887.77	2177.55	737.02	1088.78	502.51	1256.28	1256.28	217.76	10819.77	9697.49	6214.41

Pre-industrial sediments	Depth (cm)	Surface (post-fire)		Sub-surface (pre-fire)		Reference depth					
		Min	Max	Min	Max	Min	Max				
Industrial sediments	0.5	Range Hg: 0.22 (Mel) 0.74 (Ras)		Range Cd: 0.77 (Øy) 2.80 (Jord)		Range Cr: 5.70 (Mel) 26.80 (Ras)		Range V: 19.20 (Mel) 44.20 (Ras)		Range Pb: 63.50 (Svart) 232.00 (Ras)	
		Range Hg (LOI): 0.34 (Mel) 1.15 (Ras)		Range Co: 1.30 (Mel) 8.30 (Ras)		Range Ni: 7.30 (Svart) 28.70 (Ras)		Range Cu: 17.80 (Øy) 52.70 (Ras)		Range Zn: 102.00 (Svart) 294.00 (Jord)	
		Hg <	Hg (LOI) <	Cd <	Co <	Cr <	Ni <	V <	Cu <	Pb <	Zn
Industrial sediments	1.5	Range Hg: 0.14 (Svart) 0.72 (Ras)		Range Cd: 0.81 (Svart) 4.10 (Hund)		Range Cr: 7.30 (Mel) 24.40 (Ras)		Range V: 22.60 (Mel) 38.20 (Ras)		Range Pb: 50.40 (Svart) 248.00 (Ras)	
		Range Hg (LOI): 0.10 (Hund) 0.50 (Jord)		Range Co: 1.60 (Fisk) 9.10 (Ras)		Range Ni: 7.30 (Svart) 26.30 (Ras)		Range Cu: 17.80 (Svart) 52.00 (Ras)		Range Zn: 87.80 (Svart) 361.00 (Hund)	
		Hg <	Cd <	Co <	Cr <	Ni <	V <	Cu <	Pb <	Zn	
Pre-industrial sediments	33.0	Range Hg: 0.08 (Jord) 0.13 (Ras)		Range Pb: 3.00 (Hund) 10.00 (Jord)		Range V: 10.50 (Mel) 27.40 (Ras)		Range Zn: 23.00 (Hund) 56.30 (Ras)			
		Range Cd: 0.10 (Hund) 0.50 (Jord)		Range Co: 4.00 (Svart) 24.00 (Ras)		Range Ni: 5.60 (Jord) 17.70 (Ras)		Range Cu: 10.70 (Øy) 49.10 (Ras)			
		Range Co: 0.70 (Mel) 2.90 (Øy)									
Pre-industrial sediments	±11.5	Hg <		Cd <	Co <	Pb ¹ <	Cr <	Ni ² <	V <	Cu ² <	Zn

Figure 31 Prevailing trend (increasing left to right) of measured metal concentration order (coloured in shades of green) in sediments at depths 33.0, 1,5 and 0.5 cm (3.5 and 2.5 cm not included). Within boxes (outlined in black) increasing order may be disrupted. The range of metal concentrations is shown as measured metal minimum and maximum.

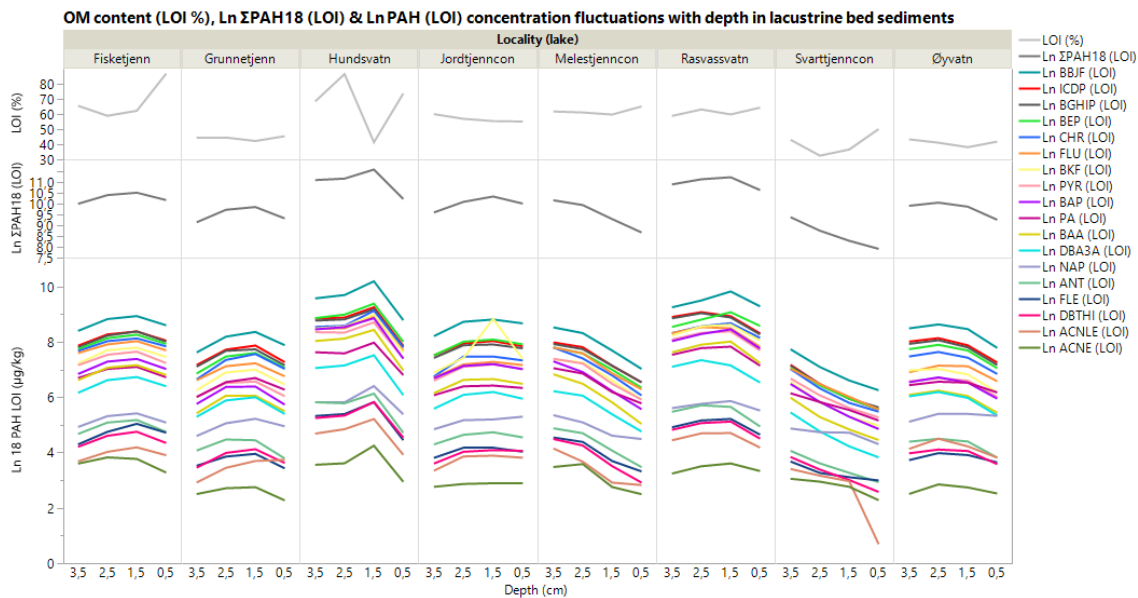


Figure 32 ΣPAH_{16+2} concentrations increase from the lowermost sediment layer to sub-surface in Fisketjenn, Hundsvatn, Grunnetjenn, Rasvassvatn and Jordtjenn_{con}. Svarttjenn_{con} and Melestjenn_{con} differ from this with declining ΣPAH_{16+2} concentrations through this section. Øyvatt has increasing ΣPAH_{16+2} concentrations from the lowermost to intermediate section, but the decline from intermediate to sub-surface section is stronger than the below increase, entailing an overall decline from the lowermost to sub-surface sector. From sub-surface to surface sediments, all ΣPAH_{16+2} decline. The individual PAHs follow the pattern of ΣPAH_{16+2} with only few exceptions (e.g. ACNLE in Grunnetjenn, and NAP and ACNE in Jordtjenn_{con}). Note the outlier BKF in Jordtjenn_{con} 1.5.

List of tables and figures

Table 1 Lake morphometric data, catchment characteristics and precipitation data retrieved through the Pyrowater project (by Lydersen) and Lydersen et al. (2014). Lakes impacted by fire (burnt) are also to a varying degree impacted by PWF logging. The three control lakes (unburnt) are located adjacent to the burnt area, outside the perimeter of the fire. 27

Table 2 Sediment age (yr), year of deposition and accumulation rates ($\text{kg m}^{-2} \text{ yr}^{-1}$) for lakes Hundsvatn, Rasvassvatn and Jordtjenn_{con}. All data assembled from the appended report (Appendix 1) on dating of core Hundsvatn, Rasvassvatn and Jordtjenn_{con} (Gamma Dating Centre Copenhagen 2011). 46

Table 3 Simple statistics on sediment OM content in Mykland lake bed sediments; OC_{min} value = 16.3 % (32.502), OC_{max} = 43.4 % (86.802) and $\text{OC}_{\text{median}}$ = 28.1 % (56.152)..... 50

Table 4 Metal concentrations in sediments. Colours code for ECC for metals in lacustrine sediments according to the Norwegian classification guide M-608 (Norwegian Environment Agency 2016). Blue code for Class I (background), green for Class II (good), yellow Class III (moderate), orange Class IV (bad) and Red class V (very bad) (table 15, Tables and figures). LOI-normalized metal concentrations for Cd_{LOI} , Cu_{LOI} , Pb_{LOI} and Hg_{LOI} are included (cf. ch. 5.3.2 Metals and sediment organic matter). There are no environmental class for V (Vanadium) and Co (not colour-coded). Also, measured concentrations of Mn and Fe are included in the table, but not evaluated against environmental condition class. 52

Table 5 Metal-to-LOI correlation coefficients on all metals in all lakes at all depths (no outliers excluded). Cells shaded green indicate significant correlations ($r > 0.3244$, $\alpha = 0.05$). Light green cells mark correlation coefficient just below threshold values of significance. Outliers Hundsvatn 1.5, Rasvassvatn 33.0 and Jordtjenn_{con} 3.5 are excluded for metal-to-LOI correlations at specified depths..... 55

Table 6 Increasing metal concentration order (prevailing trend of median values) from left to right. Within boxes outlined in black, increasing order may be disrupted (shaded grey) when considering single lakes. Note how Pb positions with Zn in the upper (depth 1.5 and 0.5 cm) sediments, compared to the relatively lower concentration levels of Pb in reference (depth 33.0 cm) sediments (highlighted yellow)..... 56

Table 7 PAH concentrations in lacustrine sediments. Colours code for ECC for PAHs in lacustrine sediments according to the Norwegian classification guide M-608 (Norwegian Environment Agency 2016). Blue code for Class I (background), green for Class II (good), yellow Class III (moderate), orange Class IV (bad) and Red class V (very bad). There are no environmental class for DBTHI, BeP, PER (biogenic) or ΣPAHs (not colour-coded).	64
Table 8 Correlation matrix on singular PAHs and LOI. PAH-to-PAH correlations are strong ($r > 0.7$). PAH-to-LOI correlations (shaded green) are good ($r > 0.5$) with significant correlation probabilities ($p < 0.02$).	65
Table 9 Formatted loading matrix from the PCA on LR PAH (outliers included). Cells shaded green indicate weighty loads on a principal component (PC). Red digits load in the opposite direction (negatively) of black digits (positively) along the PCs. BeP _{HMW} , BbjF _{HMW} , ICDP _{HMW} , DBA3A _{HMW} , BGHIP _{HMW} and BKF _{HMW} load along PC 1 (42.6 %), while along PC 2 (24.7 %) PYR _{HMW} , BaA _{HMW} and BaP _{HMW} load.	75
Table 10 Nomenclature, abbreviations and basic properties for 23 PAHs relevant to this study (based on Rognerud et al. 2007; Tobiszewski & Namieśnik 2012).	116
Table 11 Comparison of LMW and HMW PAHs (based upon Van Mouwerik et al. 1997, and references therein; Skupińska, Misiewicz & Kasprzycka-Guttman 2004; Lee & Vu 2010; Oliveira et al. 2011; Tsymbalyuk et al. 2011; Nasher et al. 2013; Pampanin & Sydnes 2013).	116
Table 12 Nomenclature of (post-)transition metals according to the periodic table of elements.	117
Table 13 Weather data for the period of the sampling campaign (Yr.no 2018).	119
Table 14 Correlation coefficients, r , for different sample sizes, n , according to Walsh (1998); a correlation is significant at level $\alpha = 0.05$ when $n \geq 5$ and $r > 2/n$	119
Table 15 Environmental quality standards (EQS) and environmental conditions class (ECC) for metals in lacustrine sediments according to M-608; Norwegian classification guide – Quality standards for water, sediment and biota (Norwegian Environment Agency 2016).	120
Table 16 Increasing (rows from left to right) order of measured metal concentrations at depth 33.0, 1.5 and 0.5 cm. Within outlined cells shaded green, metal order may be disrupted (in some cases also across neighbouring cells outlined and shaded green).	

Cells shaded yellow pay attention to Pb positioning; in reference sediments actual positioning of Pb is further left relative to the other metals in terms of increasing (left to right) metal concentration order. Vertical columns; declining (red digits) / increasing (expressed as percentages) metal concentrations across depth sections within lakes. . 121

Table 17 Formatted loading matrix from the PCA on all metals at all depths (outliers included). Cells shaded green indicate weighty loads on a principal component (PC). Red digits load in the opposite direction (negatively) of black digits (positively) along the PC. Metals load positively and quite equal along PC 1. Zn, Cd, Hg and Pb load negatively along PC 2, while V, Cr and Co load positively along PC 2..... 122

Table 18 Formatted loading matrix from the PCA (outliers included) on metals, ΣPAH and lake parameters. Cells shaded green indicate weighty loads on a principal component (PC). Red digits load in the opposite direction (negatively) of black digits (positively) along the PCs. All parameters load positively along PC 1, except pH and TOC which load in the opposite direction. Along PC 2 metals are split in two clusters (V, Cr, Co, Ni, and Zn, Cd, Hg, respectively) loading in opposite directions. 123

Table 19 Correlation table (n = 32, r >0.3536, α = 0.05) on metals (including Fe), ΣPAH_{EPA16+2}, pH, TOC, RT and LOI. When considering all metals in all lakes at all industrial depths (outliers included) simultaneously, Cu, Cd and Hg correlate to LOI, which is not seen for the rest of the metals. Metals form in two clusters (shaded in different green colours). Fe correlates to one of them. 123

Table 20 Correlation probabilities (n = 32, ρ ≤0.05) for metal correlations (including Fe), ΣPAH_{EPA16+2}, pH, TOC, RT and LOI (figure 19)..... 124

Table 21 Environmental quality standards (EQS) and environmental conditions class (ECC) for PAHs in lacustrine sediments according to the Norwegian classification guide M-608 Quality standards for water, sediment and biota (Norwegian Environment Agency 2016). 124

Table 22 LOI-normalized PAH concentrations in lacustrine sediments. Colours code for ECC for PAHs in lacustrine sediments according to the Norwegian classification guide M-608 (Norwegian Environment Agency 2016). Blue code for Class I (background), green for Class II (good), yellow Class III (moderate), orange Class IV (bad) and Red class V (very bad). There are no environmental class for DBTHI, BeP, PER (biogenic) or ΣPAHs (not colour-coded). 125

Table 23 Formatted loading matrix from the PCA on Ln PAH_{LOI} (outliers included). Cells shaded green indicate weighty loads on a principal component (PC). Red digits load in the opposite direction (negatively) of black digits (positively) along the PCs. PAHs load positively and quite equal along PC 1. Only ACNE loads along PC 2. 126

Table 24 Declining (red digits) / increasing (expressed as percentages) PAH concentrations from sub-surface to surface sediments. Measured $\Sigma\text{PAH}_{\text{EPA16+2}}$ concentration levels display a -38 % (median, range -1 to -55 %) decline. When PAHs' association to sediment OM is accounted for, $\Sigma\text{PAH}_{\text{EPA16+2}}$ LOI decline with -43 % (median, range -29 to -74 %). With only singular exceptions, all individual PAH concentrations (i.e. both measured PAH concentrations and PAH_{LOI} concentrations) decline. The PAH decline seen in Mykland surface sediments represents the first decade of the 2000s. 127

Figure 1 The perimeter of the burnt area is outlined ochre yellow, while the two nature reserves Jurdalsknuten and Myklandsvatna are outlined bright green. Sampled lakes are circled blue. Lakes with the suffix *ref.* are control lakes outside the perimeter of the fire. Solid red dot marks start of fire (Brandrud, Bratli & Sverdrup-Thygeson 2010).

Figure 2 ^{238}U decay series concerned with production of ^{210}Pb . Illustration shows the principal radionuclides (without sub-chains) and their radioactive half-lives. $^{210}\text{Pb}_{\text{ex}}$ activity = $^{210}\text{Pb}_{\text{tot}}$ activity – ^{226}Ra activity (which equals the $^{210}\text{Pb}_{\text{sup}}$) (Appleby 2001; Mabit et al. 2014). Po is the chemical element polonium (atomic number 84).

Figure 3 Figure of organic carbon content (as LOI) in lakes in Southern Norway (Rognerud et al. 2008). The area surrounding Mykland is circled black.

Figure 4 Graphic illustration of how sediment age (year of sedimentation) increases with increasing sediment depth (cm) in Hundsvatn, Rasvassvatn and Jordtjenn_{con}. The figure is generated on data from the appended report (Appendix 1) on dating of sediments, presented in table 2.

Figure 5 Sedimentation rates (cm yr⁻¹) for the lakes Hundsvatn, Rasvassvatn and Jordtjenn_{con}, generated on data from the appended report (Appendix 1) on dating of sediments, presented in table 2. Hundsvatn has four outliers (depths 9.5; 10.5; 11.5 and 12.5). $y = 0.081x$ ($r^2 = 0.99$) when the four outliers are excluded. This is similar to Jordtjenn_{con}.

Figure 6 Vertical depth profiles of LOI fluctuations throughout the sediment column. LOI levels follow a relatively uniform pattern with depth and across lakes, with Fisketjenn's LOI peak at 0.5 cm and Hundsvatn being the most distinct exceptions.

Figure 7 A Jackknife Distances outlier analysis at significance level $\alpha = 0.05$ identify two outliers positioned above the blue, dotted line which indicates the Upper Control Limit (UCL = 5.15); one sample from the burnt lake Rasvassvatn at reference depth 33.0 cm, and one from the control lake Jordtjenn_{con} at industrial depth 3.5 cm.

Figure 8 Hundsvatn at depth 1.5 cm, Rasvassvatn at reference depth 33.0 cm and Jordtjenn_{con} at industrial depth 3.5 cm position as outliers if LOI is included in the Jackknife Distances outlier analysis on all metals in all lakes at all depths.

Figure 9 Depth profiles on sediment LOI and Ln-logged (to reduce spread) metal concentrations illustrate the historic variations in sediment organic matter content and metal load for all eight lakes studied. LOI-normalized concentrations of Hg are included. Due to the complexity of the results, the number of depths illustrated are reduced (depth 2.5 cm omitted) to enhance visual interpretation / patterns.

Figure 10 PCA on all metals (measured concentrations) in all lakes at all depths (the outliers Rasvassvatn 33.0 and Jordtjenn_{con} 3.5 included). Score plot to the left and loading plot to the right. Squares represent reference depth 33.0 cm, diamonds match depth 3.5 cm, triangles correspond to sub-surface / pre-fire sediments and solid dots symbolise surface / PWF sediments (depth 0.5 cm). Xs represent the intermediate section (2.5 cm) of the industrial pre-fire sediment. The scree plot (upper left corner) propose two explanatory factors (eigenvalue 0.4905). 83.3 % of all the variance in the dataset can be explained by two principal components (PC 1 63.6 % plus PC 2 19.7 %).

Figure 11 Scatter plot including all metals at all industrial depths in all lakes (pre-industrial reference depth excluded, outliers included). $n = 32$, $r > 0.3536$, $\alpha = 0.05$. Solid circles represent sediment depth 0.5 cm, triangles 1.5 cm, crosses 2.5 cm and diamonds 3.5 cm. Yellow represent Fisketjenn, green Hundsvatn, blue Grunnetjenn, red Rasvassvatn, pink Øyvavn, orange Jordtjenn_{con}, black Svarttjenn_{con} and deep purple Melestjenn_{con}. Orange diamonds represent Jordtjenn_{con} 3.5.

Figure 12 Correlation-tree of strong (threshold $< r > 0.7$) correlations (left), and weak (threshold $< r < 0.5$) correlations (right).

Figure 13 A hierarchical two-way clustering dendrogram (method = ward) on all metals (outliers included), demonstrates that lakes rather than depths tend to cluster. Each lake is given a specific colour, depths are identified by their figures, while clusters are grouped together. The scree-plot at the bottom right corner indicates the recommended number of clusters (at knee point).

Figure 14 A Jackknife Distances outlier analysis at significance level $\alpha = 0.05$ identify Fisketjenn 0.5, Hundsvatn (all depths), Rasvassvatn (all depths) and Jordtjenn_{con} 1.5 as outliers (positioning above the blue, dotted line that indicates the Upper Control Limit [UCL = 10.32]).

Figure 15 A Fit Y ($\Sigma\text{PAH}_{\text{EPA16+2}}$) by X (LOI %) residual plot reveals that Hundsvatn and Rasvassvatn have much higher concentrations of PAHs than expected, when plotted against the content of sediment organic matter (LOI).

Figure 16 Concentration fluctuations with sediment depth across lakes reveals the prevailing concentration order of three PAH totals in Mykland lake bed sediments; $\Sigma\text{PAH}_{\text{LMW}}$ in the lowermost section and $\Sigma\text{PAH}_{\text{HMW}}$ in the intermediate section. The upper panel is $\Sigma\text{PAH}_{\text{EPA16+2}}$.

Figure 17 All individual PAH_{LOI} concentrations, and consequently $\Sigma\text{PAH}_{\text{EPA16+2}}$, increase from sediment section 3.5 to 1.5 in Fisketjenn, Hundsvatn, Grunnetjenn, Rasvassvatn and Jordtjenn_{con}. In Svarttjenn_{con} and Melestjenn_{con} there is a general concentration decline for all single PAH_{LOI} . In Øyvatn all PAH_{LMW} (including FLU) increase from depth 3.5 to 1.5 cm, while all PAH_{HMW} decline (PYR_{HMW} increase). Consequently, $\Sigma\text{PAH}_{\text{EPA16+2}}$ displays a minute decline in Øyvatn. From depth 1.5 to 0.5 cm all individual PAH_{LOI} concentrations, and consequently $\Sigma\text{PAH}_{\text{EPA16+2}}$, decline in all lakes; Fisketjenn, Hundsvatn, Grunnetjenn (ACNLE_{LMW} increases), Rasvassvatn, Øyvatn, Jordtjenn_{con} (NAP_{LMW} increases), Svarttjenn_{con} and Melestjenn_{con}. The number of depths illustrated are reduced (depth 2.5 cm omitted) to enhance visual interpretation / patterns.

Figure 18 93.3 % of all the variance in the dataset can be explained by one principal component (PC 1) when running a PCA on $\text{Ln PAH}_{\text{LOI}}$ at all depths for all lakes (outliers included). Solid dots represent PWF sediments, triangles represent pre-fire sediments, while diamond squares represent the deepest sediment layer (depth 3.5 cm).

Figure 19 Scatter plot on $\text{Ln PAH}_{\text{LOI}}$ correlation. The matrix displays strong ($r > 0.7$), positive and linear correlations between all PAHs, except PER ($r \leq 0.2649$). Only a

singular exception correlate below the 0.7 threshold value of strong correlations; ACNLE to ACNE ($r = 0.6445$).

Figure 20 A hierarchical two-way clustering dendrogram (method = ward) run on LR converted PAH concentrations, demonstrates that lakes rather than depths tend to cluster. Each lake is given a specific colour, depths are identified by their figures, while clusters are grouped together (to the right). The scree-plot at the bottom right corner indicates the recommended number (i.e. four) of clusters (at “knee point”).

Figure 21 A PCA biplot on LR PAH conclude that 77.9 % of all variance in the dataset can be expressed by three principal components. BeP_{HMW} , $BbjF_{HMW}$, $IcdP_{HMW}$, $DBa3A_{HMW}$, $BghiP_{HMW}$ and BkF_{HMW} load along PC 1 (42.6 %), while along PC 2 (24.7 %) PYR_{HMW} , BaA_{HMW} and BaP_{HMW} load. Lakes rather than depths tend to cluster. There is little difference in how the two uppermost sediment sections position in the biplot.

Figure 22 PCA on metals, $\Sigma PAH_{EPA16+2}$, LOI, TOC, pH and RT (depths 3.5 – 0.5, outliers included). Three dimensions (PC 1; 49.9 %, PC 2; 19.4 % and PC 3; 10.5 %) in the component space account for 79.8 % (cumulative percentage) of the total variance in the data set. The fourth dimension (PC 4) and on, has an eigenvalue <1.0871 , and accounts for little of the variance.

Figure 23 Smoke from the 2008 Mykland wildfire was lofted high in the air and blown to sea. Photo: Erik Holand (Nygaard & Brean 2014).

Figure 24 Satellite image of the wildfire smoke plume drifting from Mykland across the North Sea to Denmark on the 12th of June 2008 (Gjerstad 2008). Photo: NOAA/MET.no

Figure 25 Map of the burnt area, start of fire and its spread (Nygaard & Brean 2014). Upper right corner; Norway with excerpt of Aust-Agder County (furthest right). In the excerpt, Froland municipality is coloured red. Mykland locates in centre of the western part of Froland municipality (own edits of maps from Wikimedia Commons contributors 2015; Wikipedia contributors 2015).

Figure 26 Drainage pattern and meters above sea level (m.a.s.l.) for the eight investigated lakes (all lakes drain to river Tovdalsåna). Burnt headwater lakes: Hwl Fisketjenn (228+ m.a.s.l.) drains to Hundsvatn (228- m.a.s.l.), Hwl Heitjenn (278 m.a.s.l.) drains via Grunnetjenn (233 m.a.s.l.) to Hundsvatn, while Hwl 333 drains to Rasvassvatn (173 m.a.s.l.). Control lakes (not directly affected by fire): Hwl 304 drains via Jordtjenn_{con} (228+ m.a.s.l.) to Svarttjenn_{con} (191 m.a.s.l.). All lakes belong to Tovdal

drainage basin. Note that the lake just outside the perimeter of the fire, Rasvassvatn, belongs to the same catchment, Austerbekken, as the control lakes.

Figure 27 Metal concentration (Ln) fluctuations with depth (industrial sediments), including both Mn, Fe, depth 2.5 cm and the excluded lake Heitjenn. Note how Heitjenn only displays minor alterations in metal concentration levels with sediment depth.

Figure 28 Measured $\Sigma\text{PAH}_{\text{EPA16+2}}$ and LOI concentration fluctuations with depth. Note how the excluded lake Heitjenn only displays minor alterations in $\Sigma\text{PAH}_{\text{EPA16+2}}$ concentration levels with sediment depth. Also, worth noting is how depth 2.5 cm, which is omitted from the depth profile illustrations, disrupt interpretation.

Figure 29 Depth profiles on sediment LOI and Ln-logged metal concentrations illustrate historic variations in sediment organic matter content and metal load for all eight lakes studied. LOI-normalized concentrations of Hg are included. There is no obvious parallel between vertical (depth) variations of metal concentrations and LOI when plotted against each other. Worth noting is how depth 2.5 cm disrupt interpretation.

Figure 30 Concentration fluctuations with depth on single Ln PAH_{LOI} .

Figure 31 Prevailing trend (increasing left to right) of measured metal concentration order (coloured in shades of green) in sediments at depths 33.0, 1.5 and 0.5 cm (3.5 and 2.5 cm not included). Within boxes (outlined in black) increasing order may be disrupted. The range of metal concentrations is shown as measured metal minimum and maximum.

Figure 32 ΣPAH_{16+2} concentrations increase from the lowermost sediment layer to sub-surface in Fisketjenn, Hundsvatn, Grunnetjenn, Rasvassvatn and Jordtjenn_{con}.

Svarttjenn_{con} and Melestjenn_{con} differ from this with declining ΣPAH_{16+2} concentrations through this section. Øyvatn has increasing ΣPAH_{16+2} concentrations from the lowermost to intermediate section, but the decline from intermediate to sub-surface section is stronger than the below increase, entailing an overall decline from the lowermost to sub-surface sector. From sub-surface to surface sediments, all ΣPAH_{16+2} decline. The individual PAHs follow the pattern of ΣPAH_{16+2} with only few exceptions (e.g. ACNLE in Grunnetjenn, and NAP and ACNE in Jordtjenn_{con}). Note the outlier BKF in Jordtjenn_{con} 1.5.

Appendix

Footnotes

¹ An account of gamma spectrometry methodology is given in Debertin and Helmer (1988).

² Cf. www.canberra.com & <http://geo.ku.dk>

³ Main principles of CRS-modelling are exemplified in Appleby *et al.* (1979)

⁴ Svarttjenn_{con} 0.5 is not polluted with BaA, CHR, BkF, DBa3A and Pb.

⁵ Darwin (1881)

Appendix 1

Gamma Dating Centre Copenhagen

**Copenhagen, 5 April 2011
Thorbjørn J. Andersen
Department of Geography and Geology
University of Copenhagen
Øster Voldgade 10
1350 Copenhagen K
E-mail: tja@geo.ku.dk
Phone: (+45) 35 32 25 03
Fax: (+45) 35 32 25 01**

Dating of core Hundsvatn, Rasvassvatn and Jordtjenn_{con}

Dating of core Hundsvatn

Methods

The samples have been analysed for the activity of ^{210}Pb , ^{226}Ra and ^{137}Cs via gamma spectrometry at the Gamma Dating Center, Institute of Geography, University of Copenhagen. The measurements were carried out on a Canberra low-background Ge-detector. ^{210}Pb was measured via its gamma-peak at 46,5 keV, ^{226}Ra via the granddaughter ^{214}Pb (peaks at 295 and 352 keV) and ^{137}Cs via its peak at 661 keV.

Results

The core showed high surface contents of unsupported ^{210}Pb of around 840 Bq kg⁻¹ and a clear tendency for exponential decline with depth (fig 1). The calculated flux of unsupported ^{210}Pb is 42 Bq m⁻² y⁻¹ which is only about half the estimated local atmospheric supply (based on Appleby, 2001).

The content of ^{137}Cs showed a peak around 2 cm depth and generally low contents below that level.

CRS-modelling has been applied on the profile using a modified method (Appleby, 2001) where the activity below 14 cm is calculated on the basis of the regression shown in fig 2. The result is given in table 2 and fig 3 and 4.

The chronology for the core is considered to be fairly accurate due to the clear tendency for an exponential decline with depth of unsupported ^{210}Pb . The calculated chronology of the peak activity of ^{137}Cs (fig 4) is also consistent with the expected Chernobyl origin (1986) of this material. The activity of ^{137}Cs at levels dated to well before this isotopes release into nature around the mid 1950's suggests that the isotope is not completely immobile in these sediments.

5 April 2011

Thorbjørn J Andersen

Reference:

Appleby, P.G. (2001): Chronostratigraphic techniques in recent sediments. In: Last, W.M & Smol, J.P. (eds) Tracking environmental change using lake sediments. Volume 1: Basin analysis, coring and chronological techniques. Kluwer Academic Publishers, the Netherlands.

Table 1. Data core Hundsvatn

Depth	Pb-210 _{tot}	error Pb-210 _{tot}	Pb-210 _{supupp} 210Pb	error pb-210 _{sup}	Pb-210 _{unsup}	error pb-210 _{unsup}	Cs-137	error Cs-137
cm	Bq kg ⁻¹	Bq kg ⁻¹	Bq kg ⁻¹	Bq kg ⁻¹	Bq kg ⁻¹	Bq kg ⁻¹	Bq kg ⁻¹	Bq kg ⁻¹
0.5	872	63	31	31	841	70	309	14
1.5	666	52	23	21	643	56	313	15
2.5	753	52	12	0	741	52	227	11
3.5	263	23	23	10	240	25	98	10
4.5	220	19	25	12	194	23	80	9
5.5	192	17	17	5	175	18	75	11
6.5	76	7	7	14	69	16	93	8
7.5	102	10	19	7	84	12	70	11
8.5	13	1	3	7	9	7	38	6
9.5	0	0	12	12	0	12	42	6
10.5	84	8	29	11	55	14	24	10
11.5	18	2	3	3	15	3	23	8
12.5	45	4	21	13	25	13	10	8
13.5	54	5	15	0	39	5	25	5
14.5	0	0	10	5	0	5	30	5
25.5	36	3	11	15	25	15	9	5

Table 2, Chronology core Hundsvatn

Depth	Age	error age	Date	acc rate	error rate
cm	y	y	y	(kg m ⁻² y ⁻¹)	(kg m ⁻² y ⁻¹)
0.0			2010		
0.5	4	1	2006	0.04	0.00
1.5	13	2	1997	0.04	0.00
2.5	27	2	1983	0.03	0.00
3.5	44	2	1966	0.03	0.00
4.5	55	3	1955	0.04	0.01
5.5	68	3	1942	0.03	0.00
6.5	79	4	1931	0.03	0.01
7.5	89	5	1921	0.04	0.01
8.5	98	6	1912	0.05	0.04
9.5	99	6	1911	0.38	4.06
10.5	106	6	1904	0.06	0.02
11.5	119	7	1891	0.04	0.01
12.5	131	10	1879	0.04	0.02
13.5	173	15	1837	0.01	0.01

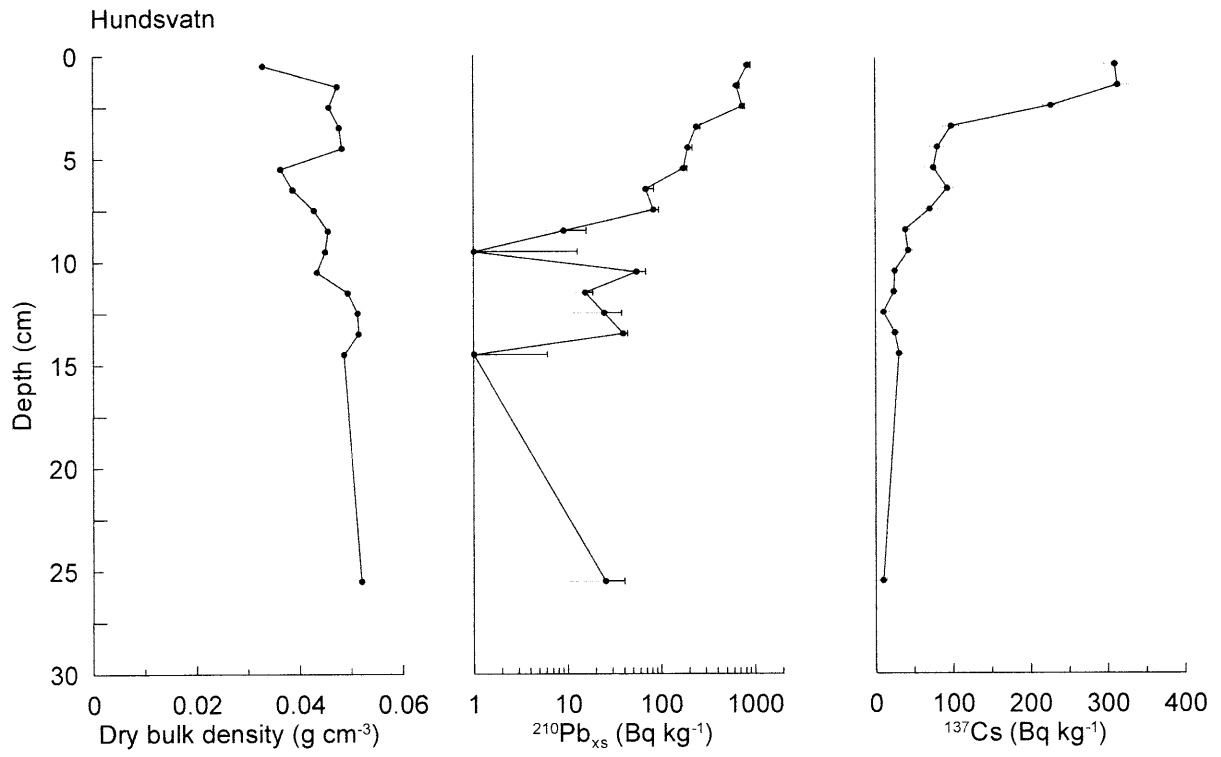


Fig 1

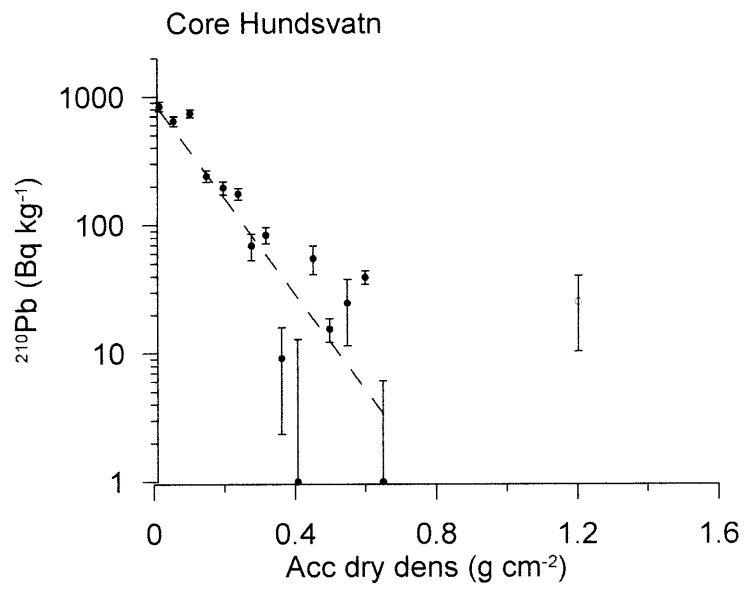


Fig 2

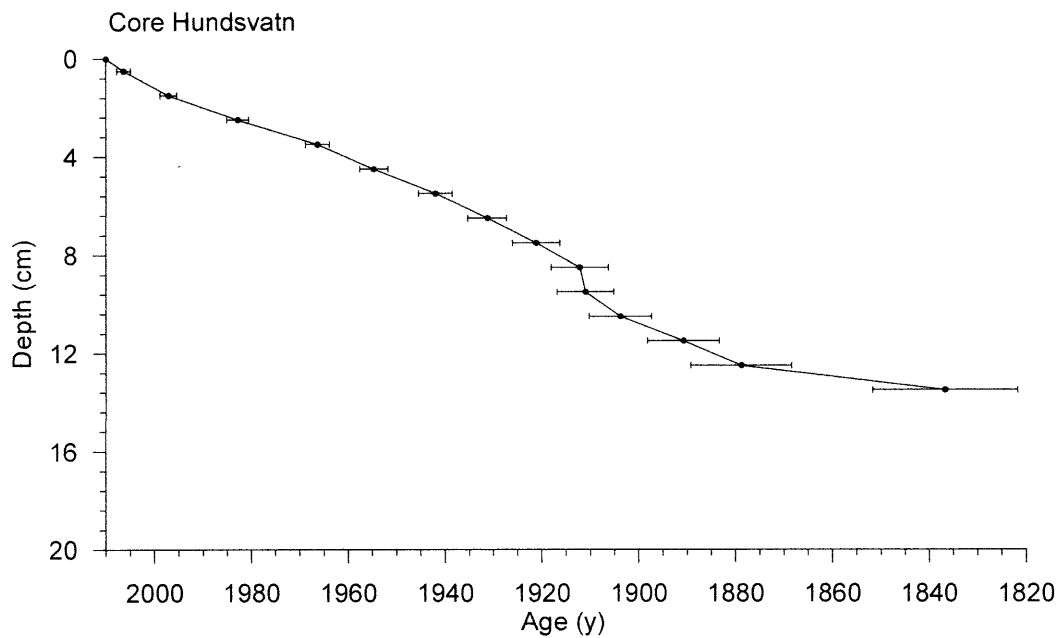


Fig 3

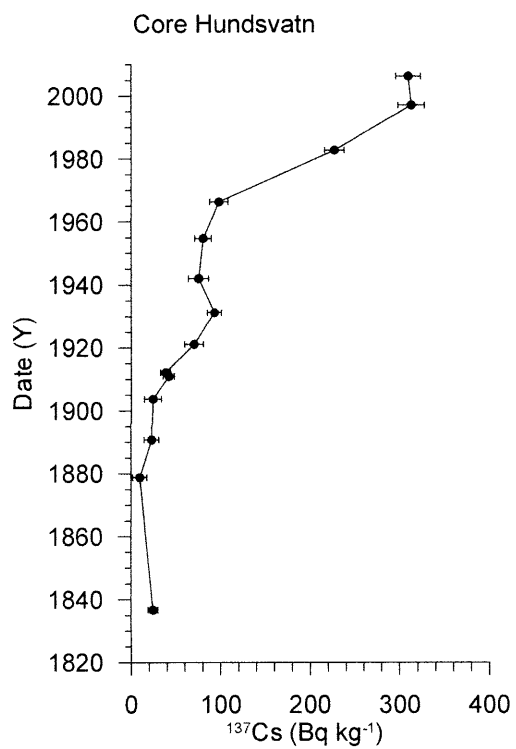


Fig 4

Dating of core Rasvatn

Methods

The samples have been analysed for the activity of ^{210}Pb , ^{226}Ra and ^{137}Cs via gamma spectrometry at the Gamma Dating Center, Institute of Geography, University of Copenhagen. The measurements were carried out on a Canberra low-background Ge-detector. ^{210}Pb was measured via its gamma-peak at 46,5 keV, ^{226}Ra via the granddaughter ^{214}Pb (peaks at 295 and 352 keV) and ^{137}Cs via its peak at 661 keV.

Results

The core showed high surface contents of unsupported ^{210}Pb of around 900 Bq kg⁻¹ and a tendency for exponential decline with depth (fig 1). The calculated flux of unsupported ^{210}Pb is 83 Bq m⁻² y⁻¹ which is about the same as the estimated local atmospheric supply (based on Appleby, 2001). Levels without unsupported ^{210}Pb was not found.

The content of ^{137}Cs showed a peak around 2 cm depth and slowly decreasing contents below that level.

CRS-modelling has been applied on the profile using a modified method (Appleby, 2001) where the activity below 15 cm is calculated on the basis of the regression shown in fig 2. The result is given in table 2 and fig 3 and 4.

The chronology for the core is considered to be fairly accurate due to the tendency for an exponential decline with depth of unsupported ^{210}Pb . The calculated chronology of the peak activity of ^{137}Cs (fig 4) is also consistent with the expected Chernobyl origin (1986) of this material. The activity of ^{137}Cs at levels dated to well before this isotopes release into nature around the mid 1950's suggests that the isotope is not completely immobile in these sediments.

5 April 2011

Thorbjørn J Andersen

Reference:

Appleby, P.G. (2001): Chronostratigraphic techniques in recent sediments. In: Last, W.M & Smol, J.P. (eds) Tracking environmental change using lake sediments. Volume 1: Basin analysis, coring and chronological techniques. Kluwer Academic Publishers, the Netherlands.

Table 1. Data core Rasvatn

Depth	Pb-210tot	error Pb-210 tot	Pb-210 supupp 210Pb	error pb-210 sup	Pb-210 un-sup	error pb-210 un-sup	Cs-137	error Cs-137
Cm	Bq kg-1	Bq kg-1	Bq kg-1	Bq kg-1	Bq kg-1	Bq kg-1	Bq kg-1	Bq kg-1
0.5	907	98	51	30	856	102	74	23
1.5	1252	93	44	2	1208	93	105	11
2.5	801	64	52	6	750	64	92	9
3.5	616	56	54	5	562	56	55	9
4.5	356	37	46	0	310	37	43	8
5.5	266	28	19	4	247	28	44	7
6.5	202	23	25	26	176	34	22	8
7.5	247	27	47	12	200	29	24	8
8.5	327	23	74	5	252	24	22	4
9.5	253	26	69	2	184	26	16	6
10.5	217	23	43	10	173	25	3	6
11.5	245	26	64	1	181	26	12	6
12.5	173	19	78	2	95	19	13	5
13.5	214	18	42	8	172	20	15	4
14.5	139	16	40	8	99	18	8	6
25.0	120	13	46	15	74	20	0	0

Table 2. Chronology core Rasvatn

Depth	Age	error age	Date	acc rate	error rate
cm	y	y	y	(kg m-2 y-1)	(kg m-2 y-1)
0.0			2010		
0.5	1	1	2009	0.10	0.01
1.5	6	1	2004	0.07	0.01
2.5	12	1	1998	0.06	0.01
3.5	18	1	1992	0.08	0.01
4.5	22	1	1988	0.10	0.01
5.5	26	1	1984	0.14	0.02
6.5	29	1	1981	0.16	0.03
7.5	32	1	1978	0.17	0.02
8.5	36	2	1974	0.13	0.01
9.5	40	2	1970	0.11	0.02
10.5	45	2	1965	0.12	0.02
11.5	51	2	1959	0.10	0.01
12.5	57	2	1953	0.11	0.02
13.5	63	2	1947	0.09	0.01
14.5	71	1	1939	0.08	0.00

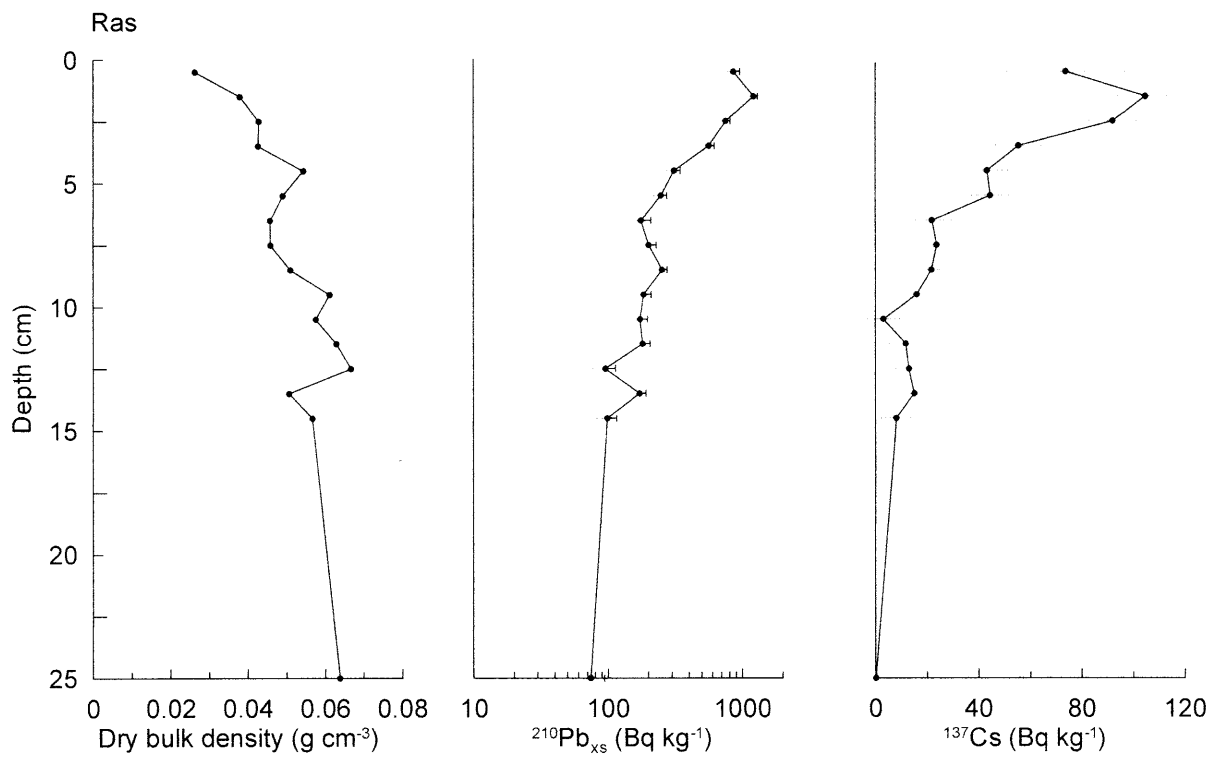


Fig 1

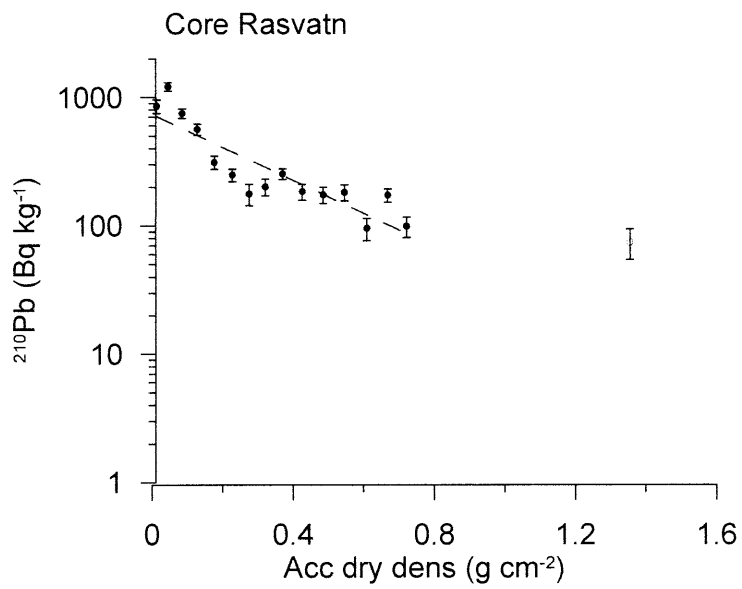


Fig 2

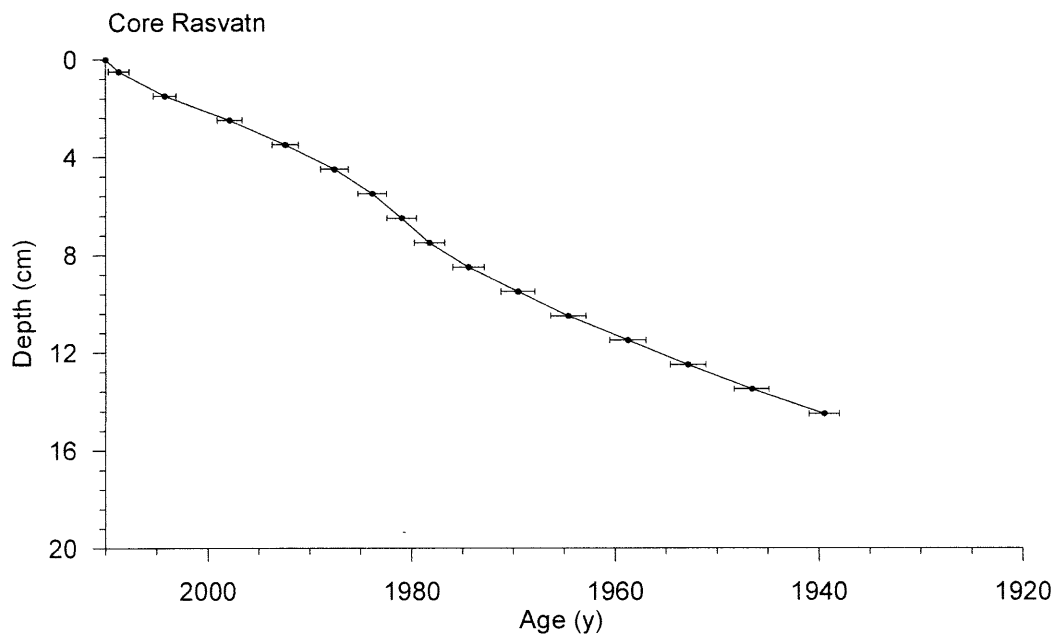


Fig 3

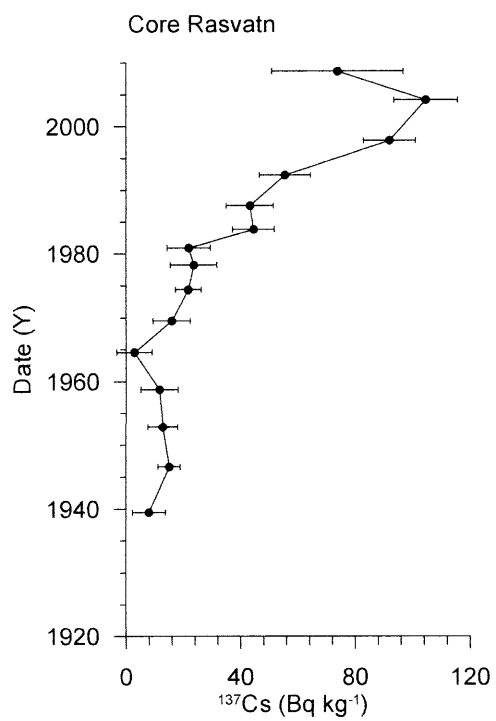


Fig 4

Dating of core Jordtjern

Methods

The samples have been analysed for the activity of ^{210}Pb , ^{226}Ra and ^{137}Cs via gamma spectrometry at the Gamma Dating Center, Institute of Geography, University of Copenhagen. The measurements were carried out on a Canberra low-background Ge-detector. ^{210}Pb was measured via its gamma-peak at 46,5 keV, ^{226}Ra via the granddaughter ^{214}Pb (peaks at 295 and 352 keV) and ^{137}Cs via its peak at 661 keV.

Results

The core showed high surface contents of unsupported ^{210}Pb of around 1900 Bq kg⁻¹ and a clear tendency for exponential decline with depth (fig 1). One sample at 14.5 cm had very high activity of unsupported ^{210}Pb , this activity of this sample cannot be explained and it is regarded as an outlier and not considered in the following calculations of chronology. The calculated flux of unsupported ^{210}Pb is 72 Bq m⁻² y⁻¹ which is about the same as the estimated local atmospheric supply (based on Appleby, 2001).

The content of ^{137}Cs showed a peak around 2 cm depth and generally low contents below that level.

CRS-modelling has been applied on the profile using a modified method (Appleby, 2001) where the activity below 14 cm is calculated on the basis of the regression shown in fig 2. The result is given in table 2 and fig 3 and 4.

The chronology for the core is considered to be fairly accurate due to the clear tendency for an exponential decline with depth of unsupported ^{210}Pb . The calculated chronology of the peak activity of ^{137}Cs (fig 4) is also consistent with the expected Chernobyl origin (1986) of this material. The activity of ^{137}Cs at levels dated to well before this isotopes release into nature around the mid 1950's suggests that the isotope is not completely immobile in these sediments.

5 April 2011

Thorbjørn J Andersen

Reference:

Appleby, P.G. (2001): Chronostratigraphic techniques in recent sediments. In: Last, W.M & Smol, J.P. (eds) Tracking environmental change using lake sediments. Volume 1: Basin analysis, coring and chronological techniques. Kluwer Academic Publishers, the Netherlands.

Table 1. Data core Jordtjern

Depth	Pb-210tot	error Pb-210 tot	Pb-210 supupp 210Pb	error pb-210 sup	Pb-210 un-sup	error pb-210 un-sup	Cs-137	error Cs-137
cm	Bq kg-1	Bq kg-1	Bq kg-1	Bq kg-1	Bq kg-1	Bq kg-1	Bq kg-1	Bq kg-1
0.5	1897	128	10	35	1887	133	145	17
1.5	1095	93	50	31	1045	98	195	27
2.5	860	56	55	4	806	56	142	8
3.5	248	20	35	11	213	23	38	6
4.5	316	25	47	10	270	27	37	6
5.5	186	16	27	14	160	22	22	8
6.5	127	12	42	8	85	14	33	7
7.5	89	8	23	2	66	8	13	6
8.5	121	11	42	20	80	23	16	6
9.5	49	5	38	13	12	13	16	5
10.5	80	6	43	7	37	9	15	3
11.5	60	5	38	2	22	6	11	3
12.5	49	5	46	8	3	10	14	6
13.5	53	5	36	5	17	7	6	6
14.5	534	40	42	9	492	41	11	7
25.5	48	5	28	1	20	5	1	4

Table 2, Chronology core Jordtjern

Depth	Age	error age	Date	acc rate	error rate
cm	y	y	y	(kg m-2 y-1)	(kg m-2 y-1)
0.0			2010		
0.5	4	1	2006	0.04	0.00
1.5	15	2	1995	0.04	0.00
2.5	28	2	1982	0.04	0.00
3.5	43	2	1967	0.05	0.01
4.5	55	3	1955	0.06	0.01
5.5	70	4	1940	0.05	0.01
6.5	81	4	1929	0.06	0.01
7.5	90	5	1920	0.07	0.01
8.5	103	7	1907	0.05	0.02
9.5	115	7	1895	0.05	0.05
10.5	125	8	1885	0.07	0.02
11.5	144	12	1866	0.04	0.02
12.5	159	17	1851	0.05	0.12
13.5	176	18	1834	0.04	0.02

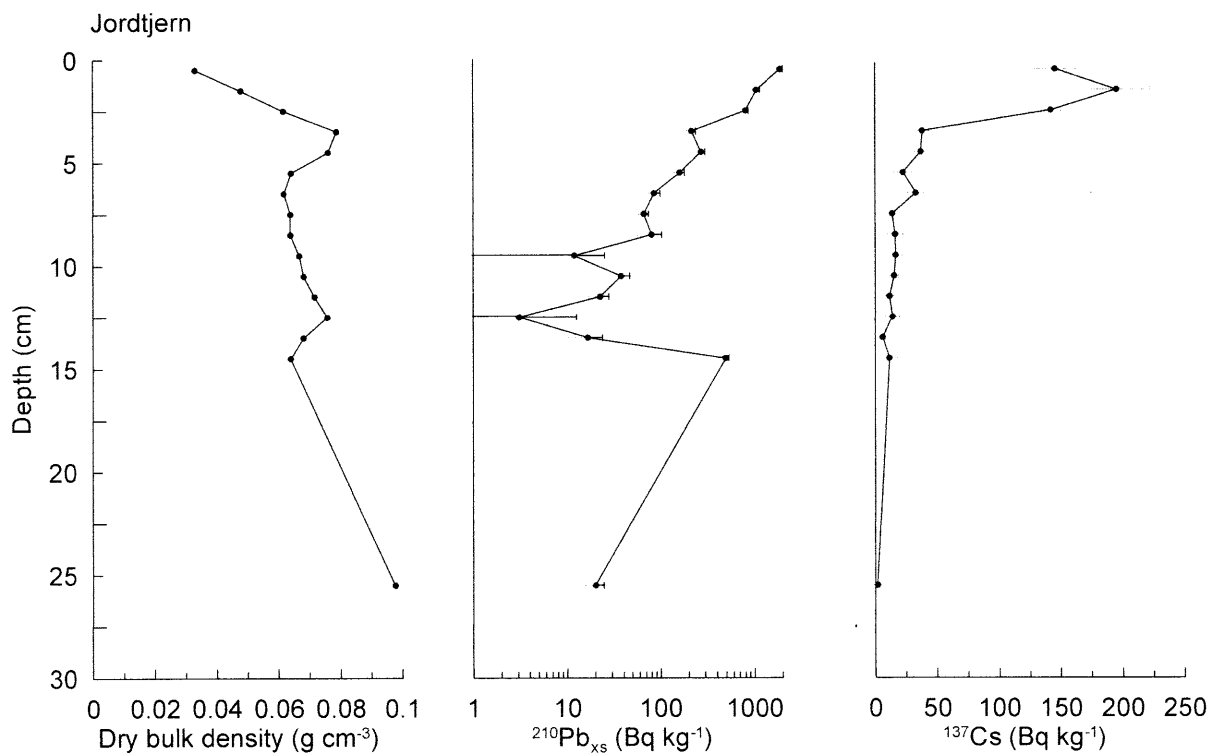


Fig 1

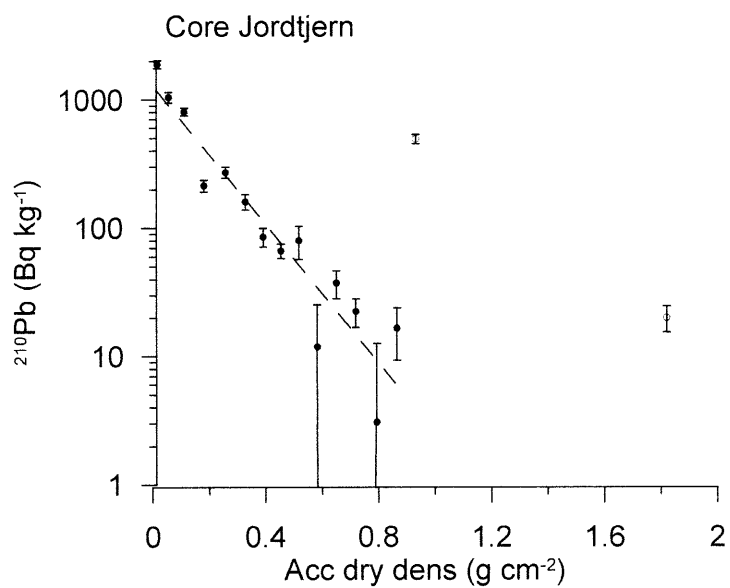


Fig 2

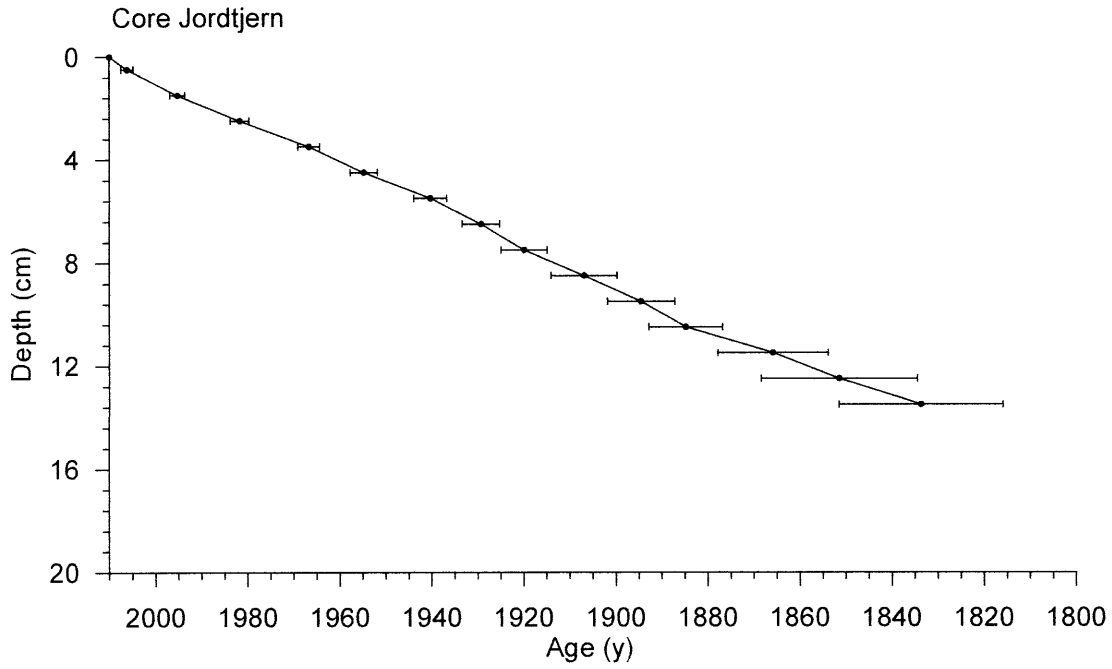


Fig 3

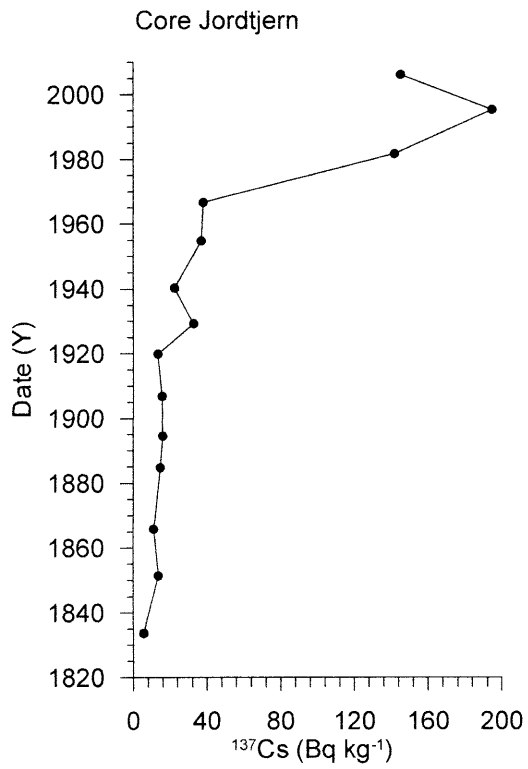


Fig 4

Appendix 2

National emissions of metals and PAHs and temporal trends in emission inventories

The total budget of national PAH emissions in Norway (2010) constitutes 127 tons, of which 23 tons leak from already contaminated soils (figure 1). Recipient environments are air, water and soils (figure 2).

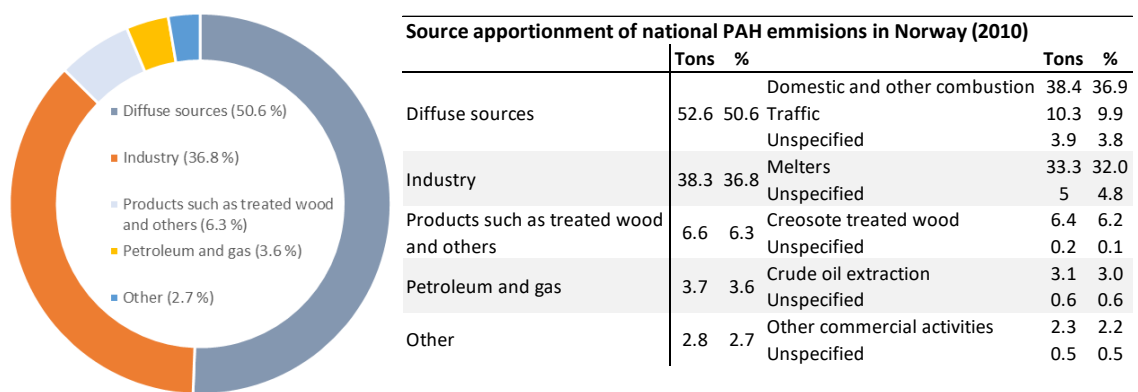


Figure 1 Percentage distribution of national PAH emissions in Norway (left), and source contributions to the right. Figure based on data from Sørensen (2012).

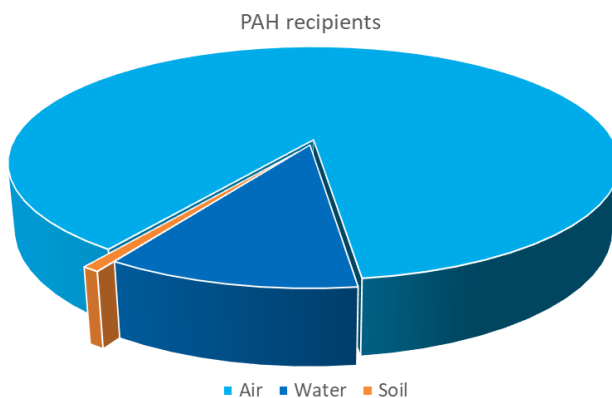


Figure 2 Recipient environments of national PAH emissions in Norway (2010). Figure based on data from (Sørensen 2012).

In addition to these emission, LRTAP of PAHs contributes in the size fraction 20 – 60 tons. Excluding contributions from contaminated soils and LRTAP, there has been a PAH reduction greater than 60 % in Norway since 1995, from 268 tons in 1995, to 104 tons in 2010 (Sørensen 2012).

Figure 3 show PAHs in terrestrial moss from different sampling stations along a south-north gradient in Norway in 2010 (Steinnes & Schlabach 2012). Far left; figures from Birkenes sampling station (N58° 23,265' – Ø8° 14,995'), close to the fire affected area Mykland.

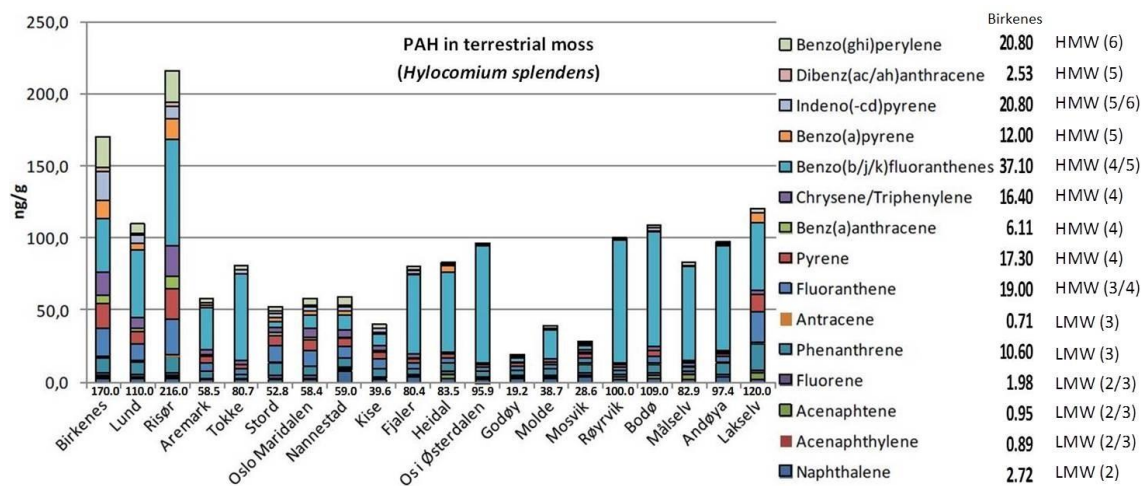


Figure 3 PAHs in terrestrial moss from different sampling stations along a south-north gradient in Norway in 2010. Figure based on Steinnes and Schlabach (2012).

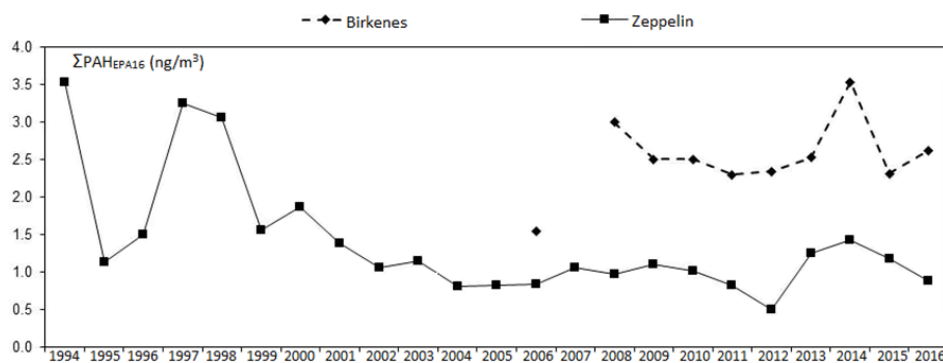


Figure Annual mean concentrations of $\Sigma\text{PAH}_{\text{EPA16}}$ (ng/m³) in air at the Norwegian Institute for Air Research's (NILU) Birkenes (Aust-Agder county) and Zeppelin (Svalbard) observatories. Annual mean concentrations of $\Sigma\text{PAH}_{\text{EPA16}}$ are about two times higher at Birkenes (monitoring started in 2008) than at Zeppelin (monitoring started in 1993, since 1994 as part of AMAP) (Nizzetto, Aas & Warner 2017).

Total emissions for several metals (i.e. Cr, Cd, Hg and Pb) are reported to decline in Norway (on national scale) during the years 1995 – 2010 (table 1), but Cu seems to increase. In 1995 Cu emissions were 748 tons (Norwegian Pollution Control Authority 2005). In 2005 an increase of 36 % since 1995 was reported (Norwegian Environment Agency 2008). That sums to 1017 tons of Cu emitted in one year in Norway.

Table 1 National metal emissions in Norway in 1995 and 2010. Table based on data from Sørensen (2012), Norwegian Environment Agency (2008) and Norwegian Pollution Control Authority (2005).

National metal emissions in Norway (1995 - 2010)			
	Tons (1995)	Tons (2010)	Reduction (%)
Chromium (Cr)	100	47	53
Cadmium (Cd)	5	1.5	72
Mercury (Hg)	2.5	0.8	67
Lead (Pb)	600	119	80
Copper (Cu)	748 ¹	1017 ³ (2005)	36 (increase) ²

¹Norwegian pollution control authority 2005

²The Norwegian Environment Agency 2008

³Own calculation

Data on national total emissions of V, Co, Ni and Zn are hardly available (internet searches through online databases like google scholar, university and library databases, governmental databases, research institute databases, statistics databases etc., turned out negative).

Consulting reports on atmospheric deposited metals in Norway, a continuous reduction in LRTAP metals V, Cr, Co, Ni (levels of Cr, Co and Ni are influenced by domestic sources), Cu, Zn, Cd, Hg and Pb since 1977 is reported for moss by Steinnes, Berg and Uggerud (2011) in 2005. This is in agreement with the results from the third Norwegian lake survey on national scale, NLS 3, where a general concentration decline of V, Co, Ni, Cu, Zn, Cd and Pb is seen in lake bed deposits along the coastal areas of southern Norway (Rognerud *et al.* 2008). Also, Aas (2011) report reduced metal (i.e. Cr, Ni, Zn, Cd, Hg and Pb) concentration in air and precipitation in 2010 compared to the 1980s and 1990s.

References

- Aas, W. (2011) Overvåking av langtransportert forurenset luft og nedbør : atmosfærisk tilførsel, 2010. *Monitoring of long-range transported air pollutants annual report for 2010*. Norwegian Institute for Air Research (NILU), Oslo.
- Nizzetto, P.B., Aas, W. & Warner, N.A. (2017) Monitoring of environmental contaminants in air and precipitation, annual report 2016. Norwegian Institute for Air Research - Norsk Institutt for Luftforskning (NILU), Norway.
- Norwegian Environment Agency (2008) Stadig mindre utslipp av miljøgifter. The Norwegian Environment Agency (Miljødirektoratet), www.miljodirektoratet.no.
- Norwegian Pollution Control Authority (2005) Nasjonale utslipp av prioriterte miljøgifter i 1995 og 2002. (ed. T.R.N.M.o.t.E. (Miljøverndepartementet)). Statens forurensningstilsyn; SFT - Norwegian Pollution Control Authority, www.miljodirektoratet.no.
- Rognerud, S., Fjeld, E., Skjelkvåle, B.L., Christensen, G. & Røyset, O.K. (2008) Nasjonal innsjøundersøkelse 2004 - 2006, del 2 sedimenter: forurensning av metaller, PAH og PCB. *National lake survey 2004 - 2006*. Norwegian Pollution Control Authority (Statens forurensningstilsyn; SFT), Oslo.
- Steinnes, E., Berg, T. & Uggerud, H.T. (2011) Three decades of atmospheric metal deposition in Norway as evident from analysis of moss samples. *Science of The Total Environment*, **412–413**, 351-358.
- Steinnes, E. & Schlabach, M. (2012) *Moseundersøkelse i Norge 2010: nivåer av organiske miljøgifter på 20 lokaliteter*. KLima- og forurensningsdirektoratet, Oslo.
- Sørensen, P. (2012) Prioriterte miljøgifter: Nasjonale utslipp - status 2010. (ed. M.T.R.N.M.o.t. Environment)), pp. 136. Klima- og forurensningsdirektoratet; KLIF - The Norwegian Climate and Pollution Agency, www.miljodirektoratet.no.

Appendix 3

Results from the Mykland sampling campaign against national trends

Based on dating of sediment cores Hundsvatn and Jordtjenn_{con} (ch. 5.1), surface (depth interval 1.0 – 0.0 cm) sediments in Mykland represent the years 2001 / 2002 \pm 2 yrs. – year 2010 (approximately the 2000s). That period covers the years when NLS 3 was conducted (NLS 3 was conducted 2004-’06). Sub-surface (depth interval 2.0 – 1.0 cm) sediments represent the ten years period in advance of 2001 / 2002 \pm 2 yrs. (approximately the 1990s), comprising the years of the former NLS (NLS 2 was conducted 1996-’97).

With the risk of being apophenic (perception of or belief in connectedness among unrelated phenomena), the fluctuation patterns of metals and PAHs found in Mykland lake sediments resembles much of the general picture for the region. The results from Mykland show

1) increased concentration levels from pre-industrial (depth 33.0 \pm 11.5 cm) to industrial (depths \leq 3.5 cm) time for all metals¹ in all lakes, which is in good correspondence to the conclusions from the three Norwegian lake surveys (NLS) on national scale, conducted in 1986 – ’88 (Rognerud & Fjeld 1990)², 1996 – ’97 (Rognerud, Fjeld & Løvik 1999) and 2004 – 2006 (Rognerud *et al.* 2008).

There is shortage of surveys from years earlier than 1990 on PAH levels in Norwegian freshwater lake bed sediments (Rognerud, Fjeld & Løvik 1997).

2) Within industrial time in advance of the 2008 wildfire (depth 3.5 – 1.5 cm, which approximate the 1960s throughout the 1990s), V, Cr (not measured in NLS 1 or sub-surface sediments in NLS 2) and Hg / Hg_{LOI} concentrations continue to increase in six (all five burnt lakes plus one unburnt control lake) out of eight Mykland lake bed sediments (constituting 75 % of the sampled lakes), which reflects the progression

¹ Exceptions: Co declines in Øyvatn, while Cr and Cu decline in Rasvassvatn (from depth 33.0 to 3.5 cm).

² NLS 1 analysed sediment concentrations only on Ni, Cd, Hg and Pb.

pattern for V and Hg in southern Norway from late '80s to early '90s (measured depth 0.5 – 0.0 cm in NLS 2 represents approximately 1987 – 1997), described in NLS 2.

During the same period (depth 3.5 – 1.5 cm), Ni and Cu increase in five out of eight Mykland lakes (decline in the three control lakes Jordtjenn_{con}, Svarttjenn_{con} and Melestjenn_{con}), leaving the overall tendency uncertain and more liable to be considered as *no tendency*. In NLS 2, concentrations of Ni and Cu are referred to as unaltered from sub-surface to surface sediments, but the median (50 %) value of Ni and Cu (the acid soluble fraction) increase (5,0 % and 2,5 %, respectively) slightly between the two uppermost sediment sections.

A marginal predominance of increasing (increase in five out of eight lakes, and by that liable to be considered as *no tendency*) Zn and Cd concentrations in Mykland sediments, contrasts the Zn and Cd decline seen from sub-surface (depth 1.0 – 0.5 cm; late half of the 1980s) to surface (depth 0.5 – 0.0 cm; early half of the 1990s) sediments in NLS 2. Methodological differences between NLS 1 and NLS 2 makes the two lake surveys unsuited for comparison of Cd and Hg concentrations.

The weak and uncertain overall tendency of an increase (62.5 % increase) in Ni, Cu, Zn and Cd concentrations in Mykland may be deviant to NLS 2 because Mykland is at risk of being influenced by the non-ferrous pyrometallurgy industry in the coastal town Arendal (34 km linear distance south-east of Mykland), intensifying atmospheric fallout.

From sub-surface (depth 1.0 – 0.5 cm represents 1977 – 1987) to surface (depth 0.5 – 0.0 cm represents 1987 – 1997) sediments, Pb concentrations decline in NLS 2. In Mykland Pb declines only in the three control lakes and Hundsvatn. That means there is no increase or decline tendency for Pb in Mykland when comparing sediments deposited in the 1960s to the ones deposited in the 1990s. This is also seen for Co (not measured in NLS 1 or sub-surface sediments in NLS 2), which decline in four out of eight lakes (all references to NLS 2 from Rognerud, Fjeld & Løvik 1999).

PAHs are not included in the regional / national lake survey program until 1997 (only surface sediments sampled), when Rognerud, Fjeld and Løvik (1997) reported high levels of PAHs in freshwater lake bed sediments (depth 0 – 2 cm) along the coastal parts of south-eastern Norway. Sediments were classified as heavily (class four out of five; 6000 – 20 000 µg kg⁻¹) to very heavily (class V; > 20 000 µg kg⁻¹) polluted,

according to the classification guide for environmental quality in marine sediments (Molvær *et al.* 1997), in force at the time.

According to the 1997 classification guide (Molvær *et al.* 1997), lake sediments in Mykland (Fisketjenn, Hundsvatn, Grunnetjenn, Rasvassvatn, Øyvatn and Jordtjenn_{con}) categorize as heavily to very heavily polluted with PAHs (measured concentrations of $\Sigma\text{PAH}_{\text{EPA16+2}}$), ranging from 6465 $\mu\text{g kg}^{-1}$ (Øyvatn) to 39 538 $\mu\text{g kg}^{-1}$ (Rasvassvatn) at depth 1.5 cm (deposited during the 1990s). Svarttjenn_{con} (1302 $\mu\text{g kg}^{-1}$) and Melestjenn_{con} (5786 $\mu\text{g kg}^{-1}$) classify as moderately (class II; 300 – 2000 $\mu\text{g kg}^{-1}$) to markedly (class III; 2000 – 6000 $\mu\text{g kg}^{-1}$) contaminated, respectively.

All individual PAH concentrations, and consequently $\Sigma\text{PAH}_{\text{EPA16+2}}$, increase from sediment depth 3.5 to 1.5 cm in Mykland (decline in Svarttjenn_{con} and Melestjenn_{con} and not a uniform trend in Øyvatn).

3) In NLS 3, a decline in V, Co, Ni, Cu, Zn, Cd and Pb concentrations is found along the south-eastern parts of coastal Norway from 1997 to 2006 (depth 0.5 – 0.0 cm). Hg concentrations are unaltered on a general basis but tend to decline in southern Norway. Cr show no tendency.

The results from Mykland correspond to the conclusion from NLS 3; Co, Ni, Zn, Cd and Pb concentrations decline from sub-surface to surface, while Cr shows no decline / increase tendency. Hg concentrations show no tendency in Mykland from pre-fire to PWF sediments, but when normalized for its LOI association, a Hg (i.e. Hg_{LOI}) decline is seen.

The absence of a Cu decline (Cu shows no tendency) in Mykland sediments can be accounted for by a possible impact from the industry in Arendal and Kristiansand. In NLS 3 a Cu increase is found in lake sediments in proximity to these cities.

Concentrations of V increase from sediment depth 1.5 to 0.5 cm in Mykland, unlike the V decline seen in NLS 3 for southern Norway from 1997 – 2006. Nevertheless, in western and northern parts of Norway a V increase has been observed (all references to NLS 3 from Rognerud *et al.* 2008). Rognerud *et al.* (2008) find it difficult to give a good explanation for the increase, but a heightened contribution from geochemical V is thinkable, as well as atmospheric deposits from eastern Europe (Rognerud, Fjeld & Løvik 1999). A paper by Schlesinger, Klein and Vengosh (2017) describes anthropogenic emissions of V to the atmosphere, and following deposits, to increase.

The paper also report V to originate from forest wildfires (Schlesinger, Klein & Vengosh 2017), but in such a scenario raised levels of V should be expected to be accompanied by other metals like Ni, Cd and Pb (Campos *et al.* 2016), which is not the case in Mykland. Thus, raised V concentration in surface sediments unlikely originate from the 2008 wildfire solely.

In NLS 3, PAH concentrations are only measured in surface (depth 1.0 – 0.0 cm) sediments, representing the years 1990 \pm 5 yr. to approximately 2006. The results reckon sediments along the coastal areas of southern and western Norway as the most polluted (Rognerud *et al.* 2008). Results are not compared to the 1997 lake survey of organic micropollutants (i.a. PAHs) on regional scale (Rognerud, Fjeld & Løvik 1997), neither is the level of sediment pollution quantified, nor environmental conditions classified.

Differences between the sampling campaign in Mykland and the three NLSs

When evaluating the results from Mykland against NLS 2, the periods (in NLS 2 temporal trends from the late half of the 1980s [sub-surface depth 1.0 – 0.5 cm represents 1984 – 1990] to early half of the 1990s [surface depth 0.5 – 0.0 cm represents 1990 – 1996]³ are described) and narrower time-span (sampled sediment layer thickness is 0.5 cm in NLS 2) in NLS 2 (Rognerud, Fjeld & Løvik 1999), both diverge from the ones representing pre-wildfire industrial time in the Mykland sampling campaign (temporal trends from the 1960s [depth 4.0 – 3.0 cm, denoted 3.5] to the 1990s [depth 2.0 – 1.0 cm, denoted 1.5] are described, cf. appended reports on dating of sediments). This influence on the comparability of the results.

Also, it is worth mentioning that metal concentrations decline / increase in the range 5 \pm 2.5 %, except Pb which decline with 16.5 %, in NLS 2 (Rognerud, Fjeld & Løvik 1999). In Mykland, alterations are in the range from 1 – 111 % during the pre-fire industrial years (depth 3.5 – 1.5 cm). More than half of these changes are greater than

³ In Rognerud, Fjeld & Løvik (1999), sediment section 1.0 – 0.5 cm is said to represent 1977 – 1987 (page 10), while on page 52 the same section represents 1984 – 1990. On the same two pages sediment section 0.5 – 0.0 cm is said to represent 1987 – 1997 and 1990 – 1996. The present paper uses time interval 1984 – 1990 on sediment section 1.0 – 0.5 cm, and 1990 – 1996 on sediment section 0.5 – 0.0 cm in NLS 2.

25 %. Such great alterations question whether the sampled Mykland lakes are affected by variables that is not accounted for, and by that degrade representativeness and suitability for comparison.

When evaluating the results from Mykland against NLS 3, once again it is important to stress the differing periods compared. In Mykland, surface sediments represent the first decade of the 2000s, while in NLS 3 sediment section 0.5 – 0.0 cm represents 1997 – 2006 (section 1.0 – 0.5 cm represents 1987 – 1996). The time-span (thickness of sediment sections) in NLS 3 is narrower (thickness 0.5 cm) than in Mykland (thickness 1.0 cm). Sampled sediment layer thickness is 1.0 cm for PAHs in NLS 3 (Rognerud *et al.* 2008). This affect the comparability of the results.

References

- Campos, I., Abrantes, N., Keizer, J.J., Vale, C. & Pereira, P. (2016) Major and trace elements in soils and ashes of eucalypt and pine forest plantations in Portugal following a wildfire. *Science of The Total Environment*, **572**, 1363-1376.
- Molvær, J., Knutzen, J., Magnusson, J., Rygg, B., Skei, J. & Sørensen, J. (1997) *Klassifisering av miljøkvalitet i fjorder og kystfarvann: veiledning*. Statens forurensningstilsyn (SFT) - Norwegian Pollution Control Authority, Oslo.
- Rognerud, S. & Fjeld, E. (1990) *Landsomfattende undersøkelse av tungmetaller i innsjøsedimenter og kvikksølv i fisk*. Norwegian Pollution Control Authority (Statens forurensningstilsyn; SFT), Oslo.
- Rognerud, S., Fjeld, E. & Løvik, J.E. (1997) *Regional undersøkelse av miljøgifter i innsjøsedimenter, delrapport 1: Organiske mikroforurensninger*. The Norwegian Institute for Water Research (Norsk Institutt for Vannforskning; NIVA), Oslo.
- Rognerud, S., Fjeld, E. & Løvik, J.E. (1999) *Landsomfattende undersøkelse av metaller i innsjøsedimenter*. The Norwegian Institute for Water Research (Norsk Institutt for Vannforskning; NIVA), Oslo.
- Rognerud, S., Fjeld, E., Skjelkvåle, B.L., Christensen, G. & Røyset, O.K. (2008) Nasjonal innsjøundersøkelse 2004 - 2006, del 2 sedimenter: forurensning av metaller, PAH og PCB. *National lake survey 2004 - 2006*. Norwegian Pollution Control Authority (Statens forurensningstilsyn; SFT), Oslo.
- Schlesinger, W., Klein, E. & Vengosh, A. (2017) *Global biogeochemical cycle of vanadium*.

Appendix 4

Qualified majority

Whether metals within a lake demonstrate a concentration decline or increase is identified by using a non-statistic approach; *qualified majority* (QM). Qualified majority is a method often used in decision making, like voting over a proposal of great significance. The threshold required to obtain qualified majority is set in advance of voting, typically $\frac{2}{3}$ or $\frac{3}{4}$ of all votes (e.g. §115 in the Constitution of the Kingdom of Norway). In this study the threshold value is set to $\geq \frac{3}{4}$, which is to be considered a rather strict criterion. This means that at least $\frac{3}{4}$ of the nine metals (regardless of which) in a single lake must either all decline or all increase. If they do, metal concentrations in that particular lake is said to decline / increase, respectively.

Does several lakes within a set of lakes (e.g. burnt lakes) share the same property of a decline / increase, metals are said to decline / increase in that group of lakes, if the decline / increase satisfy a qualified majority $> \frac{3}{4}$ across lakes (i.e. $> \frac{3}{4}$ of the lakes in a group display a decline / increase in agreement with the $\geq \frac{3}{4}$ criteria for metals).

There is a possibility that single metals demonstrate a mutual decline / increase from one depth to a shallower across several lakes, without belonging to any lake that fulfil the $\geq \frac{3}{4}$ criteria for metals to be regarded as a lake with declining / increasing metal concentrations. To capture such tendencies, these metal fluctuations are presented individually as a metal to decline / increase across lakes.

If metal fluctuations in a lake not fulfil the $\geq \frac{3}{4}$ criteria for metals, the lake is sorted as *no tendency* (metals neither decline nor increase). Nevertheless, when determining a general decline / increase across several lakes (e.g. the three burnt lakes), such categorization may camouflage the actual decline / increase tendency. This owe to the situation where sorting a lake as *no tendency* may categorize all the lakes (in a set of lakes) as *no tendency*, because the set of lakes fail to meet the $> \frac{3}{4}$ criteria for lakes, even if two out of three lakes fulfil the $\geq \frac{3}{4}$ criteria for metals.

For instance, if two out of three lakes sort as *declining tendency*, while one lake sort as *no tendency*, even though the *absolute* majority (more than 50 %) of metals decline in

that particular lake, the three lakes fail to meet the $>3/4$ qualified majority criteria for lakes as a group and categorize as *no tendency*.

To prevent unintended errors like this, all metal fluctuations (across lakes) are also considered simultaneously for a set of lakes; If the $>3/4$ criteria for lakes is met, the lakes sort under a common tendency (e.g. if there are three lakes and nine metals to be measured, 27 variations exist, out of which 21 metals must pull in the same direction to meet the $\geq 3/4$ criteria for metals). A prerequisite is that metal fluctuations within every single lake in consideration fulfil a $\geq 2/3$ qualified majority threshold, pulling in the same direction (in the example, that is a minimum of six out of nine metals in each lake).

Note that both requirements must be fulfilled.

Likewise, if two out of three lakes in the example above fulfil no more than the $\geq 2/3$ criteria for metal fluctuations (six out of nine metals) within a single lake, the three lakes may still meet the $\geq 3/4$ criteria for metals (21 out of 27 metals) and sort under common metal fluctuation tendencies, if judged as a group of lakes. This necessitates all nine metals in the third lake to pull in one single direction, that coincides with the tendency $\geq 2/3$ of the metals in each of the two other lakes demonstrate.

Pre-fire (depth 1.5 cm) deposits against PWF (depth 0.5 cm) deposits

In terms of holding the requirements of a qualified majority (threshold value $\geq 3/4$) the results outlined in chapter 5.3.4 are specified.

Calculations comprise all lakes. That include those lacking a general decline in metal concentrations from depth 1.5 to 0.5 cm within the lake (i.e. Rasvassvatn, Jordtjenn_{con} and Svarttjenn_{con}) itself. Consequently, sediment concentrations of a metal may decline from section 1.5 to 0.5 in the majority of lakes, even if the general tendency in one or more of the considered lakes where this specific metal is found to decline, do *not* hold a general metal decline tendency, or even display a metal concentration increase (e.g. Co declines in all lakes, including Jordtjenn_{con}, in which 66.67 % of the metals increase). Moreover, metals considered to decline on a general basis, are considered across lakes. This means, that even if a specific metal decline in one lake, it does not necessitate other metals considered, to decline in that very lake(s).

Metals;

From sub-surface to surface sediments Co (declines in $\frac{7}{8}$ lakes = 87.50 %, 100 % if the unaltered Co concentration in Øyvavn is considered a decline), Ni (declines in $\frac{6}{8}$ lakes = 75 %, if the unaltered Ni concentration in Svarttjenn_{con} is considered a decline), Zn (declines in $\frac{6}{8}$ lakes = 75 %, if the unaltered Zn concentration in Rasvassvatn is considered a decline), Cd (declines in $\frac{6}{8}$ lakes = 75.00 %), Hg_{LOI} (declines in $\frac{6}{8}$ lakes = 75.00 %) and Pb (87.50 %) decline in $\geq \frac{6}{8}$ (75.00 %) of the lakes. V *increases* in six out of eight (75.00 %) lakes. The remaining metals (i.e. Cr, Cu and Hg) decline from depth 1.5 to 0.5 cm in only four out of eight (50.00 %) lakes (table 16, Tables and figures).

The six metals (i.e. Co, Ni, Zn, Cd, Hg_{LOI}, Pb) to decline in $\geq \frac{6}{8}$ of the lakes are measured in all eight lakes studied, offering 48 (six metals times eight lakes) possible variations of a decline / increase. These metals decline 38 times, which is in accordance with the $\frac{3}{4}$ qualified majority ($\frac{38}{48} = 79.17$ %) for metals. On a general basis, sediment concentrations of Co, Ni, Zn, Cd, Hg_{LOI} and Pb decline from sub-surface to surface sediments.

Lakes;

Within Hundsvatn ($\frac{8}{9}$ metals decline = 88.89 %), Grunnetjenn ($\frac{6}{9}$ metals decline = 66.67 %), Øyvavn ($\frac{7}{9}$ metals decline = 77.78 %, 88.89 % if the unaltered Co concentration is considered a decline), Melestjenn_{con} (100 %) and Fisketjenn ($\frac{6}{9}$ metals decline = 66.67 %, if replacing Hg with Hg_{LOI}), six or more out of nine ($\geq \frac{2}{3} = \geq 66.67$ %) metals decline from depth 1.5 to 0.5 cm. Of the 45 metal measurements (nine metals times five lakes), 36 measurements decline (80.00 %). It is possible to conclude that a general metal concentration decline is found in five lakes. A metal decline in five out of eight ($\frac{5}{8} = 62.50$ %) lakes does not meet the $> \frac{3}{4}$ qualified majority criteria for lakes. Consequently, it is not possible to conclude that lakes hold declining metal concentrations on a general basis.

Neither is it possible to conclude that the six metals (i.e. Co, Ni, Zn, Cd, Hg_{LOI}, Pb) to decline in five lakes, decline in the five lakes (i.e. Fisketjenn, Hundsvatn, Grunnetjenn, Øyvavn, Melestjenn_{con}) that hold declining metal concentrations, because the metals to decline / increase are not uniform across lakes, meaning that the metals to constitute a declining trend in one lake may differ from the metals to represent a decline in another lake.

Nevertheless, Co, Ni, Zn, Cd, Hg_{LOI} and Pb *do* decline in Fisketjenn, Hundsvatn, Grunnetjenn, Øyvatn (if the unaltered Co concentration is considered a decline) and Melestjenn_{con} (all metals decline in Melestjenn_{con}). In addition, Cr, Cu and Hg decline in both Hundsvatn, Øyvatn and Melestjenn_{con}.

Five (55.56 %) to six (66.67 %) out of nine metals *increase* from depth 1.5 to 0.5 cm in three out of eight ($\frac{3}{8} = 37.50$ %) lakes (i.e. Rasvassvatn, Jordtjenn_{con} and Svarttjenn_{con}).